

Friis, Nicolai (2013) Cavity mode entanglement in relativistic quantum information. PhD thesis, University of Nottingham.

Access from the University of Nottingham repository:

http://eprints.nottingham.ac.uk/13795/1/Thesis_v10.pdf

Copyright and reuse:

The Nottingham ePrints service makes this work by researchers of the University of Nottingham available open access under the following conditions.

This article is made available under the University of Nottingham End User licence and may be reused according to the conditions of the licence. For more details see:
http://eprints.nottingham.ac.uk/end_user_agreement.pdf

A note on versions:

The version presented here may differ from the published version or from the version of record. If you wish to cite this item you are advised to consult the publisher's version. Please see the repository url above for details on accessing the published version and note that access may require a subscription.

For more information, please contact eprints@nottingham.ac.uk

**CAVITY MODE ENTANGLEMENT IN
RELATIVISTIC QUANTUM INFORMATION**

NICOLAI FRIIS, Mag. rer. nat.

Thesis submitted to the University of Nottingham
for the degree of Doctor of Philosophy

DECEMBER 2013

“To those who do not know mathematics it is difficult to get across a real feeling as to the beauty, the deepest beauty, of nature ... If you want to learn about nature, to appreciate nature, it is necessary to understand the language that she speaks in.”

(R. Feynman, *The Character of Physical Law* (1965) Ch. 2)

“Quantum physics means anything can happen at any time for no reason.”

(H. J. Farnsworth)

Abstract

A central aim of the field of relativistic quantum information (RQI) is the investigation of quantum information tasks and resources taking into account the relativistic aspects of nature. More precisely, it is of fundamental interest to understand how the storage, manipulation, and transmission of information utilizing quantum systems are influenced by the fact that these processes take place in a relativistic spacetime. In particular, many studies in RQI have been focused on the effects of non-uniform motion on entanglement, the main resource of quantum information protocols. Early investigations in this direction were performed in highly idealized settings that prompted questions as to the practical accessibility of these results. To overcome these limitations it is necessary to consider quantum systems that are in principle accessible to localized observers. In this thesis we present such a model, the rigid relativistic cavity, and its extensions, focusing on the effects of motion on entanglement and applications such as quantum teleportation.

We study cavities in $(1+1)$ dimensions undergoing non-uniform motion, consisting of segments of uniform acceleration and inertial motion of arbitrary duration that allow the involved velocities to become relativistic. The transitions between segments of different accelerations can be sharp or smooth and higher dimensions can be incorporated. The primary focus lies in the Bogoliubov transformations of the quantum fields, real scalar fields or Dirac fields, confined to the cavities. The Bogoliubov transformations change the particle content and the occupation of the energy levels of the cavity. We show how these effects generate entanglement between the modes of the quantum fields inside a single cavity for various initial states. The entanglement between several cavities, on the other hand, is degraded by the non-uniform motion, influencing the fidelity of tasks such as teleportation. An extensive analysis of both situations and a setup for a possible simulation of these effects in a table-top experiment are presented.

Acknowledgements

My gratitude goes to all the fantastic people that have supported me in the pursuit of my goals, specifically throughout my PhD studies. First of all I would like to thank my family and all those of my friends, which I could not have been there for as much as I would have liked, for their continued encouragement and friendship. In particular, I would like to thank *Verena Hofstätter* for her patience and ethical counsel, and a special thanks to those adventurers that came all the way to Nottingham to visit me.

I would like to express my thanks to the researchers that have guided me with their experience: *Ivette Fuentes*, for her trust, friendship, and openness, and her joy in doing physics; *Gerardo Adesso*, for the nonchalant honesty of his advice; *Jorma Louko*, for his love to detail and complicated mathematical functions; and to *Reinhold A. Bertlmann*, for his spirit, verve, and his socks. During my time in Nottingham I have been surrounded by people that I count as friends as much as colleagues: I want to thank *Antony R. Lee* for enriching my vocabulary in what he claims to be English; *David Edward Bruschi* for learning to expect the unexpected; and *Sara Tavares* for bothering to organize a conference with us. In addition I would like to thank the entire team in Nottingham, present or past, which I feel proud to have been a part of: *Mehdi Ahmadi*, *Valentina Baccetti*, *Luis C. Barbado*, *Jason Doukas*, *Andrzej Dragan*, *Karishma Hathlia*, *Giannis Kogias*, *Bartosz Regula*, *Carlos Sabín*, *Kevin Truong*, *Luke Westwood*, and *Angela White*.

A special thanks to *Marcus Huber*, for his hospitality, friendship, and unconventionality. I am also specifically grateful to *Markus Arndt*, *Jan Bouda*, *Hans J. Briegel*, *Jacob Dunningham*, *Davide Girolami*, *Lucia Hackermüller*, *Eli Hawkins*, *Beatrix C. Hiesmayr*, *Helmut Hüffel*, *Juan León*, *Robert B. Mann*, *Nicolas Menicucci*, *Daniel K. L. Oi*, *Sammy Ragy*, *Timothy C. Ralph*, *Mohsen Razavi*, *Paul Skrzypczyk*, *Vlatko Vedral*, *Silke Weinfurtnner*, and *Andreas Winter* for their kind invitations, hospitality, and financial support during academic visits, and, in particular, for giving me the opportunity to present my work at various seminars, workshops and conferences.

I am further grateful to all my co-authors, those named above as well as *Andreas Gabriel, Göran Johansson, Philipp Köhler, Eduardo Martín-Martínez, Enrique Solano, and Christoph Spengler* for all the engaging discussions, computations, correspondence, and their time and effort during the publication process.

Finally, my sincere thanks go to the funding agencies who have made many of the endeavors of the past years possible: the EPSRC (CAF Grant No. EP/G00496X/2 to Ivette Fuentes), the Royal Society, Universitas 21 and the University of Nottingham Graduate School, the London Mathematical Society, the Institute of Mathematics and its Applications small grant scheme, the CAP research network, the research support fund of the Edinburgh Mathematical Society, the Science and Technology Facilities Council, the Institute of Physics (IOP) Mathematical and Theoretical Physics group, and the IOP Gravitational Physics group.

Contents

Introduction	1
Author's Declaration	1
List of Publications	1
Aims of Relativistic Quantum Information	3
Outline of the Thesis	5
I Elements of Relativistic Quantum Information	7
1 Basic Concepts in Quantum Information	9
1.1 Pure & Mixed Quantum States	9
1.1.1 Pure States	9
1.1.2 Mixed States	10
1.2 Entanglement of Pure States	13
1.3 Entanglement of Mixed States	15
1.3.1 Detection of Entanglement	15
1.3.2 Measures of Entanglement	17
1.4 Multipartite Entanglement	20
1.4.1 Genuine Multipartite Entanglement	21
1.4.2 Detection of Genuine Multipartite Entanglement	22
1.5 Applications of Entanglement	23
1.5.1 The EPR Paradox	23
1.5.2 Bell Inequalities & Non-Locality	24
1.5.3 Quantum Teleportation	26
2 Quantum Fields in Flat and Curved Spacetimes	29
2.1 Relativistic Spacetimes	30
2.2 The Klein-Gordon Field	31
2.2.1 The Classical Klein-Gordon Field	31
2.2.2 Quantizing the Klein-Gordon Field	32
2.2.3 The Bosonic Fock Space	33

2.2.4	Bosonic Bogoliubov Transformations	35
2.3	The Dirac Field	36
2.3.1	Quantizing the Dirac Field	36
2.3.2	The Fermionic Fock Space	37
2.3.3	Bogoliubov transformations of the Dirac Field	39
3	Entanglement in Relativistic Quantum Fields	41
3.1	Entanglement in Bosonic Quantum Fields	41
3.1.1	Continuous Variables: Gaussian States	42
3.1.2	Symplectic Operations	44
3.1.3	Two-Mode Squeezed States	46
3.1.4	Entanglement of Gaussian States	47
3.2	Entanglement in Fermionic Quantum Fields	51
3.2.1	Density Operators in the Fermionic Fock Space	53
3.2.2	The Fermionic Ambiguity	54
3.2.3	The Partial Trace Ambiguity	55
3.2.4	Entanglement of Fermionic Modes	59
3.2.5	Fermionic Entanglement Beyond Two Modes	61
II	Shaking Entanglement	65
4	Constructing Non-Uniformly Moving Cavities	67
4.1	The Relativistically Rigid Cavity	68
4.2	Scalar Fields in Rigid Cavities	72
4.2.1	Cavity in Uniform Motion — Scalar Field	72
4.2.2	Matching: Inertial to Rindler — Scalar Field	74
4.3	Dirac Fields in Rigid Cavities	79
4.3.1	Cavity in Uniform Motion — Dirac Field	79
4.3.2	Matching: Inertial to Rindler — Dirac Field	85
4.4	Grafting Generic Cavity Trajectories	88
4.4.1	The Basic Building Block	88
4.4.2	Generalized Travel Scenarios	92
4.4.3	Smoothly Varying Accelerations	95
5	State Transformation by Non-Uniform Motion	99
5.1	Bosonic Fock State Transformation	100
5.1.1	Bosonic Vacuum Transformation	100
5.1.2	Transformation of Bosonic Particle States	103

5.2	Transformation of Bosonic Gaussian States	105
5.2.1	Symplectic Representation of Non-uniform Motion	105
5.2.2	Transformed Covariance Matrix Example	105
5.3	Fermionic State Transformation	107
5.3.1	Fermionic Vacuum Transformation	107
5.3.2	Transformation of Fermionic Particle & Anti-Particle States	110
6	Motion Generates Entanglement	115
6.1	Entanglement Generation in Bosonic Fock States	116
6.1.1	Bosonic Vacuum	116
6.1.2	Bosonic Single Particle States	121
6.2	Entanglement Generation in Bosonic Gaussian States	123
6.2.1	Single-Mode Squeezed States	124
6.2.2	Resonances of Entanglement Generation	127
6.3	Entanglement Generation in Fermionic States	131
6.3.1	Entanglement from the Fermionic Vacuum	132
6.3.2	Entanglement from the Fermionic Particle State	134
6.3.3	Entanglement from the Fermionic Particle-Antiparticle Pair	136
6.4	Generation of Genuine Multipartite Entanglement	137
6.4.1	Genuine Multipartite Entanglement — Bosonic Vacuum	138
6.4.2	Genuine Multipartite Entanglement — Fermionic Vacuum	139
7	Degradation of Entanglement between Moving Cavities	143
7.1	Entanglement between Two Bosonic Cavities	144
7.1.1	Bosonic Bell States	144
7.1.2	Two-Mode Squeezed States	146
7.1.3	Fidelity of Teleportation	149
7.1.4	Simulations in Superconducting Circuits	151
7.2	Entanglement between Two Fermionic Cavities	153
7.2.1	Fermionic Bell States	153
7.2.2	Non-Locality & Fidelity of Teleportation	155
	Conclusions	157
	References	161
	List of Figures	179
	Index	187

Introduction

Author's Declaration

I hereby declare that this thesis was produced by myself and is based on the results that I obtained, together with my collaborators, during the time of my PhD studies at the University of Nottingham. A summary of my publications until this date is listed below, but all of them can also be found in the reference section. In this thesis I present the results of my publications (iv)-(x) (Refs. [43, 82–84, 86–89]). I am the lead author in all of these publications apart from [43, (xi)], where authors are listed alphabetically. Accordingly, I have made major contributions to all of these articles in terms of conceptual development, computations, proofs, composition, writing, and illustrations, apart from Ref. [88, (x)], where my contribution is mostly limited to the sections on the Dirac spinor and authors are also listed alphabetically. In addition, the thesis outlines closely related results obtained by my PhD supervisor Ivette Fuentes, and my colleagues David Edward Bruschi, Andrzej Dragan, Daniele Faccio, Antony R. Lee, and Jorma Louko in Refs. [42, 44, 46, 47] during the time of my PhD.

A detailed introduction into the topic of the thesis and an outline of its contents are given after the list of publications.

List of Publications

Journal Publications

- (i) N. Friis, R. A. Bertlmann, M. Huber, and B. C. Hiesmayr,
Relativistic entanglement of two massive particles, (Ref. [81])
[Phys. Rev. A 81, 042114 \(2010\)](#) [[arXiv:0912.4863](#) [quant-ph]].
- (ii) M. Huber, N. Friis, A. Gabriel, C. Spengler, and B. C. Hiesmayr,
Lorentz invariance of entanglement classes in multipartite systems, (Ref. [111])
[Europhys. Lett. 95, 20002 \(2011\)](#) [[arXiv:1011.3374](#) [quant-ph]].

- (iii) N. Friis, P. Köhler, E. Martín-Martínez, and R. A. Bertlmann,
Residual entanglement of accelerated fermions is not nonlocal, (Ref. [85])
[Phys. Rev. A **84**, 062111 \(2011\)](#) [[arXiv:1107.3235](#) [quant-ph]].
- (iv) N. Friis, A. R. Lee, D. E. Bruschi, and J. Louko,
Kinematic entanglement degradation of fermionic cavity modes, (Ref. [87])
[Phys. Rev. D **85**, 025012 \(2012\)](#) [[arXiv:1110.6756](#) [quant-ph]].
- (v) N. Friis, D. E. Bruschi, J. Louko, and I. Fuentes, (Ref. [82])
Motion generates entanglement,
[Phys. Rev. D **85**, 081701\(R\) \(2012\)](#) [[arXiv:1201.0549](#) [quant-ph]].
- (vi) N. Friis, M. Huber, I. Fuentes, and D. E. Bruschi,
Quantum gates and multipartite entanglement resonances realized by non-uniform cavity motion, (Ref. [84])
[Phys. Rev. D **86**, 105003 \(2012\)](#) [[arXiv:1207.1827](#) [quant-ph]].
- (vii) N. Friis and I. Fuentes,
Entanglement generation in relativistic quantum fields, (Ref. [83])
[J. Mod. Opt. **60**, 22 \(2013\)](#) [[arXiv:1204.0617](#) [quant-ph]]
Invited contribution to the Special Issue: Physics in Quantum Electronics.
- (viii) N. Friis, A. R. Lee, and D. E. Bruschi
Fermionic mode entanglement in quantum information, (Ref. [86])
[Phys. Rev. A **87**, 022338 \(2013\)](#) [[arXiv:1211.7217](#) [quant-ph]].
- (ix) N. Friis, A. R. Lee, K. Truong, C. Sabín, E. Solano, G. Johansson, and I. Fuentes,
Relativistic Quantum Teleportation with Superconducting Circuits, (Ref. [89])
[Phys. Rev. Lett. **110**, 113602 \(2013\)](#) [[arXiv:1211.5563](#) [quant-ph]].
- (x) N. Friis, A. R. Lee, and J. Louko,
Scalar, spinor and photon fields under relativistic cavity motion, (Ref. [88])
[Phys. Rev. D **88**, 064028 \(2013\)](#) [[arXiv:1307.1631](#) [quant-ph]].
- (xi) D. E. Bruschi, N. Friis, I. Fuentes, and S. Weinfurtnner,
On the robustness of entanglement in analogue gravity systems, (Ref. [43])
[New J. Phys. **15**, 113016 \(2013\)](#) [[arXiv:1305.3867](#) [quant-ph]].

Pre-prints

- (xii) M. Ahmadi, D. E. Bruschi, N. Friis, C. Sabín, G. Adesso, and I. Fuentes, *Relativistic Quantum Metrology: Exploiting relativity to improve quantum measurement technologies*, (Ref. [7])
e-print [arXiv:1307.7082](https://arxiv.org/abs/1307.7082) [quant-ph] (2013).

Theses

- (xiii) N. Friis, *Relativistic Effects in Quantum Entanglement*, (Ref. [80])
[Diploma thesis, University of Vienna, 2010.](#)

Aims of Relativistic Quantum Information

The topic of this thesis is part of the research area called *Relativistic Quantum Information* (RQI). This young and thriving field aims to investigate questions that lie in the overlap of quantum information theory, quantum field theory, quantum optics and special as well as general relativity. The motivations and particular questions considered for such studies are numerous, but a central theme originating from the first papers dedicated to RQI (see, e.g., Refs. [60, 91, 96, 158, 159]) is the observer dependence of entanglement.

In a series of works [8, 9, 12, 55, 56, 62, 80, 81, 96, 111, 117, 150, 151, 188, 189] this relativity of entanglement was first investigated for inertial observers. The preliminary conclusion drawn from these papers is the following: The entanglement between internal degrees of freedom, such as spin and momentum, in systems with a fixed number of relativistic particles depends on the chosen inertial frame. However, it remains unclear, whether this mathematical observation can be tested in any experiment, since spin measurements are not independent of the particle momenta [171, 172]. In particular, investigations concerning the choice of relativistic spin operator are still a source of scientific debate [22, 52–54, 153, 173].

In parallel to the studies of Lorentz symmetry of entanglement a second branch of RQI was developed for the investigation of the effects of non-uniform motion [2, 11, 41, 85, 91, 133] and spacetime curvature [18, 90, 133–136] on the resources and protocols of quantum information processing (see Ref. [10] for a recent review). Especially the

studies of non-inertial motion established a close connection between RQI and effects of quantum field theory on curved spacetimes (see Ref. [30] for an introduction), such as the *Unruh effect* and *Hawking effect* [17, 48]. In this context the effects of the eternal, uniform acceleration of idealized point-like observers on the entanglement between global modes was the paradigm situation of interest. While such a highly simplified toy model served well as a basis to analyze qualitative features of the effects of non-uniform motion on entanglement, it is clear that it cannot be considered to be consistent with any practical situation, see, for instance, the discussion in Ref. [66]. For instance, it was left open if and how the chosen initial states could be prepared or measured for modes with support in the entire spacetime. Additionally, it seems overly restrictive to assume that accelerations need to be kept constant eternally to produce any effects. In spite of their problems the initial toy models were helpful to understand some general features and requirements of relativistic formulations of quantum information tasks.

To overcome the problems of the early models several systems were proposed that allow for localized preparation and measurements while maintaining high flexibility regarding the choice of trajectories in spacetime. One of these approaches is the so called *Unruh–DeWitt detector* [30]. This detector model describes a localized quantum system, such as a harmonic oscillator or two-level system, coupled to the quantum field along a classical trajectory. We shall not discuss the intricacies of this approach here but refer the interested reader to the relevant literature (see, e.g., Ref. [45, 110, 127]). The second major attempt to construct a theoretical description of a quantum system that can serve for the storage, processing, and transmission of quantum information in a relativistic spacetime is to confine the quantum field inside a *cavity*. This simple, yet rich theoretical model has many advantages, one of which is its experimental accessibility. For instance, cavities are well controlled systems in the context of quantum optics, as recognized by the *Nobel Prize in Physics 2012* (see, e.g., Ref. [164]), and they have been extensively studied in connection with the *dynamical Casimir effect* [15, 64, 201]. Consequently, cavities were naturally considered as objects for the rigorous relativistic study of quantum information processing in RQI [44, 66]. Apart from these two systems also other options were proposed, including wave packets [68] and covariant formulations of single particles in curved spacetimes [152]. In this thesis we shall follow the second path to describe the modes of quantum fields that are confined to cavities in relativistic motion by appropriate boundary conditions. An outline of the discussion is provided below.

Following on from the recent successes in identifying appropriate systems for RQI the field has now entered into a new phase —the connection with experiments and ap-

plications. The advances of the research on the mathematical foundations of RQI have been accompanied by breakthroughs in cutting edge experiments, such as the observation of the dynamical Casimir effect [201], or the teleportation over distances where effects of general relativity may become non-negligible [130]. It is thus now possible, and, moreover, feasible for theoretical research in RQI to be tested in Earth-based laboratories [89], which will help to provide insight into effects of space-based experiments, for instance quantum communication between satellites [168].

Additionally, the well-developed tools of RQI are now ready for state-of-the-art applications that open up entirely new directions of research, e.g., *relativistic quantum metrology* [7, (xii)] —the study of high-precision parameter estimation using relativistic settings [17, 67, 108, 109, 170]. Another area that connects to RQI is *analogue gravity* (see Ref. [21] for a review, and Refs. [24, 115, 166, 169, 197, 198] for a selection of recent advances), which aims to simulate quantum effects in curved spacetimes in compact, laboratory-based experimental setups. The techniques of RQI are here able to provide useful criteria for the presence of entanglement to identify crucial signatures of the quantumness of the expected effects.

Outline of the Thesis

This thesis aims at presenting a thorough introduction into the description of cavities as systems for quantum information processing in RQI, and the phenomena originating from this treatment. In particular, we investigate the effects of the non-uniform motion of rigid cavities in Minkowski spacetime on the entanglement between the field modes within the cavity. Several scenarios for the creation and degradation of entanglement, including applications to practical tasks such as a quantum teleportation are discussed. Due to the interdisciplinary nature of RQI, the thesis relies on background knowledge in the fields of quantum information theory, relativity, quantum field theory and quantum optics. For this reason the thesis is partitioned into two parts.

Part I provides the basic concepts that are needed from each of the above-mentioned fields. Chapter 1 introduces fundamental terminology and definitions from *quantum information theory*, focusing on entanglement theory and some simple applications. We then direct our attention to the quantization of *quantum fields in relativistic spacetimes* in Chapter 2, where we also discuss *Bogoliubov transformations*, a crucial concept for this thesis. Readers familiar with the topics covered in either of the first two chapters may skip the corresponding introductory chapters, but should be aware that most of the notation and terminology of the thesis are established there.

With the tools of Chapters 1 and 2 at hand we are in a position to discuss general features of *quantum information theory for quantum fields* in Chapter 3. First we discuss the description of bosonic fields in phase space in the so-called *covariance matrix formalism*. Having established the relevant techniques we further discuss the role of entanglement generation in bosonic quantum fields and we introduce criteria for entanglement resonances that are generalizing the results of *Bruschi et al.* from Ref. [42]. Finally, in the last section of Part I we present the intricacies of quantum information processing in fermionic Fock spaces, based on material published in Ref. [86, (viii)].

Part II, titled *shaking entanglement*, is entirely dedicated to the rigid cavity model that was, in the context of RQI, first developed for bosonic fields by *D. Bruschi, I. Fuentes, and J. Louko* [44] and subsequently generalized to bosonic Gaussian states [83, (vii)] and fermionic fields [87, (iv)] by myself and collaborators. The aim is to give a pedagogical introduction to the model of perfect, rigid cavities in motion and the corresponding effects for quantum entanglement.

Part II is organized as follows. In Chapter 4 the basic model is introduced, i.e., we discuss how bosonic and fermionic quantum fields are confined within *rigid cavities in non-uniform motion* and how generic trajectories can be constructed. This chapter also covers the results for smoothly changing accelerations from Ref. [47] by my collaborators. We continue in Chapter 5 with the *state transformation* of initial Fock states and Gaussian states.

Having set the stage we then proceed to Chapter 6, where we discuss the *entanglement generation* phenomena within the non-uniformly moving cavities. The bipartite case, based on my publications [82, (v)], and [83, (vii)], as well as Ref. [42] by my collaborators, is discussed in detail in Sections 6.1-6.3. The multipartite case, based on [84, (vi)], is finally presented in Section 6.4.

Finally, in Chapter 7 we analyze *entanglement degradation* effects between several cavities in motion, based on the results of Ref. [44] and my publications [87, (iv)] and [89, (ix)]. In particular, we apply the formalism to study the influence on the continuous-variable teleportation protocol between cavities in motion. A scheme to test these predictions in a laboratory-based experiment using superconducting circuits is briefly discussed, before we present the conclusions.

Part I

Elements of Relativistic Quantum Information

Background, Tools & Methods from *Quantum Information*,
Quantum Optics and *Quantum Field Theory*

Basic Concepts in Quantum Information

Naturally, any relativistic study of quantum information procedures requires a formal understanding of the quantities of interest in standard quantum information theory. We will give a brief introduction into the main concepts of quantum information theory, focusing on entanglement theory. In particular, we shall restrict our attention to the concepts needed for the purpose of this thesis and refer the reader to the literature for topics that lie beyond the scope of this review chapter. For a detailed introduction to quantum information theory consult, e.g., Ref. [144].

1.1 Pure & Mixed Quantum States

The essential ingredients for quantum information processing lie in the description of quantum states, and operations (state preparation, manipulation, measurements, etc.) carried out on these states. The notion of “*state*” encompasses our best knowledge of the physical system and can take on various mathematical descriptions.

1.1.1 Pure States

Let us begin with the idealized notion of a *pure state*, where the maximal amount of information about the physical system is available. In other words, a quantum system in a pure state is perfectly controlled and it is described by a state vector ψ in a *Hilbert space* \mathcal{H} .

Definition 1.1. *A Hilbert Space \mathcal{H} is a vector space over the field \mathbb{C} (or \mathbb{R}) equipped with an inner product $\langle \cdot | \cdot \rangle$. In addition, a Hilbert space is required to be complete with respect to the norm induced by the inner product.*

The inner product $\langle \cdot | \cdot \rangle$ satisfies $\langle \phi | \psi \rangle = \langle \psi | \phi \rangle^*$, where $\psi, \phi \in \mathcal{H}$. It is (*anti*-)linear

in the (first) second argument, i.e.,

$$\langle c_1\phi_1 + c_2\phi_2 \mid \psi \rangle = c_1^* \langle \phi_1 \mid \psi \rangle + c_2^* \langle \phi_2 \mid \psi \rangle, \quad (1.1a)$$

$$\langle \phi \mid c_1\psi_1 + c_2\psi_2 \rangle = c_1 \langle \phi \mid \psi_1 \rangle + c_2 \langle \phi \mid \psi_2 \rangle, \quad (1.1b)$$

where $c_{1,2} \in \mathbb{C}$, $\phi_{1,2}, \psi_{1,2} \in \mathcal{H}$, and the asterisk denotes complex conjugation. The inner product on \mathcal{H} is further *positive semi-definite*, i.e., $\langle \psi \mid \psi \rangle \geq 0$, with equality if and only if $\psi = 0$. The reflexivity of the Hilbert space, i.e., \mathcal{H} coincides with its (continuous) dual space, allows us to employ the so-called *Dirac notation*, that is, we write vectors in \mathcal{H} as $|\psi\rangle$, while the elements of the (continuous) dual Hilbert space \mathcal{H}^* are denoted as $\langle\psi| = |\psi\rangle^\dagger$. We further require physical states to be normalized, such that $\langle\psi|\psi\rangle = 1$.

We can then consider (bounded) linear operators, i.e., $A : |\psi\rangle \mapsto |\phi\rangle = A|\psi\rangle$, on such a Hilbert space, where the adjoint operator A^\dagger is defined by the relation $\langle A^\dagger\phi \mid \psi \rangle = \langle \phi \mid A\psi \rangle$. Operators that satisfy $A^\dagger|_{D(A)} = A$, with domains $D(A^\dagger) \supseteq D(A)$, are called *Hermitean*. Such operators represent physical observables, for instance, the energy of the quantum system. The eigenvalues of these operators are real and they correspond to possible outcomes of individual measurements, in which the state is projected onto the corresponding eigenstates. The expectation values

$$\langle A \rangle_\psi = \langle \psi \mid A \mid \psi \rangle, \quad (1.2)$$

which represent averaged measurement outcomes, are real as well. It can be easily seen that the projection $|\psi\rangle\langle\psi|$ into the state $|\psi\rangle$ is such a Hermitean operator. Operators U that satisfy $U^\dagger = U^{-1}$ are called *unitary* and leave the inner product invariant, $\langle U\phi \mid U\psi \rangle = \langle \phi \mid \psi \rangle$. Operations such as rotations and the dynamics of closed systems are encoded in unitaries.

An interesting feature of quantum theory is the fact that a quantum system in a pure state can be in a coherent superposition of states that correspond to different possible measurement outcomes for a given observable. For instance, the system may be in a superposition of different energy eigenstates. This *superposition principle* has far-reaching conceptual consequences, for instance for interference effects or for the notion of entanglement, see Section 1.2.

1.1.2 Mixed States

In practice the knowledge about the quantum state produced in a given preparation scheme is not perfect — one typically does not know for sure which pure state a quantum system is in. Instead of a single pure state one needs to consider an ensemble of

pure states, weighted with their relative probabilities. The appropriate descriptions for these *mixed states* are density operators ρ that we can write as convex sums of projectors on pure states, i.e.,

$$\rho = \sum_i p_i |\psi_i\rangle\langle\psi_i|, \quad (1.3)$$

where $\sum_i p_i = 1$, and the real weights p_i satisfy $0 \leq p_i \leq 1$. The operators of Eq. (1.3), also called density matrices, are *Hermitian* operators on the Hilbert space \mathcal{H} of pure states. They are *normalized*, i.e., $\text{Tr}(\rho) = \sum_i \langle\psi_i|\rho|\psi_i\rangle = 1$, where $\{|\psi_i\rangle\}$ is a complete orthonormal basis (CONB) of \mathcal{H} , satisfying $\sum_i |\psi_i\rangle\langle\psi_i| = \mathbb{1}$, and $\langle\psi_i|\psi_j\rangle = \delta_{ij}$. Furthermore, density operators are *positive semi-definite*, $\rho \geq 0$, which means that their eigenvalues are non-negative. The decomposition of ρ in Eq. (1.3) into a pure state ensemble is not unique, but can always be chosen such that the $|\psi_i\rangle$ form a CONB.

The expectation value of Eq. (1.2) can readily be generalized to mixed states by considering a weighted average of the expectation values of a complete, orthonormal ensemble of pure states, $\sum_i p_i \langle\psi_i|A|\psi_i\rangle$. By inserting the identity in terms of the same CONB and writing ρ in the decomposition of Eq. (1.3) one naturally arrives at

$$\langle A \rangle_\rho = \text{Tr}(A\rho). \quad (1.4)$$

The trace operation can further be used to define an inner product $(\cdot, \cdot)_{\text{HS}}$, via

$$(\rho, \sigma)_{\text{HS}} = \text{Tr}(\rho^\dagger\sigma), \quad (1.5)$$

which promotes the space of the density operators to a Hilbert space, the so-called *Hilbert-Schmidt space*, which we are also going to denote as \mathcal{H} in a slight abuse of notation. Every pure state is trivially represented in this space through its projector, for which $\rho^2 = \rho$, whereas this is not the case for any mixed state that cannot be represented by a single state vector. This fact can be used to quantify the *mixedness* of — the lack of knowledge about — a given density operator via the *linear entropy* $S_L(\rho)$

Definition 1.2. *The linear entropy $S_L(\rho)$ of a density matrix ρ is defined as*

$$S_L(\rho) := 1 - \text{Tr}(\rho^2).$$

The linear entropy is bounded, i.e., $0 \leq S_L(\rho) \leq 1 - \frac{1}{d}$, where $d = \dim(\mathcal{H})$, and it can be normalized by a factor $\frac{d}{d-1}$ if desired. It vanishes only for pure states, while it is strictly greater than zero for mixed states. The upper bound $(1 - \frac{1}{d})$ is attained for the maximally mixed state $\rho_{\text{mix}} = \frac{1}{d}\mathbb{1}_d$. Another conventional measure for the mixedness is the *von Neumann entropy* S_{vN} , to which S_L is a linear approximation.

Definition 1.3. The von Neumann entropy $S_{\text{vN}}(\rho)$ of a density matrix ρ is given by

$$S_{\text{vN}}(\rho) = -\text{Tr}(\rho \log(\rho)).$$

The basis of the logarithm in Definition 1.3 is often chosen to be 2, but here we are going to use the natural logarithm and denote it as “ln” in the following. We can write S_{vN} in terms of the eigenvalues λ_i of the density operator ρ , i.e.,

$$S_{\text{vN}}(\rho) = -\sum_i \lambda_i \ln(\lambda_i), \quad (1.6)$$

from which it can be seen that S_{vN} is the straightforward generalization of the classical *Shannon entropy*. As before, the von Neumann entropy is strictly zero if, and only if, the state is pure, while the largest value $\ln d$ is obtained for the maximally mixed state. Both S_L and S_{vN} are invariant under unitary transformations on \mathcal{H}

$$S_{L,\text{vN}}(U\rho U^\dagger) = S_{L,\text{vN}}(\rho). \quad (1.7)$$

The von Neumann entropy will be of further interest to us in the context of entanglement detection in Section 1.3. For now we shall turn our attention to a useful parametrization of density matrices, the *Bloch decomposition*. For a single *qubit*, a two-dimensional quantum system with Hilbert space \mathbb{C}^2 , a general mixed state may be written as

$$\rho = \frac{1}{2}(\mathbb{1}_2 + a^i \sigma_i), \quad (1.8)$$

where $a^i = \text{Tr}(\rho \sigma_i) \in \mathbb{R}$ with $a^i a_i \leq 1$ ($i = 1, 2, 3$), and we are using the *Einstein summation convention* for indices that are repeated once as superscript and once as subscript. The σ_i are the usual, traceless, Hermitean *Pauli matrices*

$$\sigma_1 = \begin{pmatrix} 0 & 1 \\ 1 & 0 \end{pmatrix}, \quad \sigma_2 = \begin{pmatrix} 0 & -i \\ i & 0 \end{pmatrix}, \quad \sigma_3 = \begin{pmatrix} 1 & 0 \\ 0 & -1 \end{pmatrix}. \quad (1.9)$$

The a^i can be interpreted as the components of a vector $\mathbf{a} = (a^i) \in \mathbb{R}^3$, the *Bloch vector*, whose length indicates the mixedness of the state. For $|\mathbf{a}| = 1$ the state is pure and lies on the surface of the so-called *Bloch sphere*, while all $|\mathbf{a}| < 1$ describe mixed states within the sphere. The state parametrization of Eq. (1.8) is very descriptive for spin- $\frac{1}{2}$ systems, where the direction of the vector $\mathbf{a} = (a^i)$ represents the spin orientation of the state ρ . The Bloch decomposition can be extended to describe single quantum systems of (finite) dimension d , called *qudits*, see Ref. [28], but we shall instead turn our attention to a generalization for composite systems that is usually referred to as

the *generalized Bloch decomposition* (also called *Fano decomposition* [76]). Any two-qubit density operator on a Hilbert space $\mathbb{C}^2 \otimes \mathbb{C}^2$ can be written as

$$\rho = \frac{1}{4}(\mathbb{1}_4 + a^i \sigma_i \otimes \mathbb{1}_2 + b^i \mathbb{1}_2 \otimes \sigma_i + t^{ij} \sigma_i \otimes \sigma_j). \quad (1.10)$$

In this decomposition $\mathbf{a} = (a^i)$ and $\mathbf{b} = (b^i)$ are the Bloch vectors of the first and second qubit, respectively, while the $t^{ij} = \text{Tr}(\rho \sigma_i \otimes \sigma_j)$ are the components of the *correlation matrix* $t[\rho]$, which encodes correlations between the two qubits. We will encounter this object again in Section 1.5.2 where it plays a role for the violation of *Bell inequalities*.

1.2 Entanglement of Pure States

Let us now turn to a more general description of composite quantum systems and their correlations. In particular, we are going to study a property called *entanglement*, a fundamental resource for quantum information tasks which is a simple consequence of applying the *superposition principle* (see p. 10) of quantum mechanics to composite systems. A pedagogical review of this topic can be found in Ref. [50], while a more extensive review is given in Ref. [107]. In this section the case of bipartite pure states is discussed, before we continue with bipartite mixed states in Section 1.3 and multipartite systems in Section 1.4. The chapter will be concluded with a brief look at applications of entanglement, such as *Bell inequalities* and *quantum teleportation* in Section 1.5.

Let us consider two Hilbert spaces, \mathcal{H}_A and \mathcal{H}_B , with dimensions $\dim(\mathcal{H}_A) = d_A$ and $\dim(\mathcal{H}_B) = d_B$, and bases $\{|\psi_i\rangle_A\}$ and $\{|\psi_j\rangle_B\}$, respectively. Any *bipartite pure state* of the composite Hilbert space $\mathcal{H}_{AB} = \mathcal{H}_A \otimes \mathcal{H}_B$, with $d_{AB} = \dim(\mathcal{H}_{AB}) = d_A d_B$, can be written in terms of these bases as

$$|\psi\rangle_{AB} = \sum_{i,j=1}^{d_A, d_B} c_{ij} |\psi_i\rangle_A \otimes |\psi_j\rangle_B, \quad (1.11)$$

such that the coefficients $c_{ij} \in \mathbb{C}$ satisfy $\sum_{i,j} |c_{ij}|^2 = 1$. However, for pure, bipartite states there exists a more economical choice of basis—the *Schmidt basis*—than the d_{AB} tensor products of the basis vectors of the individual Hilbert spaces. Let us formulate this in the *Schmidt decomposition theorem*, originally formulated in Ref. [177].

Theorem 1.1. *For every pure bipartite state $|\psi\rangle_{AB}$ there exist orthonormal bases*

$\{|\chi_i\rangle_A \in \mathcal{H}_A\}$ and $\{|\chi_i\rangle_B \in \mathcal{H}_B\}$, the Schmidt-bases, such that

$$|\psi\rangle_{AB} = \sum_{i=1}^{d_{\min}} \sqrt{p_i} |\chi_i\rangle_A \otimes |\chi_i\rangle_B,$$

where $1 \leq d_{\min} \leq \min(d_A, d_B)$, and the real Schmidt numbers $p_i \geq 0$

satisfy $\sum_i p_i = 1$.

A proof of this well-known theorem can be found, for instance, in Ref. [80, p. 30]. For any state there is an optimal decomposition in terms of a minimal number d_{opt} —the *Schmidt rank*—of linearly independent vectors $|\chi_i\rangle_A \otimes |\chi_i\rangle_B$. States of Schmidt rank 1 are called *separable*, while those with $d_{\text{opt}} = \min(d_A, d_B)$ are called *maximally entangled*.

Definition 1.4. *A bipartite pure state $|\psi\rangle_{AB} \in \mathcal{H}_{AB}$ is called separable with respect to the bipartition of \mathcal{H}_{AB} into $\mathcal{H}_A \otimes \mathcal{H}_B$ if it can be written as*

$$|\psi\rangle_{AB} = |\phi\rangle_A \otimes |\chi\rangle_B, \text{ for some } |\phi\rangle_A \in \mathcal{H}_A \text{ and } |\chi\rangle_B \in \mathcal{H}_B.$$

Having established the notion of separability, the definition of entanglement follows from Definition 1.4 by negation.

Definition 1.5. *A state is called entangled, if it is not separable.*

For entangled states, not all information about the total state can be encoded in the states of the subsystems. Consequently, the reduced state density matrices, ρ_A and ρ_B of the subsystems A and B , respectively, are mixed. The reduced states are obtained from the bipartite state ρ_{AB} by partial tracing, i.e.,

$$\rho_A = \text{Tr}_B(\rho_{AB}) = \sum_i (\mathbb{1}_A \otimes \langle \psi_i | _B) \rho_{AB} (\mathbb{1}_A \otimes | \psi_i \rangle_B), \quad (1.12)$$

where $\{|\psi_i\rangle_B\}$ is a CONB of \mathcal{H}_B and similarly $\rho_B = \text{Tr}_A(\rho_{AB})$. For compactness of notation we are going to drop the tensor product symbol, i.e., $|\psi\rangle_A \otimes |\phi\rangle_B = |\psi\rangle |\phi\rangle$ from now on and identify the corresponding subspaces by the ordering of the vectors. It is further convenient to indicate the subspaces operators are acting upon solely by their subscripts and drop any identity operators in a tensor product such that $\mathbb{1}_A \otimes \mathcal{O}_B = \mathcal{O}_B$.

For density operators ρ_{AB} corresponding to pure states $|\psi\rangle_{AB}$ the mixedness of the reductions can be entirely attributed to the entanglement—the quantum correlations—between the subsystems. Moreover, from Theorem 1.1 it can be immediately seen that ρ_A and ρ_B have the same rank and the same non-zero eigenvalues, given by the Schmidt rank and the Schmidt numbers p_i , respectively. Consequently, any function of these eigenvalues alone, in particular the (von Neumann) entropy, takes on the same value for either reduced state. This allows us to unambiguously quantify the entanglement of any bipartite pure state by the so-called *entropy of entanglement*.

Definition 1.6. *The entropy of entanglement \mathcal{E} of a bipartite pure state $|\psi\rangle_{AB}$ is defined as the von Neumann entropy S_{vN} of its reductions ρ_A and ρ_B ,*

$$\mathcal{E}(|\psi\rangle_{AB}) = S_{\text{vN}}(\rho_A) = S_{\text{vN}}(\rho_B).$$

Paradigmatic examples for entangled pure states are the two-qubit *Bell states*

$$|\phi^\pm\rangle = \frac{1}{\sqrt{2}}\left(|0\rangle|0\rangle \pm |1\rangle|1\rangle\right), \quad (1.13a)$$

$$|\psi^\pm\rangle = \frac{1}{\sqrt{2}}\left(|0\rangle|1\rangle \pm |1\rangle|0\rangle\right), \quad (1.13b)$$

where $|0\rangle$ and $|1\rangle$ form a basis in \mathbb{C}^2 . The Bell states, on the other hand, form a complete basis of $\mathbb{C}^2 \otimes \mathbb{C}^2$. They are further examples of *maximally entangled states*, i.e., pure states for which the reductions have maximal rank, or, in other words, for which the reduced states are maximally mixed.

1.3 Entanglement of Mixed States

For mixed states the notion of separability is somewhat more involved, since it needs to leave the possibility of incoherent mixtures of uncorrelated product states $\rho_A \otimes \rho_B$.

Definition 1.7. A bipartite mixed state $\rho_{AB} \in \mathcal{H}_{AB}$ is called separable with respect to the bipartition of \mathcal{H}_{AB} into $\mathcal{H}_A \otimes \mathcal{H}_B$ if it can be written as

$$\rho_{AB} = \sum_i p_i \rho_A^i \otimes \rho_B^i,$$

for some ensembles $\{\rho_A^i \in \mathcal{H}_A\}$ and $\{\rho_B^i \in \mathcal{H}_B\}$.

As before, a state is called entangled, if it is not separable.

By this definition all separable states can be created using *local operations and classical communication* (LOCC), i.e., any operations restricted to either of the subsystems and classical communication between the corresponding observers, usually referred to as *Alice* and *Bob*. However, in general it is not straightforward to determine whether a given state admits a decomposition of the form of Definition 1.7, but we shall discuss some useful *separability criteria* and *measures of entanglement* in Sections 1.3.1 and 1.3.2, respectively.

1.3.1 Detection of Entanglement

In contrast to the pure state case, it is not unambiguously possible to attribute the mixedness of the subsystems to the overall entanglement. Neither is it conclusive to compute the entropy of entanglement for the pure states in a particular decomposition of ρ_{AB} , since there is no preferred pure state decomposition for any mixed state. Nonetheless, a sufficient (but not necessary) criterium for the presence of bipartite entanglement can be formulated in the following *entropy inequalities*. A state ρ_{AB} is entangled if the entropy of any of the reductions, ρ_A or ρ_B , is larger than the entropy of ρ_{AB} ,

i.e., ρ_{AB} is entangled if

$$S(\rho_{AB}) - S(\rho_A) < 0, \quad (1.14a)$$

$$\text{or } S(\rho_{AB}) - S(\rho_B) < 0, \quad (1.14b)$$

where we have omitted the label for the chosen entropy. A proof for the von Neumann entropy S_{vN} as well as selected other entropy measures can be found in Ref. [190].

Let us now consider a more geometric method for the detection of entanglement—*entanglement witnesses* as in, e.g., Refs. [29, 50]. From Definition 1.7 it can be easily seen that the separable states form a closed, convex subset $\mathcal{S} \subset \mathcal{H}$ of the Hilbert space of states, while all entangled states form the complement. Since any entangled state is represented by a single point in \mathcal{H} , which is trivially a compact, convex subset of \mathcal{H} , the *Hahn-Banach theorem* of functional analysis allows to separate this point from \mathcal{S} by a hyperplane, see Ref. [167, p. 75]. Such a hyperplane can be interpreted as a linear functional on \mathcal{H} , realized by a Hermitean operator. Let us phrase this in the following *entanglement witness theorem*, which was introduced in Ref. [103].

Theorem 1.2. *For any entangled state ρ there exists an entanglement witness, i.e., a Hermitean operator \mathcal{O}_W , such that $(\mathcal{O}_W, \rho)_{\text{HS}} < 0$, while $(\mathcal{O}_W, \sigma)_{\text{HS}} \geq 0$ for all separable states $\sigma \in \mathcal{S}$.*

Although this does not directly supply an operational criterion for the detection of entanglement many operational criteria can be considered special cases of the entanglement witness theorem, see, e.g., Ref. [27]. One example is the *Clauser-Horne-Shimony-Holt (CHSH) criterion* for two qubits, that we are going to discuss in Section 1.5.2.

In a similar approach it was suggested by A. Peres in Ref. [157] to use the *partial transposition* $\mathbb{1}_A \otimes T_B$ to detect entanglement. Since the transposition preserves the positivity of operators, it is easy to see from Definition 1.7 that separable states remain positive under partial transposition. In Ref. [103] M., R., and P. Horodecki were then able to use Theorem 1.2 to prove that this condition for separability is sufficient only as long as $d_{AB} = d_A d_B \leq 6$. Let us phrase this in the following theorem, known as *positive partial transpose (PPT) criterion*, or *Peres-Horodecki criterion*.

Theorem 1.3. *A bipartite state $\rho_{AB} \in \mathbb{C}^2 \otimes \mathbb{C}^2$ or $\mathbb{C}^2 \otimes \mathbb{C}^3$ is separable if, and only if, the partial transposition (see p. 19) of ρ_{AB} is positive, i.e.,*

$$\rho_{AB}^{T_B} = (\mathbb{1}_A \otimes T_B)\rho_{AB} \geq 0.$$

The subsystems A and B in the PPT theorem can of course be exchanged. We see that for two-qubit states, or states of one qubit and one qutrit, all entangled states have a *negative partial transpose* (NPT), while in general there exist entangled states with positive partial transpose, called *bound entangled* states. It was shown in Ref. [104] that these PPT entangled states are undistillable, i.e., it is not possible to obtain any pure, maximally entangled states from n copies of the given mixed state by LOCC, but we shall not be further concerned with entanglement distillation in this thesis (see, e.g., Ref. [50] for a pedagogical review of this topic). However, we shall return to the PPT criterion for the construction of useful entanglement measures —*negativity measures*—in Section 1.3.2, and, in the context of bosonic Gaussian states in Section 3.1.4.

1.3.2 Measures of Entanglement

As we have seen, it is not trivial to establish criteria for the separability of a given mixed state. Consequently, there are also many issues in the definition of mixed state entanglement measures, and many candidates have been proposed to suit the plethora of requirements. An extensive review of the various available entanglement measures, entanglement monotones, and their connections can be found in Ref. [162]. For the purpose of this thesis we shall restrict the discussion to two representatives of these measures, the *entanglement of formation* and related *concurrence*, followed by an overview of the so-called *negativity measures*. Let us begin with a list of requirements which are usually imposed on (bipartite) *entanglement measures* $E(\rho)$.

Definition 1.8. *An entanglement measure is a map from density operators ρ to the non-negative real numbers $E(\rho) \in \mathbb{R}_0^+$ that satisfies:*

- (i) $E(\rho) = 0$ for all separable states $\rho \in \mathcal{S}$.
- (ii) $E(\rho)$ is non-increasing under LOCC.

It is sometimes customary in the literature to add further requirements for genuine entanglement measures, the most popular of which are continuity, reduction to the entropy of entanglement (recall Definition 1.6) for pure states, i.e., $E(|\psi\rangle\langle\psi|) = \mathcal{E}(|\psi\rangle)$, convexity, i.e., $E(\sum_i p_i \rho_i) \leq \sum_i p_i E(\rho_i)$, and (full) additivity $E(\rho_{AB} \otimes \rho_{CD}) = E(\rho_{AB}) + E(\rho_{CD})$. In the case of such additional requirements for a genuine entanglement measure, Definition 1.8 is said to define an *entanglement monotone*. For our purposes it will suffice to introduce the above convention. It should also be noted that requirement (ii) implies that entanglement is invariant under *local unitary operations* $U_A \otimes U_B$ since the corresponding inverse transformations are also LOCC.

Convex Roof Constructions

A mathematically intuitive way of generalizing the entropy of entanglement \mathcal{E} of Definition 1.6 to mixed state ensembles is the *entanglement of formation* $E_F(\rho)$ introduced in Ref. [26].

Definition 1.9. The entanglement of formation $E_F(\rho)$ of a bipartite state ρ is given by

$$E_F(\rho) := \inf_{\{(p_i, |\psi_i\rangle)\}} \sum_i p_i \mathcal{E}(|\psi_i\rangle),$$

where the infimum is taken over all pure state ensembles $(p_i, |\psi_i\rangle)$

that realize $\rho = \sum_i p_i |\psi_i\rangle\langle\psi_i|$.

The entanglement of formation constitutes an entanglement measure in the sense of Definition 1.8 and is an example for a so-called *convex roof construction*. Therefore it is convex by construction and trivially reduces to the von Neumann entropy for pure states. In spite of the elegance of its formal definition, the entanglement of formation is in general not a practical measure of entanglement, since the minimization in Definition 1.9 cannot be carried out in a closed form for arbitrary systems. However, for some situations that exhibit high symmetry, or are specifically simple, this calculation can be performed analytically. In particular, for the simple case of two qubits, a closed expression is provided by (see Refs. [26, 205])

$$E_F(\rho) = h\left(\frac{1 + \sqrt{1 - C^2(\rho)}}{2}\right), \quad (1.15)$$

where $h(p)$ is the *Shannon entropy* $H(\{p, 1-p\})$ of the Bernoulli distribution $\{p, 1-p\}$,

$$h(p) = -p \ln(p) - (1-p) \ln(1-p), \quad (1.16)$$

and $C(\rho)$ is the so-called (*Wootters*) *concurrence* for two-qubits

$$C(\rho) = \max\{0, \sqrt{\lambda_1} - \sqrt{\lambda_2} - \sqrt{\lambda_3} - \sqrt{\lambda_4}\}. \quad (1.17)$$

The $\lambda_i \in \mathbb{R}_0^+$ are the eigenvalues of the matrix $\rho(\sigma_2 \otimes \sigma_2)\rho^*(\sigma_2 \otimes \sigma_2)$ in decreasing order, $\lambda_1 \geq \lambda_{2,3,4}$. Since the entanglement of formation is a monotonous function of the concurrence only, the latter is sometimes used instead of E_F even though it derives its meaning via its relation to E_F . In Section 3.1.4 we shall encounter another simple situation, symmetric two-mode Gaussian states on infinite dimensional Hilbert spaces, for which the entanglement of formation can be computed explicitly as well [95]. The quantity $C^2(\rho) = \tau(\rho)$, where $C(\rho)$ is the two-qubit concurrence of Eq. (1.17), can be defined as the convex roof construction over the linear entropy [148], i.e.,

$$\tau(\rho_{AB}) := \inf_{\{(p_i, |\psi_i\rangle)\}} \sum_i p_i S_L(\text{Tr}_B[|\psi_i\rangle\langle\psi_i|]), \quad (1.18)$$

in complete analogy to the entanglement of formation in Definition 1.9. The definition of this measure—the *tangle*—now naturally extends to two systems of arbitrary dimensions. Beyond two qubits the tangle is generally an upper bound to — not identical to — the square of the corresponding concurrence (see, e.g., Ref. [147]). Nonetheless, a very useful feature of the tangle is that it captures the so-called *monogamy of entanglement*. For three qubits A , B and C the tangle satisfies the *Coffman-Kundu-Wootters* (CKW) inequality

$$\tau(\rho_{AB}) + \tau(\rho_{AC}) \leq \tau(\rho_{A(BC)}), \quad (1.19)$$

where $\rho_{AB} = \text{Tr}_C(\rho_{ABC})$, $\rho_{AC} = \text{Tr}_B(\rho_{ABC})$ and $\tau(\rho_{A(BC)})$ is the tangle with respect to the bipartition $A|BC$. The inequality (1.19) was proven in Ref. [59], and subsequently extended to an arbitrary number of qubits in Ref. [148]. Loosely speaking, the monogamy of entanglement means that a given qubit cannot be maximally entangled with more than one qubit at a time. Any gain in entanglement between qubits A and C must be compensated by a reduction in entanglement between A and B . The monogamy inequalities using the tangle do not generally hold beyond qubits (see, e.g., Ref. [149]), but possible extensions to qudits relying on other measures of entanglement have been proposed [119], for instance squashed entanglement satisfies monogamy restraints in arbitrary dimensions [120]. Monogamy can further be restored for Gaussian states in infinite dimensional systems [100].

Despite the useful properties of the convex roof measures, it is more desirable for our purposes here to consider easily computable measures of entanglement, one of which we shall turn to now.

NPT Entanglement

The *negativity* measures, based on the PPT criterion (Theorem 1.3) and introduced in Ref. [194], quantify —loosely speaking—how much a given state fails to be positive after partial transposition. To implement the partial transposition we write a general bipartite mixed state $\rho \in \mathcal{H}_{AB}$ in terms of local bases $\{|i\rangle \in \mathcal{H}_A\}$ and $\{|j\rangle \in \mathcal{H}_B\}$ as

$$\rho = \sum_{i,i',j,j'} \rho_{ij,i'j'} |i\rangle\langle i'| \otimes |j\rangle\langle j'|. \quad (1.20)$$

The partial transposition of ρ_{AB} is then obtained by exchanging the indices on the operators on one of the subspaces,

$$\rho^{T_B} = (\mathbb{1}_A \otimes T_B)\rho = \sum_{i,i',j,j'} \rho_{ij,i'j'} |i\rangle\langle i'| \otimes |j'\rangle\langle j|. \quad (1.21)$$

Definition 1.10. The negativity $\mathcal{N}(\rho)$ of a bipartite state ρ is given by

$$\mathcal{N}(\rho) := \frac{1}{2} \sum_i (|\lambda_i| - \lambda_i),$$

where the $\lambda_i \in [-\frac{1}{2}, 1]$ are the eigenvalues of ρ^{TB} .

In other words, the negativity is the modulus of the sum of the, at most [165, 174], $(d_A - 1)(d_B - 1)$ negative eigenvalues of the partial transposition, where as usual, $d_A = \dim(\mathcal{H}_A)$ and $d_B = \dim(\mathcal{H}_B)$. Alternatively, the negativity can be defined in terms of the trace norm $\|\cdot\|_1$, i.e., $\mathcal{N}(\rho) = \frac{1}{2}(\|\rho^{TB}\|_1 - 1)$, where $\|\rho\|_1 = \text{Tr} \sqrt{\rho^\dagger \rho}$. By Definition 1.8 the negativity is an entanglement measure, and is further convex, but the negativity does not reduce to the entropy of entanglement for pure states and it is not additive. The latter issue can be amended by defining the so-called *logarithmic negativity* $E_{\mathcal{N}}$ as

$$E_{\mathcal{N}}(\rho) = \log_2 \|\rho^{TB}\|_1 = \log_2(2\mathcal{N}(\rho) + 1), \quad (1.22)$$

which is additive, but still does not reduce to the entropy of entanglement in the pure case, and it is not convex [161]. Clearly, because of their relation to Theorem 1.3 neither of the negativities is able to capture bound entanglement. Nonetheless, the negativity measures are widely used because of their computational simplicity. Finally, we can relate the entanglement of formation and the negativity measures. It was shown in Ref. [192] that for a two-qubit state with given concurrence C [recall Eq. (1.17)] the negativity is bounded by

$$\frac{1}{2}(\sqrt{(1-C)^2 + C^2} - (1-C)) \leq \mathcal{N} \leq \frac{1}{2}C. \quad (1.23)$$

We will use the measures described above to quantify the bipartite entanglement between modes of quantum fields. However, in such scenarios we will naturally encounter also systems of more than two modes. It is therefore of interest to take a brief look at entanglement in multipartite systems, as we will do in the next section.

1.4 Multipartite Entanglement

In a multipartite system with a fixed number of subsystems A, B, \dots, N the entanglement structure is much more involved than in the bipartite case, but also much richer. In general these structures are not well understood beyond three qubits, see, e.g., Refs. [50, 92, 98], but already in the tripartite case several inequivalent classes of multipartite entanglement are known. We shall mainly be concerned with the detection of *genuine multipartite entanglement* (GME), discussed in Section 1.4.2, but first we are going to introduce this concept.

1.4.1 Genuine Multipartite Entanglement

We can start as before by defining N -partite states in $\mathcal{H}_{AB\dots N} = \mathcal{H}_A \otimes \mathcal{H}_B \otimes \dots \otimes \mathcal{H}_N$ that do not contain any entanglement.

Definition 1.11. *A pure, N -partite state $|\psi\rangle_{AB\dots N} \in \mathcal{H}_{AB\dots N}$ is called fully separable, if it can be written as $|\psi\rangle_{AB\dots N} = |\phi_A\rangle \otimes |\phi_B\rangle \otimes \dots \otimes |\phi_N\rangle$, for some $|\phi_A\rangle \in \mathcal{H}_A$, $|\phi_B\rangle \in \mathcal{H}_B$, \dots , $|\phi_N\rangle \in \mathcal{H}_N$.*

The state is called n -separable if it can be written as a tensor product with respect to some partition of $\mathcal{H}_{AB\dots N}$ into $n \leq N$ subsystems.

For $n = 2$, i.e., for pure bi-separable states, one essentially obtains the pure, bipartite case where the two subsystems contain additional structure. While Definition 1.11 is straightforward, it is nonetheless involved to test whether a given state is n -separable. In contrast to the bipartite case only very specific states admit a generalized Schmidt decomposition (see Ref. [156]). To check a general given state for n -separability thus requires to compute the reductions of all the subsystems and verify that they are pure. We shall therefore define *genuine multipartite entanglement* for pure states in the following way:

Definition 1.12. *A pure state $|\psi\rangle_{AB\dots N}$ is called genuinely N -partite entangled if it is not bi-separable in $\mathcal{H}_{AB\dots N}$.*

For mixed states we simply extend the notion of n -separability to the convex sum.

Definition 1.13. *A mixed state $\rho_{AB\dots N}$ is called n -separable if it admits at least one decomposition into a convex sum of pure n -separable states.*

Conversely, a mixed state $\rho_{AB\dots N}$ is genuinely N -partite entangled if it is not bi-separable ($n = 2$) in $\mathcal{H}_{AB\dots N}$.

While these definitions seem straightforward, let us consider some of their implications. Firstly, if a given state is n -separable, then it is automatically also n' -separable for all $n' < n$. The sets \mathcal{S}_n of n -separable states are thus convexly nested in each other, i.e., $\mathcal{S}_n \subset \mathcal{S}_{n-1} \subset \dots \subset \mathcal{S}_1$. What complicates matters is the fact that the individual states in the decomposition of a bi-separable mixed state into bi-separable pure states need not be separable with respect to the same bi-partitions.

Therefore, a given mixed state can be n -separable, even though it is entangled with respect to specific partitions. This feature makes it rather difficult to determine whether a given state is n -separable. However, as we will discuss shortly, one can construct witness inequalities whose violation detects GME [92].

1.4.2 Detection of Genuine Multipartite Entanglement

For the detection of genuine multipartite entanglement a seemingly mundane property of n -separable pure states can be used—permutational symmetry in the exchange of corresponding subsystems of two copies of the state. Let us start with two copies, $|\psi\rangle_{A_1 A_2}$ and $|\psi\rangle_{B_1 B_2}$, of a bi-separable pure state $|\psi\rangle_{1,2} = |\phi\rangle_1 |\chi\rangle_2$, where A_i and B_i ($i = 1, 2$) label the i -th subsystem of two otherwise identical copies A and B , respectively. The subsystems A_2 and B_2 of the first and second copy may be freely exchanged,

$$\pi_{(A_1|A_2)_2} |\psi\rangle_{A_1 A_2} \otimes |\psi\rangle_{B_1 B_2} = |\psi\rangle_{A_1 B_2} \otimes |\psi\rangle_{B_1 A_2}, \quad (1.24)$$

where we have defined the permutation operator $\pi_{(A_1|A_2)_2}$, that exchanges the second subsystem of the two copies with respect to the partition $(A_1|A_2)$. This statement trivially extends to multipartite entanglement, i.e., a pure state that is n -separable with respect to a n -partition $\mathbb{P}(n) = (A_1|A_2|\dots|A_n)$ is invariant under permutations $\pi_{\mathbb{P}(n)_i}$, i.e., exchanges of the i -th subsystems A_i and B_i of the two copies. Using this statement the following theorem was formulated in Ref. [92].

Theorem 1.4. *Every N -partite, n -separable state ρ satisfies*

$$\left(\langle \Phi | \rho^{\otimes 2} \prod_i \pi_{\mathbb{P}(n)_i} | \Phi \rangle \right)^{\frac{1}{2}} \leq \sum_{\mathbb{P}(n)} \left(\prod_{i=1}^n \langle \Phi | \pi_{\mathbb{P}(n)_i}^\dagger \rho^{\otimes 2} \pi_{\mathbb{P}(n)_i} | \Phi \rangle \right)^{\frac{1}{2n}},$$

for every fully separable $(2N)$ -partite pure state $|\Phi\rangle$.

Proof. Let us quickly sketch the proof for this inequality. If ρ is a pure, N -partite, n -separable state, then it must be n -separable with respect to one of the n -partitions $\mathbb{P}(n)$ in the sum on the right hand side. The corresponding term of the sum over all $\mathbb{P}(n)$ then cancels with the left hand side since the fully separable state $|\Phi\rangle$ can trivially be written as a tensor product of two N -partite states, i.e., $|\Phi\rangle = |\Phi_A\rangle |\Phi_B\rangle$, and $\rho = |\psi\rangle\langle\psi|$ is pure. The remaining terms on the right hand side are products of $(2n)$ th roots of diagonal entries ρ_{kk} of the density operator ρ , and therefore strictly positive. Thus the inequality is trivially satisfied. To extend the proof to mixed states one simply notes that the left hand side is the modulus—a convex function—of a density matrix

element ρ_{kl} , while the $(2n)$ th roots on the right hand side are concave functions of the matrix elements, i.e.,

$$\left| \sum_i p_i \rho_{kl}^i \right| \leq \sum_i p_i |\rho_{kl}^i|, \quad (1.25a)$$

$$\left(\sum_i p_i \rho_{kk}^i \right)^{\frac{1}{2n}} \geq \sum_i p_i \left(\rho_{kk}^i \right)^{\frac{1}{2n}}, \quad (1.25b)$$

which concludes the proof. □

We will use detection inequalities of this type to study GME between modes of quantum fields in cavities in Section 6.4.

1.5 Applications of Entanglement

1.5.1 The EPR Paradox

We have previously introduced the mathematical notion of entanglement—establishing that the superposition principle, applied to composite systems, gives rise to this intriguing property. But one might ask what distinguishes entanglement from other correlations. For this purpose, let us turn to the *EPR thought experiment* formulated by *Albert Einstein, Boris Podolsky, and Nathan Rosen* (EPR) in 1935. In their seminal paper “*Can Quantum-Mechanical Description of Physical Reality Be Considered Complete?*” (Ref. [73]) they used an entangled state to argue that quantum theory does not meet their criteria of *locality, reality, and completeness*.

- (i) *Locality*: There are no instantaneous interactions between distant physical systems.
- (ii) *Realism*: If the value of a physical quantity can be predicted with certainty without disturbing the system, then this quantity corresponds to an *element of physical reality*.
- (iii) *Completeness*: A theory is *complete* if every element of physical reality is assigned to a corresponding element in the theory.

In short, their argument asserts that the existence of maximally entangled states in quantum mechanics gives rise to elements of reality that are not accounted for in quantum mechanics, which, according to EPR, is therefore incomplete. In spite of the far-reaching conceptual consequences of this paradox it was mostly ignored or considered to be a purely philosophical problem. In particular the reply by *Niels Bohr* in Ref. [33] supported this point of view. It was not until 1957 that the problem pointed out by EPR was appreciated, when *David Bohm* and *Yakir Aharonov* published their version [32] of

the paradox, which we shall present here using the language of quantum information theory.

Let us consider two spatially distant qubits, A and B , in the Bell state $|\psi^-\rangle_{AB}$ of Eq. (1.13b). If both subsystems are measured in the basis $\{|0\rangle, |1\rangle\}$ then the measurement results are always perfectly anti-correlated. In particular, if “0” is measured in subsystem A , then A can predict the outcome of B to be “1” with certainty, endowing this result with physical reality according to requirement (ii) above. However, the same argument can be made for any other single qubit basis such that all of these results should have simultaneous physical reality. Quantum mechanics on the other hand states that measurements in different bases do not generally commute. Therefore the corresponding results cannot have independent physical reality, which leads to the apparent paradox.

Since it seemed imprudent to remove the requirement for locality, an obvious solution was considered to be to equip quantum mechanics with a set of *hidden variables* that determine the measurement outcomes, thus completing the theory in the sense of requirement (iii). Those “completions” of quantum mechanics in terms of so-called *hidden variable theories* (HVTs) are severely constrained by no-go theorems such as *Bell’s theorem* [19] or *contextuality* arguments (see Refs. [121, 139, 155]), some of which we are going to discuss in Section 1.5.2.

1.5.2 Bell Inequalities & Non-Locality

In 1964 *John Stewart Bell* elevated the discussion of the EPR paradox to a new level. He formulated an inequality that allowed to decide experimentally whether or not completeness in the sense of the EPR argument can be achieved by a local HVT. We will not consider Bell’s original inequality here, but instead consider a more easily testable version—the *Clauser-Horne-Shimony-Holt* (CHSH) *inequality* introduced in Ref. [58]. However, irrespectively of the specific type of *Bell inequality* that is being tested we can formulate Bell’s theorem in the following way.

Theorem 1.5. *All HVTs that are local and realistic in the sense of the EPR requirements (i) and (ii), respectively, are incompatible with the predictions of quantum mechanics for the outcome of certain experiments.*

Let us put this theorem into a mathematical framework in terms of the CHSH inequality. Let us consider two distant parties, Alice and Bob, who are measuring dichotomic quantities $A(\mathbf{a})$ and $B(\mathbf{b})$, respectively, where $\mathbf{a} = (a^i)$ and $\mathbf{b} = (b^i)$ cor-

respond to the measurement settings. To implement the reality requirement (ii) of the HVT one can assume that the measurement results also depend on some set λ of hidden parameters. The locality assumption (i) simply means that the outcomes $A(B)$ are independent of the measurement settings $\mathbf{b}(\mathbf{a})$ of the other party, i.e., $A(\mathbf{a}, \lambda) = \pm 1, 0$ and $B(\mathbf{b}, \lambda) = \pm 1, 0$, where ± 1 represent successful measurements, while 0 corresponds to failed detections. The expectation value $\langle (\mathbf{a}, \mathbf{b}) \rangle_\lambda$ for the joint measurements of A and B for a hidden variable λ with (normalized) distribution $\rho(\lambda)$ is then given by

$$\langle (\mathbf{a}, \mathbf{b}) \rangle_\lambda = \int d\lambda \rho(\lambda) A(\mathbf{a}, \lambda) B(\mathbf{b}, \lambda). \quad (1.26)$$

We can then formulate Theorem 1.5 in terms of the CHSH inequality [58].

Theorem 1.6. *The expectation values $\langle (\mathbf{a}, \mathbf{b}) \rangle_\lambda$ of a local, realistic theory satisfy*

$$\langle (\mathbf{a}, \mathbf{b}) \rangle_\lambda - \langle (\mathbf{a}, \tilde{\mathbf{b}}) \rangle_\lambda + \langle (\tilde{\mathbf{a}}, \mathbf{b}) \rangle_\lambda + \langle (\tilde{\mathbf{a}}, \tilde{\mathbf{b}}) \rangle_\lambda \leq 2.$$

For a pedagogical proof see, e.g., Ref. [80, pp. 47-48]. For the purpose of checking this theorem in a quantum mechanical computation the CHSH inequality can be reformulated in terms of the following two-qubit observable on $\mathbb{C}^2 \otimes \mathbb{C}^2$,

$$\mathcal{O}_{\text{CHSH}} = a^m \sigma_m \otimes (b^n + \tilde{b}^n) \sigma_n + \tilde{a}^m \sigma_m \otimes (b^n - \tilde{b}^n) \sigma_n, \quad (1.27)$$

where summation over repeated indices is implied, and the σ_n are the Pauli matrices (1.9). The quantum mechanical expectation value of the observable in (1.27) can reach $\langle \mathcal{O}_{\text{CHSH}} \rangle_{\text{QM}} \leq 2\sqrt{2} > 2$, both in theory and in experiment (see, e.g., Ref. [79]), in clear violation of the CHSH inequality. The possible violation of a Bell inequality by a given state, often referred to as *non-locality*, has a profound connection with the separability of that state. In fact, one can easily construct an entanglement witness in full analogy to Theorem 1.2.

Theorem 1.7. *A two-qubit state ρ can violate the CHSH inequality*

$$(\rho, 2\mathbb{1} - \mathcal{O}_{\text{CHSH}})_{\text{HS}} \geq 0,$$

where $\mathcal{O}_{\text{CHSH}}$ is given by (1.27), only if it is entangled.

In fact, it was shown in Ref. [97] that the CHSH inequality can be violated for every entangled pure state. This is in general no longer the case for mixed states. The issue that Theorem 1.7 has in common with the entanglement witnesses discussed earlier, is to determine a suitable operator for a given state ρ . However, for the CHSH inequality this problem can be circumvented by the following theorem—the *CHSH criterion*—proven in Ref. [102].

Theorem 1.8. *The maximally possible value of the CHSH expectation value $\langle \mathcal{O}_{\text{CHSH}} \rangle_\rho$ for a given two-qubit state ρ is given by $\langle \mathcal{O}_{\text{CHSH}}^{\text{max}} \rangle_\rho = 2\sqrt{\mu_1 + \mu_2}$, where μ_1 and μ_2 are the two largest eigenvalues of $M_\rho = t[\rho]^T t[\rho]$, and $t[\rho]$ is the correlation matrix $t[\rho]_{ij} = \text{Tr}(\rho \sigma_i \otimes \sigma_j)$ of Eq. (1.10).*

The criterion does not require us to determine the measurement directions \mathbf{a} , \mathbf{b} , $\tilde{\mathbf{a}}$, and $\tilde{\mathbf{b}}$, but instead provides us with a simple way to use Theorem 1.7 for the detection of entanglement. In Section 1.5.3 we will study the protocol known as *quantum teleportation* and following Ref. [106] we shall discover the connection this protocol has to the violation of the CHSH inequality.

1.5.3 Quantum Teleportation

To conclude this chapter we are now going to discuss a paradigmatic protocol of quantum information processing —*quantum teleportation*— introduced in Ref. [25] and generalized to mixed resource states in Ref. [163].

The Teleportation Protocol

The setup is the following: two observers, *Alice* and *Bob*, share a two-qubit state ρ_{AB} . Alice additionally has access to an unknown pure, single-qubit state $|\phi\rangle_X$ in a subsystem that we label by X . Alice wishes to send the state of the third qubit to Bob using only classical communication and local operations. To this end she performs a *Bell measurement*, i.e., she projects the subsystems X and A into the Bell basis $\{|\phi^\pm\rangle, |\psi^\pm\rangle\}$ of Eq. (1.13). With probability p_k the total state is then transformed to the state

$$\frac{1}{p_k} [(P_k)_{XA} \otimes \mathbb{1}_B] [(P_\phi)_X \otimes \rho_{AB}] [(P_k)_{XA} \otimes \mathbb{1}_B], \quad (1.28)$$

where $k = 1, 2, 3, 4$, labels the four Bell states, P_χ denotes a projector on the state $|\chi\rangle$, $P_\chi = |\chi\rangle\langle\chi|$, and the probability p_k for the outcome k is given by

$$p_k = \text{Tr} \left([(P_k)_{XA} \otimes \mathbb{1}_B] [(P_\phi)_X \otimes \rho_{AB}] \right). \quad (1.29)$$

Finally, Alice communicates the outcome k to Bob by sending two bits of classical information. Bob can then perform a local unitary operation U_k on subsystem B to obtain the state

$$\rho_k = \frac{1}{p_k} \text{Tr}_{XA} \left([(P_k)_{XA} \otimes (U_k)_B] [(P_\phi)_X \otimes \rho_{AB}] [(P_k)_{XA} \otimes (U_k^\dagger)_B] \right). \quad (1.30)$$

For a pure, maximally entangled resource state, e.g., for $\rho_{AB} = |\psi^\pm\rangle\langle\psi^\pm|$, the transmission of the quantum state $|\phi\rangle$ becomes perfect, i.e., $\rho_k = |\phi\rangle\langle\phi| \forall k$.

Optimized Teleportation & Teleportation Fidelity

For general mixed states ρ_{AB} the teleportation is afflicted with errors and the scheme can therefore profit from variations. For instance, one can define a generic teleportation protocol $\mathbb{T}[\rho_{XAB}]$ that allows for (trace preserving) local operations and classical communication [105, 193] between Alice's and Bob's subsystems, (XA) and B , respectively, i.e., transformations that cannot increase the shared entanglement between A and B . For such a protocol the final state of subsystem B is given by

$$\rho_{B,\mathbb{T}} = \text{Tr}_{XA} \left(\mathbb{T}[(P_\phi)_X \otimes \rho_{AB}] \right). \quad (1.31)$$

A figure of merit for this protocol is the *teleportation fidelity* $\mathcal{F}(\mathbb{T}, \rho_{AB})$, defined as [105]

$$\mathcal{F}_{\mathbb{T}}(\rho_{AB}) = \int d\phi \langle \phi | \rho_{B,\mathbb{T}} | \phi \rangle, \quad (1.32)$$

where the integral is carried out over a uniform distribution of input states $|\phi\rangle$. This teleportation fidelity can be understood as the overlap between the final state $\rho_{B,\mathbb{T}}$ and the target state $|\phi\rangle$, averaged over all inputs. For a separable state the teleportation fidelity cannot exceed $\frac{2}{3}$, in other words $\mathcal{F}_{\mathbb{T}}(\rho_{\text{sep}}) \leq \frac{2}{3}$ (see, e.g., Ref. [193]). Consequently, any state for which the fidelity can exceed the value of $\frac{2}{3}$ is called *useful* for teleportation. Interestingly, the fidelity of the standard teleportation protocol can be related to the violation of the CHSH inequality [106]—any state that violates the CHSH inequality is useful for teleportation. The corresponding fidelity, maximized over Bob's local rotations U_k , is given by

$$\mathcal{F}_{\text{max}}(\rho_{AB}) = \frac{1}{2} \left(1 + \frac{1}{3} \sum_i \sqrt{\mu_i} \right), \quad (1.33)$$

where the μ_i are the eigenvalues of $M_{\rho_{AB}} = t[\rho_{AB}]^T t[\rho_{AB}]$ from Theorem 1.8. As the $\mu_i \leq 1$ one finds $\sum_i \sqrt{\mu_i} \geq \sqrt{\mu_1 + \mu_2}$, where $\mu_3 \leq \mu_{1,2}$. It then immediately follows that

$$\mathcal{F}_{\text{max}}(\rho_{AB}) \geq \frac{1}{2} \left(1 + \frac{1}{12} \langle \mathcal{O}_{\text{CHSH}}^{\text{max}} \rangle_{\rho_{AB}} \right), \quad (1.34)$$

which is larger than $\frac{2}{3}$ only if $\langle \mathcal{O}_{\text{CHSH}}^{\text{max}} \rangle_{\rho_{AB}} > 2$. All mixed two-qubit states that violate the CHSH inequality are useful for teleportation. However, it should be noted that states that do not violate a Bell inequality can still be useful for some teleportation schemes (see Ref. [163]).

We will consider the effects on the possible teleportation fidelity between modes of both fermionic and bosonic quantum fields confined to different cavities in non-uniform motion in Chapter 7. Now, let us turn to the description of these quantum fields.

Quantum Fields in Flat and Curved Spacetimes

Let us now turn to the second pillar of RQI: *relativity*, in particular, relativistic quantum field theory. We shall here consider the quantization of relativistic fields and study quantum information procedures in the corresponding Fock spaces. We note here in passing that it is possible to consider only a sector of the Fock space with a fixed number of relativistic particles in a covariant way. Such situations have been studied extensively in the context of RQI (see, e.g., Refs. [8, 9, 12, 22, 52, 53, 60, 81, 96, 111, 117, 151, 152, 158, 171–173, 188, 189], or see Ref. [80] for an introduction to the topic), but the discussion of these results lies beyond the scope of this thesis. Here we are interested in studying a genuine relativistic multi-particle theory that allows for particle creation phenomena.

Naturally, the question arises: *Why is it necessary to consider quantum fields in RQI?* First and foremost, one may answer that field quantization is needed to endow the solutions of relativistic field equations with an appropriate interpretation where the usual procedure of interpreting wave functions fails. In this context quantum field theory provides a natural extension of quantum mechanics. We will further elaborate on this problem in Section 2.2. Another reason for the necessity to consider quantum fields in the context of RQI lies in the observer dependence of particle content [30] and entanglement [10]. Any model with a fixed particle number cannot hope to capture the intriguing effects attributed to non-uniform motion and spacetime structure, such as the *Unruh effect*, the *Hawking effect*, the *dynamical Casimir effect*, or the effects of non-uniformly moving cavities that we are going to discuss in Part II. We will now establish the basic framework of quantization in (non-interacting) quantum field theory that is needed in the following chapters. For a thorough introduction to the numerous additional aspects of quantum field theory we direct the interested reader to standard textbooks, e.g., Refs. [30, 160].

Our aim in this chapter is the quantization of Lorentz invariant field equations. We shall be concerned with two representatives of the irreducible, unitary representations of the *Poincaré* group — relativistic fields: In Section 2.2 we will discuss the *real scalar field* and in Section 2.3 the *Dirac field* will be introduced. First we are going to establish some conventions for the description of relativistic spacetimes in Section 2.1.

2.1 Relativistic Spacetimes

We are interested in constructing our quantum fields in a *spacetime*, i.e., a smooth, connected, differentiable manifold M , which can be locally covered with coordinates $\{x^\mu \mid \mu = 0, 1, 2, \dots, n - 1\}$ in open subsets of \mathbb{R}^n . For a more thorough introduction to curved spacetimes and general relativity see, for example, Ref. [196]. Practically, we are here interested in the $(3 + 1)$ -dimensional case and we shall work in units where $c = \hbar = 1$ from now on. In addition the spacetime is equipped with a *Lorentzian metric tensor* g :

Definition 2.1. *A Lorentzian metric is a non-degenerate, symmetric, bilinear form $g(\cdot, \cdot)$ with signature $(-, +, +, +)$ that maps two elements of each tangent space of M to a real number. The line element is given by*

$$ds^2 = g_{\mu\nu} dx^\mu dx^\nu. \quad (2.1)$$

Summation is implied for repeated indices. Alternatively and equivalently, the convention $(+, -, -, -)$ may be chosen for the signature of the metric, which would result in sign changes in several of the following definitions. We shall keep the convention stated in Definition 2.1 throughout this document.

A special case of the general (curved) metric $g_{\mu\nu}$ is the flat space *Minkowski metric* $\eta_{\mu\nu} = \text{diag}\{-1, 1, 1, 1\}$ with the line element $ds^2 = \eta_{\mu\nu} dx^\mu dx^\nu = -dt^2 + dx^2 + dy^2 + dz^2$. The metric is not positive-definite, i.e., it is not Riemannian, but we can classify vectors and distances into three categories. Following our sign convention for the metric we define:

Definition 2.2. *A vector $v = v^\mu$, with $g(v, v) = g_{\mu\nu} v^\mu v^\nu = v^\mu v_\mu$ is called*

time-like	if $v^\mu v_\mu < 0$,
null	if $v^\mu v_\mu = 0$,
space-like	if $v^\mu v_\mu > 0$.

Likewise, a curve $x^\mu(\lambda)$ is called time-like/null/space-like if its tangent vector $v^\mu = dx^\mu(\lambda)/d\lambda$ is time-like/null/space-like at every point.

All massive particles and, consequently, all observers follow time-like curves — world-lines, while light is confined to null rays. Along any time-like curve \mathcal{C}_t the proper time τ , i.e., the time that elapses on a clock moving along the curve, is given by

$$\tau = \int_{\mathcal{C}_t} \sqrt{-ds^2} = \int_{\mathcal{C}_t} \sqrt{-g_{\mu\nu} dx^\mu dx^\nu}, \quad (2.2)$$

where the line element ds^2 is given by Eq. (2.1). Similarly, along any space-like path \mathcal{C}_x the proper length l can be defined as

$$l = \int_{\mathcal{C}_x} \sqrt{ds^2} = \int_{\mathcal{C}_x} \sqrt{g_{\mu\nu} dx^\mu dx^\nu}. \quad (2.3)$$

For practical purposes the symmetries of a given metric g are of great interest. Such symmetries are represented by *isometries* G , i.e., diffeomorphisms (a differentiable bijection with a differentiable inverse) that leave the metric invariant. Any one-parameter group of isometries such that

$$G(a)g = e^{a\xi}g = g, \quad (2.4)$$

is generated by a *Killing vector* ξ that satisfies the *Killing equation*

$$\nabla_\mu \xi_\nu + \nabla_\nu \xi_\mu = 0. \quad (2.5)$$

Here ∇_μ is the covariant derivative with respect to the metric g (see Ref. [196] for details). Alternatively, Killing vector fields may be defined via the *Lie derivative* of the metric, i.e., $\mathcal{L}_\xi g = 0$, see Ref. [196]. For the analysis of quantum fields Killing vectors play an essential role in distinguishing positive and negative frequency solutions of the field equations, as we shall see in Section 2.2.2.

2.2 The Klein-Gordon Field

2.2.1 The Classical Klein-Gordon Field

As a first representative of a quantum field let us consider the *real scalar field* $\phi(x)$. We start from the classical *Lagrangian* (density) for the free field ϕ on a general (curved) background described by the metric g , i.e.,

$$\mathcal{L} = -\frac{1}{2} \sqrt{-\det g} (g^{\mu\nu} (\partial_\mu \phi) (\partial_\nu \phi) + m^2 \phi^2). \quad (2.6)$$

This Lagrangian describes a non-interacting field that is not coupled to the gravitational field (see, for instance, Ref. [30, p. 43]). The constant m will later be interpreted as the mass of the particles in the quantized theory. Having included the factor of $\sqrt{-\det g}$ in the Lagrangian we can straightforwardly write the action S as

$$S = \int d^4x \mathcal{L}(\phi, \partial_\mu \phi). \quad (2.7)$$

Varying the action (2.7) with respect to the field, and demanding the action to be stationary, i.e., $\delta S = 0$, one finds the usual *Euler-Lagrange equations*

$$\frac{\partial \mathcal{L}}{\partial \phi} - \partial_\mu \left(\frac{\partial \mathcal{L}}{\partial (\partial_\mu \phi)} \right) = 0. \quad (2.8)$$

Note that Eq. (2.8) is covariant because $(\partial \mathcal{L} / \partial (\partial_\mu \phi))$ transforms as a vector density. For the Lagrangian (2.6) this *action principle* yields the *curved spacetime Klein-Gordon equation*

$$\partial_\mu (\sqrt{-\det g} g^{\mu\nu} \partial_\nu \phi) - \sqrt{-\det g} \mathbf{m}^2 \phi = 0. \quad (2.9)$$

If the spacetime is equipped with a (translational) symmetry represented by a Killing vector ξ^μ , then the *Noether current* J^μ , given by

$$J^\mu = \xi^\nu T^\mu{}_\nu = \frac{1}{\sqrt{-\det g}} \xi^\nu \left(\frac{\partial \mathcal{L}}{\partial (\partial_\mu \phi)} \partial_\nu \phi - \delta^\mu{}_\nu \mathcal{L} \right), \quad (2.10)$$

where $T^\mu{}_\nu$ is the *stress-energy-momentum tensor*, is conserved, i.e., $\nabla_\mu J^\mu = 0$.

2.2.2 Quantizing the Klein-Gordon Field

Let us now turn to the solutions ϕ_n — the *mode functions* — of the Klein-Gordon equation (2.9). Following Ref. [30] we define the (pseudo) inner product

$$(\phi_1, \phi_2)_{\text{KG}} = -i \int_\Sigma d\Sigma^\mu (\phi_1 \partial_\mu \phi_2^* - \phi_2^* \partial_\mu \phi_1), \quad (2.11)$$

where Σ is a spacelike Cauchy surface (assuming global hyperbolicity of the spacetime) — a surface that is intersected by every inextendible, causal (time-like or null) curve exactly once — and $d\Sigma^\mu = g^{\mu\nu} d\Sigma_\nu$, with $g_{\mu\lambda} g^{\lambda\nu} = \delta_\mu{}^\nu$. The volume form $d\Sigma_\mu$ for the three-surface Σ is given by [187, p. 10]

$$d\Sigma_\mu = \frac{1}{3!} \sqrt{-\det g} \epsilon_{\mu\mu_1\mu_2\mu_3} dx^{\mu_1} \wedge dx^{\mu_2} \wedge dx^{\mu_3}, \quad (2.12)$$

where $\epsilon_{\mu\mu_1\mu_2\mu_3}$, with $\epsilon_{0123} = 1$, is the totally antisymmetric Levi-Civita symbol. Note that the inner product is independent of the chosen hypersurface Σ , see Ref. [30]. One can choose a complete set of orthonormal solutions with respect to the pseudo inner product (2.11) such that $(\phi_m, \phi_n)_{\text{KG}} = -(\phi_m^*, \phi_n^*)_{\text{KG}} = \delta_{mn}$, and $(\phi_m, \phi_n^*)_{\text{KG}} = 0$. The positive and negative frequency solutions (see below) to the Klein-Gordon equation then form Hilbert spaces, respectively. We should note here that we have assumed a discrete set of solutions for the sake of simplicity, but the treatment can easily be reformulated for a continuous spectrum.

In a general spacetime there is no preferred splitting into the solutions $\{\phi_n\}$ and $\{\phi_n^*\}$. Such a distinction can be uniquely made with respect to a time-like Killing vector

field ξ^μ and the corresponding conservation of energy [see Eq. (2.10)]. The solutions can then be naturally split into positive frequency solutions ϕ_n and negative frequency solutions ϕ_n^* according to the signs of their eigenvalues,

$$i \xi \phi_n = +\omega_n \phi_n, \quad (2.13a)$$

$$i \xi \phi_n^* = -\omega_n \phi_n^*, \quad (2.13b)$$

where $\omega_n > 0$. Because the Klein-Gordon product of Eq. (2.11) is not positive-definite, linear combinations of *mode functions* ϕ_n and ϕ_n^* cannot be interpreted as single particle wave functions. It thus becomes necessary to promote the *Klein Gordon field* to an operator of the form

$$\phi = \sum_n (\phi_n a_n + \phi_n^* a_n^\dagger), \quad (2.14)$$

where the *annihilation operators* a_n and the *creation operators* a_n^\dagger satisfy the *commutation relations*

$$[a_m, a_n^\dagger] = \delta_{mn}, \quad (2.15a)$$

$$[a_m, a_n] = [a_m^\dagger, a_n^\dagger] = 0. \quad (2.15b)$$

In Chapter 4 we are going to consider explicit solutions to the Klein-Gordon equation in both Minkowski and Rindler coordinates, both subject to appropriate cavity boundary conditions.

2.2.3 The Bosonic Fock Space

We now turn to the physical interpretation of the annihilation and creation operators. As their names suggest, the operators a_n annihilate a particle in the state ϕ_n , while the operators a_n^\dagger create such a particle. The corresponding *Fock space* is a Hilbert space that is constructed from a vacuum state $|0\rangle$ that does not contain any particles. Mathematically, the vacuum state is defined via the relation

$$a_n |0\rangle = 0 \quad \forall n. \quad (2.16)$$

Any single boson (1-b) state $|\phi^{1-b}\rangle$ can be simply obtained by acting on the vacuum with a linear combination of creation operators, i.e.,

$$|\phi^{1-b}\rangle = \sum_i \theta_i |\phi_i\rangle, \quad (2.17)$$

where $\theta_i \in \mathbb{C}$, $|\phi_i\rangle = a_i^\dagger |0\rangle$ and $\sum_i |\theta_i|^2 = 1$. The states $|\phi_n\rangle$ form a complete basis of the single boson Hilbert space \mathcal{H}_{1-b} . The vacuum state, on the other hand, is an

element of the Hilbert space $\mathcal{H}_{0\text{-b}} = \mathbb{C}$. When a second particle is added we need to keep in mind that the particles are indistinguishable from each other, such that we have to symmetrize the tensor product with respect to the exchange of the two particles

$$|\phi_m, \phi_n\rangle = a_m^\dagger a_n^\dagger |0\rangle = |\phi_m\rangle \circ |\phi_n\rangle := \frac{1}{\sqrt{2}} \left(|\phi_m\rangle \otimes |\phi_n\rangle + |\phi_n\rangle \otimes |\phi_m\rangle \right). \quad (2.18)$$

The two-boson states are thus elements of the *symmetrized* tensor product space of two single-boson Hilbert spaces, i.e.,

$$\mathcal{H}_{2\text{-b}} = S\left(\mathcal{H}_{1\text{-b}} \otimes \mathcal{H}_{1\text{-b}}\right). \quad (2.19)$$

Similarly, states with higher particle content need to be symmetrized as well, and we can write the *bosonic Fock space* \mathbb{F} as the direct sum over all boson numbers of the symmetrized Hilbert spaces, i.e.,

$$\mathbb{F}(\mathcal{H}_{1\text{-b}}) = \bigoplus_{m=0}^{\infty} S\left(\mathcal{H}_{1\text{-b}}^{\otimes m}\right) = \mathcal{H}_{0\text{-b}} \oplus \mathcal{H}_{1\text{-b}} \oplus S\left(\mathcal{H}_{1\text{-b}} \otimes \mathcal{H}_{1\text{-b}}\right) \oplus \dots, \quad (2.20)$$

where $\mathcal{H}^{\otimes m}$ denotes the m -fold tensor product and we write $\mathcal{H}_{0\text{-b}}$ as $\mathcal{H}_{1\text{-b}}^{\otimes 0}$. A general state in the space \mathbb{F} can be written as

$$|\Phi^{\mathbb{F}}\rangle = \theta_0 |0\rangle + \sum_{i \neq 0} \theta_i |\phi_i\rangle + \sum_{j,k} \theta_{jk} |\phi_j, \phi_k\rangle + \dots, \quad (2.21)$$

where $\theta_0, \theta_i, \theta_{jk}, \dots \in \mathbb{C}$, and the vectors “ $|\cdot\rangle$ ” in all sectors of fixed particle content are understood as being extended to the total Fock space \mathbb{F} via the direct sum with zero vectors for all other sectors, e.g., $|\phi_i\rangle = 0_{0\text{-b}} \oplus |\phi_i\rangle \oplus 0_{2\text{-b}} \oplus \dots$. For ease of notation we are going to make some adjustments to the way we denote these states. We shall use the *occupation number notation* where non-zero numbers of particles in each mode are indicated by integers with the corresponding mode labels as subscripts, for instance, $|\phi_m, \phi_n\rangle = |1_m\rangle |1_n\rangle$, such that

$$\langle 1_m | \langle 1_n | 1_i \rangle | 1_j \rangle = \delta_{ni} \delta_{mj} + \delta_{nj} \delta_{mi}, \quad (2.22)$$

and we have dropped the symbol “ \circ ” for the symmetrized tensor product. For several excitations in the same mode i our conventions imply

$$a_i |n_i\rangle = \sqrt{n_i} |n_i - 1\rangle, \quad (2.23a)$$

$$a_i^\dagger |n_i\rangle = \sqrt{n_i + 1} |n_i + 1\rangle. \quad (2.23b)$$

We note here in passing that we have chosen the split notation $|1_m\rangle |1_n\rangle$, rather than $|1_m, 1_n\rangle$ because this proves to be a more useful notation for computations with fermions in Part II. Thus, we can rewrite Eq. (2.21) as

$$|\Phi^{\mathbb{F}}\rangle = \theta_0 |0\rangle + \sum_{i \neq 0} \theta_i |1_i\rangle + \sum_{j,k} \theta_{jk} |1_j\rangle |1_k\rangle + \dots \quad (2.24)$$

2.2.4 Bosonic Bogoliubov Transformations

In Sections 2.2.2 and 2.2.3 we have quantized the scalar field for a particular set of mode functions ϕ_n and we have further classified them into positive and negative frequency solutions using a time-like Killing vector field. However, typically such choices are not unique, in other words, a different basis $\{\tilde{\phi}_n, \tilde{\phi}_n^*\}$ can be chosen. Furthermore, if a different time-like Killing vector is chosen to separate particles (positive frequency) and antiparticles (negative frequency) then also the particle content of a given state will be affected. The transformations that connect the two choices of solutions are called *Bogoliubov transformations*.

Definition 2.3. A bosonic Bogoliubov transformation is an isomorphism (a bijective map) between two representations of the commutation relation algebra of Eq. (2.15). The transformation is unitary with respect to the (pseudo) inner product $(\cdot, \cdot)_{\text{KG}}$ of Eq. (2.11) and the inner product of the bosonic Fock space.

For two given sets of mode functions $\{\phi_n, \phi_n^*\}$ and $\{\tilde{\phi}_n, \tilde{\phi}_n^*\}$ with mode operators $\{a_n, a_n^\dagger\}$ and $\{\tilde{a}_n, \tilde{a}_n^\dagger\}$, respectively, we can write the Bogoliubov transformation as a linear transformation of the mode functions and mode operators,

$$\tilde{\phi}_m = \sum_n (\alpha_{mn} \phi_n + \beta_{mn} \phi_n^*), \quad (2.25a)$$

$$\tilde{a}_m = \sum_n (\alpha_{mn}^* a_n - \beta_{mn}^* a_n^\dagger), \quad (2.25b)$$

respectively, where the complex numbers

$$\alpha_{mn} = (\tilde{\phi}_m, \phi_n)_{\text{KG}}, \quad (2.26a)$$

$$\beta_{mn} = -(\tilde{\phi}_m, \phi_n^*)_{\text{KG}}, \quad (2.26b)$$

are called the *Bogoliubov coefficients*. If the β -type coefficients are absent, the remaining α coefficients do not change the particle content of a given state, but simply shift excitations between different modes. The coefficients α_{mn} can hence be understood as a form of generalized rotation in the space of positive or negative frequency solutions, respectively. The coefficients β_{mn} , on the other hand, change the particle content, which can be easily seen from Eq. (2.25b) since β_{mn} relates annihilation and creation operators. The unitarity of the transformation demands that the Bogoliubov coefficients satisfy

$$\sum_n (\alpha_{nm}^* \alpha_{nl} - \beta_{nm} \beta_{nl}^*) = \delta_{ml}, \quad (2.27a)$$

$$\sum_n (\alpha_{nm} \beta_{nl}^* - \beta_{nm}^* \alpha_{nl}) = 0. \quad (2.27b)$$

The linear transformations of the mode operators can alternatively be written as unitary operations on the states in the Fock space. These transformations are realized by exponentials of Hermitean operators that are quadratic in the mode operators. In other words, all linear, unitary transformations on the Fock space can be represented by Bogoliubov transformations. Throughout this thesis we will make extensive use of Bogoliubov transformations to describe physical transformations of states in the Fock space.

2.3 The Dirac Field

Now, let us turn to the description of fermionic fields, in particular, the *Dirac field*.

2.3.1 Quantizing the Dirac Field

Mirroring the approach when introducing the scalar field we start from a Lagrangian density for the Dirac field in a curved spacetime, given by

$$\mathcal{L} = \sqrt{-\det g} \left(\frac{i}{2} [\bar{\psi} \gamma^\mu \nabla_\mu \psi - (\nabla_\mu \bar{\psi}) \gamma^\mu \psi] - m \bar{\psi} \psi \right). \quad (2.28)$$

where ∇_μ is the appropriate covariant derivative (see, e.g., Ref. [13, 199] for details), m is the mass of the field excitations, γ^μ are the curved space *Dirac γ matrices* satisfying the anticommutation relation

$$\{\gamma^\mu, \gamma^\nu\} = -2g^{\mu\nu}, \quad (2.29)$$

and $\bar{\psi}$ denotes the Dirac conjugate $\bar{\psi} = \psi^\dagger \gamma^0$. For a more detailed construction of this Lagrangian see Ref. [30, p. 85].

As in Section 2.2.1 we invoke an action principle to obtain the Euler-Lagrange equations [see Eqs. (2.7) and (2.8)] which here yields the *curved space Dirac equation*

$$(i\gamma^\mu \nabla_\mu - m) \psi = 0. \quad (2.30)$$

One is then interested in a complete set of solutions that are orthonormal with respect to the inner product

$$(\psi_1, \psi_2)_D = \int_\Sigma d\Sigma^\mu \bar{\psi}_1 \gamma_\mu \psi_2, \quad (2.31)$$

with the conventions for $d\Sigma^\mu$ as used in Eq. (2.11). In the presence of a time-like Killing vector field the solutions can be meaningfully classified into positive and negative frequency solutions. However, since we will allow the excitations of the Dirac field to

carry electric charge we will choose different symbols for the mode operators that annihilate or create particles or antiparticles. In addition we use non-negative (negative) numbers to label the (anti)particle solutions, such that the quantized field can be written as

$$\psi = \sum_{n \geq 0} b_n \psi_n + \sum_{n < 0} c_n^\dagger \psi_n, \quad (2.32)$$

where the operators b_n annihilate a Dirac fermion in the state ψ_n , while the c_n annihilate an antifermion. As before we have simplified the discussion to a discrete spectrum for further convenience. The mode operators satisfy the *anticommutation relations*

$$\{b_m, b_n^\dagger\} = \{c_m, c_n^\dagger\} = \delta_{mn}, \quad (2.33a)$$

$$\{b_m, b_n\} = \{c_m, c_n\} = \{b_m, c_n\} = \{b_m, c_n^\dagger\} = 0, \quad (2.33b)$$

where $\{\dots\}$ denotes the anticommutator. We will study some explicit examples for solutions to the Dirac equation in Chapter 4 when we consider Dirac fields contained in cavities. For now we are more interested in the construction of the fermionic Fock space.

2.3.2 The Fermionic Fock Space

In analogy to our approach in the bosonic case, let us now construct the fermionic Fock space. As previously, we start from a vacuum state that is annihilated by all annihilation operators, $b_m |0\rangle = c_n |0\rangle = 0 \forall m \geq 0, n < 0$. The creation operators b_m^\dagger and c_n^\dagger acting upon the vacuum state $|0\rangle$ will populate the vacuum with single excitations of particles and antiparticles, respectively, i.e.,

$$|\psi_m\rangle = b_m^\dagger |0\rangle, \quad (2.34a)$$

$$|\psi_n\rangle = c_n^\dagger |0\rangle, \quad (2.34b)$$

where we assume that the mode labels $m \geq 0$ and $n < 0$ distinguish the particle and antiparticle mode solutions. As can be quickly seen from this property and Eq. (2.33a), the states $|\psi_i\rangle$ are orthonormal and they further form a complete basis of the single-fermion Hilbert space \mathcal{H}_{1-f} , whereas $|0\rangle \in \mathcal{H}_{0-f} \neq \mathcal{H}_{1-f}$. We write a general state in the fermionic single-excitation space \mathcal{H}_{1-f} as

$$|\psi^{1-f}\rangle = \sum_i \mu_i |\psi_i\rangle, \quad (2.35)$$

with $\mu_i \in \mathbb{C}$ and $\sum_i |\mu_i|^2 = 1$ such that $\langle \psi^{1-f} | \psi^{1-f} \rangle = 1$. The form of the states of Eq. (2.35) may be further restricted by superselection rules. For instance, conservation

of charge would exclude any superpositions of states of different charge. We shall not explicitly include such restrictions, but any superselection rule can be applied to the Fock space construction we present here. Let us now turn to states of multiple fermions. A second fermion can be added to the state (2.34) by the action of another creation operator b_m^\dagger or c_n^\dagger , e.g.,

$$b_m^\dagger b_n^\dagger |0\rangle \propto |\psi_m, \psi_n\rangle. \quad (2.36)$$

Clearly, the anticommutation relations (2.33) require the two-fermion state to be antisymmetric with respect to the exchange of the mode labels m and n . We therefore define

$$|\psi_m, \psi_n\rangle = b_m^\dagger b_n^\dagger |0\rangle = |\psi_m\rangle \wedge |\psi_n\rangle = \frac{1}{\sqrt{2}} \left(|\psi_m\rangle \otimes |\psi_n\rangle - |\psi_n\rangle \otimes |\psi_m\rangle \right). \quad (2.37)$$

The two-fermion states are thus elements of the antisymmetrized tensor product space of two single-fermion Hilbert spaces, i.e.,

$$\mathcal{H}_{2-f} = \bar{S}(\mathcal{H}_{1-f} \otimes \mathcal{H}_{1-f}), \quad (2.38)$$

and a general state within this space can be written as

$$|\psi^{2-f}\rangle = \sum_{i,j} \mu_{ij} |\psi_i, \psi_j\rangle, \quad (2.39)$$

where the coefficients $\mu_{ij} \in \mathbb{C}$ form an antisymmetric matrix. States with more than two fermions can then be constructed by antisymmetrizing over the corresponding number of single-fermion states. Finally, the *fermionic Fock space* $\bar{\mathbb{F}}$ is simply given as the direct sum over all fermion numbers of the antisymmetrized Hilbert spaces, i.e.,

$$\bar{\mathbb{F}}(\mathcal{H}_{1-f}) = \bigoplus_{m=0}^{\infty} \bar{S}(\mathcal{H}_{1-f}^{\otimes m}) = \mathcal{H}_{0-f} \oplus \mathcal{H}_{1-f} \oplus \bar{S}(\mathcal{H}_{1-f} \otimes \mathcal{H}_{1-f}) \oplus \dots \quad (2.40)$$

where, as before, $\mathcal{H}^{\otimes m}$ denotes the m -fold tensor product and we write \mathcal{H}_{0-f} as $\mathcal{H}_{1-f}^{\otimes 0}$. A general state in the space $\bar{\mathbb{F}}$ can be written as

$$|\Psi^{\bar{\mathbb{F}}}\rangle = \mu_0 |0\rangle + \sum_{i \neq 0} \mu_i |\psi_i\rangle + \sum_{j,k} \mu_{jk} |\psi_j\rangle \wedge |\psi_k\rangle + \dots, \quad (2.41)$$

where $\mu_0, \mu_i, \mu_{jk}, \dots \in \mathbb{C}$, and the vectors “ $|\cdot\rangle$ ” in all sectors of fixed particle content are understood as being extended to the total Fock space $\bar{\mathbb{F}}$ via the direct sum with zero vectors for all other sectors, e.g., $|\psi_i\rangle = 0_{0-f} \oplus |\psi_i\rangle \oplus 0_{2-f} \oplus \dots$. Let us now simplify the notation. To distinguish more clearly from the bosonic case we will from now on denote states in the fermionic Fock space by double-lined Dirac notation, i.e., $\|\cdot\rangle\rangle$ instead of $|\cdot\rangle$, where the antisymmetric “wedge” product is implied when two

vectors are multiplied, i.e., $\| \cdot \rangle \| \cdot \rangle = \| \cdot \rangle \wedge \| \cdot \rangle$. Furthermore, let us again use the common *occupation number notation* and write 1_n instead of ψ_n to denote an excitation in the mode n . With this convention in mind we can rewrite Eq. (2.41) as

$$\| \Psi \rangle = \mu_0 \| 0 \rangle + \sum_{i \neq 0} \mu_i \| 1_i \rangle + \sum_{j,k} \mu_{jk} \| 1_j \rangle \| 1_k \rangle + \dots \quad (2.42)$$

For the adjoint space we use the convention [compare to Eq. (2.37)]

$$\langle\langle 1_n \| \langle\langle 1_m \| := \langle\langle 0 \| b_n b_m = \left(b_m^\dagger b_n^\dagger \| 0 \rangle \right)^\dagger = -\frac{1}{\sqrt{2}} \left(\langle \psi_n | \otimes \langle \psi_m | - \langle \psi_m | \otimes \langle \psi_n | \right), \quad (2.43)$$

which allows us to write

$$\langle\langle 1_m \| \langle\langle 1_n \| 1_i \rangle \| 1_j \rangle = \delta_{ni} \delta_{mj} - \delta_{nj} \delta_{mi}, \quad (2.44)$$

which is convenient for computations in the fermionic Fock space. It should be noted that, in standard quantum information notation, e.g., as used in Chapter 1, the position of a “ket” corresponds to a particular ordering of the subspaces with respect to the tensor product structure of the total space. Here, however, there is no tensor product structure corresponding to different modes according to which the vectors $\| \cdot \rangle$ can be naturally ordered. We shall return to this issue in Section 3.2 in Chapter 3.

2.3.3 Bogoliubov transformations of the Dirac Field

Similarly as for the bosonic case (see Definition 2.3) one can define a change of basis in the set of mode solutions to the Dirac equation as a fermionic Bogoliubov transformation.

Definition 2.4. *A fermionic Bogoliubov transformation is an isomorphism (a bijective map) between two representations of the anticommutation relation algebra of Eq. (2.33). The transformation is unitary with respect to the inner product $(\cdot, \cdot)_D$ of Eq. (2.31) and the inner product of the fermionic Fock space.*

Given two sets of mode solutions to the Dirac equation (2.32), $\{\psi_m\}$ and $\{\tilde{\psi}_n\}$ we can write the *fermionic Bogoliubov transformation* as

$$\tilde{\psi}_m = \sum_n A_{mn} \psi_n. \quad (2.45)$$

Although our notation allows us to use only a single symbol for all fermionic Bogoliubov coefficients, it is obvious that coefficients $A_{mn} = (\psi_n, \tilde{\psi}_m)_D$ with $m, n \geq 0$ or $m, n < 0$ are α -type coefficients, while those with subscripts with mixed signs represent β -type coefficients responsible for particle creation phenomena. The unitarity of the transformation is expressed as the unitarity of the matrix $A = (A_{mn})$, i.e.,

$$A^\dagger A = \mathbf{1}. \quad (2.46)$$

Entanglement in Relativistic Quantum Fields

With the definitions and methodology of Chapters 1 and 2 at our disposal we now turn to some elementary concerns in relativistic quantum information (RQI) — entanglement in relativistic quantum fields. The appropriate relativistic treatment of quantum correlations requires to work with quantum fields and the corresponding Fock spaces. As in the previous chapter we separate the discussion of bosonic and fermionic quantum fields into Sections 3.1 and 3.2, respectively. Starting with bosons we review the tools available (see, e.g., Ref. [1] for a detailed introduction) for the important class of *Gaussian states* in Sections 3.1.1–3.1.4. We include a short discussion of teleportation with Gaussian states and the construction of *entanglement resonances* as introduced in Ref. [42] and Ref. [43, (xi)]. Finally, quantum information techniques for *fermionic Fock spaces* originally presented in Ref. [86, (viii)] are examined in Section 3.2.

3.1 Entanglement in Bosonic Quantum Fields

The first question encountered when studying entanglement in bosonic Fock spaces is the choice of bipartitions. In other words, one has to address the question of selecting appropriate subsystems. Since the particle content is not fixed it becomes necessary to consider instead the entanglement between different modes of the quantum field. The Fock space is not naturally equipped with a tensor product structure with respect to different modes. Nonetheless, the symmetrization in Eq. (2.20) allows a unique one-to-one mapping between states in $\mathbb{F}(\mathcal{H}_{1-b})$ and a tensor product space $\mathcal{H}_1 \otimes \mathcal{H}_2 \otimes \mathcal{H}_3 \otimes \dots$, where the subscripts (1, 2, 3, ...) label the modes of the quantum field. Note that such an argument cannot be made in a straightforward way for fermions, as discussed in Section 3.2.

In addition, working in a bosonic Fock space naturally raises the question how the

infinite dimensions are handled. Practically there are two simple ways to circumvent this complication. The first option is to justify a truncation to finite dimensions by considering density operators in $\mathbb{F}(\mathcal{H}_{1-b})$ that have finite rank. We shall consider such an approach in Section 5.1. The other option is to switch from the Fock space to the *phase space*, which we shall explore in the following sections.

3.1.1 Continuous Variables: Gaussian States

Instead of the Hilbert space description we have used in Chapter 1 quantum systems can be represented by a *characteristic function* in *phase space*, e.g., the *Wigner function* $W(q, p)$ for n -modes, given by (see, e.g., [93, p. 173])

$$W(q, p) = \frac{1}{\pi^n} \int_{\mathbb{R}^n} d^n \tilde{q} \langle q - \tilde{q} | \rho | q + \tilde{q} \rangle e^{i \tilde{q}^T p}, \quad (3.1)$$

where $q, p \in \mathbb{R}^n$ and $|q\rangle$ are the eigenstates of the quadrature operator $\hat{q}_i := \frac{1}{\sqrt{2}}(a_i + a_i^\dagger)$, i.e., $\hat{q}_i |q\rangle = q_i |q\rangle$ with $q = (q_1, q_2, \dots, q_i, \dots, q_n)^T$. The Wigner function is a *quasi probability distribution* since it can take on negative values. Note that the quadratures q and p are phase space variables, but do not necessarily correspond to positions and momenta in spacetime. For the class of *Gaussian states* the defining feature is that the Wigner function, or other characteristic functions of choice (see Ref. [1, p. 30]), are multivariate Gaussian distributions. Such distributions are completely determined by the vector of first moments $\langle \mathbb{X} \rangle_\rho$, where

$$\mathbb{X} := (\hat{q}_1, \hat{p}_1, \hat{q}_2, \hat{p}_2, \dots, \hat{q}_n, \hat{p}_n)^T, \quad (3.2)$$

and the real, symmetric *covariance matrix* Γ with components

$$\Gamma_{ij} := \langle \mathbb{X}_i \mathbb{X}_j + \mathbb{X}_j \mathbb{X}_i \rangle_\rho - 2 \langle \mathbb{X}_i \rangle_\rho \langle \mathbb{X}_j \rangle_\rho. \quad (3.3)$$

Here $\langle \cdot \rangle_\rho$ is the expectation value in the state ρ , see Eq. (1.4), and the operators a_n and a_n^\dagger have been combined into the *quadrature operators*

$$\hat{q}_n := \frac{1}{\sqrt{2}}(a_n + a_n^\dagger), \quad (3.4a)$$

$$\hat{p}_n := \frac{-i}{\sqrt{2}}(a_n - a_n^\dagger). \quad (3.4b)$$

From Eq. (2.15) it immediately follows that the Hermitean quadrature operators satisfy the canonical commutation relations

$$[\hat{q}_k, \hat{p}_l] = i \delta_{kl}, \quad (3.5a)$$

$$[\hat{q}_k, \hat{q}_l] = [\hat{p}_k, \hat{p}_l] = 0. \quad (3.5b)$$

Let us now consider some examples for Gaussian states. The simplest and most fundamental representative is the vacuum state $|0\rangle$, for which the first moments vanish and, in our conventions, the covariance matrix is proportional to the identity matrix, $\Gamma_{\text{vac}} = \mathbb{1}$. The family of *coherent states* $|\alpha\rangle$ is obtained from the vacuum by displacements in phase space. Physically, coherent states can be used, for instance, for the description of the electromagnetic field of a laser beam. Note that the notation using the symbol α is customary in the literature (see, e.g., Ref. [93, p. 150]) and is not to be confused with the notation for the matrix of Bogoliubov coefficients α_{mn} from Eq. (2.26a). For any mode k the displacement operator

$$D_k(\alpha) = e^{\alpha a_k^\dagger + \alpha^* a_k} \quad (3.6)$$

with $\alpha \in \mathbb{C}$, takes the vacuum state to a coherent state, $\hat{D}_k(\alpha)|0\rangle = |\alpha_k\rangle$. The displacement shifts the corresponding first moments to $\langle \hat{q}_k \rangle = \sqrt{2} \text{Re}(\alpha)$ and $\langle \hat{p}_k \rangle = \sqrt{2} \text{Im}(\alpha)$, respectively, while it leaves the covariance matrix unchanged, i.e., $\Gamma_\alpha = \mathbb{1}$. A *single-mode squeezed state*, on the other hand, is obtained by a quadratic combination of creation and annihilation operators acting on the vacuum, i.e., for mode k we have

$$U_S(s_k) = e^{\frac{s_k}{2}(a_k^\dagger{}^2 - a_k^2)} \quad (3.7)$$

where $s_k \in \mathbb{R}$ is the single-mode squeezing parameter for mode k . While coherent states can be thought of as quasi-classical, i.e., they approximate the classical description of light as closely as possible (see, e.g., Ref. [93, p. 148]), squeezed states are considered to be truly non-classical. For our discussion it is sufficient to consider a real squeezing parameter, since squeezing along other quadratures can be achieved by applying additional local rotations. The covariance matrix for a single-mode squeezed state $|s_k\rangle = U_S(s_k)|0\rangle$ is given by

$$\Gamma_S(s_k) = \begin{pmatrix} e^{2s_k} & 0 \\ 0 & e^{-2s_k} \end{pmatrix}. \quad (3.8)$$

As can be easily seen from the form of $\Gamma_S(s_k)$, a positive squeezing parameter indicates squeezing in the p -quadrature, while the orthogonal q -quadrature is broadening, such that the product of the covariances remains constant, satisfying the Heisenberg bound. All the Gaussian states we have mentioned so far are pure, i.e., $\det(\Gamma) = 1$. As a last example in this section let us consider the family of mixed *thermal states*. The covariance matrix for a thermal state of mode k with frequency ω_k at temperature T is given by $\Gamma_{\text{th}} = \coth\left(\frac{\hbar\omega_k}{2k_B T}\right)\mathbb{1}$, where we have explicitly inserted Planck's constant \hbar and Boltzmann's constant k_B for clarity. For vanishing first moments, the average particle number \bar{n}_k of mode k is given by

$$\bar{n}_k = \langle a_k^\dagger a_k \rangle = \frac{1}{4} [\text{Tr}(\Gamma) - 2], \quad (3.9)$$

such that the average particle number of the thermal state is distributed according to Bose-Einstein statistics, i.e., $\bar{n}_k = (\exp[\frac{\hbar\omega_k}{k_B T}] - 1)^{-1}$.

3.1.2 Symplectic Operations

To formalize our treatment of the phase space the canonical commutation relations (3.5) can be conveniently combined to define the *symplectic form* Ω via the relation

$$[\mathbb{X}_k, \mathbb{X}_l] = i \Omega_{kl}, \quad (3.10)$$

such that the symplectic form for n modes has the matrix representation

$$\Omega = \bigoplus_{i=1}^n \Omega_i \quad \text{with} \quad \Omega_i = \begin{pmatrix} 0 & 1 \\ -1 & 0 \end{pmatrix}. \quad (3.11)$$

The symplectic form can be used to express a *bona fide* condition, i.e., $\Gamma + i\Omega \geq 0$, which is satisfied by any covariance matrix Γ representing a physical state. Linear transformations S that leave Ω invariant, i.e.,

$$S \Omega S^T = \Omega, \quad (3.12)$$

are called *symplectic transformations* and they correspond to unitaries on the Fock space that are generated by Hamiltonians that are quadratic in the quadrature operators, see, e.g., Eq. (3.7). Such transformations, along with displacements (3.6) and partial tracing over any number of modes preserve the Gaussian character of states. The symplectic transformations on n modes form the *real, symplectic group* $\text{Sp}(2n, \mathbb{R})$. It is precisely this group of operations that can be realized by Bogoliubov transformations of the kind of Eq. (2.25b), and displacements can be incorporated by adding a constant offset $\underline{\alpha}$ to each mode

$$\tilde{a}_m = \sum_n (\alpha_{mn}^* a_n - \beta_{mn}^* a_n^\dagger) + \underline{\alpha}_m, \quad (3.13)$$

where the parameters $\underline{\alpha}_m$ correspond to the displacements [see Eq. (3.6)] of each mode. Symplectic transformations can be written explicitly in terms of the Bogoliubov coefficients in a straightforward fashion [83, (vii)],

$$S = \begin{pmatrix} \mathcal{M}_{11} & \mathcal{M}_{12} & \mathcal{M}_{13} & \dots \\ \mathcal{M}_{21} & \mathcal{M}_{22} & \mathcal{M}_{23} & \dots \\ \mathcal{M}_{31} & \mathcal{M}_{32} & \mathcal{M}_{33} & \dots \\ \vdots & \vdots & \vdots & \ddots \end{pmatrix}, \quad (3.14)$$

i.e., we decompose the transformation matrix into the 2×2 sub-blocks \mathcal{M}_{mn} given by

$$\mathcal{M}_{mn} = \begin{pmatrix} \text{Re}(\alpha_{mn} - \beta_{mn}) & \text{Im}(\alpha_{mn} + \beta_{mn}) \\ -\text{Im}(\alpha_{mn} - \beta_{mn}) & \text{Re}(\alpha_{mn} + \beta_{mn}) \end{pmatrix}. \quad (3.15)$$

The transformed covariance matrix $\tilde{\Gamma}$ is then simply obtained as

$$\tilde{\Gamma} = S \Gamma S^T, \quad (3.16)$$

and partial tracing over any modes is achieved by simply removing the corresponding rows and columns from the covariance matrix. It is convenient to characterize different types of symplectic transformations, following Ref. [204] we distinguish:

- (i) *Passive symplectic transformations* S_P are represented by orthogonal, symplectic matrices $S_P^T S_P = \mathbb{1}$ and they form a subgroup of $\text{Sp}(2n, \mathbb{R})$. Practically, passive transformations can be realized, for instance, by passive/linear optical elements, such as (ideal) *beam splitters* or *phase space rotations*.
- (ii) *Active symplectic transformations* S_A are represented by symmetric, symplectic matrices $S_A^T = S_A$. Active transformations, such as single- and two-mode squeezing, can be realized by active/non-linear optical elements and they change the energy and average particle number, as opposed to passive transformations.

Every symplectic transformation can be decomposed into passive and active transformations, in particular we may decompose any symplectic matrix as $S = S_P S_A$, see Ref. [16]. We have already encountered the single-mode squeezing operation (3.7) as an example for an active symplectic transformation and it gains additional significance via the *Boch-Messiah reduction* [38].

Theorem 3.1. *Every n -mode symplectic transformation S can be written in the Bloch-Messiah decomposition*

$$S = S_P (S_S(s_1) \oplus S_S(s_2) \oplus \cdots \oplus S_S(s_n)) S_P',$$

where $S_S(s_i)$ is the symplectic representation of the single-mode squeezing of Eq. (3.7) in mode i , while S_P and S_P' are passive n -mode operations.

A proof of Theorem 3.1 can be found in Ref. [38]. Finally, let us consider the diagonalization in phase space. Every n mode covariance matrix can be brought to the so-called *Williamson normal form* Γ_W , given by

$$\Gamma_W = \bigoplus_{i=1}^n \begin{pmatrix} \nu_i & 0 \\ 0 & \nu_i \end{pmatrix}, \quad (3.17)$$

by a symplectic transformation, $\Gamma_W = S \Gamma S^T$, see Ref. [200]. The *symplectic eigenvalues* $\nu_i \geq 1$, which are invariant under global symplectic transformations, form the symplectic spectrum of the covariance matrix and they can be computed as the eigenvalues

of $|i\Omega\Gamma|$. In addition to the symplectic spectrum the determinant of the covariance matrix, $\det(\Gamma)$, is a global symplectic invariant. This can be easily seen from Eq. (3.12), which implies that $\det(S) = 1$ for all symplectic operations S . We now have all the ingredients for the discussion of entanglement in phase space.

3.1.3 Two-Mode Squeezed States

The powerful tools of Gaussian states can be used to study the entanglement between different bosonic modes. As we have mentioned, a complete description of Gaussian states is provided by the first and second moments. However, the first moments can be arbitrarily adjusted using the displacements of Eq. (3.6) — operations that act *locally* on the phase spaces of particular modes. Therefore, all necessary information about the entanglement between Gaussian states is encoded solely in the *covariance matrix* Γ . For the intents and purposes of this thesis it is sufficient to consider two-mode Gaussian states only, but the analysis can be extended to more modes if so desired [6]. The paradigm for an entangled Gaussian state is the *two-mode squeezed state*, which can be produced, for example, in parametric down conversion using non-linear optical crystals, see, e.g., Ref. [93, pp. 391]. For two modes k and k' we can create such a state by acting on the vacuum with the operator

$$U_{\text{TMS}}(r) = e^{r(a_k^\dagger a_{k'}^\dagger - a_k a_{k'})}, \quad (3.18)$$

where $r \in \mathbb{R}$ is called two-mode squeezing parameter. Similar as in the case of single-mode squeezing it is possible to redefine the operator in Eq. (3.18) using a complex squeezing parameter. However, this is equivalent to applying local rotations — squeezing along different directions. For a real squeezing parameter the two-mode covariance matrix $\Gamma_{\text{TMS}}(r)$ representing the state $U_{\text{TMS}}(r) |0\rangle$ is given by

$$\Gamma_{\text{TMS}}(r) = \begin{pmatrix} \cosh(2r) & 0 & \sinh(2r) & 0 \\ 0 & \cosh(2r) & 0 & -\sinh(2r) \\ \sinh(2r) & 0 & \cosh(2r) & 0 \\ 0 & -\sinh(2r) & 0 & \cosh(2r) \end{pmatrix}. \quad (3.19)$$

The corresponding symplectic transformation $S_{\text{TMS}}(r)$, such that $S_{\text{TMS}}(r)\Gamma_{\text{vac}}S_{\text{TMS}}^T(r) = \Gamma_{\text{TMS}}(r)$, is given by $S_{\text{TMS}}(r) = \Gamma_{\text{TMS}}(\frac{r}{2})$. Alternatively, one may initially prepare the two modes in an antisymmetrically (i.e., $s_k = -s_{k'} = s$) single-mode squeezed state $\Gamma_S(s) \oplus \Gamma_S(-s)$ by applying local squeezing operations and combine the two modes on an ideal, balanced beam splitter to obtain a two-mode squeezed state $\Gamma_{\text{TMS}}(r = s)$ — a straightforward application of the Bloch-Messiah reduction (Theorem 3.1). The ideal beam splitter for the modes k and k' is realized by a passive symplectic transformation

represented [see Eqs. (3.14) and (3.15)] by the Bogoliubov coefficients $\alpha_{kk} = -\alpha_{k'k'} = \cos \Theta$ and $\alpha_{kk'} = \alpha_{k'k} = \sin \Theta$, while all other coefficients are zero, and the beam splitter is called balanced for $\Theta = \frac{\pi}{4}$. This construction is in fact even more profound, every pure, two-mode Gaussian state is locally equivalent to a two-mode squeezed state. In other words, for pure, two-mode Gaussian states the entanglement is fully characterized by the squeezing parameter r and every such state can be brought to the form of Eq. (3.19) by local rotations and single-mode squeezings that do not change the entanglement.

The Standard Form of Two-mode Gaussian States

For general, mixed states of two modes k and k' , given by the covariance matrix

$$\Gamma = \begin{pmatrix} \Gamma_k & C \\ C^T & \Gamma_{k'} \end{pmatrix}, \quad (3.20)$$

where $\Gamma_k, \Gamma_{k'}$ and C are real 2×2 matrices, it is customary to introduce the standard form Γ_{St} , given by

$$\Gamma_{\text{St}} = \begin{pmatrix} \Gamma_{\text{St-}k} & C_{\text{St}} \\ C_{\text{St}} & \Gamma_{\text{St-}k'} \end{pmatrix}, \quad (3.21)$$

where $\Gamma_{\text{St-}k} = \text{diag}\{\gamma_k, \gamma_k\}$, $\Gamma_{\text{St-}k'} = \text{diag}\{\gamma_{k'}, \gamma_{k'}\}$, and $C_{\text{St}} = \text{diag}\{\gamma_+, \gamma_-\}$, with $\gamma_k, \gamma_{k'}, \gamma_{\pm} \in \mathbb{R}$. Every covariance matrix can be converted to its standard form by local symplectic operations $S_k \oplus S_{k'}$ [182], and the standard form is unique if an ordering is specified for γ_{\pm} , e.g., $\gamma_+ \geq |\gamma_-|$. The determinants of the 2×2 sub-blocks, i.e., $\det(\Gamma_{\text{St-}k}) = \det(\Gamma_k)$, $\det(\Gamma_{\text{St-}k'}) = \det(\Gamma_{k'})$, and $\det(C_{\text{St}}) = \det(C)$, are *local symplectic invariants*. Two-mode Gaussian states for which $\Gamma_{\text{St-}k} = \Gamma_{\text{St-}k'}$ are called *symmetric*.

3.1.4 Entanglement of Gaussian States

We now turn to the quantification of entanglement of Gaussian states. As mentioned, the entanglement between two modes in a pure, Gaussian state is completely characterized by the two-mode squeezing parameter r . However, we wish to find a quantification that also relates to our previous treatment of non-Gaussian states in Chapter 1. Fortunately, we can directly connect to the tools introduced in Section 1.3.2. As shown in Ref. [182] the Peres-Horodecki criterion (Theorem 1.3) provides a necessary and sufficient condition for entanglement of two-mode Gaussian states.

The partial transposition is implemented on the phase space by a mirror operation — a sign flip — of the p -quadrature of one of the modes. The “partially transposed”

covariance matrix $\tilde{\Gamma}$ is then simply $\tilde{\Gamma} = \tilde{T}_{k'} \Gamma \tilde{T}_{k'}$, where $\tilde{T}_{k'} = \mathbb{1} \oplus \text{diag}\{1, -1\}$. In complete analogy to the usual partial transposition, the symplectic eigenvalues [see Eq. (3.17)] of $\tilde{\Gamma}$ do not necessarily correspond to a physical state anymore. The smallest eigenvalue $\tilde{\nu}_- \geq 0$ of $|i\Omega\tilde{\Gamma}|$, where $\text{spectr}(i\Omega\tilde{\Gamma}) = \{\pm\tilde{\nu}_-, \pm\tilde{\nu}_+\}$ with $\tilde{\nu}_+ \geq \tilde{\nu}_-$, can be smaller than 1, see Ref. [182].

Theorem 3.2. *A two-mode Gaussian state represented by the covariance matrix Γ is entangled if, and only if the smallest eigenvalue of $|i\Omega\tilde{\Gamma}|$ is smaller than 1,*

$$0 \leq \tilde{\nu}_- < 1.$$

The smallest symplectic eigenvalue $\tilde{\nu}_-$ (we will omit the suffix “of the partial transpose” from now on and rely on the distinction made by the “ $\tilde{}$ ” symbol) can then be used to construct the usual negativity measures.

Entanglement Measures for Gaussian States

Both the logarithmic negativity $E_{\mathcal{N}}$ [see Eq. (1.22)] and the negativity \mathcal{N} (see Definition 1.10) are monotonously decreasing functions of $\tilde{\nu}_-$ [5] such that we can write the simple expressions

$$E_{\mathcal{N}}(\Gamma) = \max\{0, -\log_2(\tilde{\nu}_-)\}, \quad (3.22a)$$

$$\mathcal{N}(\Gamma) = \max\{0, (1 - \tilde{\nu}_-)/2\tilde{\nu}_-\}. \quad (3.22b)$$

For symmetric two-mode states, i.e., for which the local symplectic invariants $\Gamma_{\text{St-}k}$ and $\Gamma_{\text{St-}k'}$ are the same, it is even possible to compute the entanglement of formation E_{F} (see Definition 1.9). The involved minimization procedure reveals that the corresponding state decomposition is realized within the set of two-mode Gaussian states [95] and the entanglement of formation can be expressed as

$$E_{\text{F}} = \begin{cases} \mathfrak{h}(\tilde{\nu}_-) & \text{if } 0 \leq \tilde{\nu}_- < 1 \\ 0 & \text{if } \tilde{\nu}_- \geq 1 \end{cases}, \quad (3.23)$$

where the entropic function $\mathfrak{h}(\tilde{\nu}_-)$ is defined as

$$\mathfrak{h}(\tilde{\nu}_-) := \frac{(1 + \tilde{\nu}_-)^2}{4\tilde{\nu}_-} \ln \frac{(1 + \tilde{\nu}_-)^2}{4\tilde{\nu}_-} - \frac{(1 - \tilde{\nu}_-)^2}{4\tilde{\nu}_-} \ln \frac{(1 - \tilde{\nu}_-)^2}{4\tilde{\nu}_-}. \quad (3.24)$$

Operationally it is also quite straightforward to check if a given covariance matrix is a symmetric two-mode Gaussian state — a necessary and sufficient condition is $\det(\Gamma_k) = \det(\Gamma_{k'})$. Moreover, for symmetric states the smallest symplectic eigenvalue $\tilde{\nu}_-$ provides a unique characterization of the entanglement, i.e., all (known) entanglement

measures are monotonously decreasing functions of $\tilde{\nu}_-$ and they provide the same ordering of entangled states [4]. Unfortunately, this is no longer true for non-symmetric two-mode Gaussian states — the answer to the question “*Is one state more entangled than another?*” generally depends on the chosen measure of entanglement [4].

As an example, let us consider again the two-mode squeezed state of Eq. (3.19). The smallest symplectic eigenvalue for this state is directly related to the two-mode squeezing parameter r via the relation $\tilde{\nu}_-(r) = e^{-2|r|}$. It can be easily seen that maximal entanglement can only be achieved in the limit $r \rightarrow \infty$. Practically, squeezing parameters of approximately $\frac{1}{2} \ln(2)$ can be reached in the current experiments with optical squeezing in the microwave regime, see, e.g., Refs. [72, 78, 138].

Teleportation with Gaussian States

Let us illustrate the role of continuous variable entanglement with the help of the teleportation protocol. In Section 1.5.3 we have discussed this fascinating application of entangled resource states for two qubits. A continuous variable teleportation protocol for the teleportation of coherent states (3.6) may be introduced in complete analogy to the qubit scenario, see Refs. [39, 191]. In this version of the teleportation scheme the observers share an entangled two-mode Gaussian state with vanishing first moments. Alice wishes to teleport an unknown coherent state, i.e., its first moments, to Bob. To this end she mixes the unknown state with her mode of the resource state on a balanced beam splitter (see p. 46) and performs *homodyne detection* — projective measurements in quadrature eigenstates (see Ref. [77, pp. 49] for details) — on the two outputs. As usual she sends the measurement results to Bob via a classical channel. Bob, in turn, can then perform the necessary displacements to retrieve, approximately, the unknown input state.

A crucial difference to the qubit teleportation lies in the imperfection of the shared entanglement. Perfect correlations between two modes of a continuous variable state — EPR correlations — would require an infinite amount of squeezing. The *teleportation fidelity* $\mathcal{F}(\Gamma)$ for the continuous variable teleportation protocol with an entangled resource state represented by the covariance matrix Γ is given by [131]

$$\mathcal{F} = \frac{2}{\sqrt{4 + 2 \text{Tr}(N) + \det(N)}}, \quad (3.25)$$

where the 2×2 matrix $N = Z\Gamma_k Z + ZC + C^T Z + \Gamma_{k'}$ is given in terms of the sub-blocks of the two-mode covariance matrix from Eq. (3.20) and $Z = \text{diag}\{1, -1\}$. The fidelity is strictly smaller than 1 for finite squeezing. We note in passing a typographical error in

Eq. (1) of Ref. [89, (ix)] as compared to Eq. (3.25) above. As in the qubit case the teleportation fidelity may be optimized over local operations that do not increase the shared entanglement [3]. The fidelity \mathcal{F}_{opt} , optimized over all local Gaussian operations, can be bounded by functions that depend only on the smallest symplectic eigenvalue of the partial transpose [131], i.e.,

$$\frac{1 + \check{\nu}_-}{1 + 3\check{\nu}_-} \leq \mathcal{F}_{\text{opt}} \leq \frac{1}{1 + \check{\nu}_-}. \quad (3.26)$$

The upper bound becomes tight for symmetric two-mode Gaussian states, see Ref. [3]. We shall make use of these tools to study the effects of non-uniform motion on the continuous variable teleportation protocol in Chapter 7.

Entanglement Resonances

The last sections have demonstrated that the entanglement of Gaussian states can be easily described, quantified and used for tasks such as quantum teleportation. In addition it is useful to understand how entanglement can be enhanced by successive symplectic transformations, for instance in applications in analogue gravity systems [43, (xi)], or non-uniform cavity motion, see Refs. [42] and [84, (vi)].

As we have established in Section 3.1.2 any symplectic transformation can be decomposed into a passive, orthogonal transformation S_{P} and an active, symmetric transformation $S_{\text{A}} = S_{\text{A}}^T$, i.e., $S = S_{\text{P}}S_{\text{A}}$ (see Ref. [16]). For two modes the passive transformations include rotations and beam splitters, while the active transformations can involve single-mode and two-mode squeezing. Let us now consider a symplectic transformation S for two modes that leaves the quadratures of the individual modes on equal footing, i.e., without any overall single-mode squeezing. The active part of the transformation thus consists only of pure two-mode squeezing, $S_{\text{A}} = S_{\text{TMS}}(r)$.

In addition, we assume that the initial covariance matrix of the two modes is proportional to the identity, $\Gamma = \mathbb{1}$. This is the case if the initial state is the vacuum state or, given that the two modes have the same frequency, a thermal state at temperature T (see p. 43). For simplicity let us pick the vacuum state. If the physical transformation that is embodied by the symplectic matrix $S = S_{\text{P}}S_{\text{TMS}}(r)$ can be repeated, then the entanglement will grow with the number of repetitions if the *resonance condition* (see [42] and [43, (xi)])

$$[S, S^T] = 0. \quad (3.27)$$

is satisfied. This condition has a very intuitive interpretation. The condition is fulfilled if the state Γ_{TMS} that is created by the two-mode squeezing, $\Gamma_{\text{TMS}} = S_{\text{TMS}} S_{\text{TMS}}^T$ is invariant under the passive transformation S_{P} , i.e.,

$$S_{\text{P}} \Gamma_{\text{TMS}} S_{\text{P}}^T = \Gamma_{\text{TMS}}. \quad (3.28)$$

At this stage it is essential to note that the two-mode squeezing operations form a one parameter subgroup of the symplectic group $\text{Sp}(2n, \mathbb{R})$,

$$S_{\text{TMS}}(r_1) S_{\text{TMS}}(r_2) = S_{\text{TMS}}(r_1 + r_2). \quad (3.29)$$

It is then straightforward to see that the resonance condition of Eq. (3.27) indicates when the repeated symplectic transformation realizes consecutive squeezing along the same direction and, consequently, accumulates entanglement. Such procedures have been suggested for various physical systems, including entanglement generation in BECs for analogue gravity experiments [43, (xi)] and for modes of quantum fields in non-uniformly moving cavities, see Refs. [42] and [84, (vi)]. We will turn our attention back on entanglement resonances in Section 6.2.2.

For now, let us return to fermionic systems and analyze the description of quantum information tasks for anticommuting field operators.

3.2 Entanglement in Fermionic Quantum Fields

Fermionic systems have been analyzed as agents for quantum information processing in a multitude of studies, ranging from discussions of fermionic modes of relativistic quantum fields [11, 48, 82, 84, 85, 87, 90, 133, 142, 181, 183], and fermionic lattices [207], to discussions of the entanglement between fixed numbers of indistinguishable particles [51, 71, 94, 113, 128, 154, 175, 176, 180, 202, 203]. In the latter case, only pure states of fixed particle numbers are considered and a selection of entanglement measures are available, see, e.g., Ref. [203]. However, these restrictions seem to be much more limiting than required. From the point of view of quantum information theory it is natural to ask for an extension to incoherent mixtures of quantum states, see Section 1.1.2. Furthermore, from the perspective of a relativistic description particle numbers are not usually conserved, i.e., the particle content of a given pure state is observer dependent (see, e.g., the discussion in Section 2.2.4 or 2.3.3). The description of fermionic entanglement should therefore include coherent and incoherent mixtures of different particle numbers. Any required superselection rules, e.g., for (electric) charge [185] or parity, can then be considered as special cases of such a framework.

In the light of this fact it is therefore reasonable to consider the entanglement between fermionic modes, in a similar way as is conventionally done for bosonic modes, see, for instance, the treatment in Section 3.1. In this section we give an account of the material published in Ref. [86, (viii)], albeit with slightly altered notations to better fit the framework of this thesis. We show that the entanglement of a system of fermionic modes can be defined unambiguously by enforcing a physically reasonable definition of its subsystems. This procedure is completely independent of any superselection rules.

A central question that appears in practical situations is: *Can fermionic modes be considered as qubits?* The short answer to this question is “No.” Due to the *Pauli exclusion principle*, fermionic modes are naturally restricted to two degrees of freedom, i.e., each mode can be unoccupied or contain a single excitation. This has provided many researchers with an *ad hoc* justification for the comparison with qubits — two-level systems used in quantum information, which has incited debates among scientists, see, e.g., the exchange in Refs. [36, 37, 140, 141]. In limited situations certain techniques from the study of qubits can indeed be applied to fermionic systems. However, while mappings between fermionic systems and qubits are possible in principle, e.g., via the Jordan-Wigner transformation [20], the problem lies in the consistent mapping between the subsystems. In the following we shall give a more precise answer to the question above, along with a detailed description of the problem as published in Ref. [86, (viii)].

Any superselection rules further restrict the possible operations that can be performed on single-mode subsystems, and it was argued that this should lead to a modified definition of the entanglement between modes [203]. At least for fixed particle content this problem can be circumvented [99]. Moreover, even if quantum correlations are not directly accessible, a transfer of the entanglement to systems that are not encumbered by such restrictions should be possible. In other words, entanglement may be swapped from the fermionic modes to systems that are not subject to superselection rules, thus justifying the use of unmodified measures for mode entanglement.

The main aim of Section 3.2 is establishing a clear framework for the implementation of fermionic field modes as vessels for quantum information tasks. To this end we present an analysis of the problem at hand, i.e., how the modes in a fermionic Fock space can be utilized as subsystems for quantum information processing. We present a framework that is based on simple physical requirements in which this can be achieved. We further discuss the issues and restrictions in mapping fermionic modes to qubits

and we show how previous work and proposed solutions, e.g., invoking superselection rules [37], fit into this framework.

Section 3.2 is structured as follows: In Section 3.2.1 we start with a brief discussion of the implementation of density operators in the fermionic Fock space introduced in Section 2.3.2. We then go on to formulate the “fermionic ambiguity” that has been pointed out in Ref. [140] in Section 3.2.2. Subsequently, we reinterpret this as an ambiguity in the definition of mode subsystems, which can be resolved by physical consistency conditions, in Section 3.2.3. Finally, we discuss the implications for the quantification of entanglement between two fermionic modes in Section 3.2.4, before we investigate situations beyond two modes in Section 3.2.5.

3.2.1 Density Operators in the Fermionic Fock Space

In complete analogy to the usual case of mixed states (1.3) on tensor product spaces we can now construct incoherent mixtures of pure states in a fermionic Fock space. For simplicity, we now restrict our analysis to a finite dimensional n -mode fermionic Fock space $\bar{\mathbb{F}}_n$ [see Eq. (2.40)]

$$\bar{\mathbb{F}}_n(\mathcal{H}_{1-f}) = \bigoplus_{m=0}^n \bar{S}(\mathcal{H}_{1-f}^{\otimes m}). \quad (3.30)$$

Let us first consider the projector on the state $|\Psi\rangle\rangle$ from Eq. (2.42), i.e.,

$$\begin{aligned} |\Psi\rangle\rangle\langle\langle\Psi| = & |\mu_0|^2 |0\rangle\rangle\langle\langle 0| + \sum_{i,i'} \mu_i \mu_{i'}^* |1_i\rangle\rangle\langle\langle 1_{i'}| + \sum_i \left(\mu_i \mu_0^* |1_i\rangle\rangle\langle\langle 0| + \text{H. c.} \right) \\ & + \sum_{j,j',k,k'} \mu_{jk} \mu_{j'k'}^* |1_j\rangle\rangle\langle\langle 1_{j'}| |1_k\rangle\rangle\langle\langle 1_{k'}| + \dots, \end{aligned} \quad (3.31)$$

where “H. c.” denotes the Hermitean conjugate, $(\mathcal{O} + \text{H. c.}) = (\mathcal{O} + \mathcal{O}^\dagger)$. We can check that such an object satisfies the criteria for a density operator:

- (i) It can be immediately noticed that (3.31) provides a *Hermitean* operator.
- (ii) The *normalization*, i.e., $\text{Tr}(|\Psi\rangle\rangle\langle\langle\Psi|) = 1$, is guaranteed by the normalization of $|\Psi\rangle\rangle$. In other words, the trace of (3.31) is well defined and independent of the chosen (complete, orthonormal) basis in $\bar{\mathbb{F}}_n$.
- (iii) *Positivity*: Finally, the eigenvalues of $|\Psi\rangle\rangle\langle\langle\Psi|$ are well defined, i.e., (3.31) can be represented as a diagonal matrix with diagonal entries $\{1, 0, 0, \dots\}$, which clearly is a positive semidefinite spectrum.

Incoherent mixtures of such pure states can then simply be formed using convex sums, i.e.,

$$\varrho = \sum_n p_n \|\Psi_n\rangle\rangle\langle\langle\Psi_n\|, \quad (3.32)$$

where $\sum_n p_n = 1$, to construct the elements of the *Hilbert-Schmidt space* $\mathcal{H}_S(\bar{\mathbb{F}}_n)$ over the fermionic Fock space. Properties (i) and (ii) can trivially be seen to be satisfied for such *mixed* states. The positivity of (3.32) — condition (iii), however, requires some additional comments. The operator ϱ can be diagonalized by a unitary transformation U on $\bar{\mathbb{F}}_n$, which in turn can be constructed from exponentiation of Hermitean or anti-Hermitean operators formed from algebra elements b_n, b_m^\dagger, c_n and c_m^\dagger . Operationally this procedure is rather elaborate. A simpler approach is the diagonalization of a matrix representation of ϱ . As we shall see in Section 3.2.2, the matrix representation of ϱ is not unique, but all possible representations $\pi_i(\varrho)$ are unitarily equivalent, such that their eigenvalues all coincide with those of ϱ , i.e.,

$$\text{spectr}(\pi_i(\varrho)) = \text{spectr}(\varrho) \quad \forall i. \quad (3.33)$$

3.2.2 The Fermionic Ambiguity

Let us now turn to the apparent ambiguity in such fermionic systems when quantum information tasks are considered. It was pointed out in Ref. [140] that the anticommutation relations (2.33) do not suggest a natural choice for the basis vectors of the fermionic Fock space for the multi-particle sector, i.e., for two fermions in the modes m and n , either

$$\|1_m\rangle\rangle\|1_n\rangle\rangle \quad \text{or} \quad \|1_n\rangle\rangle\|1_m\rangle\rangle = -\|1_m\rangle\rangle\|1_n\rangle\rangle \quad (3.34)$$

could be used to represent the physical state. This becomes of importance when we try to map the states in a fermionic n -mode Fock space to vectors in an n -fold tensor product space, i.e.,

$$\pi_i : \bar{\mathbb{F}}_n \longrightarrow \mathcal{H}_1 \otimes \dots \otimes \mathcal{H}_n \quad (3.35a)$$

$$\|\psi\rangle\rangle \xrightarrow{\pi_i} |\psi_{(i)}\rangle \quad (3.35b)$$

$$\varrho \xrightarrow{\pi_i} \pi_i(\varrho) \quad (3.35c)$$

where the spaces $\mathcal{H}_i = \mathbb{C}^2$ ($i = 1, \dots, n$) are identical, single-qubit Hilbert spaces. The mappings π_i are unitary, i.e., $\langle\langle\phi\|\psi\rangle\rangle = \langle\phi_{(i)}|\psi_{(i)}\rangle$ and $\text{Tr}(\varrho\sigma) = \text{Tr}(\pi_i(\varrho)\pi_i(\sigma))$. This implies that the maps π_i for different i are unitarily equivalent. In particular, the different matrix representations $\pi_i(\varrho)$ are related by multiplication of selected rows

and columns of the matrix by (-1) . In the language of quantum information theory the states $\psi_{(i)}$ are related by *global unitary* transformations. It thus becomes apparent that the entanglement of $\pi_i(\varrho)$ with respect to a bipartition

$$\mathcal{H}_{\mu_1} \otimes \dots \otimes \mathcal{H}_{\mu_m} | \mathcal{H}_{\mu_{m+1}} \otimes \dots \otimes \mathcal{H}_{\mu_n} \quad (3.36)$$

will generally depend on the chosen mapping. Clearly, this is an unfavorable situation, but the inequivalence of entanglement measures for different such mappings has been noted before (see, e.g., Refs. [35, 37, 51]), while other investigations [82, 84, 87] did not suffer from any problems due to this ambiguity. Recently, the authors of Ref. [37] suggested that the ambiguity can be resolved by restrictions imposed by charge superselection rules, while Refs. [140, 142] suggested a solution by enforcing a particular operator ordering. We will discuss both of these approaches in Section 3.2.3, where we present simple and physically intuitive criteria for quantum information processing on a fermionic Fock space. Most importantly, we will show in Sections 3.2.3 and 3.2.5 that mappings of the type of (3.35) can only be considered to be consistent for special cases, e.g., when the analysis is limited to two fermionic modes obeying charge superselection.

3.2.3 The Partial Trace Ambiguity

While the sign ambiguity in the sense of the different mappings π_i is the superficial cause of the issue, we want to discuss now a separate, and in some sense more fundamental problem: partial traces over “mode subspaces.” We are interested in the entanglement between modes of a fermionic quantum field. However, in the structure of the Fock space, there is no tensor product decomposition into Hilbert spaces for particular modes [see, e.g., Eq. (2.37)]. Only a tensor product structure with respect to individual fermions is available, but since the particles are indistinguishable, the entanglement between two particles in this sense has to be defined very carefully [203]. This issue is not unique for fermions and is sometimes referred to as “*fluffy bunny*” entanglement (see Ref. [202]).

For the decomposition into different modes we only have a wedge product structure available. In Ref. [37] the authors suggest that entanglement should be considered with respect to this special case of the “braided tensor product.” As far as the construction of the density operators with respect to such a structure is concerned, we agree with this view (see Section 3.2.1), and no ambiguities arise regarding the description of the total n -mode system. However, the crucial problem lies in the definition of the partial tracing over a subset of the n modes. This is best illustrated for a simple exam-

ple: Consider a system of two fermionic modes labelled κ and κ' , where we assume without loss of generality that both are positive frequency modes. A general, mixed state of these two modes can be written as

$$\begin{aligned} \varrho_{\kappa\kappa'} = & c_1 \|0\rangle\langle 0| + c_2 \|1_{\kappa'}\rangle\langle 1_{\kappa'}| + c_3 \|1_{\kappa}\rangle\langle 1_{\kappa}| + c_4 \|1_{\kappa}\rangle\langle 1_{\kappa'}| + c_5 \|1_{\kappa'}\rangle\langle 1_{\kappa}| \\ & + \left(d_1 \|0\rangle\langle 1_{\kappa'}| + d_2 \|0\rangle\langle 1_{\kappa}| + d_3 \|0\rangle\langle 1_{\kappa'}| + d_4 \|0\rangle\langle 1_{\kappa}| + d_5 \|1_{\kappa'}\rangle\langle 1_{\kappa}| \right. \\ & \left. + d_6 \|1_{\kappa'}\rangle\langle 1_{\kappa'}| + d_7 \|1_{\kappa}\rangle\langle 1_{\kappa}| + \text{H.c.} \right), \end{aligned} \quad (3.37)$$

where appropriate restrictions on the coefficients $c_i \in \mathbb{R}$ and $d_j \in \mathbb{C}$ apply to ensure the positivity and normalization of $\varrho_{\kappa\kappa'}$. Here we have, for now, disregarded superselection rules. Let us now determine the corresponding reduced density operators (on the Fock space) for the individual modes κ and κ' . Usually one would select a basis of the subsystem that is being traced over, e.g., for tracing over mode κ' one could choose $\{\|0\rangle, \|1_{\kappa'}\rangle\}$. This clearly cannot work since basis vectors with different numbers of excitations are orthogonal. We thus have to define the partial trace in a different way. This is equally true for bosonic fields as well. However, in contrast to the fermionic case, no ambiguities arise in such a redefinition for bosonic fields. For the diagonal elements of the reduced fermionic states the redefinition of the partial trace is straightforward as well. These elements are obtained from

$$\text{Tr}_m(\|0\rangle\langle 0|) := \|0\rangle\langle 0|, \quad (3.38a)$$

$$\text{Tr}_m(\|1_n\rangle\langle 1_n|) := (1 - \delta_{mn}) \|1_n\rangle\langle 1_n| + \delta_{mn} \|0\rangle\langle 0|, \quad (3.38b)$$

$$\text{Tr}_m(\|1_m\rangle\langle 1_n|) := \|1_n\rangle\langle 1_n| \quad (m \neq n), \quad (3.38c)$$

where $n, m = \kappa, \kappa'$. While the diagonal elements are unproblematic and do not suffer from any ambiguities, we have to be more careful with the off-diagonal elements. Three of these will not contribute, i.e.,

$$\text{Tr}_m(\|1_m\rangle\langle 1_n|) = \text{Tr}_m(\|0\rangle\langle 1_m|) = \text{Tr}_m(\|1_n\rangle\langle 1_m|) = 0, \quad (3.39)$$

and two more are unproblematic as well, i.e.,

$$\text{Tr}_m(\|0\rangle\langle 1_n|) := (1 - \delta_{mn}) \|0\rangle\langle 1_n|. \quad (3.40)$$

The last element,

$$\text{Tr}_m(\|1_m\rangle\langle 1_m|) = -\text{Tr}_m(\|1_m\rangle\langle 1_n|) = \pm \|0\rangle\langle 1_n|, \quad (3.41)$$

however, presents an ambiguity. If a mapping π_i to a two-qubit Hilbert space is performed, the choice of map will determine the corresponding sign in the partial trace

over either of the qubits. The differences in entanglement related to the fact that $\pi_i(\varrho)$ and $\pi_j(\varrho)$ are related by a global unitary are thus explained by the relative sign between the contributions of Eq. (3.40) and Eq. (3.41) to the same element of the reduced density matrix.

However, simple *physical requirements* restrict the choice in this relative sign. Any reduced state formalism has to satisfy the simple criterion that the reduced density operator contains all the information about the subsystem that can be obtained from the global state when measurements are performed only on the respective subsystem alone. Let us put this statement in more mathematical terms. For any bipartition $A|B$ of a Hilbert space \mathcal{H} (with respect to any braided tensor product structure on \mathcal{H}) and any state $\rho \in \mathcal{H}$ the partial trace operation Tr_B must satisfy

$$\langle \mathcal{O}_n(A) \rangle_\rho = \langle \mathcal{O}_n(A) \rangle_{\text{Tr}_B(\rho)}, \quad (3.42)$$

where $\langle \mathcal{O} \rangle_\rho$ denotes the expectation value of the operator \mathcal{O} in the state ρ and $\{\mathcal{O}_n(A)\}$ is the set of all (Hermitean) operators that act on the subspace A only. For the operator $\varrho_{\kappa\kappa'}$ from Eq. (3.37) the condition (3.42) can be written as

$$\text{Tr}(\mathcal{O}_n(\kappa)\varrho_{\kappa\kappa'}) = \text{Tr}(\mathcal{O}_n(\kappa)\varrho_\kappa), \quad (3.43)$$

where $\varrho_\kappa = \text{Tr}_{\kappa'}(\varrho_{\kappa\kappa'})$. This consistency condition uniquely determines the relative signs between different contributions to the same elements of ϱ_κ . Let us consider the (Hermitean) operators $(b_\kappa + b_\kappa^\dagger)$ and $i(b_\kappa - b_\kappa^\dagger)$. Their expectation values for the global state $\varrho_{\kappa\kappa'}$ are given by

$$\text{Tr}((b_\kappa + b_\kappa^\dagger)\varrho_{\kappa\kappa'}) = 2 \text{Re}(d_2 + d_5), \quad (3.44a)$$

$$\text{Tr}(i(b_\kappa - b_\kappa^\dagger)\varrho_{\kappa\kappa'}) = 2 \text{Im}(d_2 + d_5). \quad (3.44b)$$

For the mode κ' , on the other hand, we compute

$$\text{Tr}((b_{\kappa'} + b_{\kappa'}^\dagger)\varrho_{\kappa\kappa'}) = 2 \text{Re}(d_1 - d_6), \quad (3.45a)$$

$$\text{Tr}(i(b_{\kappa'} - b_{\kappa'}^\dagger)\varrho_{\kappa\kappa'}) = 2 \text{Im}(d_1 - d_6). \quad (3.45b)$$

Equations (3.44) and (3.45) determine the sign in Eq. (3.41) and we find the reduced states

$$\begin{aligned} \varrho_\kappa = \text{Tr}_{\kappa'}(\varrho_{\kappa\kappa'}) &= (c_1 + c_2) \|0\rangle\langle 0\| + (c_3 + c_4) \|1_\kappa\rangle\langle 1_\kappa\| \\ &+ \left((d_2 + d_5) \|0\rangle\langle 1_\kappa\| + \text{H.c.} \right), \end{aligned} \quad (3.46a)$$

$$\begin{aligned} \varrho_{\kappa'} = \text{Tr}_\kappa(\varrho_{\kappa\kappa'}) &= (c_1 + c_3) \|0\rangle\langle 0\| + (c_2 + c_4) \|1_{\kappa'}\rangle\langle 1_{\kappa'}\| \\ &+ \left((d_1 - d_6) \|0\rangle\langle 1_{\kappa'}\| + \text{H.c.} \right), \end{aligned} \quad (3.46b)$$

for the modes κ and κ' , respectively. Notice that this formally corresponds to tracing “inside out,” that is, first (anti)commuting operators towards the projector on the vacuum state before removing them, such that

$$\mathrm{Tr}_m(b_m^\dagger \| 0 \rangle \langle 0 \| b_m b_n) = \| 0 \rangle \langle 0 \| 1_n \| . \quad (3.47)$$

We have now arrived at a point where we can make a general statement about the consistency conditions. Let us formulate this in the following theorem.

Theorem 3.3. *Given a density operator $\varrho_{1,\dots,n} \in \mathcal{H}_S(\overline{\mathbb{F}}_n)$ for n fermionic modes (labelled $1, \dots, n$) the consistency conditions (3.42) completely determine the reduced states on $\mathcal{H}_S(\overline{\mathbb{F}}_m)$ for any m with $1 < m < n$.*

Proof. This can be seen in the following way: for any matrix element

$$\varphi b_{\mu_1}^\dagger \dots b_{\mu_i}^\dagger \| 0 \rangle \langle 0 \| b_{\nu_1} \dots b_{\nu_j} \quad (3.48)$$

of an $(n-1)$ -mode reduced state $\varrho_{1,\dots,(n-1)} = \mathrm{Tr}_n(\varrho_{1,\dots,n})$, where $\varphi \in \mathbb{C}$ and the sets

$$\mu := \{\mu_1, \dots, \mu_i\} \subseteq \{1, 2, \dots, (n-1)\} \quad (3.49a)$$

$$\text{and } \nu := \{\nu_1, \dots, \nu_j\} \subseteq \{1, 2, \dots, (n-1)\} \quad (3.49b)$$

label subsets of the mode operators for the $(n-1)$ modes, can have contributions from at most two matrix elements of $\varrho_{1,\dots,n}$, i.e.,

$$\mathrm{Tr}_n(\varphi_1 b_{\mu_1}^\dagger \dots b_{\mu_i}^\dagger \| 0 \rangle \langle 0 \| b_{\nu_1} \dots b_{\nu_j}), \quad (3.50a)$$

$$\text{and } \mathrm{Tr}_n(\varphi_2 b_{\mu_1}^\dagger \dots b_{\mu_i}^\dagger b_n^\dagger \| 0 \rangle \langle 0 \| b_n b_{\nu_1} \dots b_{\nu_j}). \quad (3.50b)$$

The composition of φ into $\varphi_1 \in \mathbb{C}$ and $\varphi_2 \in \mathbb{C}$, i.e., $\varphi = \varphi_1 \pm \varphi_2$, is determined by the consistency conditions of Eq. (3.42). For every matrix element (3.48) with corresponding partial trace contributions from (3.50) there exists a pair of Hermitean operators

$$\mathcal{O}_x(\lambda, \tau) = b_{\lambda_1} \dots b_{\lambda_k} b_{\tau_1}^\dagger \dots b_{\tau_l}^\dagger + b_{\tau_1} \dots b_{\tau_l} b_{\lambda_k}^\dagger \dots b_{\lambda_1}^\dagger, \quad (3.51a)$$

$$\mathcal{O}_p(\lambda, \tau) = b_{\lambda_1} \dots b_{\lambda_k} b_{\tau_1}^\dagger \dots b_{\tau_l}^\dagger - i b_{\tau_1} \dots b_{\tau_l} b_{\lambda_k}^\dagger \dots b_{\lambda_1}^\dagger, \quad (3.51b)$$

with $\lambda := \{\lambda_1, \dots, \lambda_k\} = \mu/\nu$ and $\tau := \{\tau_1, \dots, \tau_l\} = \nu/\mu$, that uniquely determine the relative sign of φ_1 and φ_2 . These operators are unique up to an overall multiplication with scalars. The tracing procedure can be repeated when any other of the $(n-1)$ remaining modes are traced over. Since the order of the partial traces is of no importance for the final reduced state, all reduced density operators are completely determined. \square

Consequently, the reduced density matrices in the fermionic Fock space can be considered as proper density operators, i.e., they are Hermitean, normalized, and their eigenvalues are well defined and non-negative. Moreover, since the eigenvalues are free of ambiguities, all functions of these eigenvalues, in particular, all entropy measures for density operators, are well defined. Also, the operator ordering that was suggested in Ref. [140] is consistent with our consistency condition. Let us stress here that this analysis does not depend on any superselection rules that might be imposed in addition. We will see how these enter the problem when mappings to qubits are attempted in Section 3.2.4.

3.2.4 Entanglement of Fermionic Modes

We are now in a position to reconsider a measure of entanglement between fermionic modes. We can define the entanglement of formation \bar{E}_F for fermionic systems with respect to a chosen bipartition $A|B$ as

$$\bar{E}_F(\varrho) = \inf_{\{(p_n, \|\Psi_n\rangle\rangle)\}} \sum_n p_n \mathcal{E}(\|\Psi_n\rangle\rangle), \quad (3.52)$$

in complete analogy to the previous Definition 1.9. Here the minimum is taken over all pure state ensembles $\{(p_n, \|\Psi_n\rangle\rangle)\}$ that realize ϱ according to Eq. (3.32) and $\mathcal{E}(\|\Psi\rangle\rangle)$ denotes the entropy of entanglement (Definition 1.6) of the pure state $\|\Psi\rangle\rangle$. Since the entropy of entanglement is a function of the eigenvalues of the reduced states $\text{Tr}_B(\|\Psi\rangle\rangle\langle\langle\Psi\|)$ or $\text{Tr}_A(\|\Psi\rangle\rangle\langle\langle\Psi\|)$ alone, we can conclude that this is a well-defined quantity. As pointed out in Ref. [51], the minimization in Eq. (3.52) can be restricted to pure state decompositions that respect superselection rules. Since this restriction limits the set of states over which the minimization is carried out, the quantity without this restriction will be a lower bound to the “physical” entanglement of formation. For two fermionic modes the minimization over all states that respect superselection rules can indeed be carried out (see Ref. [51]). However, in general this step will be problematic.

Let us now turn to some computable entanglement measures, in particular, let us investigate if and how the *negativity* \mathcal{N} (see Definition 1.10 or Ref. [194]) and the *concurrence* C (see Eq. (1.17) or Ref. [26]) can be computed to quantify fermionic mode entanglement. Both of these measures are operationally based on the tensor product structure of qubits, since the partial transposition is a map that is well defined only for basis vectors on a tensor product space. To employ this measure, let us therefore try to find a mapping π_i to such a tensor product structure that is consistent with the conditions of Eq. (3.42). Starting with the two-mode state $\varrho_{\kappa\kappa'}$ of Eq. (3.37), we are looking for

a map π that takes $\{||0\rangle\rangle, ||1_\kappa\rangle\rangle, ||1_{\kappa'}\rangle\rangle, ||1_\kappa\rangle\rangle ||1_{\kappa'}\rangle\rangle\}$ to $\{|00\rangle, |01\rangle, |10\rangle, |11\rangle\}$, where $|mn\rangle = |m\rangle \otimes |n\rangle \in \mathcal{H}_\kappa \otimes \mathcal{H}_{\kappa'}$, such that

$$\varrho \longmapsto \pi(\varrho), \quad (3.53a)$$

$$\varrho_\kappa \longmapsto \pi(\varrho_\kappa) = \text{Tr}_{\kappa'}(\pi(\varrho)), \quad (3.53b)$$

$$\varrho_{\kappa'} \longmapsto \pi(\varrho_{\kappa'}) = \text{Tr}_\kappa(\pi(\varrho)). \quad (3.53c)$$

The condition for a consistent mapping can be represented in the following diagram:

$$\begin{array}{ccc} \varrho_{\kappa\kappa'} & \xrightarrow{\pi} & \pi(\varrho_{\kappa\kappa'}) \\ \text{Tr}_{\kappa'} \downarrow & & \downarrow \text{Tr}_{\kappa'} \\ \varrho_\kappa & \xrightarrow{\pi} & \pi(\varrho_\kappa) \end{array} \quad (3.54)$$

In other words, a mapping $\pi : \varrho \mapsto \pi(\varrho)$ from the space $\mathcal{H}_S(\overline{\mathbb{F}}_2)$ to $\mathcal{H}_\kappa \otimes \mathcal{H}_{\kappa'}$ is considered to be consistent if it commutes with the partial trace operation. It is quite simple to check that these requirements generally cannot be met, i.e., writing $\varrho_{\kappa\kappa'}$ of Eq. (3.37) as a matrix with respect to the basis $\{||0\rangle\rangle, ||1_\kappa\rangle\rangle, ||1_{\kappa'}\rangle\rangle, ||1_\kappa\rangle\rangle ||1_{\kappa'}\rangle\rangle\}$ we get

$$\varrho = \begin{pmatrix} c_1 & d_1 & d_2 & d_3 \\ d_1^* & c_2 & d_4 & d_5 \\ d_2^* & d_4^* & c_3 & d_6 \\ d_3^* & d_5^* & d_6^* & c_4 \end{pmatrix}. \quad (3.55)$$

A mapping of the desired type should be obtained by multiplying any number of rows and the corresponding columns by (-1) and considering the resulting matrix as the representation $\pi(\varrho)$ on $\mathcal{H}_\kappa \otimes \mathcal{H}_{\kappa'}$. The desired result should have a relative sign switch between d_1 and d_6 , while the signs in front of d_2 and d_5 should be the same. This clearly is not possible unless some of the coefficients vanish identically, e.g., by imposing superselection rules. For example, conservation of charge would require the coefficients d_1, d_2, d_5, d_6 , and, depending on the charge of the modes κ and κ' , either d_3 or d_4 to vanish identically. In this way only incoherent mixtures of pure states with different charge are allowed, but no coherent superpositions.

We thus find that *two fermionic modes can only be consistently represented as two qubits when charge superselection is respected*. In that case only one off-diagonal element can be non-zero and the sign of this element is insubstantial, i.e., it does not influence the reduced states or the value of any entanglement measure. In particular, the results for entanglement generation and degradation between two fermionic modes presented in

Refs. [82, 85, 87, (iii-v)] respect both charge superselection and the consistency conditions of Eq. (3.42).

Let us return to the choice of entanglement measure for the permitted mappings to two qubits. We now restrict the entanglement of formation \bar{E}_F as defined in Eq. (3.52) to states that obey charge superselection, as suggested in Ref. [51]. As discussed earlier, this means the usual entanglement of formation E_F of Definition 1.9 provides a lower bound to \bar{E}_F , i.e.,

$$E_F \leq \bar{E}_F. \quad (3.56)$$

For two qubits $E_F = E_F(C)$ is a monotonically increasing function of the concurrence C . We propose an analogous functional dependence of $\bar{E}_F = \bar{E}_F(\bar{C})$ on a parameter \bar{C} , that we call “fermionic concurrence.” Evidently, the function $\bar{C}(\varrho)$ is an entanglement monotone that is bounded from below by the usual concurrence C . As can be seen from Eq. (1.23) (see also Ref. [192]), the negativity \mathcal{N} further provides a lower bound to the concurrence, i.e., in our convention of Definition 1.10, $2\mathcal{N} \leq C$. Consequently, the negativity provides a lower bound to \bar{C} , i.e.,

$$2\mathcal{N} \leq C \leq \bar{C}. \quad (3.57)$$

For two modes it is thus at least possible to compute lower bounds to entanglement measures explicitly. It was suggested in Ref. [203] that conventional entanglement measures overestimate the quantum correlations that can physically be extracted from fermionic systems. The operations that can be performed on each single-mode subsystem are limited by (charge) superselection as well. However, we conjecture that the inaccessible entanglement between the fermionic modes can always be swapped to two (uncharged) bosonic modes for which the local bases can be chosen arbitrarily.

3.2.5 Fermionic Entanglement Beyond Two Modes

Finally, let us consider the entanglement between more than two fermionic modes. In principle, any measure of entanglement that is based on entropies of the subsystems is well defined on the fermionic Fock space, as we have discussed. However, we would like to employ computable measures. Let us therefore start by attempting a consistent mapping from three fermionic modes to three qubits, in analogy to the two-mode case in Section 3.2.4. For simplicity we assume that the modes κ , κ' , and κ'' all have equal

charge such that the most general mixed state of these modes can be written as

$$\begin{aligned}
 \rho_{\kappa\kappa'\kappa''} = & \mu_1 |0\rangle\langle 0| + \mu_2 |1_{\kappa''}\rangle\langle 1_{\kappa''}| + \mu_3 |1_{\kappa'}\rangle\langle 1_{\kappa'}| + \mu_4 |1_{\kappa'}\rangle |1_{\kappa''}\rangle\langle 1_{\kappa''}| \langle 1_{\kappa'}| \\
 & + \mu_5 |1_{\kappa}\rangle\langle 1_{\kappa}| + \mu_6 |1_{\kappa}\rangle |1_{\kappa''}\rangle\langle 1_{\kappa''}| \langle 1_{\kappa}| + \mu_7 |1_{\kappa}\rangle |1_{\kappa'}\rangle\langle 1_{\kappa'}| \langle 1_{\kappa}| \\
 & + \mu_8 |1_{\kappa}\rangle |1_{\kappa'}\rangle |1_{\kappa''}\rangle\langle 1_{\kappa''}| \langle 1_{\kappa'}| \langle 1_{\kappa}| + \left(\nu_1 |1_{\kappa''}\rangle\langle 1_{\kappa'}| + \nu_2 |1_{\kappa''}\rangle\langle 1_{\kappa}| \right. \\
 & + \nu_3 |1_{\kappa'}\rangle\langle 1_{\kappa}| + \nu_4 |1_{\kappa'}\rangle |1_{\kappa''}\rangle\langle 1_{\kappa''}| \langle 1_{\kappa}| + \nu_5 |1_{\kappa'}\rangle |1_{\kappa''}\rangle\langle 1_{\kappa'}| \langle 1_{\kappa}| \\
 & \left. + \nu_6 |1_{\kappa}\rangle |1_{\kappa''}\rangle\langle 1_{\kappa'}| \langle 1_{\kappa}| + \text{H.c.} \right). \tag{3.58}
 \end{aligned}$$

The relevant consistency conditions to construct the three different reduced two-mode density matrices $\rho_{\kappa\kappa'}$, $\rho_{\kappa\kappa''}$ and $\rho_{\kappa'\kappa''}$ are given by

$$\text{Tr}\left((b_{\kappa}^{\dagger}b_{\kappa'} + b_{\kappa'}^{\dagger}b_{\kappa})\rho_{\kappa\kappa'}\right) = 2\text{Re}(\nu_3 + \nu_4), \tag{3.59a}$$

$$\text{Tr}\left((b_{\kappa}^{\dagger}b_{\kappa''} + b_{\kappa''}^{\dagger}b_{\kappa})\rho_{\kappa\kappa''}\right) = 2\text{Re}(\nu_2 - \nu_5), \tag{3.59b}$$

$$\text{Tr}\left((b_{\kappa'}^{\dagger}b_{\kappa''} + b_{\kappa''}^{\dagger}b_{\kappa'})\rho_{\kappa'\kappa''}\right) = 2\text{Re}(\nu_1 + \nu_6). \tag{3.59c}$$

Again, the correct partial traces are obtained by tracing "inside out" [see Eq. (3.47)]. This is not a coincidence. The prescription for the partial trace to anticommute operators towards the projector of the vacuum state before eliminating them takes into account the number of anticommutations occurring in computations of the expectation values of Eq. (3.42). A matrix representation of the three-mode state $\rho_{\kappa\kappa'\kappa''}$ is given by

$$\rho_{\kappa\kappa'\kappa''} = \begin{pmatrix} \mu_1 & 0 & 0 & 0 & 0 & 0 & 0 & 0 \\ 0 & \mu_2 & \nu_1 & 0 & \nu_2 & 0 & 0 & 0 \\ 0 & \nu_1^* & \mu_3 & 0 & \nu_3 & 0 & 0 & 0 \\ 0 & 0 & 0 & \mu_4 & 0 & \nu_4 & \nu_5 & 0 \\ 0 & \nu_2^* & \nu_3^* & 0 & \mu_5 & 0 & 0 & 0 \\ 0 & 0 & 0 & \nu_4^* & 0 & \mu_6 & \nu_6 & 0 \\ 0 & 0 & 0 & \nu_5^* & 0 & \nu_6^* & \mu_7 & 0 \\ 0 & 0 & 0 & 0 & 0 & 0 & 0 & \mu_8 \end{pmatrix}. \tag{3.60}$$

Similar as before, one can try to interpret Eq. (3.60) as a matrix representation of a three-qubit state and exchange the signs of the basis vectors in the three qubit state such that the consistency conditions of Eq. (3.59) are met, i.e., opposite signs in front of ν_2 and ν_6 , while the signs in front of the pairs ν_3, ν_4 and ν_1, ν_6 are each the same. This is not possible, even though superselection rules are respected. This suggests that the superselection rules only coincidentally aid the fermionic qubit mapping for two modes. They simply force all the problematic coefficients to disappear. However, for more than two modes we find here that a mapping to a tensor product space cannot be

performed consistently in general. Therefore, computing a measure like the negativity to determine the entanglement between more than two modes appears to be meaningless. Due to the lack of practical alternatives, the minimization over all states consistent with charge superselection to find \bar{E}_F of Eq. (3.52) should be considered since the restriction of the set of permissible states could make this computation feasible.

Let us briefly summarize the key aspects of Section 3.2. We have discussed the implementation of fermionic modes as fundamental objects for quantum information tasks. The foundation of this task is the rigorous construction of the notion of mode subsystems in a fermionic Fock space. We have demonstrated that this can be achieved despite the absence of a simple tensor product structure. Our simple consistency conditions give a clear picture of this process, which can be easily executed operationally by performing partial traces “inside out.” Thus we show that fermionic mode entanglement, quantified by the (fermionic) entanglement of formation or any other function of the eigenvalues of the reduced states, is indeed a well-defined concept, free of any ambiguities and independent of any superselection rules.

However, problems arise when mappings from the fermionic Fock space to qubit spaces are attempted. We have explicitly demonstrated in two examples, for two and three modes, that such mappings cannot generally succeed. Only in the limited case where only two modes are considered and the quantum states obey charge superselection can one meaningfully speak of an equivalence between the two fermionic modes and two qubits. In this case the application of tools such as the negativity or concurrence is justified. We have argued that these measures will at least provide a lower bound to genuine measures of fermionic mode entanglement.

Nonetheless, open questions remain. In particular, it is not clear if any practically computable measures exist for situations beyond two qubits. In Ref. [84, (vi)], which we will discuss in Section 6.4, we have employed the witnesses for genuine multipartite entanglement presented in Theorem 1.4 (see also Refs. [92, 112]) for fermionic modes. These witnesses are completely compatible with the framework we have presented here, but they can only provide lower bounds to entropic entanglement measures.

Finally, we have conjectured that the entanglement in fermionic modes is accessible even in spite of superselection rules that restrict the possible operations performed on single modes by means of entanglement swapping. The investigation of this question, while beyond the scope of this thesis, will certainly be of future interest.

Part II

Shaking Entanglement

Quantum Correlations in *Non-Uniformly* Moving Cavities

Constructing Non-Uniformly Moving Cavities

It is the aim of this chapter to establish the mathematical model for relativistically rigid cavities that has been introduced by *David Bruschi, Ivette Fuentes, and Jorma Louko* in Ref. [44] in the context of quantum information procedures, but shares features with earlier work, see e.g., Refs. [14, 61, 63–65]. The framework has later been extensively expanded, including extensions to $(1 + 1)$ dimensional cavities for massless fermionic fields [87, (iv)] and smoothly varying accelerations for cavities containing bosonic fields [47]. Recently, the cavity model has been further extended in Ref. [88, (x)] to allow for fully $(3 + 1)$ dimensional quantum fields, including massive and massless scalar fields, massive and massless Dirac fields, as well as the electromagnetic field.

The initial motivation for a relativistic cavity model originates in RQI. Relativistic quantum fields are affected by the kinematics of spacetime, changes in boundary conditions, and the presence of horizons. Therefore, well known phenomena such as the Hawking-effect, or the Unruh-effect, associated to black holes and accelerated motion respectively (see, e.g., Ref. [30]), are expected to influence relativistic quantum information processing [10]. However, for a meaningful, operational description of RQI it is essential to enforce some notion of localization. In other words, the “local” (in the sense of the tensor product) observer needs unrestricted control over his quantum system, which, in turn, requires the system to be spatially localizable with respect to the observer. This is certainly not the case for global modes of a quantum field in the whole Minkowski spacetime. Such solutions can be regarded as a means to handle a scattering theory, but for the purpose of RQI other approaches have to be considered.

The ideas for localization in RQI are numerous, e.g., by considering wave-packets [68,

69], or Unruh-DeWitt type detectors [40, 45, 127]. The confinement of a quantum field in a cavity of finite length is the method that we shall discuss here. This framework will not remove issues inherent to quantum field theory, for instance, we are not proposing our method as a solution to conceptual problems of relativistic quantum measurement theories [184]. However, it seems reasonable to assume that measurements in a laboratory involve length scales of, say, centimeters, rather than lightyears, which may well also practically remove the conceptual issues raised in [184]. With these restrictions in mind, the relativistic cavity model provides a conceptually satisfying theoretical apparatus to study the fundamental connection between non-uniform motion, particle creation and quantum correlations.

Recently, the relativistic cavity model, using a scalar field as representative for electromagnetic radiation [88, (x)], has generated interest also as a possible system for experimental tests employing *superconducting circuits*. The conceptual similarity to the *dynamical Casimir effect* (see Section 4.4.3), which has recently been verified for such materials [123, 201], in principle allows for analogous tests of more general effects of non-uniform motion. Such an experimental setup was proposed in Ref. [89, (ix)] and we shall discuss the setup in Chapter 7. The fermionic cavity model, on the other hand, is motivated by the prospect of simulating effects of non-uniform motion in analogue fermionic solid state systems, see, e.g., Refs. [31, 114, 208].

This chapter is structured as follows: in Section 4.1 we discuss the geometric aspects of rigid cavities in Minkowski spacetime. In Sections 4.2 and 4.3 we then go on to study respectively the quantized scalar field and Dirac field in inertial and uniformly accelerated cavities. We match the segments of uniform motion to construct rigid cavities that are moving non-uniformly. In Section 4.4 different trajectories — travel scenarios — are constructed, including smoothly varying accelerations.

Note that we are using unit where $\hbar = c = 1$ throughout.

4.1 The Relativistically Rigid Cavity

Before we start to consider quantum fields in cavities, let us ask about the cavity itself. In particular we have to inquire “*How can we describe a rigid cavity in relativity?*” We attempt to answer this question by explaining the notion of rigidity we have chosen for our model. Ultimately, every model needs to be compared with empirical data, but we will argue here that the construction introduced in Ref. [44] is a conceptually satisfying approach.

Inertial Rigid Cavity

The starting point is an ideally lossless, inertial cavity of fixed length L in a $(1 + 1)$ dimensional Minkowski spacetime. We pick a co-moving inertial frame with coordinates (t, x) such that for all times t the boundaries of the cavity are located at x_L and x_R , respectively, where $x_R - x_L = L > 0$, see Fig. 4.1.

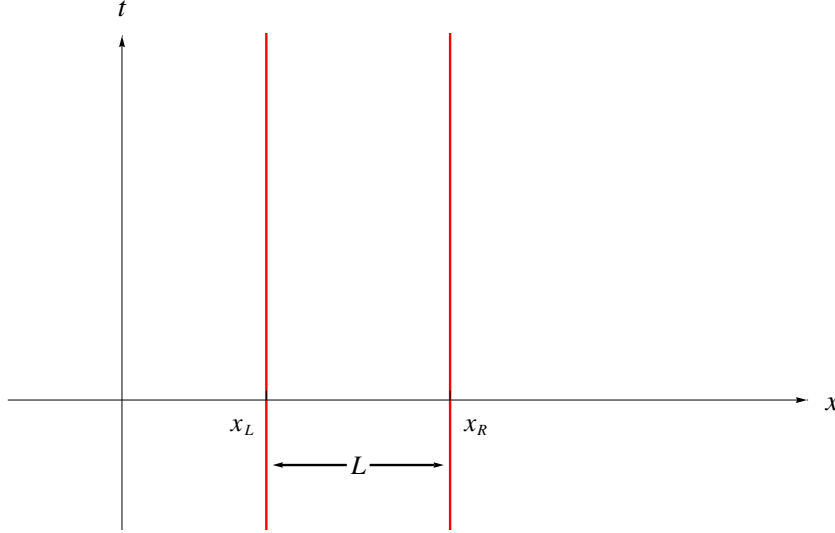


Figure 4.1: Inertial rigid cavity: From the point of view of a co-moving observer with coordinates (t, x) , the inertial, rigid cavity has boundaries at $x = x_L$ and $x = x_R$, such that the cavity has the proper length $L = x_R - x_L$.

From the point of view of inertial observers that are moving with a constant velocity v with respect to this cavity its length L_v is seen to be Lorentz contracted, i.e., $L_v = L\sqrt{1 - v^2}$, where L is the proper length [see Eq. (2.3)] as measured by the observer co-moving with the cavity. In technical terms, $x(t) = x_L$ and $x(t) = x_R$ are integral curves of the global time-like Killing vector ∂_t , see Definition 2.2 and Eq. 2.5. In other words, the cavity walls are “dragged along” by the Killing vector ∂_t . In principle the coordinates could have been picked such that $x_L = 0$ and $x_R = L$ but the choice of $x_L > 0$ will be more convenient for the accelerating cavity.

Accelerated Motion — Rindler Coordinates

In order to accelerate the cavity walls we consider appropriate coordinates — *Rindler coordinates* (η, χ) , see Ref. [187]. For the quadrant $|t| < x$ (without loss of generality we accelerate towards increasing x) we choose the hyperbolic Rindler coordinates

$$t = \chi \sinh(\eta), \quad (4.1a)$$

$$x = \chi \cosh(\eta), \quad (4.1b)$$

where $0 < \chi < \infty$ and $-\infty < \eta < \infty$, see Fig. 4.2. Let us see why these coordinates are suitable for accelerated motion. From Eqs. (4.1) one can easily see that the lines of constant χ are time-like (see Definition 2.2) and can therefore be used to describe an (ideally point-like) observer. From Eq. (2.2) it can be straightforwardly verified that the proper time τ along a worldline $\chi = \text{const.}$ is given by $\tau = \chi\eta$. The coordinate time η is thus proportional to the proper time for fixed χ . Parameterizing the worldline by τ and taking the second derivative with respect to the proper time one arrives at

$$a^\mu(\tau) = \frac{d^2}{d\tau^2}x^\mu(\tau) = \frac{1}{\chi} \begin{pmatrix} \sinh(\tau/\chi) \\ \cosh(\tau/\chi) \end{pmatrix}. \quad (4.2)$$

The magnitude \mathbf{a} of this vector (with respect to the $(1+1)$ dimensional Minkowski metric $\text{diag}\{-1, +1\}$), i.e., where $\mathbf{a}^2 = a^\mu a_\mu$, is called the *proper acceleration* and it is here given by $\mathbf{a} = 1/\chi$. Physically the proper acceleration is the Newtonian acceleration along the worldline as measured in the instantaneous rest frame. In conclusion, lines of constant χ correspond to worldlines of (ideally point-like) observers with fixed proper acceleration $1/\chi$ towards increasing values of x and proper time $\chi\eta$. If so chosen, leftward acceleration can be described by a second set of Rindler coordinates for the quadrant $|t| < -x$ with the replacement $x \rightarrow -x$ in Eqs. (4.1), see p. 77.

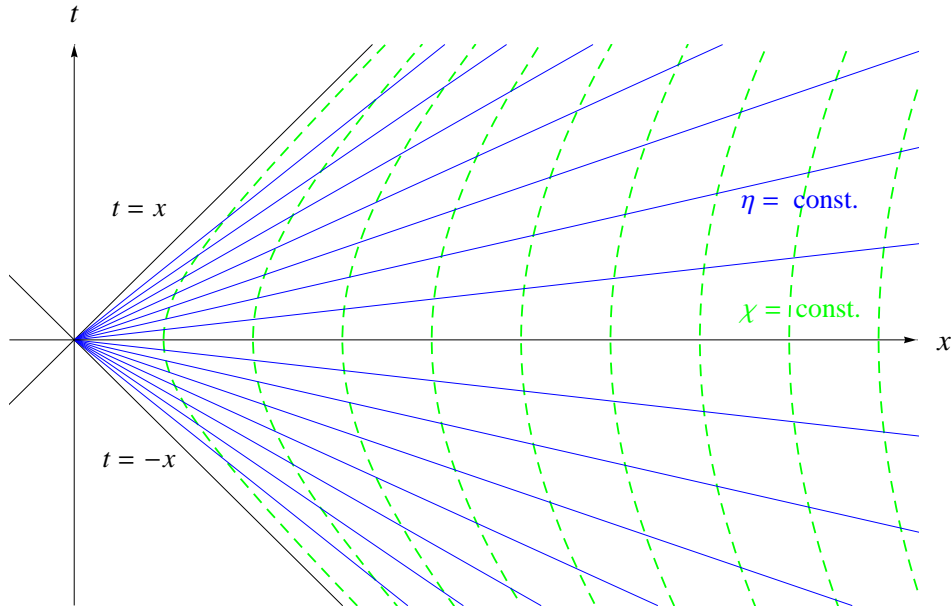


Figure 4.2: Rindler coordinates: Lines of constant χ (dashed green confocal hyperbolae) and constant η (solid blue radial lines) are shown for selected values of the coordinates in the right Rindler wedge $|t| < x$. The Rindler horizon is indicated by the solid black lines $t = x$ and $t = -x$. The hyperbolae $\chi = \text{const.}$ describe a family of (point-like) observers that are eternally uniformly accelerated.

Accelerated Rigid Cavity

To use Rindler coordinates in the construction of an accelerating cavity it is still necessary to give some thought to the notion of *rigidity*. Let us consider one cavity wall that is following a worldline of constant $\chi = \chi_L$. At every instant of the coordinate time η the plane of simultaneity from the perspective of an observer identified with the cavity wall is the line of constant η . Note that the proper distance [Eq. (2.3)] between two different hyperbolae $\chi = \chi_L = \text{const.}$ and $\chi = \chi_R = \text{const.}$ along lines of fixed η is constant as well. Thus, a cavity of length $L = \chi_R - \chi_L$ with walls that are uniformly accelerating with *different* proper accelerations $1/\chi_L$ and $1/\chi_R$, respectively, can be considered to be rigid. The argument can be extended to any part of the cavity between the two walls, e.g., an observer placed in the centre of the cavity whose proper acceleration is given by $2/(\chi_R + \chi_L)$ experiences the walls at fixed proper distance $L/2$ throughout the journey. In analogy to the inertial case the uniformly accelerated boundaries can now be considered to be “dragged along” by the Killing vector $\partial_\eta = x\partial_t + t\partial_x$.

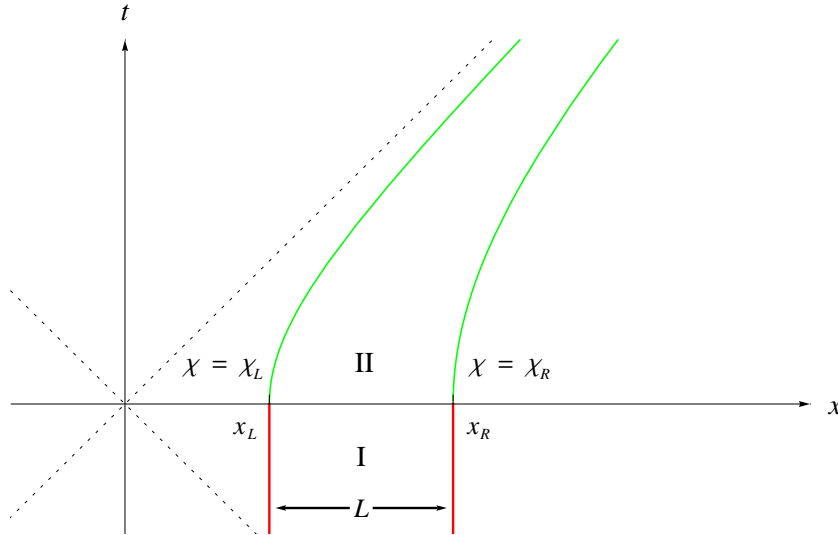


Figure 4.3: Relativistically rigid cavity: The rigid inertial (region I) and uniformly accelerated (region II) cavities can be combined by pasting together the boundaries $x = x_L$ and $x = x_R$, with $\chi = \chi_L$ and $\chi = \chi_R$, respectively, at $\eta = t = 0$. The proper length with respect to a co-moving observer is $L = x_R - x_L$. The dashed lines indicate the light cone at the origin.

At last, the inertial cavity depicted in Fig 4.1 can be uniformly accelerated by pasting the inertial and uniformly accelerated trajectories of the cavity walls along slices of fixed η , such that $\chi_L = x_L$ and $\chi_R = x_R$. The tangent vectors of the trajectories are orthogonal to the corresponding line $\eta = \text{const.}$ in the sense of the Minkowski metric (see p. 30), see Fig. 4.3. We shall extend this framework to generic trajectories in Section 4.4.

4.2 Scalar Fields in Rigid Cavities

For the quantization of the fields we adopt the same strategy as for the geometric construction. We first consider the quantization procedure for the scalar field individually for an inertial and a uniformly accelerated cavity before we match the two. The whole programme is then repeated for the Dirac field in Section 4.3.

4.2.1 Cavity in Uniform Motion — Scalar Field

Scalar Field in Inertial Cavity

Let us consider a real, scalar field ϕ in a $(1+1)$ dimensional Minkowski spacetime with metric $ds^2 = \eta_{\mu\nu} dx^\mu dx^\nu = -dt^2 + dx^2$. The field satisfies the *Klein-Gordon equation* [see Eq. (2.9)]

$$(-\square + m^2)\phi(t, x) = 0, \quad (4.3)$$

where $\square = \eta^{\mu\nu} \partial_\mu \partial_\nu$ is the scalar Laplacian and $m \geq 0$ is the mass to be associated with the excitations of the quantum field. To confine the mode solutions ϕ_n to the inertial cavity discussed in Section 4.1 we impose the *Dirichlet boundary conditions*

$$\phi_n(t, x_L) = \phi_n(t, x_R) = 0. \quad (4.4)$$

Alternatively, other boundary conditions, for instance Neumann boundary conditions may be chosen. This is of relevance when a Maxwell field is considered in a cavity, for which the two polarization degrees of freedom behave like Dirichlet and Neumann scalar fields, respectively [88, (x)]. The qualitative features of the scalar field cavity model under these two types of conditions are the same, and the Dirichlet conditions seem to be the intuitively most natural restrictions to model perfectly reflecting cavity walls for the scalar field. Therefore, we shall be content to focus our discussion on the Dirichlet boundary condition of Eq. (4.4) above. For the situation here the Klein-Gordon (pseudo) inner product of Eq. (2.11) reads

$$(\phi_m, \phi_n)_{\text{KG}} = -i \int_{x_L}^{x_R} dx (\phi_m \partial_t \phi_n^* - \phi_n^* \partial_t \phi_m). \quad (4.5)$$

A standard basis of orthonormal [w.r.t. the inner product (4.5)] solutions to Eq. (4.3), subject to the boundary conditions of Eq. (4.4), can be found to be

$$\phi_n(t, x) = \frac{1}{\sqrt{\omega_n L}} \sin\left(\frac{n\pi(x - x_L)}{L}\right) e^{-i\omega_n t}. \quad (4.6)$$

The field modes ϕ_n are labelled by the discrete index $n = 1, 2, 3, \dots$, and are of positive frequency

$$\omega_n = \frac{1}{L} \sqrt{M^2 + (\pi n)^2}, \quad (4.7)$$

where we have introduced the dimensionless parameter $M := mL$, with respect to the Minkowski time-translation Killing vector ∂_t . The phase in Eq. (4.6) has been chosen such that $\partial_x \phi_n > 0$ at $(t, x) = (0, x_L)$. In the inertial region the field can be decomposed as

$$\phi = \sum_n (\phi_n a_n + \phi_n^* a_n^\dagger), \quad (4.8)$$

where the field operators a_n and a_n^\dagger satisfy the commutation relations of Eqs. (2.15).

Scalar Field in Uniformly Accelerated Cavity

To quantize the field in the accelerated region II of Fig. 4.3 we again employ the Rindler coordinates (η, χ) of Eq. (4.1) for which the line element is

$$ds^2 = -\chi^2 d\eta^2 + d\chi^2. \quad (4.9)$$

Since now $\sqrt{-\det g} = \chi$ and $g^{\mu\nu} = \text{diag}\{-1/\chi^2, 1\}$ we can rewrite the Klein-Gordon equation (2.9) in Rindler coordinates,

$$(-\partial_\eta^2 + (\chi\partial_\chi)^2 - m^2\chi^2)\phi(\eta, \chi) = 0. \quad (4.10)$$

Before applying the boundary conditions it is useful to make the ansatz $\phi(\eta, \chi) = f(\chi)e^{-i\Omega\eta}$ for the solutions such that Eq. (4.10) can be cast into the form

$$(\chi^2\partial_\chi^2 + \chi\partial_\chi - [m^2\chi^2 + (i\Omega)^2])f(\chi) = 0. \quad (4.11)$$

With a simple coordinate re-scaling $\chi \rightarrow m\chi$, where $\partial_\chi \rightarrow m^{-1}\partial_\chi$ and we assume $m > 0$, it becomes apparent that Eq. (4.11) is the *modified Bessel equation* [145]. At this stage we enforce the Dirichlet boundary conditions

$$\tilde{\phi}_n(\eta, \chi_L) = \tilde{\phi}_n(\eta, \chi_R) = 0, \quad (4.12)$$

for the region II field modes $\tilde{\phi}_n$ in complete analogy to Eq. (4.4). The inner product of Eq. (2.11) for the metric (4.9) now reads [187]

$$(\tilde{\phi}_m, \tilde{\phi}_n)_{\text{KG}} = -i \int_{\chi_L}^{\chi_R} d\chi \chi^{-1} (\tilde{\phi}_m \partial_\eta \tilde{\phi}_n^* - \tilde{\phi}_n^* \partial_\eta \tilde{\phi}_m). \quad (4.13)$$

A basis of mode functions that are orthogonal in the inner product (4.13) and that are of positive frequency with respect to the time-like boost Killing vector ∂_η are given by

$$\tilde{\phi}_n(\eta, \chi) = N_n e^{-i\Omega_n \eta} [I_{-i\Omega_n}(\mathbf{m}\chi_L) I_{i\Omega_n}(\mathbf{m}\chi) - I_{i\Omega_n}(\mathbf{m}\chi_L) I_{-i\Omega_n}(\mathbf{m}\chi)], \quad (4.14)$$

where N_n is a normalization constant, the modes are labelled $n = 1, 2, 3, \dots$, and the quantities $I_{\pm i\Omega_n}(\mathbf{m}\chi)$ are the *modified Bessel functions of the first kind* [145]. Finally, the Rindler frequencies Ω_n , which are ordered by ascending mode label, i.e., $\Omega_m > \Omega_n$ for $m > n$, are determined by the second boundary condition $\tilde{\phi}_n(\eta, \chi_R) = 0$. The particular form of Ω_n and the choice of N_n are best discussed in the context of the transition between the inertial region I and the accelerated region II, which we shall do in the following Section 4.2.2. The quantum field in region II is now naturally decomposed into the modes $\tilde{\phi}_n$ as

$$\phi = \sum_n (\tilde{\phi}_n \tilde{a}_n + \tilde{\phi}_n^* \tilde{a}_n^\dagger), \quad (4.15)$$

where the field operators \tilde{a}_n and \tilde{a}_n^\dagger satisfy $[\tilde{a}_m, \tilde{a}_n^\dagger] = \delta_{mn}$ and $[\tilde{a}_m, \tilde{a}_n] = 0$.

4.2.2 Matching: Inertial to Rindler — Scalar Field

Consider now the transition between the inertial region I and the uniformly accelerated region II. At $t = 0$ the cavity walls suddenly accelerate, such that their velocity changes smoothly but their proper accelerations have finite jumps, $0 \rightarrow 1/\chi_L$ and $0 \rightarrow 1/\chi_R$, respectively. We model the instantaneous change in the mode structure by a linear transformation — a *Bogoliubov transformation*, see Definition 2.3, which is of the form

$$\tilde{\phi}_m = \sum_n ({}_o\alpha_{mn} \phi_n + {}_o\beta_{mn} \phi_n^*), \quad (4.16)$$

as illustrated in Fig. 4.4. From the field decompositions (4.8) and (4.15) the Minkowski to Rindler Bogoliubov coefficients ${}_o\alpha_{mn}$ and ${}_o\beta_{mn}$ can be written as

$${}_o\alpha_{mn} = (\tilde{\phi}_m, \phi_n)_{\text{KG}}, \quad (4.17a)$$

$${}_o\beta_{mn} = -(\tilde{\phi}_m, \phi_n^*)_{\text{KG}}, \quad (4.17b)$$

where one may either evaluate the inner product (4.5) at $t = 0$ or, equivalently, (4.13) at $\eta = 0$. Unfortunately, even though it is straightforward to write the abstract definitions of Eq. (4.17), the corresponding integrals do not yield expressions in terms of known elementary functions. However, it is convenient to perform a suitable power expansion of the integrand. To this end it is useful to parameterize the cavity geometry by the quantities L and h , where the dimensionless parameter

$$h = \mathbf{a}_c L \quad (4.18)$$

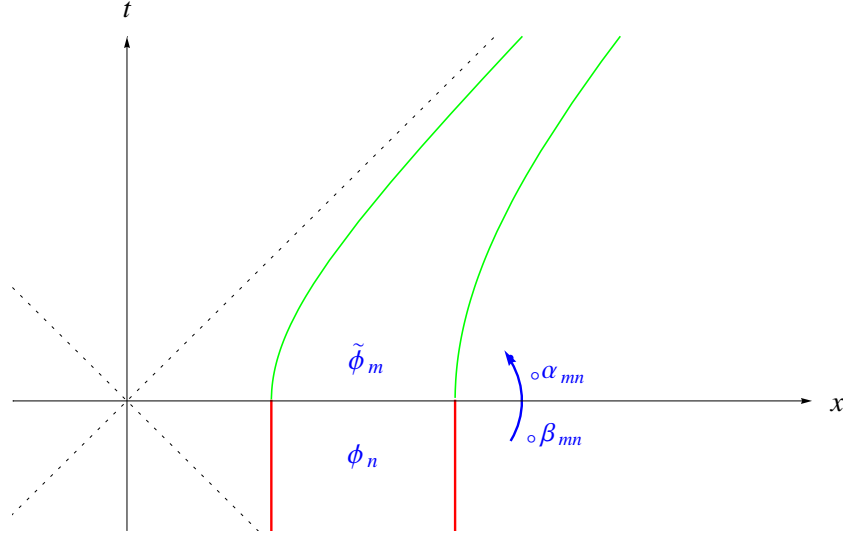


Figure 4.4: Minkowski to Rindler Bogoliubov transformation — scalar field: The cavity modes ϕ_n in the inertial region and the modes $\tilde{\phi}_m$ in the uniformly accelerated region are related by a Bogoliubov transformation with coefficients ${}_{\circ}\alpha_{mn}$ and ${}_{\circ}\beta_{mn}$, see Eq. (4.16).

is the product of the proper acceleration $\mathbf{a}_c = 2/(\chi_R + \chi_L)$ (see p. 70) at the centre of the cavity and its width $L = (\chi_R - \chi_L)$. The cavity boundaries, expressed through h and L read

$$\chi_L = \left(\frac{1}{h} - \frac{1}{2} \right) L, \quad (4.19a)$$

$$\chi_R = \left(\frac{1}{h} + \frac{1}{2} \right) L, \quad (4.19b)$$

where $0 < h < 2$ such that the acceleration at both ends remains finite. We shall work perturbatively in h from now on, i.e., we are interested in finding Taylor-Maclaurin expansions around $h = 0$ for all quantities of interest. First, noting that the coordinate time η is dimensionless we find that the proper time observed at the centre of the cavity is given by $L\eta/h$. The angular frequencies $\tilde{\omega}_n$ with respect to this proper time are then obtained from the dimensionless Rindler frequencies Ω_n as

$$\tilde{\omega}_n = \frac{h}{L} \Omega_n = \frac{n\pi h}{2L \operatorname{artanh}(h/2)} = \omega_n (1 + O(h^2)), \quad (4.20)$$

where $O(x)$ denotes a quantity for which $O(x)/x$ is finite for $x \rightarrow 0$. To leading order in the expansion the Minkowski and Rindler mode functions, ϕ_n and $\tilde{\phi}_n$, must be equal up to a phase factor, which we set to unity in the normalization constant N_n of Eq. (4.14) such that $\partial_\chi \tilde{\phi}_n > 0$ at $(\eta, \chi) = (0, \chi_L)$. Since both the order and the arguments of the modified Bessel functions $I_{\pm i\Omega_n}(m\chi_L)$ in Eq. (4.14) diverge at $h = 0$ we have to use the corresponding uniform asymptotic expansions [70] to obtain the perturbative

expansion of the inner products in (4.17). With some computational effort expansions of the Bogoliubov coefficients are obtained as

$${}_o\alpha_{mn} = {}_o\alpha_{mn}^{(0)} + {}_o\alpha_{mn}^{(1)} h + {}_o\alpha_{mn}^{(2)} h^2 + O(h^3), \quad (4.21a)$$

$${}_o\beta_{mn} = {}_o\beta_{mn}^{(1)} h + {}_o\beta_{mn}^{(2)} h^2 + O(h^3), \quad (4.21b)$$

where the superscripts (n) indicate the coefficients of h^n . The leading order is ${}_o\alpha_{mn}^{(0)} = \delta_{mn}$, while ${}_o\alpha_{nn}^{(1)} = {}_o\beta_{nn}^{(1)} = 0$. For $m \neq n$ we find the linear terms

$${}_o\alpha_{mn}^{(1)} = -\frac{\pi^2 mn (1 - (-1)^{m+n})}{L^4 \sqrt{\omega_m \omega_n} (\omega_m - \omega_n)^3}, \quad (4.22a)$$

$${}_o\beta_{mn}^{(1)} = \frac{\pi^2 mn (1 - (-1)^{m+n})}{L^4 \sqrt{\omega_m \omega_n} (\omega_m + \omega_n)^3}, \quad (4.22b)$$

with ω_n given by Eq. (4.7). Note that the linear coefficients vanish for mode pairs (m, n) with equal parity, i.e., ${}_o\alpha_{mn}^{(1)} = {}_o\beta_{mn}^{(1)} = 0$ if $(m+n)$ is even. The second order coefficients can be obtained with the same procedure, but we will not need their explicit form in the following. However, we shall note that it has been verified that the Bogoliubov coefficients up to and including second order are satisfying the Bogoliubov identities (2.27) when terms proportional to h^2 are kept. In addition, the second order coefficients ${}_o\alpha_{mn}^{(2)}$ and ${}_o\beta_{mn}^{(2)}$ are proportional to $(1 + (-1)^{m+n})$ and, consequently, vanish for index pairs (m, n) with opposite parity, i.e., if $(m+n)$ is odd.

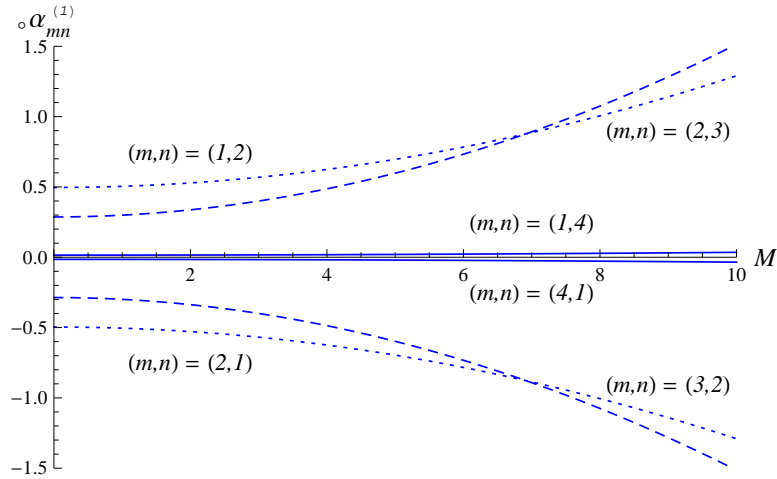


Figure 4.5: Minkowski to Rindler Bogoliubov coefficients — scalar field α 's: The behaviour of the leading order “mode mixing” Bogoliubov coefficients ${}_o\alpha_{mn}^{(1)}$ from (4.22a) is shown for increasing mass of the $(1+1)$ -dimensional real scalar field with Dirichlet boundary conditions. A selection of the coefficients ${}_o\alpha_{mn}^{(1)}$ is plotted against the dimensionless combination $M := mL$. The coefficients are proportional to M^2 as $M \rightarrow \infty$, while the intersections with the vertical axis give the massless limit, $m \rightarrow 0$, of Eq. (4.22a).

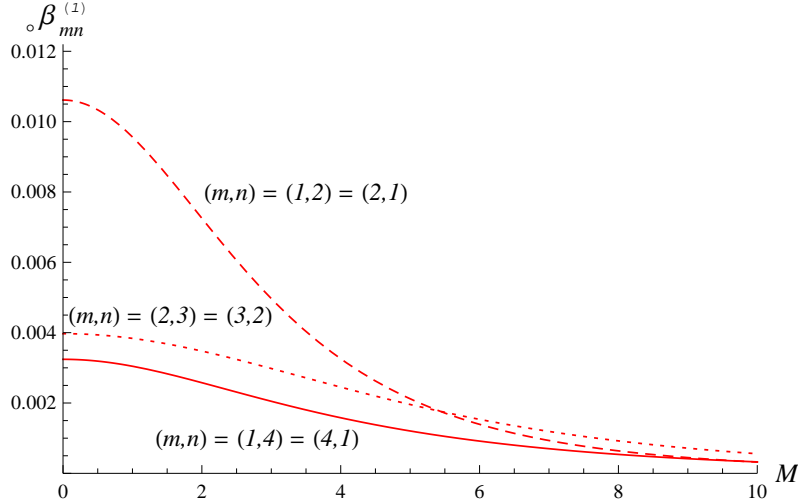


Figure 4.6: Minkowski to Rindler Bogoliubov coefficients — scalar field β 's: The behaviour of the leading order “particle creation” Bogoliubov coefficients $\circ\beta_{mn}^{(1)}$ from (4.22b) is shown for increasing mass of the $(1+1)$ -dimensional real scalar field with Dirichlet boundary conditions. A selection of the coefficients $\circ\beta_{mn}^{(1)}$ is plotted against the dimensionless combination $M := mL$. The coefficients are proportional to M^{-4} as $M \rightarrow \infty$, while the intersections with the vertical axis give the massless limit, $m \rightarrow 0$, of Eq. (4.22b).

We trust the perturbative expansion for $h \ll 1$ when the indices of the coefficients are bounded from above by any constant. For non-zero mass we additionally require that $Mh \ll 1$ but within this regime we allow for $M \gg 1$ such that $M^2h \lesssim 1$. In that case the dominant contributions to the coefficients $\circ\alpha_{mn}^{(1)}$ behave as M^2 , while the coefficients $\circ\beta_{mn}^{(1)}$ are suppressed as M^{-4} . Further considerations regarding the perturbative regime will be presented as demanded by the applications, for instance in Chapter 5. Finally, even though it was assumed that $m > 0$ to obtain (4.14) it can be verified that the limit $m \rightarrow 0$ in (4.21) coincides with the results obtained if the mass m is set to zero from the start, see, e.g., Ref. [44].

Leftward Acceleration

As explained in Section 4.1 we have so far considered acceleration towards increasing values of x . For accelerations towards decreasing x we may repeat the whole procedure laid out in the previous sections in a similar way. Instead of (4.1) we may introduce Rindler coordinates (η', χ') for the quadrant $|t| < -x$ via

$$t = \chi' \sinh(\eta'), \quad (4.23a)$$

$$x = -\chi' \cosh(\eta'). \quad (4.23b)$$

The metric now reads $ds^2 = -\chi'^2 d\eta'^2 + d\chi'^2$, as before in (4.9) but with the primed Rindler coordinates. For the inertial cavity the positions of the left and right cavity boundaries are now at $-x_R$ and $-x_L$, respectively, i.e., the cavity geometry has been mirrored with respect to $x = 0$. For the leftward accelerated region the left and right wall now follow segments of the hyperbolae $\chi' = \chi_R$ and $\chi' = \chi_L$, respectively, see Fig. 4.7. The Bogoliubov coefficients, i.e., the inner products (4.17) of the mirrored

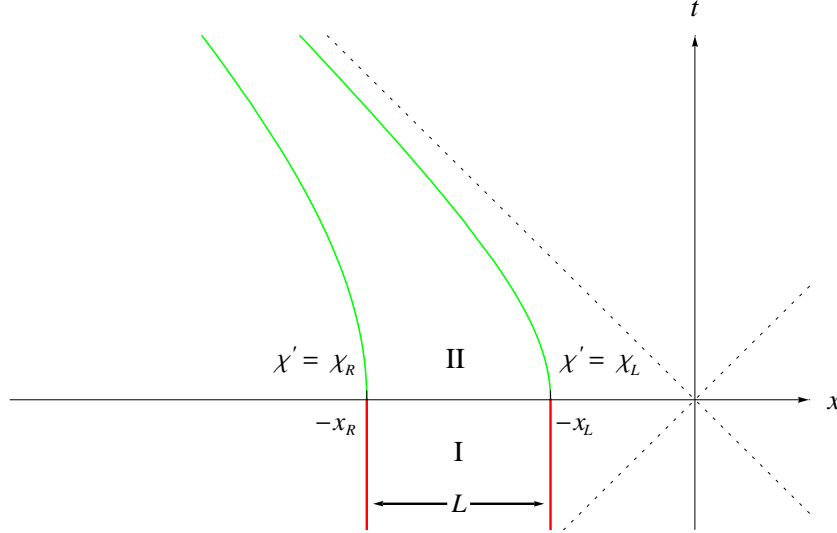


Figure 4.7: Acceleration to the left: The cavity is mirrored to the left Rindler wedge $|t| < -x$. The spatial reflection leaves the Bogoliubov coefficients unchanged but the inverted signs of the odd modes have to be taken into account when matching the phases of the modes.

cavity modes ϕ'_n and $\tilde{\phi}'_m$, are left unchanged by such a reflection. However, to match our previous phase convention we require $\partial_x \phi_n|_{t=0} > 0$ and $\partial_{\eta'} \tilde{\phi}'_m|_{\eta=0} > 0$ at the left boundaries. For the even modes $m, n = 1, 3, 5, \dots$, this is automatically satisfied, but we have to compensate for the sign flip of the odd modes $m, n = 2, 4, \dots$, acquired due to the reflection. Therefore we include factors of $(-1)^{n+1}$ and $(-1)^{m+1}$ for the Minkowski and (left wedge) Rindler modes, respectively. In conclusion we find that the coefficients for leftward acceleration are obtained from the rightward acceleration coefficients ${}_o\alpha_{mn}$ and ${}_o\beta_{mn}$ in (4.17) by inclusion of a factor $(-1)^{m+n}$. Practically this may be implemented by assuming the expansions (4.21), including \hbar^2 contributions, to hold for both cases with positive (negative) h indicating acceleration towards increasing (decreasing) values of x .

As a last comment before we turn to the Dirac field in Section 4.3 we note that the case of linear acceleration in $(1 + 1)$ dimensions immediately generalizes to higher dimensions. The momenta in the spatial directions transverse to the acceleration simply contribute to the mass in the $(1 + 1)$ dimensional analysis, see Eq. (5.12).

4.3 Dirac Fields in Rigid Cavities

It is the aim of this section to consider a *Dirac spinor* field that is confined to an accelerating cavity. The motivation for this approach is two-fold. First, we wish to gain insight into the influence of particle statistics on the mechanisms of the transformation to identify features of the effects of non-uniform motion that are independent of the chosen quantum field. Second, possible applications in solid state systems [31, 114, 208] may offer the possibility of experimental verification of particle creation effects in fermionic systems. We proceed in a similar way as in Section 4.2.1, presenting the results obtained in Refs. [87, (iv)] and [88, (x)].

4.3.1 Cavity in Uniform Motion — Dirac Field

Dirac Field in Inertial Cavity

Let us consider a Dirac field ψ in $(1+1)$ dimensional Minkowski spacetime with metric $ds^2 = \eta_{\mu\nu} dx^\mu dx^\nu = -dt^2 + dx^2$. The Dirac equation [see Eq. (2.30)] now reads

$$(i \gamma^\mu \partial_\mu - m)\psi = 0, \quad (4.24)$$

where the Dirac gamma matrices satisfy $\{\gamma^\mu, \gamma^\nu\} = -2\eta^{\mu\nu}$, and m again denotes the mass of the field quanta. As for the scalar field, additional spatial dimensions can be added, but the formalism reduces to the $(1+1)$ dimensional case by Fourier decomposition, such that the momenta transverse to the chosen direction supply strictly positive contributions to the mass $m > 0$, see Eq. (5.12). Working in the $(1+1)$ dimensional case we can work only with 2×2 representations of γ^0 and γ^1 , for instance

$$\gamma^0 = \begin{pmatrix} 1 & 0 \\ 0 & -1 \end{pmatrix}, \quad \gamma^1 = \begin{pmatrix} 0 & 1 \\ -1 & 0 \end{pmatrix}. \quad (4.25)$$

The matrices further satisfy $(\gamma^0)^2 = -(\gamma^1)^2 = \mathbb{1}$ and it is convenient to multiply (4.24) by γ^0 to rewrite the Dirac equation as

$$i \partial_t \psi = H_D \psi = (-i \gamma^0 \gamma^1 \partial_x + m \gamma^0) \psi. \quad (4.26)$$

We then introduce a basis $\{u_\pm\}$ consisting of eigenspinors of $\gamma^0 \gamma^1$ such that

$$\gamma^0 \gamma^1 u_\pm = \pm u_\pm, \quad (4.27a)$$

$$\gamma^0 u_\pm = u_\mp. \quad (4.27b)$$

The basis is orthonormal in the sense that $u_\pm^\dagger u_\pm = 1$, and $u_\pm^\dagger u_\mp = 0$. For the representation of Eq. (4.25) the basis takes the specific form

$$u_\pm = \frac{1}{\sqrt{2}} \begin{pmatrix} 1 \\ \pm 1 \end{pmatrix}. \quad (4.28)$$

As for the scalar field we separate the variables to find the linearly independent solutions of Eq. (4.26), which can be expressed as

$$\psi_{+,k} = (\cos[\xi(k)] u_+ + \sin[\xi(k)] u_-) e^{ikx - i\omega_k t}, \quad (4.29a)$$

$$\psi_{-,k} = (\sin[\xi(k)] u_+ + \cos[\xi(k)] u_-) e^{-ikx - i\omega_k t}, \quad (4.29b)$$

where k is a non-zero real number, $\xi(k) := \frac{1}{2} \arctan(\frac{m}{k})$, and the eigenvalues ω_k of the Dirac Hamiltonian H_D of Eq. (4.26) are given by

$$\omega_k = \text{sgn}(k) \sqrt{m^2 + k^2}. \quad (4.30)$$

The functions $\psi_{+,k}$ and $\psi_{-,k}$ represent right-movers and left-movers respectively. We are now in a position to introduce the cavity for the Dirac field with boundaries at $x = x_L$ and $x = x_R$ as discussed in Section 4.1. A natural way to restrict the fermions to this region is to require the (spatial) probability current to vanish at the boundaries, i.e.,

$$\bar{\psi}_1 \gamma^1 \psi_2 \Big|_{x=x_L} = \bar{\psi}_1 \gamma^1 \psi_2 \Big|_{x=x_R} = 0, \quad (4.31)$$

where $\bar{\psi} = \psi^\dagger \gamma^0$ as in Section 2.3. Following the procedure laid out in Ref. [34] to obtain the deficiency indices for the Dirac Hamiltonian H_D on the finite interval $[x_L, x_R]$ we find that the self-adjoint extensions of H_D are determined by two independent phases. Physically these represent the phase shifts at the reflections on the cavity walls. Imposing the boundary conditions of Eq. (4.31) individually at each wall gives the solutions

$$\begin{aligned} x_L : \quad \psi = & [e^{-i\frac{\pi}{4}} \cos(\xi(k) - \xi_L) - e^{i\frac{\pi}{4}} \sin(\xi(k) + \xi_L)] e^{-ikx_L} \psi_{+,k} \\ & + [e^{i\frac{\pi}{4}} \cos(\xi(k) - \xi_L) - e^{-i\frac{\pi}{4}} \sin(\xi(k) + \xi_L)] e^{ikx_L} \psi_{-,k}, \end{aligned} \quad (4.32a)$$

$$\begin{aligned} x_R : \quad \psi = & [e^{-i\frac{\pi}{4}} \cos(\xi(k) - \xi_R) - e^{i\frac{\pi}{4}} \sin(\xi(k) + \xi_R)] e^{-ikx_R} \psi_{+,k} \\ & + [e^{i\frac{\pi}{4}} \cos(\xi(k) - \xi_R) - e^{-i\frac{\pi}{4}} \sin(\xi(k) + \xi_R)] e^{ikx_R} \psi_{-,k}. \end{aligned} \quad (4.32b)$$

The real parameters ξ_L and ξ_R , parameterizing the $U(1)$ phases mentioned above, specify the boundary conditions at the left and right cavity wall, respectively. To single out physically significant choices of these parameters we turn to the *MIT bag boundary conditions* [57, 74], named after the affiliation of the authors of [57] — the Massachusetts Institute of Technology. These boundary conditions, originally developed for the description of composite hadrons, emerge when the field inside the “bag” is matched to a field with a different mass outside the boundaries and the latter mass is subsequently taken to infinity. In this sense the MIT bag boundary conditions are the analogue of the Dirichlet boundary conditions in (non-relativistic) quantum mechanics, which arise

in the limit when the height of the walls of a potential well are taken to infinity, see Ref. [23]. Using our notation here the MIT bag boundary conditions read

$$(1 - i\gamma^1)\psi|_{x=x_L} = (1 + i\gamma^1)\psi|_{x=x_R} = 0. \quad (4.33)$$

Applying the conditions (4.33) to Eqs. (4.32a) and (4.32b), respectively, we find that the MIT bag boundary conditions correspond to the choices $\xi_L = 0$ and $\xi_R = \frac{\pi}{2}$. When the Dirac field is confined to the cavity by application of the boundary conditions at both walls the corresponding (normalized) mode function spinors are found to be

$$\psi_{k_n} = \sqrt{\frac{\omega_{k_n}^2}{2L(\omega_{k_n}^2 + [m/L])}} \left(e^{-i\xi(k_n)} e^{-ik_n x_L} \psi_{+,k_n} + i e^{i\xi(k_n)} e^{ik_n x_L} \psi_{-,k_n} \right), \quad (4.34)$$

where ψ_{\pm,k_n} and $\xi(k_n)$ are as in (4.29), the frequencies are given by Eq. (4.30), and the $k_n \in \mathbb{R}$, labelled by consecutive integers n , take on the discrete values that satisfy the *transcendental equation*

$$\frac{\tan(k_n L)}{k_n L} = -\frac{1}{mL}. \quad (4.35)$$

The positive and negative frequencies appear symmetrically in the spectrum, see Fig. 4.8.

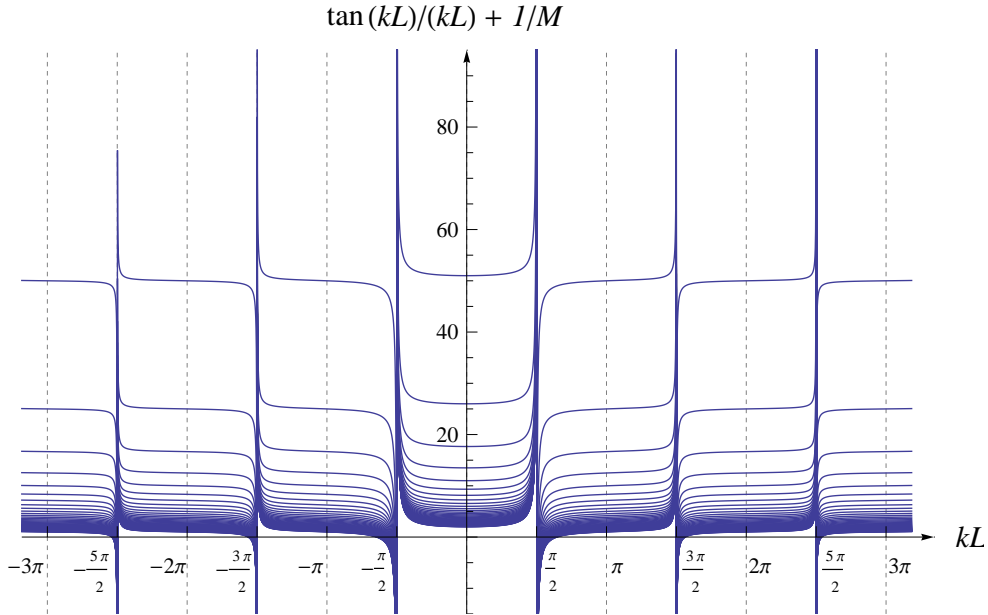


Figure 4.8: Transcendental equation: For fixed parameters m and L the allowed frequencies ω_{k_n} from Eq.(4.30) for the Dirac field modes in the cavity are determined by the positive and negative numbers k_n that satisfy the transcendental equation (4.35). The roots of the function $\tan(kL)/(kL) + 1/M$ determine the possible values of $(k_n L)$. Curves are shown here for discrete steps, $M \in \{\frac{2l}{100} | l = 1, 2, \dots, 50\}$ (l increasing from top to bottom), of the dimensionless combination $M = mL$.

The phase in Eq.(4.34) has been chosen such that the spinors at $(t, x) = (0, x_L)$ are positive multiples of $(u_+ + iu_-)$. The Dirac field within the cavity can now be decomposed as

$$\psi = \sum_{m \geq 0} \psi_{k_m} b_m + \sum_{n < 0} \psi_{k_n} c_n^\dagger, \quad (4.36)$$

where we have chosen the convention that $m \geq 0$ and $n < 0$ label positive and negative frequency solutions, respectively. The solutions appear symmetrically in the spectrum even though they are not symmetrically labelled, i.e., the lowest energy solutions are labelled by $m = 0$ and $n = -1$. The operators b_m^\dagger and c_n^\dagger create particles and antiparticles, respectively, in the modes $m \geq 0$ and $n < 0$, respectively, and they satisfy the anticommutation relations of (2.33). Finally, we consider the massless limit, $m \rightarrow 0$, for which the possible values of k_n coincide with the frequencies of Eq. (4.30), such that

$$\omega_{k_n} = k_n = \frac{\pi}{L} \left(n + \frac{1}{2} \right), \quad (4.37)$$

which corresponds to the case $(s, \theta) = (\frac{1}{2}, \frac{\pi}{2})$ discussed in Ref. [87, (iv)]. Note that there is no zero mode. With the notation of (4.37) the cavity spinors (4.34) for the massless Dirac field take the form

$$\psi_{k_n} = \frac{1}{\sqrt{2L}} \left(e^{i\omega_{k_n}(x-x_L)} u_+ + i e^{-i\omega_{k_n}(x-x_L)} u_- \right) e^{-i\omega_{k_n} t}. \quad (4.38)$$

Dirac Field in Uniformly Accelerated Cavity

For the Dirac field in the accelerated region we have to determine the form of the Dirac equation (2.30) in Rindler coordinates. To this end we express the covariant derivative $\nabla_\mu \psi = (\partial_\mu - \Gamma_\mu) \psi$ (see, e.g., Ref. [13] and mind our sign convention for the metric) in terms of the *spin connection coefficients* Γ_μ (Note that we have chosen the symbol Γ_μ here to adhere to usual conventions for this object even though we have used Γ to denote the covariance matrix in Section 3.1 and the two concepts are unrelated.). The spin connection coefficients for the Rindler coordinates (4.1) can be obtained from a straightforward procedure [137] which yields $\Gamma_\chi = 0$ and

$$\Gamma_\eta = -\frac{1}{2} \gamma^0 \gamma^1, \quad (4.39)$$

where the γ^μ are the Minkowski space gamma matrices from (4.25). With this the Dirac equation for the right Rindler wedge becomes

$$i \partial_\eta \tilde{\psi} = \left(-i \gamma^0 \gamma^1 [\chi \partial_\chi + \frac{1}{2}] + m \gamma^0 \chi \right) \tilde{\psi}. \quad (4.40)$$

For a formal derivation of (4.40) involving the explicit construction of the dyads see, e.g., Refs. [13, 125, 126]. We proceed, as in the inertial case, by finding the linearly

independent solutions to this equation, given by

$$\tilde{\psi}_{+,\Omega} = (I_{i\Omega-\frac{1}{2}}(\mathbf{m}\chi) u_+ + I_{i\Omega+\frac{1}{2}}(\mathbf{m}\chi) u_-) e^{-i\Omega\eta}, \quad (4.41a)$$

$$\tilde{\psi}_{-,\Omega} = (I_{-i\Omega+\frac{1}{2}}(\mathbf{m}\chi) u_+ + I_{-i\Omega-\frac{1}{2}}(\mathbf{m}\chi) u_-) e^{-i\Omega\eta}, \quad (4.41b)$$

where Ω are the real dimensionless Rindler frequencies, while the $I_{\pm i\Omega \pm \frac{1}{2}}(\mathbf{m}\chi)$ and $I_{\pm i\Omega \mp \frac{1}{2}}(\mathbf{m}\chi)$ are the *modified Bessel functions of the first kind* [145]. Let us briefly illustrate how to arrive at this form of the solutions by concentrating on the solutions (4.41a). We insert the ansatz

$$\tilde{\psi}_{+,\Omega} = (\tilde{I}_+(\chi) u_+ + i\tilde{I}_-(\chi) u_-) e^{-i\Omega\eta}, \quad (4.42)$$

where $\tilde{I}_{\pm}(\chi)$ are yet unknown functions, into Eq. (4.40). Consecutively, the orthonormality of the spinors u_{\pm} from (4.27) is used, i.e., u_+^{\dagger} or u_-^{\dagger} are applied from the left to arrive at either of the equations

$$(i\Omega - \frac{1}{2} - \chi\partial_{\chi}) \tilde{I}_+(\chi) + \mathbf{m}\chi \tilde{I}_-(\chi) = 0, \quad (4.43a)$$

$$(i\Omega + \frac{1}{2} + \chi\partial_{\chi}) \tilde{I}_-(\chi) - \mathbf{m}\chi \tilde{I}_+(\chi) = 0. \quad (4.43b)$$

Assuming $(\mathbf{m}\chi) \neq 0$, the function \tilde{I}_- can be expressed from (4.43a) and inserted into (4.43b), or vice versa for \tilde{I}_+ , to obtain the *modified Bessel equation* [145]

$$(\chi^2\partial_{\chi}^2 + \chi\partial_{\chi} - [\mathbf{m}^2\chi^2 + (i\Omega \mp \frac{1}{2})^2]) \tilde{I}_{\pm}(\chi) = 0, \quad (4.44)$$

revealing $\tilde{I}_{\pm}(\chi) = I_{i\Omega \mp \frac{1}{2}}(\mathbf{m}\chi)$, as claimed in (4.41a). As before, we apply the vanishing current boundary conditions (4.31) at the cavity walls $\chi = \chi_L$ and χ_R individually, i.e.,

$$\chi_L : \quad (4.45a)$$

$$\begin{aligned} \tilde{\psi} = & [(1 + e^{i\tilde{\xi}_L} \tanh[\mathbf{m}\chi_L]) I_{-i\Omega-\frac{1}{2}}(\mathbf{m}\chi_L) - (e^{i\tilde{\xi}_L} + \tanh[\mathbf{m}\chi_L]) I_{-i\Omega+\frac{1}{2}}(\mathbf{m}\chi_L)] \tilde{\psi}_{+,\Omega} \\ & + [(e^{i\tilde{\xi}_L} + \tanh[\mathbf{m}\chi_L]) I_{i\Omega-\frac{1}{2}}(\mathbf{m}\chi_L) - (1 + e^{i\tilde{\xi}_L} \tanh[\mathbf{m}\chi_L]) I_{i\Omega+\frac{1}{2}}(\mathbf{m}\chi_L)] \tilde{\psi}_{-,\Omega}, \end{aligned}$$

$$\chi_R : \quad (4.45b)$$

$$\begin{aligned} \tilde{\psi} = & [(1 + e^{i\tilde{\xi}_R} \tanh[\mathbf{m}\chi_R]) I_{-i\Omega-\frac{1}{2}}(\mathbf{m}\chi_R) - (e^{i\tilde{\xi}_R} + \tanh[\mathbf{m}\chi_R]) I_{-i\Omega+\frac{1}{2}}(\mathbf{m}\chi_R)] \tilde{\psi}_{+,\Omega} \\ & + [(e^{i\tilde{\xi}_R} + \tanh[\mathbf{m}\chi_R]) I_{i\Omega-\frac{1}{2}}(\mathbf{m}\chi_R) - (1 + e^{i\tilde{\xi}_R} \tanh[\mathbf{m}\chi_R]) I_{i\Omega+\frac{1}{2}}(\mathbf{m}\chi_R)] \tilde{\psi}_{-,\Omega}, \end{aligned}$$

where the real parameters $\tilde{\xi}_L$ and $\tilde{\xi}_R$ specify the boundary conditions at χ_L and χ_R , respectively. Once again we specialize to the *MIT bag boundary conditions* [57, 74], here of the form

$$(1 - i\gamma^1) \tilde{\psi}|_{\chi=\chi_L} = (1 + i\gamma^1) \tilde{\psi}|_{\chi=\chi_R} = 0, \quad (4.46)$$

which singles out $\tilde{\xi}_L = 0$ and $\tilde{\xi}_R = \pi$. Enforcing both boundary conditions we arrive at the cavity spinor solutions

$$\begin{aligned} \tilde{\psi}_{\Omega_n} = N_{\Omega_n} & \left([I_{-i\Omega_n - \frac{1}{2}}(\mathbf{m}\chi_L) - I_{-i\Omega_n + \frac{1}{2}}(\mathbf{m}\chi_L)] \tilde{\psi}_{+, \Omega_k(n)} \right. \\ & \left. + [I_{i\Omega_n - \frac{1}{2}}(\mathbf{m}\chi_L) - I_{i\Omega_n + \frac{1}{2}}(\mathbf{m}\chi_L)] \tilde{\psi}_{-, \Omega_n} \right), \end{aligned} \quad (4.47)$$

where the discrete frequencies Ω_n , satisfying the transcendent equation

$$\text{Re} \left([I_{-i\Omega_n - \frac{1}{2}}(\mathbf{m}\chi_L) - I_{-i\Omega_n + \frac{1}{2}}(\mathbf{m}\chi_L)] [I_{-i\Omega_n - \frac{1}{2}}(\mathbf{m}\chi_R) + I_{-i\Omega_n + \frac{1}{2}}(\mathbf{m}\chi_R)] \right) = 0, \quad (4.48)$$

are labelled by consecutive integers n . The normalization constant N_{Ω_n} appearing in Eq. (4.47) is determined from the inner product

$$(\psi_1, \psi_2)_D = \int_{\chi_L}^{\chi_R} d\chi \psi_1^\dagger \psi_2, \quad (4.49)$$

which follows from (2.31) by noting that $\gamma^\eta = (1/\chi)\gamma^0$. The forms of Ω_n and N_{Ω_n} become more apparent when we match the accelerated cavity to the inertial one. We further note that the exchange $\Omega \rightarrow -\Omega$ takes the order of the modified Bessel functions to their complex conjugates. Consequently, Eq.(4.48) is invariant under this mapping and the spectrum is again symmetric with respect to positive and negative frequency modes. We select the mode labelling such that integers $n \geq 0$ ($n < 0$) indicate solutions of positive (negative) frequency with respect to the time-like Killing vector ∂_η , such that we can decompose the field as

$$\psi = \sum_{n \geq 0} \tilde{\psi}_{\Omega_n} \tilde{b}_n + \sum_{n < 0} \tilde{\psi}_{\Omega_n} \tilde{c}_n^\dagger. \quad (4.50)$$

The operators \tilde{b}_n, \tilde{c}_n and their Hermitean conjugates satisfy the anticommutation relations from (2.33). As a last consideration here we take the limit $\mathbf{m} \rightarrow 0$ and obtain

$$\tilde{\psi}_{\Omega_n} = \frac{e^{-i\Omega_n \eta}}{\sqrt{2\chi \ln(\chi_R/\chi_L)}} \left(\left(\frac{\chi}{\chi_L} \right)^{i\Omega_n} u_+ + i \left(\frac{\chi}{\chi_L} \right)^{-i\Omega_n} u_- \right), \quad (4.51)$$

where the massless Rindler frequencies Ω_n are given by

$$\Omega_n = \frac{\pi}{\ln(\chi_R/\chi_L)} \left(n + \frac{1}{2} \right) = \frac{(n + \frac{1}{2})\pi}{2 \operatorname{artanh}(h/2)}, \quad (4.52)$$

where h is as in (4.19), and the normalization N_{Ω_n} in (4.47) was chosen so that the phases of the Minkowski and Rindler modes match at $t = \eta = 0$, i.e., at $(\eta, \chi) = (0, \chi_L)$ the modes (4.51) are positive multiples of $(u_+ + iu_-)$. Equations (4.51) and (4.52) again reproduce the case $(s, \theta) = (\frac{1}{2}, \frac{\pi}{2})$ analyzed in Ref. [87, (iv)].

4.3.2 Matching: Inertial to Rindler — Dirac Field

We match the inertial and accelerated cavity containing the Dirac field at the junction $t = \eta = 0$, as laid out in Section 4.1, where we assume the acceleration to be towards increasing values of x . The Minkowski (region I in Fig. 4.3) spinors (4.34) and the Rindler (region II in Fig. 4.3) spinors (4.47) are related by a Bogoliubov transformation (see Section 2.3.3 and Fig. 4.9)

$$\tilde{\psi}_{\Omega_m} = \sum_n {}_oA_{mn} \psi_{k_n} \quad (4.53)$$

where the Bogoliubov coefficients are of the form

$${}_oA_{mn} = (\psi_{k_n}, \tilde{\psi}_{\Omega_m})_D, \quad (4.54)$$

and the Dirac inner product is given by (4.49). Since both sets of modes are normalized the matrix ${}_oA = ({}_oA_{mn})$ is unitary

$$\sum_j {}_oA_{jk}^* {}_oA_{jl} = \delta_{kl}. \quad (4.55)$$

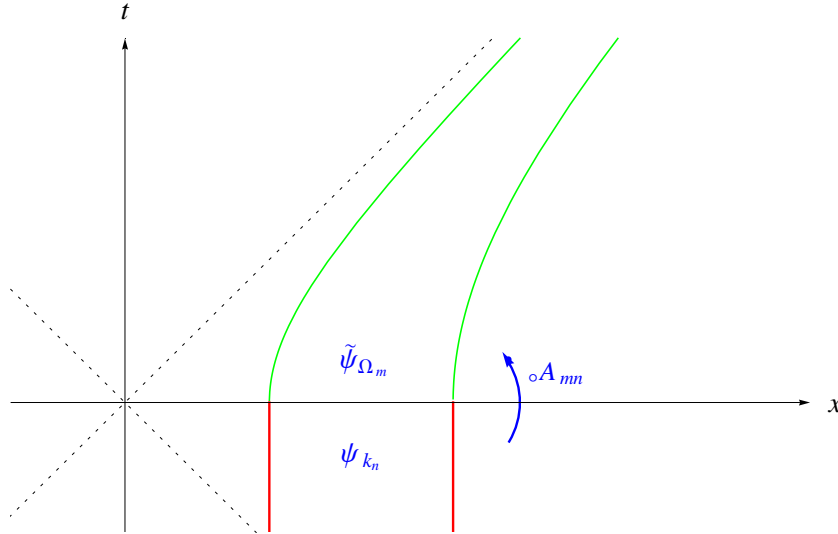


Figure 4.9: Minkowski to Rindler Bogoliubov transformation — Dirac field: The cavity modes ψ_{k_n} in the inertial region and the modes $\tilde{\psi}_{\Omega_m}$ in the uniformly accelerated region are related by a Bogoliubov transformation with coefficients ${}_oA_{mn}$, see Eq. (4.53).

As in Section 4.2.2 we now turn to the small \hbar approximation. In other words, we wish to find the Taylor-Maclaurin expansion of the Bogoliubov coefficients ${}_oA_{mn}$ as functions of the parameter $h = \mathbf{a}_c L$ around the value $h = 0$. In this regime a comparison of (4.34) and (4.47) reveals that the leading order of the Rindler frequencies is proportional to h^{-1} . This complicates the uniform expansion of the modified Bessel

functions because their order approaches the imaginary axis as h goes to zero. For details on the intricacies of the uniform expansions see Ref. [146]. We therefore choose a slightly different procedure than in Section 4.2.2, i.e., we perform the power expansion in h directly for the differential equation to which Eq. (4.41) provides the solutions. This task is simplified by the introduction of a new dimensionless variable λ , where

$$\chi = \frac{L}{h}(1 + h\lambda), \quad (4.56)$$

such that at χ_L and χ_R we have $\lambda_L = -\frac{1}{2}$ and $\lambda_R = \frac{1}{2}$, respectively. This procedure reveals

$$\Omega_n = \frac{L}{h} \omega_{k_n} (1 + O(h^2)), \quad (4.57)$$

where the k_n are determined by Eq. (4.35). Note that we have used the same symbol Ω_n for the Rindler frequencies of both the scalar [see (4.20)] and Dirac field [see (4.57)], but they do not generally match and neither do the corresponding Minkowski frequencies ω_n [see (4.7)] and ω_{k_n} [see (4.30)]. Finally, a lengthy but straightforward computation provides the Bogoliubov coefficients for the Dirac cavity field between the inertial region I and the accelerated region II (see Fig. 4.3)

$${}_oA_{mn} = {}_oA_{mn}^{(0)} + {}_oA_{mn}^{(1)} h + {}_oA_{mn}^{(2)} h^2 + O(h^3), \quad (4.58)$$

where the superscript (n) in brackets indicates the coefficients of h^n , and ${}_oA_{mn}^{(0)} = \delta_{mn}$. The non-vanishing coefficients linear in h are

$${}_oA_{mn}^{(1)} = \frac{2((-1)^{m+n} - 1) |k_m k_n| C_{k_m}^2 C_{k_n}^2 (C_{k_m} + C_{k_n})(C_{k_m} C_{k_n} + m^2)}{\sqrt{L^2 \omega_{k_m}^2 + mL} \sqrt{L^2 \omega_{k_n}^2 + mL} (C_{k_m} - C_{k_n})^3 (C_{k_m} C_{k_n} - m^2)^3}, \quad (4.59)$$

for $m \neq n$, and $C_{k_n} = k_n + \omega_{k_n}$, where ω_{k_n} is given by (4.30). The consecutive indices $m, n \geq 0$ (< 0) label positive (negative) frequency modes. Coefficients that relate modes of the same frequency sign correspond to α -type coefficients for bosonic fields, while those that connect positive and negative frequency modes are β -type coefficients, responsible for particle creation. It is interesting to note that the MIT bag boundary conditions prevent particle creation in pairs of modes with equal energies, i.e., the leading order coefficients ${}_oA_{mn}^{(1)}$ vanish identically for modes m and n with $\omega_{k_m} = -\omega_{k_n}$. The linear coefficients in (4.59) form an anti-Hermitian matrix, as required, and they consistently reduce to the case $s = \frac{1}{2}$ of Ref. [87, (iv)] in the massless limit, i.e., for $m \neq n$ and $m \rightarrow 0$ we have

$${}_oA_{mn}^{(1)} = \frac{((-1)^{m+n} - 1)(m + n + 1)}{2\pi^2(m - n)^3}. \quad (4.60)$$

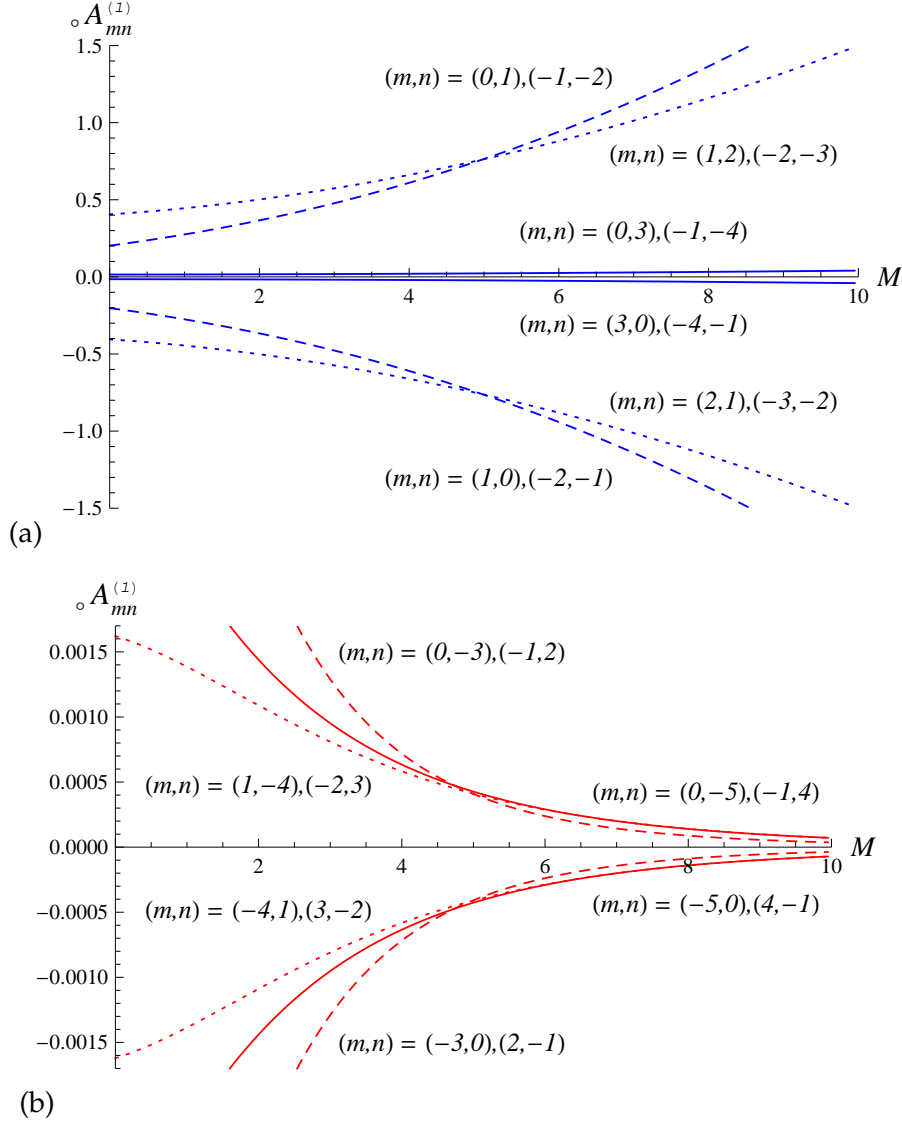


Figure 4.10: Minkowski to Rindler Bogoliubov coefficients — Dirac field: The behaviour of the leading order Bogoliubov coefficients ${}_0A_{mn}^{(1)}$ from (4.59) for the $(1 + 1)$ -dimensional Dirac field with MIT bag boundary conditions is shown for increasing mass. The coefficient ${}_0A_{mn}^{(1)}$ is plotted against the dimensionless combination $M := mL$. Figure 4.10 (a) shows a selection of Bogoliubov coefficients that relate modes with the same sign of the frequency (α -type coefficients): These mode-mixing coefficients are proportional to M^2 as $M \rightarrow \infty$. Figure 4.10 (b) shows a selection of Bogoliubov coefficients that relate positive frequency modes with negative frequency modes (β -type coefficients). These particle creation coefficients are proportional to M^{-6} as $M \rightarrow \infty$. For all curves the intersections with the vertical axis are given by the massless coefficients of Eq. (4.60).

On the other hand, for large mass, taking the limit $M = mL \rightarrow \infty$, it can be shown from (4.59) that the mode-mixing α -type coefficients behave as M^2 (Fig. 4.10 (a)), while the β -type coefficients decrease as M^{-6} (Fig. 4.10 (b)). As in the bosonic case we em-

phasize that the perturbative expansions can be trusted for $h \ll 1$ when the indices of the coefficients are bounded from above by any constant. For non-zero mass we additionally require $Mh \ll 1$ but we allow for $M \gg 1$ within this regime as long as $M^2 h \lesssim 1$.

The second order coefficients ${}_o A_{mn}^{(2)}$ are complicated and won't be needed explicitly in this work, but we note that they are proportional to $(1 + (-1)^{m+n})$ as their scalar field counterparts (see Section 4.2.2) and it has been verified [88, (x)] that the unitarity conditions (4.55) are satisfied when terms of order h^2 are included. A similar argument (see Ref. [88, (x)]) as for the bosonic field (see pp. 4.2.2) can be applied to consider leftward acceleration. For this procedure it is required to keep in mind that a spatial reflection changes the sign of the spatial components of γ^μ in the Dirac equation, reversing the roles of u_+ and u_- . As before, matching the conventions established for the phases leads to the conclusion that leftwards acceleration can be described to second order in h by the exchange $h \rightarrow -h$.

4.4 Grafting Generic Cavity Trajectories

With Eqs. (4.22) and (4.59) we have established, to leading order in h , the Bogoliubov transformations for the real scalar field and Dirac field, respectively, for an instantaneous transition from an inertial to a uniformly accelerated cavity according to the geometry depicted in Fig. 4.3. This allows us to study the effects on the states of the quantum field when the cavity is suddenly accelerated. Conceptually the role of the observer is clearly laid out. Without loss of generality we may consider the observer at the centre of the cavity, who experiences excitations with frequencies $\tilde{\omega}_n$ from (4.20). Nonetheless, the fact that the cavity in Fig. 4.3 is accelerated eternally evokes the question how more general non-uniform motion of the cavity can be described. We are now going to investigate exactly this issue.

4.4.1 The Basic Building Block

The key to understanding more general cavity trajectories (see Section 4.4.2) lies in the transition from an inertial cavity, back to an inertial cavity, with a single intermediate period of uniform acceleration — the *basic building block*. Let us first briefly return to the geometry of the rigid cavity as inspected in Section 4.1. As we have noted there the inertial and uniformly accelerated cavities are connected along a slice of fixed Rindler coordinate time η . We follow this recipe also when inverting the procedure. Stopping

the acceleration of the cavity at $\eta = \eta_1 = \text{const.}$ we maintain rigidity, see Fig. 4.11. The cavity walls of the inertial cavity after the acceleration (region III in Fig. 4.11) are again parallel and at a distance L , as measured by the co-moving observer. For an observer that is at rest with respect to the initial cavity in region I the cavity in region III is moving at a constant speed such that the final cavity's length is Lorentz contracted. It is interesting to note that the requirement of rigidity in relativity suggests that different parts of the cavity need to accelerate at different rates and for different durations (in terms of proper time).

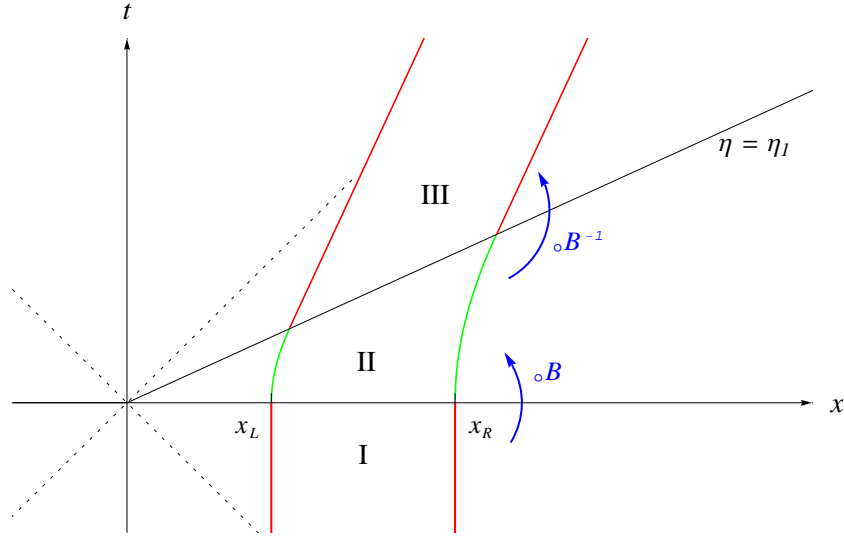


Figure 4.11: Basic building block: The rigid cavity is at rest initially (region I), then undergoes a period of uniform acceleration from $t = 0$ to Rindler coordinate time $\eta = \eta_1$ (region II) and is thereafter again inertial (region III). The transitions between periods of inertial motion and uniform acceleration induce Bogoliubov transformations ${}_oB$ (I \rightarrow II) and ${}_oB^{-1}$ (II \rightarrow III).

To construct the Bogoliubov transformation (see Sections 2.2.4 and 2.3.3) corresponding to the basic building block let us denote the abstract transformation between the inertial region I and the accelerated region II by ${}_oB$. For now, we postpone to distinguish between bosons and fermions. For each case all the Bogoliubov coefficients can be combined into formally infinite-dimensional matrix representations of ${}_oB$. From the Lorentz symmetry between regions I and III it becomes evident that the transformation at the junction between regions II and III can be chosen to be simply the inverse transformation ${}_oB^{-1}$. This means that the same phase conventions are chosen for the region III solutions at $\eta = \eta_1$ as we have previously established at $\eta = 0$ for the region I solutions and the phases acquired by the Rindler modes in region II are accounted for

separately by a diagonal matrix $\tilde{G}(\eta_1)$, such that

$${}_B B = {}_o B^{-1} \tilde{G}(\eta_1) {}_o B. \quad (4.61)$$

Let us now consider the representations of (4.61) for bosons and fermions separately.

The Bosonic Building Block

For the scalar field we represent ${}_o B$ and its inverse by the matrices ${}_o \mathcal{A}$ and ${}_o \mathcal{A}^{-1}$, respectively, in which we combine the matrices ${}_o \alpha = ({}_o \alpha_{mn})$ and ${}_o \beta = ({}_o \beta_{mn})$, i.e.,

$${}_o \mathcal{A} = \begin{pmatrix} {}_o \alpha & {}_o \beta \\ {}_o \beta^* & {}_o \alpha^* \end{pmatrix}, \quad {}_o \mathcal{A}^{-1} = \begin{pmatrix} {}_o \alpha^\dagger & -{}_o \beta^T \\ -{}_o \beta^\dagger & {}_o \alpha^T \end{pmatrix}. \quad (4.62)$$

From the Bogoliubov identities (2.27) one can easily verify that the inverse of ${}_o \mathcal{A}$ is formed by the map $({}_o \alpha, {}_o \beta) \rightarrow ({}_o \alpha^\dagger, -{}_o \beta^T)$ such that ${}_o \mathcal{A}^{-1} {}_o \mathcal{A} = \mathbf{1}$. The bosonic basic building block transformation can then be written as

$${}_B \mathcal{A} = {}_o \mathcal{A}^{-1} \tilde{G}(\eta_1) {}_o \mathcal{A}, \quad (4.63)$$

where $\tilde{G}(\eta_1) = G(\eta_1) \oplus G^*(\eta_1)$, and the diagonal matrix $G = \text{diag}\{G_n | n = 1, 2, \dots\}$ has entries $G_n(\eta_1) = \exp(i\Omega_n \eta_1)$. The transformation ${}_B \mathcal{A}$ can be decomposed into matrices ${}_B \alpha$ and ${}_B \beta$, i.e.,

$${}_B \alpha = {}_o \alpha^\dagger G {}_o \alpha - {}_o \beta^T G^* {}_o \beta^*, \quad (4.64a)$$

$${}_B \beta = {}_o \alpha^\dagger G {}_o \beta - {}_o \beta^T G^* {}_o \alpha^*, \quad (4.64b)$$

analogously to the decomposition (4.62), such that the modes ϕ_n in region I and the Minkowski modes in region III, denoted by $\hat{\phi}_m$, are related by

$$\hat{\phi}_m = \sum_n ({}_B \alpha_{mn} \phi_n + {}_B \beta_{mn} \phi_n^*). \quad (4.65)$$

We now wish to obtain the small \hbar expansion of the Bogoliubov coefficients ${}_B \alpha_{mn}$ and ${}_B \beta_{mn}$. The phase factors $G_n(\eta_1)$ can be conveniently written in such an expansion as

$$G_n(\eta_1) = \exp(i\Omega_n \eta_1) = \exp(i\omega_n \tilde{\tau}_1) + O(\hbar^2) = G_n^{(0)}(\tilde{\tau}_1) + O(\hbar^2) \quad (4.66)$$

by substituting the proper time $\tilde{\tau} = L\eta/h$ at the centre of the cavity and the Minkowski frequencies ω_n [see Eq. (4.20)]. Given Eq. (4.66) as well as the expansions (4.21) and (4.22) of the Minkowski to Rindler coefficients we obtain

$${}_B \alpha = {}_B \alpha^{(0)} + {}_B \alpha^{(1)} \hbar + O(\hbar^2) \quad (4.67a)$$

$$= G^{(0)} + (G^{(0)} {}_o \alpha^{(1)} + {}_o \alpha^{(1)\dagger} G^{(0)}) \hbar + O(\hbar^2),$$

$${}_B \beta = {}_B \beta^{(1)} \hbar + O(\hbar^2) = (G^{(0)} {}_o \beta^{(1)} - {}_o \beta^{(1)T} G^{(0)*}) \hbar + O(\hbar^2). \quad (4.67b)$$

Using the antisymmetry and symmetry, respectively, of the real matrices ${}_o\alpha^{(1)}$ and ${}_o\beta^{(1)}$ (4.22) we can conveniently write the coefficients of ${}_B\alpha^{(1)}$ and ${}_B\beta^{(1)}$ as

$${}_B\alpha_{mn}^{(1)} = {}_o\alpha_{mn}^{(1)} (G_m^{(0)} - G_n^{(0)}), \quad (4.68a)$$

$${}_B\beta_{mn}^{(1)} = {}_o\beta_{mn}^{(1)} (G_m^{(0)} - G_n^{(0)*}). \quad (4.68b)$$

The Fermionic Building Block

For the fermionic representation ${}_B A$ of the basic building block transformation in Fig. 4.11 we write

$${}_B A = {}_o A^{-1} G(\eta_1) {}_o A = {}_o A^\dagger G(\eta_1) {}_o A, \quad (4.69)$$

where the phases for the spinor modes are encoded in the matrix

$$G = \text{diag}\{G_n | \dots, -2, -1, 0, 1, \dots\}, \quad (4.70)$$

and the individual phases G_n are as in (4.66) but with the appropriate frequencies Ω_n and ω_{k_n} for the Dirac spinors. With this the spinor mode solutions of the final inertial region III, denoted by $\widehat{\psi}_m$, are obtained from the region I solutions ψ_n by

$$\widehat{\psi}_m = \sum_n {}_B A_{mn} \psi_n. \quad (4.71)$$

The power expansion of ${}_B A$ for $h \ll 1$ is of the form

$${}_B A = G^{(0)} + (G^{(0)} {}_o A^{(1)} - {}_o A^{(1)} G^{(0)}) h + O(h^2), \quad (4.72)$$

where we have used the unitarity of the Minkowski to Rindler transformation, which implies that ${}_o A^{(1)}$ is anti-Hermitian. In components the linear order of the fermionic Bogoliubov coefficients for the basic building block reads

$${}_B A_{mn}^{(1)} = {}_o A_{mn}^{(1)} (G_m^{(0)} - G_n^{(0)}). \quad (4.73)$$

As a special case, let us consider the massless quantum fields. If $m = 0$ the frequencies of both the scalar and Dirac field are equally spaced. Consequently, the Bogoliubov coefficients for the basic building block are periodic in the duration of the acceleration. In Chapter 6 we shall reconsider this periodicity for select examples of more generic travel scenarios, which are investigated in the following Section 4.4.2.

4.4.2 Generalized Travel Scenarios

With the basic building block transformations of Eqs. (4.63) and (4.69) at hand we are now in a position to construct more complicated trajectories. The key ingredient is to notice that two basic building blocks can be straightforwardly connected by an intermediate period of inertial coasting of proper time τ . The inertial segment is represented by a matrix $\mathcal{G}(\tau)$, composed as \tilde{G} in (4.63) for the scalar field or as (4.70) for the Dirac field, but the basic phase factors G_n are replaced by their leading order terms $G_n^{(0)}$. With this notation the Bogoliubov transformation \mathcal{B} for a generic travel scenario connecting two inertial regions with n intermediate periods of uniform acceleration can be written as

$$\mathcal{B} = {}_B B_n \mathcal{G}(\tau_{n-1}) {}_B B_{n-1} \dots \mathcal{G}(\tau_2) {}_B B_2 \mathcal{G}(\tau_1) {}_B B_1. \quad (4.74)$$

The individual building block transformations ${}_B B_i$ are given by their representatives ${}_B A_i = {}_B A(\eta_i, h_i)$ from (4.63) and ${}_B A_i = {}_B A(\eta_i, h_i)$ from (4.69) for the scalar and Dirac field, respectively. Assuming that the accelerations h_i of all segments are small, i.e., $|h_i| \ll 1$ we can perform a power expansion for all of these parameters. The leading order of (4.74) is then given by

$$\mathcal{B}^{(0)} = \mathcal{G}(\tau_{\text{tot}}) = \mathcal{G}\left(\sum_{i=1}^{n-1} \tau_i + \sum_{j=1}^n \tilde{\tau}_j\right), \quad (4.75)$$

where τ_{tot} is the total proper time as measured at the centre of the cavity between the initial and final inertial segment. The coefficients $\mathcal{B}_{mn}^{(1i)}$ of the linear term $\sum_i \mathcal{B}^{(1i)} h_i$ in the expansion are all proportional to the linear Minkowski to Rindler coefficients, ${}_o \alpha_{mn}^{(1)}$, and ${}_o \beta_{mn}^{(1)}$, or ${}_o A_{mn}^{(1)}$ from (4.22) and (4.59), respectively, and therefore share their basic structure. The linear terms $\mathcal{B}_{mn}^{(1i)}$ vanish identically for pairs of modes (m, n) that have the same parity, i.e., for which $(m + n)$ is even, in particular for $m = n$. Up to and including second order terms in the expansion the direction of the acceleration in the i -th building block may be controlled by the sign of h_i (see pp. 77). Assuming for simplicity of notation that every h_i can be written as $\epsilon_i h$, for a fixed h and $\epsilon_i \in \mathbb{R}$, we can thus conclude that the coefficients for a generic travel scenario have a power expansion of the form

$$\alpha_{mn} = G_m^{(0)} \delta_{mn} + \alpha_{mn}^{(1)} h + \alpha_{mn}^{(2)} h^2 + O(h^3), \quad (4.76a)$$

$$\beta_{mn} = \beta_{mn}^{(1)} h + \beta_{mn}^{(2)} h^2 + O(h^3), \quad (4.76b)$$

$$A_{mn} = G_m^{(0)} \delta_{mn} + A_{mn}^{(1)} h + A_{mn}^{(2)} h^2 + O(h^3), \quad (4.76c)$$

where the appropriate forms of $G_m^{(0)} = G_m^{(0)}(\tau_{\text{tot}})$ apply for the scalar and Dirac field, and the diagonal first order coefficients vanish, i.e., $\alpha_{nn}^{(1)} = \beta_{nn}^{(1)} = 0$ and $A_{nn}^{(1)} = 0$. We

insert the expansions (4.76) into the *Bogoliubov identities* for bosonic (2.27) and fermionic fields (2.46), respectively, to express these unitarity requirements for the linear coefficients in the perturbative expansion as

$$G_m^{(0)*} \alpha_{mn}^{(1)} + G_n^{(0)} \alpha_{nm}^{(1)*} = 0, \quad (4.77a)$$

$$G_m^{(0)*} \beta_{mn}^{(1)} - G_n^{(0)*} \beta_{nm}^{(1)} = 0, \quad (4.77b)$$

$$G_m^{(0)*} A_{mn}^{(1)} + G_n^{(0)} A_{nm}^{(1)*} = 0. \quad (4.77c)$$

It is convenient to consider also the second order of the Bogoliubov identities, i.e.,

$$G_m^{(0)*} \alpha_{mn}^{(2)} + G_n^{(0)} \alpha_{nm}^{(2)*} = - \sum_l (\alpha_{lm}^{(1)*} \alpha_{ln}^{(1)} - \beta_{lm}^{(1)} \beta_{ln}^{(1)*}), \quad (4.78a)$$

$$G_m^{(0)*} \beta_{mn}^{(2)} - G_n^{(0)*} \beta_{nm}^{(2)} = - \sum_l (\alpha_{lm}^{(1)*} \beta_{ln}^{(1)} - \beta_{lm}^{(1)} \alpha_{ln}^{(1)*}), \quad (4.78b)$$

$$G_m^{(0)*} A_{mn}^{(2)} + G_n^{(0)} A_{nm}^{(2)*} = - \sum_l A_{lm}^{(1)*} A_{ln}^{(1)}, \quad (4.78c)$$

which will be helpful in the following chapters. Let us now illustrate the construction of generic trajectories for a specific example in the next section.

Trip to Alpha-Centauri

A particular example of interest is a travel scenario where the cavity undergoes two periods of uniform acceleration such that the cavity comes to rest in the same inertial frame it started from, but is possibly located at a remote location in spacetime. To illustrate this travel scenario one may think of a spaceship carrying the cavity on a *one-way trip to Alpha Centauri* [44].

We decompose the Bogoliubov transformation into two basic building blocks of the same duration $\tilde{\tau}$ as measured at the centre of the cavity and equal, but opposite accelerations, here represented by $\pm h$ in a slight abuse of notation. In between we leave a period of inertial coasting for the (proper) time τ , such that the total transformation is of the form

$${}_{\alpha c} \mathcal{B} = {}_B B(\tilde{\tau}, -h) \mathcal{G}(\tau) {}_B B(\tilde{\tau}, h). \quad (4.79)$$

For the scalar field we substitute ${}_B \mathcal{A}$ from (4.63) for ${}_B B$ and immediately obtain the decompositions

$${}_{\alpha c} \alpha = {}_B \alpha(\tilde{\tau}, -h) G^{(0)}(\tau) {}_B \alpha(\tilde{\tau}, h) + {}_B \beta(\tilde{\tau}, -h) G^{(0)*}(\tau) {}_B \beta^*(\tilde{\tau}, h), \quad (4.80a)$$

$${}_{\alpha c} \beta = {}_B \alpha(\tilde{\tau}, -h) G^{(0)}(\tau) {}_B \beta(\tilde{\tau}, h) + {}_B \beta(\tilde{\tau}, -h) G^{(0)*}(\tau) {}_B \alpha^*(\tilde{\tau}, h), \quad (4.80b)$$

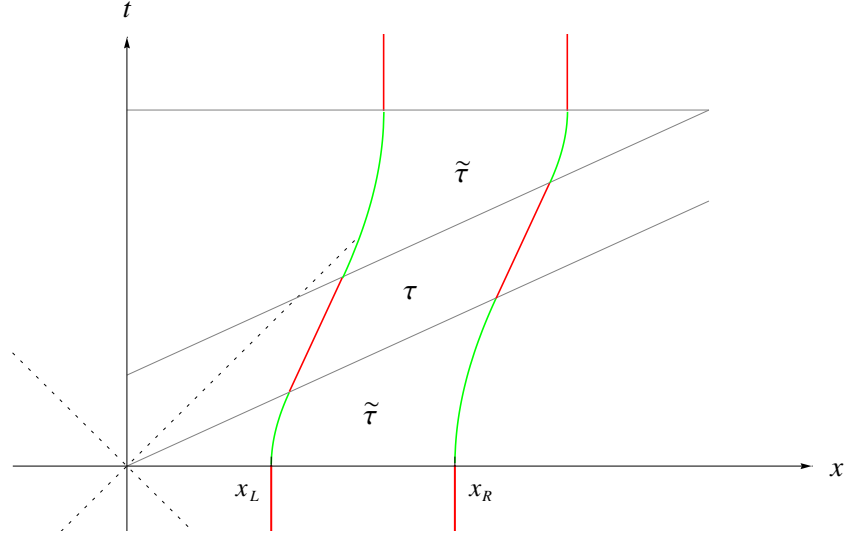


Figure 4.12: Trip to Alpha Centauri: The travel scenario contains two periods of uniform acceleration of the same duration $\tilde{\tau}$ and proper acceleration as measured at the centre of the cavity. One of these segments is towards increasing, the other towards decreasing values of x . The periods of uniform acceleration are separated by a segment of inertial coasting at fixed velocity for the (proper) time τ , allowing the cavity to reach a (possibly) remote location such as *Alpha Centauri* [44].

from which we obtain the power expansion coefficients

$$\alpha_{\text{c}}\alpha_{mn}^{(0)} = \delta_{mn} G_m^{(0)}(2\tilde{\tau} + \tau), \quad (4.81\text{a})$$

$$\begin{aligned} \alpha_{\text{c}}\alpha_{mn}^{(1)} = \text{o}\alpha_{mn}^{(1)} & \left[G_m^{(0)}(2\tilde{\tau} + \tau) - G_m^{(0)}(\tilde{\tau} + \tau)G_n^{(0)}(2\tilde{\tau}) \right. \\ & \left. - G_m^{(0)}(\tilde{\tau})G_n^{(0)}(\tilde{\tau} + \tau) + G_n^{(0)}(2\tilde{\tau} + \tau) \right], \end{aligned} \quad (4.81\text{b})$$

$$\begin{aligned} \alpha_{\text{c}}\beta_{mn}^{(1)} = \text{o}\beta_{mn}^{(1)} & \left[G_m^{(0)}(2\tilde{\tau} + \tau) - G_m^{(0)}(\tilde{\tau} + \tau)G_n^{(0)*}(2\tilde{\tau}) \right. \\ & \left. - G_m^{(0)}(\tilde{\tau})G_n^{(0)*}(\tilde{\tau} + \tau) + G_n^{(0)*}(2\tilde{\tau} + \tau) \right]. \end{aligned} \quad (4.81\text{c})$$

A similar computation for the fermionic Bogoliubov transformation reveals

$$\alpha_{\text{c}}A_{mn}^{(0)} = \delta_{mn} G_m^{(0)}(2\tilde{\tau} + \tau), \quad (4.82\text{a})$$

$$\begin{aligned} \alpha_{\text{c}}A_{mn}^{(1)} = \text{o}A_{mn}^{(1)} & \left[G_m^{(0)}(2\tilde{\tau} + \tau) - G_m^{(0)}(\tilde{\tau} + \tau)G_n^{(0)}(2\tilde{\tau}) \right. \\ & \left. - G_m^{(0)}(\tilde{\tau})G_n^{(0)}(\tilde{\tau} + \tau) + G_n^{(0)}(2\tilde{\tau} + \tau) \right], \end{aligned} \quad (4.82\text{b})$$

with the appropriate frequencies for the Dirac spinor modes in the phase factors. Finally, let us consider the possibility of smooth transitions between segments of inertial motion and uniform acceleration in Section 4.4.3.

4.4.3 Smoothly Varying Accelerations

As a last step in the construction of generic travel scenarios let us reconsider the assumptions of sharp transitions between inertial motion and uniform accelerations. Certainly, accelerations can be thought of as switching instantaneously if the change in acceleration occurs much faster than the characteristic timescale of the cavity. Such a timescale can be constructed from the propagation speed in the cavity and its length.

However, it is also of interest to study the effects of non-uniform motion for which the acceleration is allowed to vary smoothly in time, without sharp jumps. Let us construct the corresponding Bogoliubov transformation as a limit of Eq. (4.74), following Ref. [47]. Since the acceleration can now take on arbitrary values we can remove the inertial segments and we fix only an initial time τ_0 and a final time τ , such that we have

$$\mathcal{B}(\tau, \tau_0) = \lim_{\substack{N \rightarrow \infty \\ \tilde{\tau} \rightarrow 0}} \mathcal{B}B(\tilde{\tau}_N, h_N) \mathcal{B}B(\tilde{\tau}_{N-1}, h_{N-1}) \dots \mathcal{B}B(\tilde{\tau}_1, h_1) \quad (4.83)$$

where the total time is fixed

$$\sum_{n=1}^N \tilde{\tau}_n = \tau - \tau_0 = \text{const.} \quad (4.84)$$

An infinitesimal increase in time, i.e., $\tau \rightarrow \tau + d\tau$, is then achieved by applying the transformation $\mathcal{B}B(d\tau, h)$ to $\mathcal{B}(\tau, \tau_0)$ of (4.83) from the left,

$$\mathcal{B}(\tau + d\tau, \tau_0) = \mathcal{B}B(d\tau, h) \mathcal{B}(\tau, \tau_0). \quad (4.85)$$

Neglecting terms of $O(d\tau^2)$ the infinitesimal basic building block transformation can be written as

$$\mathcal{B}B(d\tau, h) = {}_oB^{-1}(h) \tilde{G}(h, d\tau) {}_oB(h) = {}_oB^{-1}(h) (\mathbb{1} + i\tilde{\Omega}(h) d\tau) {}_oB(h), \quad (4.86)$$

where we define the matrix $\tilde{\Omega}$ individually for the scalar and Dirac field,

$$\text{scalar: } \tilde{\Omega}(h) := \text{diag}\{\Omega_n | n = 1, 2, \dots\} \oplus \text{diag}\{-\Omega_n | n = 1, 2, \dots\}, \quad (4.87a)$$

$$\text{Dirac: } \tilde{\Omega}(h) := \text{diag}\{\Omega_n | n = \dots, -2, -1, 0, 1, \dots\}. \quad (4.87b)$$

This enables us to write the derivative of $\mathcal{B}(\tau, \tau_0)$ with respect to the proper time τ as

$$\frac{\partial}{\partial \tau} \mathcal{B}(\tau, \tau_0) = \lim_{d\tau \rightarrow 0} \frac{\mathcal{B}(\tau + d\tau, \tau_0) - \mathcal{B}(\tau, \tau_0)}{d\tau} = i {}_oB^{-1}(h) \tilde{\Omega}(h) {}_oB(h) \mathcal{B}(\tau, \tau_0). \quad (4.88)$$

The simple differential equation (4.88) can be immediately recognized to be of the form of the *Schrödinger equation*. Since $h = h(\tau)$ is now time-dependent the solution to Eq. (4.88) is given in terms of a *time-ordered integral* (see, e.g., Ref. [160, pp. 84])

$$\mathcal{B}(\tau, \tau_0) = T \exp \left(i \int_{\tau_0}^{\tau} {}_oB^{-1}(h(\tau')) \tilde{\Omega}(h(\tau')) {}_oB(h(\tau')) d\tau' \right). \quad (4.89)$$

From (4.89) it can be seen that the transformation reduces to the acquisition of phases for any time interval for which $h = \text{const.}$. In addition, no small h approximation has been performed yet and it can therefore be argued quite generally, that any effects of mode mixing and particle creation are due to the *changes* in acceleration. In other words, the non-uniformity of the acceleration is responsible for any effects. In the case of the small h approximation we find the leading terms of the expansion for the scalar field from (4.88) and (4.21) as

$${}_s\alpha_{nn} = G_n^{(0)}(\tau - \tau_0) + O(h^2), \quad (4.90a)$$

and for $m \neq n$ the leading order coefficients are

$${}_s\alpha_{mn} = i L (\omega_m - \omega_n) {}_o\alpha_{mn}^{(1)} G_m^{(0)}(\tau - \tau_0) \int_{\tau_0}^{\tau} e^{i(\omega_m - \omega_n)(\tau' - \tau_0)} \mathbf{a}_c(\tau') d\tau', \quad (4.90b)$$

$${}_s\beta_{mn} = i L (\omega_m + \omega_n) {}_o\beta_{mn}^{(1)} G_m^{(0)}(\tau - \tau_0) \int_{\tau_0}^{\tau} e^{i(\omega_m + \omega_n)(\tau' - \tau_0)} \mathbf{a}_c(\tau') d\tau', \quad (4.90c)$$

where $G_m^{(0)}(\tau) = \exp(i\omega_m\tau)$, ω_m is given by (4.7), and we have assumed the cavity length L to be fixed, while the proper acceleration $\mathbf{a}_c(\tau)$ at the centre of the cavity varies smoothly. The product $h(\tau) = \mathbf{a}_c(\tau)L \ll 1$ is assumed to be small throughout the journey. The linear order in the expansion of the Bogoliubov coefficients is thus given by a *Fourier transform* of the time-dependent acceleration. A similar calculation involving (4.88) and (4.58) supplies the fermionic counterparts [88, (x)]

$${}_sA_{nn} = G_n^{(0)}(\tau - \tau_0) + O(h^2), \quad (4.91a)$$

$${}_sA_{mn} = i L (\omega_m - \omega_n) {}_oA_{mn}^{(1)} G_m^{(0)}(\tau - \tau_0) \int_{\tau_0}^{\tau} e^{i(\omega_m - \omega_n)(\tau' - \tau_0)} \mathbf{a}_c(\tau') d\tau', \quad (4.91b)$$

$(m \neq n)$

with the frequencies determined by (4.30) and (4.35). Since all the linear coefficients for the scalar and Dirac field are proportional to the Minkowski to Rindler coefficients we can conclude that the linear coefficients vanish for mode pairs of equal parity, i.e., if $(m+n)$ is even, regardless of the travel scenario or the smoothness of the acceleration.

The magnitude of the coefficients for a given travel scenario depends on the jumps in the acceleration. If $\mathbf{a}_c(\tau)$ changes much slower than the oscillating terms in (4.90) or (4.91) the effects governed by the magnitude of the coefficients are significantly reduced. One such effect is the *dynamical Casimir effect* (see, e.g., Refs. [63, 64, 124, 143]), in which one or both of the boundaries of a cavity undergo periodic motion at a resonance frequency to produce pairs of particles. The cavity model as described in this chapter accounts for this effect in its incarnation where the two walls are kept at a fixed distance throughout this oscillation, e.g., by letting the acceleration in (4.90) be sinusoidal [46, 47].

State Transformation by Non-Uniform Motion

The analysis of Chapter 4 has provided the Bogoliubov transformations between the mode functions and mode operators of a rigid cavity undergoing non-uniform motion. The cavity is assumed to confine massive scalar or Dirac fields in (1+1) dimensions and additional spatial dimensions can be included by their strictly positive contributions to the mass. The motion of the cavity is assumed to be inertial at the start and finish of the journey, but is non-uniform in between, possibly including smooth as well as sharp transitions between different accelerations. For practical reasons a perturbative approach is adopted. The coefficients of the Bogoliubov transformation between the initial “in-region” and the final “out-region” are obtained as Taylor-Maclaurin expansions in the parameter $h = \mathbf{a}_c L \ll 1$, where \mathbf{a}_c is the proper acceleration at the centre of the cavity, and the length L of the cavity is considered to be fixed. A discussion of the numerical values for the expansion parameter can be found in Section 7.1.4. For a generic travel scenario the expansions of the coefficients are of the form given in (4.76). The in-region mode functions and annihilation operators for bosons and fermions are denoted by ϕ_n, a_n , and ψ_n, b_n, c_n , respectively, while the out-region quantities are denoted as $\hat{\phi}_n, \hat{a}_n, \hat{\psi}_n, \hat{b}_n$, and \hat{c}_n .

The purpose of the present chapter is to implement these Bogoliubov transformations on the corresponding *Fock spaces* (see Sections 2.2.3 and 2.3.2) as well as in *phase space* (see Section 3.1). We separate the description of the bosonic and fermionic transformations. In Sections 5.1 and 5.2 we study the transformation in the bosonic Fock space and phase space, respectively, before we turn to the fermionic Fock space transformations in Section 5.3.

This chapter combines results that were derived as part of the research conducted for related investigations by myself [82–84, 87, 89, (iv)–(vii), (ix)] and others [44].

5.1 Bosonic Fock State Transformation

5.1.1 Bosonic Vacuum Transformation

To construct the Bogoliubov transformation on the bosonic Fock space (see Section 2.2.3) the natural starting point is the vacuum, i.e., relating the in-region vacuum state $|0\rangle$ and the out-region vacuum $|\widehat{0}\rangle$. Since the Bogoliubov transformation is linear in the mode operators it can be represented by exponentials of quadratic combinations of the operators a_m and a_n^\dagger , see Section 3.1.2. Such a transformation can further be split into passive and active transformations (see p. 45). The former leave the vacuum invariant, while the active transformations are generated by quadratic combinations of the form

$$\sum_{p,q} (V_{pq} \widehat{a}_p^\dagger \widehat{a}_q^\dagger - V_{pq}^* \widehat{a}_p \widehat{a}_q), \quad (5.1)$$

with $V_{pq} \in \mathbb{C}$. Since $a_n |\widehat{0}\rangle = 0$, and a quick application of the commutation relations (2.15) shows that also $[\widehat{a}_p^\dagger \widehat{a}_q^\dagger, \widehat{a}_{p'} \widehat{a}_{q'}] |\widehat{0}\rangle = 0$, the transformation between the vacua can be written as [75]

$$|0\rangle = N_{\text{vac}} \exp(W) |\widehat{0}\rangle = N_{\text{vac}} \exp\left(\frac{1}{2} \sum_{p,q} V_{pq} \widehat{a}_p^\dagger \widehat{a}_q^\dagger\right) |\widehat{0}\rangle, \quad (5.2)$$

where we have included a factor of $\frac{1}{2}$ for convenience. If the in-region and out-region Fock spaces are unitarily equivalent the state is normalized by a finite constant N_{vac} . We shall return to this criterion on page 101. The next step of our investigation is to determine the symmetric matrix $V = (V_{pq})$ in (5.2). We exploit the property that the in-region vacuum $|0\rangle$ is annihilated by all operators a_n , where we insert the Hermitian conjugate of the inverse Bogoliubov transformation from (2.25b) to write

$$a_n |0\rangle = N_{\text{vac}} \sum_m (\alpha_{mn} \widehat{a}_m + \beta_{mn}^* \widehat{a}_m^\dagger) \exp(W) |\widehat{0}\rangle = 0. \quad (5.3)$$

The *Hadamard Lemma* of the Baker-Campbell-Hausdorff formula, i.e.,

$$X e^Y = e^Y (X + [X, Y] + \frac{1}{2!} [[X, Y], Y] + \dots), \quad (5.4)$$

is then used to commute a_n and $\exp(W)$. One straightforwardly obtains the commutators

$$[\widehat{a}_m, W] = \sum_p V_{pm} \widehat{a}_p^\dagger, \quad (5.5a)$$

$$[\widehat{a}_m^\dagger, W] = [[\widehat{a}_m, W], W] = 0. \quad (5.5b)$$

Combining (5.3)-(5.5) we arrive at the condition

$$\sum_m V_{pm} \alpha_{mn} + \beta_{pn}^* = 0. \quad (5.6)$$

Since the matrix $\alpha = (\alpha_{mn})$ is invertible [195] we can rephrase (5.6) to directly express V as

$$V = -\beta^* \alpha^{-1}. \quad (5.7)$$

Returning to the perturbative treatment we employ the expansions (4.76) to get

$$V_{pq}^{(0)} = 0, \quad (5.8a)$$

$$V_{pq}^{(1)} = -G_q^{(0)*} \beta_{pq}^{(1)*}, \quad (5.8b)$$

$$V_{pq}^{(2)} = G_p^{(0)*} G_q^{(0)*} \sum_m \beta_{mp}^{(1)*} \alpha_{mq}^{(1)} - G_q^{(0)*} \beta_{pq}^{(2)*}, \quad (5.8c)$$

where we have used the identity (4.77b) to rewrite the second order terms (5.8c).

Unitarity of the Transformation — Bosons

A subtlety in the transformation is the question whether the in-region and out-region Fock spaces are unitarily equivalent. In other words, it is not guaranteed that Eq. (5.2) is well-defined. The condition for the unitarity of the transformation is that the matrix V from (5.7) is *Hilbert-Schmidt* (see, e.g., Ref. [101, 122, 178, 179]), i.e., the norm induced by the inner product (1.5) is finite. Indeed, assuming that α is bounded it is enough [75, 122, 195] to require this for the matrix $\beta = (\beta_{mn})$ such that the normalization constant in (5.2) is finite. We examine this condition perturbatively to leading order in \hbar , where only the coefficients $\beta_{mn}^{(1)}$ contribute, see (5.8b). The Hilbert-Schmidt condition to leading order is then

$$\sum_{m,n} |\beta_{mn}^{(1)}|^2 < \infty. \quad (5.9)$$

In spite of the plethora of available travel scenarios there are essentially two cases of interest, the sharp transition from Minkowski to Rindler solutions with coefficients ${}_o\beta_{mn}^{(1)}$ from (4.22b), and the smoothly changing accelerations with coefficients ${}_s\beta_{mn}^{(1)}$ from (4.90c). Starting with the sharp transitions, we first consider the case $M = 0$, for which we get

$$\sum_{m,n} |{}_o\beta_{mn}^{(1)}(M=0)|^2 = \frac{8}{\pi^4} \sum_{\substack{m \text{ even} \\ n \text{ odd}}} \frac{m n}{(m+n)^6} = \frac{1}{48\pi^4} (28 \zeta(3) - 31 \zeta(5)), \quad (5.10)$$

where $\zeta(z)$ is the *Riemann zeta function*, which is finite for $\text{Re}(z) > 1$ and real for $z \in \mathbb{R}$. For $M > 0$ elementary estimates for the left hand side of (5.9) are obtained by treating the sum as a *Riemann sum*. Substituting $x = m\pi/M$ and $y = n\pi/M$ the Riemann sum can be written as [88, (x)]

$$M^2 \sum_{m,n} |{}_o\beta_{mn}^{(1)}(M)|^2 \rightarrow \frac{2}{\pi^2} \int_{\substack{x>0 \\ y>0}} \frac{x^2 y^2 dx dy}{\sqrt{1+x^2} \sqrt{1+y^2} (\sqrt{1+x^2} + \sqrt{1+y^2})^6} = \frac{1}{90\pi^2}, \quad (5.11)$$

suggesting the Hilbert-Schmidt condition is satisfied for the $(1 + 1)$ dimensional scalar cavity field for all M . To extend this line of argument to additional spatial dimensions we note that the transverse momenta k_{\perp} enter into the dimensionless parameter M via the substitution

$$M \rightarrow \sqrt{\mathbf{m}^2 + k_{\perp}^2} L. \quad (5.12)$$

For the Hilbert-Schmidt condition it is necessary to sum over the transverse momenta of the additional n dimensions and the estimate of (5.11) involves integrals of the form

$$\int_{x_i > 0} dx_1 \dots dx_n \frac{1}{1 + \sum_{i=1}^n x_i^2}, \quad (5.13)$$

which diverge for $n \geq 2$. These contributions suggest that the Hilbert-Schmidt condition for the sharp transitions is still satisfied in $(2 + 1)$ dimensions, while the unitarity requirement fails in $(3 + 1)$ (or higher) spacetime dimensions. However, a remedy for this predicament is provided by the Bogoliubov transformations for smoothly varying accelerations. The corresponding coefficients ${}_s\beta_{mn}^{(1)}$ (4.90b) are given by Fourier transforms of the acceleration $\mathbf{a}_c(\tau)$. If the acceleration changes smoothly the rapid fall-off of the Fourier transform at infinity guarantees that the leading order of the sum

$$\sum_{k_{\perp}} \sum_{m,n} |{}_s\beta_{mn}^{(1)}|^2 \quad (5.14)$$

remains finite for all spacetime dimensions. Hence, unitarity is established.

Perturbative Expansion of the Transformed Bosonic Vacuum

We return to the transformation of the vacuum state with the perturbative expansion of the normalization constant N_{vac} . We insert (5.8) into (5.2) and require $\langle 0 | 0 \rangle = 1$ to obtain

$$N_{\text{vac}} = 1 - \frac{1}{4} \sum_{p,q} |\beta_{pq}^{(1)}|^2 h^2 + O(h^4). \quad (5.15)$$

Consecutively we can express the transformed vacuum state as

$$\begin{aligned} |0\rangle &= |\widehat{0}\rangle + h \frac{1}{2} \sum_{p,q} V_{pq}^{(1)} \widehat{a}_p^{\dagger} \widehat{a}_q^{\dagger} |\widehat{0}\rangle + h^2 \frac{1}{2} \sum_{p,q} \left(V_{pq}^{(2)} \widehat{a}_p^{\dagger} \widehat{a}_q^{\dagger} - \frac{1}{2} |\beta_{pq}^{(1)}|^2 \right. \\ &\quad \left. + \frac{1}{4} \sum_{p',q'} V_{pq}^{(1)} V_{p'q'}^{(1)} \widehat{a}_p^{\dagger} \widehat{a}_q^{\dagger} \widehat{a}_{p'}^{\dagger} \widehat{a}_{q'}^{\dagger} \right) |\widehat{0}\rangle + O(h^3), \end{aligned} \quad (5.16)$$

with $V_{pq}^{(1)}$ and $V_{pq}^{(2)}$ given by (5.8b) and (5.8c), respectively. To leading order the state remains unchanged, while the linear corrections add pairs of excitations to the superposition. To linear order the changes to the state are governed by the coefficients $\beta_{mn}^{(1)}$.

The density operator corresponding to (5.16) is then simply

$$\begin{aligned}
 |0\rangle\langle 0| &= |\widehat{0}\rangle\langle \widehat{0}| + h \frac{1}{2} \sum_{p,q} (V_{pq}^{(1)} \widehat{a}_p^\dagger \widehat{a}_q^\dagger |\widehat{0}\rangle\langle \widehat{0}| + \text{H. c.}) \\
 &+ h^2 \frac{1}{2} \sum_{p,q} \left[(V_{pq}^{(2)} \widehat{a}_p^\dagger \widehat{a}_q^\dagger |\widehat{0}\rangle\langle \widehat{0}| + \text{H. c.}) - |\beta_{pq}^{(1)}|^2 |\widehat{0}\rangle\langle \widehat{0}| \right. \\
 &+ \frac{1}{4} \sum_{p',q'} (V_{pq}^{(1)} V_{p'q'}^{(1)} \widehat{a}_p^\dagger \widehat{a}_q^\dagger \widehat{a}_{p'}^\dagger \widehat{a}_{q'}^\dagger |\widehat{0}\rangle\langle \widehat{0}| + \text{H. c.}) \\
 &\left. + \frac{1}{2} \sum_{p',q'} V_{pq}^{(1)} V_{p'q'}^{(1)*} \widehat{a}_p^\dagger \widehat{a}_q^\dagger |\widehat{0}\rangle\langle \widehat{0}| \widehat{a}_{p'} \widehat{a}_{q'} \right] + O(h^3),
 \end{aligned} \tag{5.17}$$

where ‘‘H. c.’’ denotes the Hermitean conjugate, $(\mathcal{O} + \text{H. c.}) = (\mathcal{O} + \mathcal{O}^\dagger)$. Noting that V_{pq} is symmetric and the diagonal leading order terms vanish, $V_{nn}^{(1)} = 0$, the right hand side of Eq. (5.17) can be quickly seen to be normalized, i.e., $\text{Tr}(|0\rangle\langle 0|) = 1 + O(h^3)$.

5.1.2 Transformation of Bosonic Particle States

To obtain the out-region decomposition of any other Fock states we express the in-region creation operators in terms of their Bogoliubov transformation to the out-region operators, i.e.,

$$a_m^\dagger = \sum_n (\alpha_{nm}^* \widehat{a}_n^\dagger + \beta_{nm} \widehat{a}_n). \tag{5.18}$$

Consecutively, we apply the operators to the vacuum state in the decomposition (5.16) and expand the Bogoliubov coefficients as in (4.76). To illustrate the procedure we consider Fock states with a single excitation in a particular mode and such with an excitation each in two different modes.

Bosonic Single Particle States

For the single excitation in an in-region mode labelled by k we apply the creation operator a_k^\dagger to the vacuum to study the transformation of the state $a_k^\dagger |0\rangle = |1_k\rangle$. The power expansion in h gives

$$\begin{aligned}
 |1_k\rangle &= G_k^{(0)*} |\widehat{1}_k\rangle + h \left(\sum_m \alpha_{mk}^{(1)*} \widehat{a}_m^\dagger + \frac{1}{2} G_k^{(0)*} \sum_{p,q} V_{pq}^{(1)} \widehat{a}_p^\dagger \widehat{a}_q^\dagger \widehat{a}_k^\dagger \right) |\widehat{0}\rangle \\
 &+ h^2 \left[\sum_m \left(\alpha_{mk}^{(2)*} \widehat{a}_m^\dagger + \sum_p \beta_{pk}^{(1)} V_{pm}^{(1)} \widehat{a}_m^\dagger \right) + \frac{1}{2} G_k^{(0)*} \sum_{p,q} \left(\sum_m G_k^{(0)} \alpha_{mk}^{(1)*} V_{pq}^{(1)} \widehat{a}_p^\dagger \widehat{a}_q^\dagger \widehat{a}_m^\dagger \right. \right. \\
 &\left. \left. + V_{pq}^{(2)} \widehat{a}_p^\dagger \widehat{a}_q^\dagger \widehat{a}_k^\dagger - \frac{1}{2} |\beta_{pq}^{(1)}|^2 \widehat{a}_k^\dagger + \frac{1}{4} \sum_{p',q'} V_{pq}^{(1)} V_{p'q'}^{(1)} \widehat{a}_p^\dagger \widehat{a}_q^\dagger \widehat{a}_{p'}^\dagger \widehat{a}_{q'}^\dagger \widehat{a}_k^\dagger \right) \right] |\widehat{0}\rangle + O(h^3),
 \end{aligned} \tag{5.19}$$

where $V_{pq}^{(1)}$ and $V_{pq}^{(2)}$ are given by (5.8b) and (5.8c), as previously. In addition to the creation of particle pairs the linear order terms now feature the coefficients $\alpha_{mk}^{(1)}$ shifting

the excitation of mode k to other modes. The density operator for the state (5.19) is given by

$$\begin{aligned}
 |1_k\rangle\langle 1_k| &= |\widehat{1}_k\rangle\langle \widehat{1}_k| + h \left[\sum_m \left(G_k^{(0)} \alpha_{mk}^{(1)*} \widehat{a}_m^\dagger | \widehat{0} \rangle \langle \widehat{1}_k | + \text{H. c.} \right) \right. \\
 &+ \frac{1}{2} \sum_{p,q} \left(V_{pq}^{(1)} \widehat{a}_p^\dagger \widehat{a}_q^\dagger | \widehat{1}_k \rangle \langle \widehat{1}_k | + \text{H. c.} \right) \left. \right] + h^2 \left[\sum_{m,m'} \alpha_{mk}^{(1)*} \alpha_{m'k}^{(1)} \widehat{a}_m^\dagger | \widehat{0} \rangle \langle \widehat{0} | \widehat{a}_{m'} \right. \\
 &+ \sum_m \left\{ G_k^{(0)} \alpha_{mk}^{(2)*} \widehat{a}_m^\dagger | \widehat{0} \rangle \langle \widehat{1}_k | + \frac{1}{2} \sum_{p,q} G_k^{(0)*} \alpha_{mk}^{(1)} V_{pq}^{(1)} \widehat{a}_p^\dagger \widehat{a}_q^\dagger | \widehat{1}_k \rangle \langle \widehat{0} | \widehat{a}_m \right. \\
 &+ G_k^{(0)} \sum_p \beta_{pk}^{(1)} V_{pm}^{(1)} \widehat{a}_m^\dagger | \widehat{0} \rangle \langle \widehat{1}_k | + \text{H. c.} \left. \right\} + \frac{1}{2} \sum_{p,q} \left\{ \left(\sum_m G_k^{(0)} \alpha_{mk}^{(1)*} V_{pq}^{(1)} \widehat{a}_p^\dagger \widehat{a}_q^\dagger \widehat{a}_m^\dagger \right. \right. \\
 &+ V_{pq}^{(2)} \widehat{a}_p^\dagger \widehat{a}_q^\dagger \widehat{a}_k^\dagger - \frac{1}{2} |\beta_{pq}^{(1)}|^2 \widehat{a}_k^\dagger + \frac{1}{4} \sum_{p',q'} V_{pq}^{(1)} V_{p'q'}^{(1)} \widehat{a}_p^\dagger \widehat{a}_q^\dagger \widehat{a}_{p'}^\dagger \widehat{a}_{q'}^\dagger \left. \right) | \widehat{0} \rangle \langle \widehat{1}_k | \\
 &\left. + \frac{1}{4} \sum_{p',q'} V_{pq}^{(1)} V_{p'q'}^{(1)*} \widehat{a}_p^\dagger \widehat{a}_q^\dagger | \widehat{1}_k \rangle \langle \widehat{1}_k | \widehat{a}_{p'} \widehat{a}_{q'} + \text{H. c.} \right\} \left. \right] + O(h^3),
 \end{aligned} \tag{5.20}$$

The normalization of (5.20) can be verified using the Bogoliubov identity (4.78a) and the trace

$$\begin{aligned}
 \text{Tr} \left(\widehat{a}_p^\dagger \widehat{a}_q^\dagger | \widehat{1}_k \rangle \langle \widehat{1}_k | \widehat{a}_{p'} \widehat{a}_{q'} \right) &= \left(\delta_{pp'} \delta_{qq'} + \delta_{pq'} \delta_{qp'} \right) \left(2\delta_{pk}(1 - \delta_{qk}) \right. \\
 &\left. + 2\delta_{qk}(1 - \delta_{pk}) + (1 - \delta_{pk})(1 - \delta_{qk}) + 6\delta_{pk}\delta_{qk} \right),
 \end{aligned} \tag{5.21}$$

where (2.23b) is taken into account. As before with (5.16) the state remains pure, as required by the unitarity of the transformation, if no modes are traced over. We shall consider tracing over subsets of the modes in Chapters 6 and 7 to study entanglement of the remaining modes.

Bosonic Particle Pair

For the state $|1_k\rangle|1_{k'}\rangle$ we apply the creation operator $a_{k'}^\dagger$ to (5.19). For simplicity of notation in this illustration we keep terms up to linear order in h and obtain

$$\begin{aligned}
 |1_k\rangle|1_{k'}\rangle &= G_k^{(0)*} G_{k'}^{(0)*} |\widehat{1}_k\rangle|\widehat{1}_{k'}\rangle + h \left[\frac{1}{2} \left(G_k^{(0)*} \beta_{kk'}^{(1)} + G_{k'}^{(0)*} \beta_{k'k}^{(1)} \right) | \widehat{0} \rangle \right. \\
 &+ \sum_m G_k^{(0)*} \alpha_{mk'}^{(1)*} \widehat{a}_m^\dagger | \widehat{1}_k \rangle + \sum_m G_{k'}^{(0)*} \alpha_{mk}^{(1)*} \widehat{a}_m^\dagger | \widehat{1}_{k'} \rangle \\
 &\left. - \frac{1}{2} G_k^{(0)*} G_{k'}^{(0)*} \sum_{p,q} G_q^{(0)*} \beta_{pq}^{(1)*} \widehat{a}_p^\dagger \widehat{a}_q^\dagger | \widehat{1}_k \rangle | \widehat{1}_{k'} \rangle \right] + O(h^2).
 \end{aligned} \tag{5.22}$$

The corresponding density operator is given by the projector on $|1_k\rangle|1_{k'}\rangle$. As can be inferred from (5.17) and (5.20) the density operator decomposition becomes more and more involved when additional excitations are added. For more complicated states it thus becomes cumbersome to study the Bogoliubov transformation in this fashion.

5.2 Transformation of Bosonic Gaussian States

5.2.1 Symplectic Representation of Non-uniform Motion

A computationally much simpler way of handling more complicated states is the *symplectic representation* of the Bogoliubov transformation in phase space as explained in Section 3.1.2. The symplectic transformation S for an arbitrary travel scenario can be decomposed into blocks \mathcal{M}_{mn} as given in (3.14), see Ref. [83, (vii)]. For fixed m and n the 2×2 matrix \mathcal{M}_{mn} is given by (3.15), which we may expand in a power series in h ,

$$\mathcal{M}_{ij} = \mathcal{M}_{ij}^{(0)} + \mathcal{M}_{ij}^{(1)} h + \mathcal{M}_{ij}^{(2)} h^2 + O(h^3), \quad (5.23)$$

where the non-vanishing leading order coefficient matrices in the expansion are given by

$$\mathcal{M}_{ii}^{(0)} = \begin{pmatrix} \cos(\omega_i \tilde{\tau}) & \sin(\omega_i \tilde{\tau}) \\ -\sin(\omega_i \tilde{\tau}) & \cos(\omega_i \tilde{\tau}) \end{pmatrix}, \quad (5.24)$$

with ω_i given by (4.7). The coefficient matrices of h^n take the form

$$\mathcal{M}_{ij}^{(n)} = \begin{pmatrix} \operatorname{Re}(\alpha_{ij}^{(n)} - \beta_{ij}^{(n)}) & \operatorname{Im}(\alpha_{ij}^{(n)} + \beta_{ij}^{(n)}) \\ -\operatorname{Im}(\alpha_{ij}^{(n)} - \beta_{ij}^{(n)}) & \operatorname{Re}(\alpha_{ij}^{(n)} + \beta_{ij}^{(n)}) \end{pmatrix}, \quad (5.25)$$

where $\alpha_{ij}^{(n)}$ and $\beta_{ij}^{(n)}$ are as in (4.76).

5.2.2 Transformed Covariance Matrix Example

Specializing to *Gaussian states* we are interested in the effect of the non-uniform motion described in Chapter 4 on the covariance matrix, which encodes all the information about the entanglement of the state. The symplectic transformation S for a given travel scenario takes the in-region covariance matrix Γ to

$$\hat{\Gamma} = S \Gamma S^T. \quad (5.26)$$

We examine a particular example for an initial state more closely. A fully separable state, represented by the covariance matrix $\Gamma = \bigoplus_n \Gamma_n$ of an arbitrary number of modes with individual covariance matrices Γ_n ($n = 1, 2, \dots$). The transformed covariance matrix $\hat{\Gamma}$ decomposes into the diagonal blocks $\hat{\Gamma}_m$ for the individual modes, and off-diagonal blocks \hat{C}_{mn} encoding the correlations between modes m and n . In terms of the matrices \mathcal{M}_{mn} from (3.15) these 2×2 matrices read

$$\hat{\Gamma}_m = \sum_i \mathcal{M}_{mi} \Gamma_i \mathcal{M}_{mi}^T, \quad (5.27a)$$

$$\hat{C}_{mn} = \sum_i \mathcal{M}_{mi} \Gamma_i \mathcal{M}_{ni}^T. \quad (5.27b)$$

Transformed Single-mode Squeezed States

To examine our example more closely we select particular initial states Γ_n , i.e., we assume that each single mode can be *squeezed* with squeezing parameters $s_n \in \mathbb{R}$, such that the matrices Γ_n are given by (3.8)

$$\Gamma_n(s_n) = \begin{pmatrix} e^{2s_n} & 0 \\ 0 & e^{-2s_n} \end{pmatrix}. \quad (5.28)$$

Employing the perturbative expansion of (5.23) we get $\hat{\Gamma}_m$ from (5.27a) as a power series in h ,

$$\hat{\Gamma}_m = \hat{\Gamma}_m^{(0)} + \hat{\Gamma}_m^{(1)} h + \hat{\Gamma}_m^{(2)} h^2 + O(h^3). \quad (5.29)$$

The symmetric coefficient matrices in the expansion are expressed in components order by order, that is

$$(\hat{\Gamma}_m^{(0)})_{11} = \cosh(2s_m) + \sinh(2s_m) \cos(2\omega_m \tilde{\tau}), \quad (5.30a)$$

$$(\hat{\Gamma}_m^{(0)})_{22} = \cosh(2s_m) - \sinh(2s_m) \cos(2\omega_m \tilde{\tau}), \quad (5.30b)$$

$$(\hat{\Gamma}_m^{(0)})_{12} = -\sinh(2s_m) \sin(2\omega_m \tilde{\tau}). \quad (5.30c)$$

The coefficients of h in the expansion of $\hat{\Gamma}_m$ in (5.29) vanish identically but the second order coefficients are non-zero and given by

$$\begin{aligned} (\hat{\Gamma}_m^{(2)})_{11} &= 2 \cosh(2s_m) \operatorname{Re}(G_m^{(0)} [\alpha_{mm}^{(2)*} - \beta_{mm}^{(2)}]) + \sinh(2s_m) \operatorname{Re}(G_m^{(0)} [\alpha_{mm}^{(2)} - \beta_{mm}^{(2)*}]) \\ &+ \sum_n \left[\cosh(2s_m) \left(|\alpha_{mn}^{(1)}|^2 - 2 \operatorname{Re}(\alpha_{mn}^{(1)} \beta_{mn}^{(1)}) + |\beta_{mn}^{(1)}|^2 \right) \right. \\ &\quad \left. + \sinh(2s_m) \operatorname{Re} \left((\alpha_{mn}^{(1)})^2 - 2\alpha_{mn}^{(1)} \beta_{mn}^{(1)*} + (\beta_{mn}^{(1)})^2 \right) \right], \end{aligned} \quad (5.31a)$$

$$\begin{aligned} (\hat{\Gamma}_m^{(2)})_{22} &= 2 \cosh(2s_m) \operatorname{Re}(G_m^{(0)} [\alpha_{mm}^{(2)*} + \beta_{mm}^{(2)}]) - \sinh(2s_m) \operatorname{Re}(G_m^{(0)} [\alpha_{mm}^{(2)} + \beta_{mm}^{(2)*}]) \\ &+ \sum_n \left[\cosh(2s_m) \left(|\alpha_{mn}^{(1)}|^2 + 2 \operatorname{Re}(\alpha_{mn}^{(1)} \beta_{mn}^{(1)}) + |\beta_{mn}^{(1)}|^2 \right) \right. \\ &\quad \left. - \sinh(2s_m) \operatorname{Re} \left((\alpha_{mn}^{(1)})^2 + 2\alpha_{mn}^{(1)} \beta_{mn}^{(1)*} + (\beta_{mn}^{(1)})^2 \right) \right], \end{aligned} \quad (5.31b)$$

$$\begin{aligned} (\hat{\Gamma}_m^{(2)})_{12} &= 2 \cosh(2s_m) \operatorname{Im}(G_m^{(0)} \beta_{mm}^{(2)}) - 2 \sinh(2s_m) \operatorname{Im}(G_m^{(0)} \alpha_{mm}^{(2)}) \\ &+ \sum_n \left[2 \cosh(2s_m) \operatorname{Im}(\alpha_{mn}^{(1)} \beta_{mn}^{(1)}) - \sinh(2s_m) \operatorname{Im}((\alpha_{mn}^{(1)})^2 + (\beta_{mn}^{(1)})^2) \right]. \end{aligned} \quad (5.31c)$$

Similarly, the off-diagonal blocks \hat{C}_{mn} are expanded as

$$\hat{C}_{mn} = \hat{C}_{mn}^{(1)} h + \hat{C}_{mn}^{(2)} h^2 + O(h^3), \quad (5.32)$$

where the lowest order in the expansion is linear in h . The corresponding components of these coefficients are given by

$$\begin{aligned} (\widehat{C}_{mn}^{(1)})_{11} &= \cosh(2s_m) \operatorname{Re}(G_m^{(0)} [\alpha_{nm}^{(1)*} - \beta_{nm}^{(1)}]) + \cosh(2s_n) \operatorname{Re}(G_n^{(0)} [\alpha_{mn}^{(1)*} - \beta_{mn}^{(1)}]) \\ &\quad + \sinh(2s_m) \operatorname{Re}(G_m^{(0)} [\alpha_{nm}^{(1)} - \beta_{nm}^{(1)*}]) + \sinh(2s_n) \operatorname{Re}(G_n^{(0)} [\alpha_{mn}^{(1)} - \beta_{mn}^{(1)*}]), \end{aligned} \quad (5.33a)$$

$$\begin{aligned} (\widehat{C}_{mn}^{(1)})_{22} &= \cosh(2s_m) \operatorname{Re}(G_m^{(0)} [\alpha_{nm}^{(1)*} + \beta_{nm}^{(1)}]) + \cosh(2s_n) \operatorname{Re}(G_n^{(0)} [\alpha_{mn}^{(1)*} + \beta_{mn}^{(1)}]) \\ &\quad - \sinh(2s_m) \operatorname{Re}(G_m^{(0)} [\alpha_{nm}^{(1)} + \beta_{nm}^{(1)*}]) - \sinh(2s_n) \operatorname{Re}(G_n^{(0)} [\alpha_{mn}^{(1)} + \beta_{mn}^{(1)*}]), \end{aligned} \quad (5.33b)$$

$$\begin{aligned} (\widehat{C}_{mn}^{(1)})_{12} &= \cosh(2s_m) \operatorname{Im}(G_m^{(0)} [\beta_{nm}^{(1)} + \alpha_{nm}^{(1)*}]) + \cosh(2s_n) \operatorname{Im}(G_n^{(0)} [\beta_{mn}^{(1)} - \alpha_{mn}^{(1)*}]) \\ &\quad - \sinh(2s_m) \operatorname{Im}(G_m^{(0)} [\alpha_{nm}^{(1)} + \beta_{nm}^{(1)*}]) - \sinh(2s_n) \operatorname{Im}(G_n^{(0)} [\alpha_{mn}^{(1)} - \beta_{mn}^{(1)*}]), \end{aligned} \quad (5.33c)$$

$$\begin{aligned} (\widehat{C}_{mn}^{(1)})_{21} &= \cosh(2s_m) \operatorname{Im}(G_m^{(0)} [\beta_{nm}^{(1)} - \alpha_{nm}^{(1)*}]) + \cosh(2s_n) \operatorname{Im}(G_n^{(0)} [\beta_{mn}^{(1)} + \alpha_{mn}^{(1)*}]) \\ &\quad - \sinh(2s_m) \operatorname{Im}(G_m^{(0)} [\alpha_{nm}^{(1)} - \beta_{nm}^{(1)*}]) - \sinh(2s_n) \operatorname{Im}(G_n^{(0)} [\alpha_{mn}^{(1)} + \beta_{mn}^{(1)*}]). \end{aligned} \quad (5.33d)$$

We shall study the entanglement of the transformed single mode squeezed states in Chapter 6. For now, let us briefly return to the Fock space treatment, this time for the fermions.

5.3 Fermionic State Transformation

5.3.1 Fermionic Vacuum Transformation

We pursue the construction of the Bogoliubov transformation on the *fermionic Fock space* (see Section 2.3.2) in a completely analogous fashion as the previous bosonic case in Section 5.1 by starting from the fermionic vacuum state $\|0\rangle\rangle$. Following Ref. [(iv)][87], a similar argument as that made for bosons on page 100 allows us to make the ansatz

$$\|0\rangle\rangle = \tilde{N}_{\text{vac}} \exp(\mathcal{W}) \|\widehat{0}\rangle\rangle = \tilde{N}_{\text{vac}} \exp\left(\frac{1}{2} \sum_{\substack{p \geq 0 \\ q < 0}} \mathcal{V}_{pq} \widehat{b}_p^\dagger \widehat{c}_q^\dagger\right) \|\widehat{0}\rangle\rangle, \quad (5.34)$$

where $\mathcal{V}_{pq} \in \mathbb{C}$ and \tilde{N}_{vac} is a normalization constant. We then examine the property $b_n \|0\rangle\rangle = 0$ by inserting the Bogoliubov transformation of b_n ,

$$b_n = \sum_{m \geq 0} A_{mn} \widehat{b}_m + \sum_{m < 0} A_{mn} \widehat{c}_m^\dagger. \quad (5.35)$$

Now turning again to the Hadamard Lemma of (5.4) the commutators

$$[\widehat{b}_m, \mathcal{W}] = \sum_{q < 0} \mathcal{V}_{mq} \widehat{c}_q^\dagger, \quad (5.36a)$$

$$[\widehat{c}_m^\dagger, \mathcal{W}] = [[\widehat{b}_m, \mathcal{W}], \mathcal{W}] = 0, \quad (5.36b)$$

provide the criterion (for $n \geq 0, q < 0$)

$$\sum_{m \geq 0} A_{mn} \mathcal{V}_{mq} = -A_{qn}, \quad (5.37a)$$

while the same procedure using $c_n || 0 \rangle\rangle = 0$ gives (for $n < 0, p \geq 0$)

$$\sum_{m < 0} A_{mn}^* \mathcal{V}_{pm} = A_{pn}^*. \quad (5.37b)$$

If one of the blocks of $A = (A_{mn})$ where the indices are either both non-negative or both negative is invertible then the conditions (5.37a) or (5.37b), respectively, uniquely determine the matrix \mathcal{V} . If both blocks are invertible (5.37a) and (5.37b) are equivalent by virtue of the unitarity of A , i.e., $A^\dagger A = \mathbb{1}$.

Unitarity of the Transformation — Fermions

To ensure that the fermionic in-region and out-region vacua can indeed be unitarily related a closer examination of the Hilbert-Schmidt condition is in order. For the fermionic case it manifests as the condition that the blocks of $A = (A_{mn})$ that relate positive and negative frequency solutions are *Hilbert-Schmidt*, see Ref. [122]. In complete analogy to (5.9) the leading order presents the requirement

$$\sum_{\substack{p \geq 0 \\ q < 0}} |A_{pq}^{(1)}|^2 < \infty. \quad (5.38)$$

We proceed, as before, with the sharp transitions between the Minkowski and Rindler solutions in (1+1) dimensions, and we consider first the case of zero mass. The leading order coefficients for $M = 0$ are given by (4.60)

$$\sum_{\substack{p \geq 0 \\ q < 0}} |{}_o A_{pq}^{(1)}(M = 0)|^2 = \frac{1}{96\pi^4} (28\zeta(3) - 31\zeta(5)) < \infty, \quad (5.39)$$

where $\zeta(z)$ is the *Riemann zeta function*. For the massive case we use an analysis as in (5.11), where we consider an estimate in terms of a *Riemann sum* [88, (x)]. Substituting $x = m\pi/M$ and $y = n\pi/M$ we write

$$\begin{aligned} M^2 \sum_{\substack{p \geq 0 \\ q < 0}} |{}_o A_{pq}^{(1)}(M)|^2 &\rightarrow \frac{8}{\pi^2} \int_{\substack{x > 0 \\ y > 0}} \frac{(\sqrt{1+x^2} + x - \sqrt{1+y^2} - y)^2}{(\sqrt{1+x^2} + x + \sqrt{1+y^2} + y)^6} \\ &\times \frac{[(\sqrt{1+x^2} + x)(\sqrt{1+y^2} + y) - 1]^2}{[(\sqrt{1+x^2} + x)(\sqrt{1+y^2} + y) + 1]^6} \times \frac{x^2 y^2 (\sqrt{1+x^2} + x)^4 (\sqrt{1+y^2} + y)^4}{(1+x^2)(1+y^2)} dx dy, \end{aligned} \quad (5.40)$$

where ${}_0A_{pq}^{(1)}$ are the coefficients of (4.59). The integral in (5.40), where we have set $x = |p|/\mu$ and $y = |q|/\mu$, can be evaluated by the substitution $x = (u - u^{-1})/2$ and $y = (v - v^{-1})/2$, which reveals

$$M^2 \sum_{\substack{p \geq 0 \\ q < 0}} |{}_0A_{pq}^{(1)}(M)|^2 \rightarrow \frac{7}{45\pi^2} - \frac{1}{64} < \infty. \quad (5.41)$$

We can thus conclude that the Hilbert-Schmidt condition is satisfied for the $(1 + 1)$ dimensional Dirac cavity field for all M . The addition of extra spatial dimensions suffers from the same limitations as the bosonic case [see Eq. (5.13)] such that the unitarity of the Bogoliubov transformation for sharp transitions holds only in $(1 + 1)$ and $(2 + 1)$ dimensions, but fails in $(3 + 1)$ dimensions and beyond. For smooth accelerations the rapid fall-off of the Fourier transform in Eq. (4.91b) again guarantees the unitarity for all cases. With this in mind we return to the transformation of the vacuum state.

Perturbative Expansion of the Transformed Fermionic Vacuum

We now perform the perturbative expansion of Eq. (5.37a) with the coefficients of (4.76c), which yields

$$\mathcal{V}_{pq} = \mathcal{V}_{pq}^{(1)} h + \mathcal{V}_{pq}^{(2)} h^2 + O(h^3), \quad (5.42)$$

where the expansion coefficients are given by

$$\mathcal{V}_{pq}^{(1)} = -G_p^{(0)*} A_{qp}^{(1)}, \quad (5.43a)$$

$$\mathcal{V}_{pq}^{(2)} = -G_p^{(0)*} A_{qp}^{(2)} - G_p^{(0)*} G_q^{(0)} \sum_{m \geq 0} A_{mp}^{(1)} A_{mq}^{(1)*}. \quad (5.43b)$$

With this the normalization constant in (5.34) is immediately obtained as

$$\tilde{N}_{\text{vac}} = 1 - \frac{1}{2} \sum_{\substack{p \geq 0 \\ q < 0}} |A_{pq}^{(1)}|^2 h^2 + O(h^4). \quad (5.44)$$

In the following we will assume that the first (second) index of \mathcal{V}_{pq} is always non-negative (negative) unless otherwise stated. The vacuum state can then be straightforwardly expanded in terms of powers of h ,

$$\begin{aligned} \|0\rangle\rangle &= \|\hat{0}\rangle\rangle + h \sum_{p,q} \mathcal{V}_{pq}^{(1)} \hat{b}_p^\dagger \hat{c}_q^\dagger \|\hat{0}\rangle\rangle + h^2 \sum_{p,q} \left(\mathcal{V}_{pq}^{(2)} \hat{b}_p^\dagger \hat{c}_q^\dagger - \frac{1}{2} |A_{pq}^{(1)}|^2 \right. \\ &\quad \left. + \frac{1}{2} \sum_{p',q'} \mathcal{V}_{pq}^{(1)} \mathcal{V}_{p'q'}^{(1)} \hat{b}_p^\dagger \hat{c}_q^\dagger \hat{b}_{p'}^\dagger \hat{c}_{q'}^\dagger \right) \|\hat{0}\rangle\rangle + O(h^3), \end{aligned} \quad (5.45)$$

where we keep in mind the fermionic anticommutation relations (2.33b) that imply that no second particle or antiparticle can be added to the same mode — the *Pauli exclusion*

principle. To progress further it is convenient to introduce an additional label in the fermionic Fock states of Section 2.3.2. We distinguish excitations of positive (negative) frequency modes by a superscript sign + (−) on the double-lined ket notation, i.e.,

$$b_p^\dagger \parallel 0 \rangle\rangle = \parallel 1_p \rangle\rangle^+ , \quad (5.46a)$$

$$c_q^\dagger \parallel 0 \rangle\rangle = \parallel 1_q \rangle\rangle^- , \quad (5.46b)$$

and similarly for the co-vectors. With this notation at hand we may rewrite Eq. (5.45),

$$\begin{aligned} \parallel 0 \rangle\rangle &= \parallel \hat{0} \rangle\rangle + h \sum_{p,q} \mathcal{V}_{pq}^{(1)} \parallel \hat{1}_p \rangle\rangle^+ \parallel \hat{1}_q \rangle\rangle^- + h^2 \sum_{p,q} \left[\mathcal{V}_{pq}^{(2)} \parallel \hat{1}_p \rangle\rangle^+ \parallel \hat{1}_q \rangle\rangle^- - \frac{1}{2} |\mathcal{V}_{pq}^{(1)}|^2 \parallel \hat{0} \rangle\rangle \right. \\ &\quad \left. + \frac{1}{2} \sum_{p',q'} \mathcal{V}_{pq}^{(1)} \mathcal{V}_{p'q'}^{(1)} (1 - \delta_{pp'}) (1 - \delta_{qq'}) \parallel \hat{1}_p \rangle\rangle^+ \parallel \hat{1}_q \rangle\rangle^- \parallel \hat{1}_{p'} \rangle\rangle^+ \parallel \hat{1}_{q'} \rangle\rangle^- \right] + O(h^3), \end{aligned} \quad (5.47)$$

where we have suppressed the symbol for the anti-symmetrized tensor product (see Section 2.3.2). To conclude this section we form the density operator for the transformed vacuum state

$$\begin{aligned} \parallel 0 \rangle\rangle \langle\langle 0 \parallel &= \parallel \hat{0} \rangle\rangle \langle\langle \hat{0} \parallel + h \sum_{p,q} \left[\mathcal{V}_{pq}^{(1)} \parallel \hat{1}_p \rangle\rangle^+ \parallel \hat{1}_q \rangle\rangle^- \langle\langle \hat{0} \parallel + \text{H. c.} \right] - h^2 \sum_{p,q} \left[|\mathcal{V}_{pq}^{(1)}|^2 \parallel \hat{0} \rangle\rangle \langle\langle \hat{0} \parallel \right. \\ &\quad \left. - \frac{1}{2} \sum_{p',q'} \left(\mathcal{V}_{pq}^{(1)} \mathcal{V}_{p'q'}^{(1)} (1 - \delta_{pp'}) (1 - \delta_{qq'}) \parallel \hat{1}_p \rangle\rangle^+ \parallel \hat{1}_q \rangle\rangle^- \parallel \hat{1}_{p'} \rangle\rangle^+ \parallel \hat{1}_{q'} \rangle\rangle^- \langle\langle \hat{0} \parallel + \text{H. c.} \right) \right. \\ &\quad \left. - \left(\mathcal{V}_{pq}^{(2)} \parallel \hat{1}_p \rangle\rangle^+ \parallel \hat{1}_q \rangle\rangle^- \langle\langle \hat{0} \parallel + \text{H. c.} \right) - \sum_{p',q'} \mathcal{V}_{pq}^{(1)} \mathcal{V}_{p'q'}^{(1)*} \parallel \hat{1}_p \rangle\rangle^+ \parallel \hat{1}_q \rangle\rangle^- \langle\langle \hat{1}_{q'} \parallel^+ \langle\langle \hat{1}_{p'} \parallel \right] + O(h^3). \end{aligned} \quad (5.48)$$

5.3.2 Transformation of Fermionic Particle & Anti-Particle States

We continue with the *fermionic Fock states* with particle or antiparticle content, by applying the respective creation operators b_n^\dagger ($n \geq 0$) and c_n^\dagger ($n < 0$) with Bogoliubov decompositions

$$b_n^\dagger = \sum_{m \geq 0} A_{mn}^* \hat{b}_m^\dagger + \sum_{m < 0} A_{mn}^* \hat{c}_m, \quad (5.49a)$$

$$c_n^\dagger = \sum_{m \geq 0} A_{mn} \hat{b}_m + \sum_{m < 0} A_{mn} \hat{c}_m^\dagger. \quad (5.49b)$$

Fermionic Single Particle States

For the single fermion state $\parallel 1_\kappa \rangle\rangle^+$, an excitation in a mode labelled by $\kappa \geq 0$, we apply the operator b_κ^\dagger of (5.49a), with coefficients expanded as in (4.76c) to the vacuum

state (5.47) and we get

$$\begin{aligned}
 \|1_\kappa\rangle\rangle^+ &= G_\kappa^{(0)*} \|\widehat{1}_\kappa\rangle\rangle^+ + h \left[\sum_{m \geq 0} A_{m\kappa}^{(1)*} \|\widehat{1}_m\rangle\rangle^+ + G_\kappa^{(0)*} \sum_{p,q} \mathcal{V}_{pq}^{(1)} (1 - \delta_{p\kappa}) \|\widehat{1}_\kappa\rangle\rangle^+ \|\widehat{1}_p\rangle\rangle^+ \|\widehat{1}_q\rangle\rangle^- \right] \\
 &+ h^2 \left\{ \sum_{m \geq 0} A_{m\kappa}^{(2)*} \|\widehat{1}_m\rangle\rangle^+ + \sum_{p,q} \left[\sum_{m \geq 0} A_{m\kappa}^{(1)*} \mathcal{V}_{pq}^{(1)} (1 - \delta_{mp}) \|\widehat{1}_m\rangle\rangle^+ \|\widehat{1}_p\rangle\rangle^+ \|\widehat{1}_q\rangle\rangle^- \right. \right. \\
 &- A_{q\kappa}^{(1)*} \mathcal{V}_{pq}^{(1)} \|\widehat{1}_p\rangle\rangle^+ + G_\kappa^{(0)*} \mathcal{V}_{pq}^{(2)} (1 - \delta_{p\kappa}) \|\widehat{1}_\kappa\rangle\rangle^+ \|\widehat{1}_p\rangle\rangle^+ \|\widehat{1}_q\rangle\rangle^- - \frac{1}{2} G_\kappa^{(0)*} |\mathcal{V}_{pq}^{(1)}|^2 \|\widehat{1}_\kappa\rangle\rangle^+ \\
 &- \frac{1}{2} G_\kappa^{(0)*} \sum_{p',q'} \mathcal{V}_{pq}^{(1)} \mathcal{V}_{p'q'}^{(1)} (1 - \delta_{pp'}) (1 - \delta_{qq'}) (1 - \delta_{\kappa p}) (1 - \delta_{\kappa p'}) \\
 &\left. \left. \times \|\widehat{1}_\kappa\rangle\rangle^+ \|\widehat{1}_p\rangle\rangle^+ \|\widehat{1}_{p'}\rangle\rangle^+ \|\widehat{1}_q\rangle\rangle^- \|\widehat{1}_{q'}\rangle\rangle^- \right] \right\} + O(h^3). \tag{5.50}
 \end{aligned}$$

To leading order the state remains unchanged apart from the phase that is picked up during time evolution. At linear order in h Eq. (5.50) illustrates the role of the α and β -type coefficients. The block of $A_{mn}^{(1)}$ where both indices are non-negative shifts the available excitation into a superposition of excitations in positive frequency modes. On the other hand, the block of $A_{mn}^{(1)}$ that mixes negative and non-negative indices is responsible for terms in the superposition with additional pairs of particles and antiparticles. The appropriate expression, to second order in h , for the density operator of the pure state $\|1_\kappa\rangle\rangle^+$ is given by

$$\begin{aligned}
 \|1_\kappa\rangle\rangle^+ \langle\langle 1_\kappa \| &= \|\widehat{1}_\kappa\rangle\rangle^+ \langle\langle \widehat{1}_\kappa \| + h \left[\sum_{p,q} \mathcal{V}_{pq}^{(1)} (1 - \delta_{p\kappa}) \|\widehat{1}_\kappa\rangle\rangle^+ \|\widehat{1}_p\rangle\rangle^+ \|\widehat{1}_q\rangle\rangle^- \langle\langle \widehat{1}_\kappa \| \right. \\
 &+ G_\kappa^{(0)} \sum_{m \geq 0} A_{m\kappa}^{(1)*} \|\widehat{1}_m\rangle\rangle^+ \langle\langle \widehat{1}_\kappa \| + \text{H. c.} \left. \right] + h^2 \left\{ \sum_{m,m' \geq 0} A_{m\kappa}^{(1)*} A_{m'\kappa}^{(1)} \|\widehat{1}_m\rangle\rangle^+ \langle\langle \widehat{1}_{m'} \| \right. \\
 &+ \sum_{\substack{p,q \\ m \geq 0}} \left(G_\kappa^{(0)*} A_{m\kappa}^{(1)} \mathcal{V}_{pq}^{(1)} (1 - \delta_{p\kappa}) \|\widehat{1}_\kappa\rangle\rangle^+ \|\widehat{1}_p\rangle\rangle^+ \|\widehat{1}_q\rangle\rangle^- \langle\langle \widehat{1}_m \| + \text{H. c.} \right) + \sum_{p,q,p',q'} \mathcal{V}_{pq}^{(1)} \mathcal{V}_{p'q'}^{(1)*} \\
 &\times (1 - \delta_{p\kappa}) (1 - \delta_{p'\kappa}) \|\widehat{1}_\kappa\rangle\rangle^+ \|\widehat{1}_p\rangle\rangle^+ \|\widehat{1}_q\rangle\rangle^- \langle\langle \widehat{1}_{q'} \| \langle\langle \widehat{1}_{p'} \| \langle\langle \widehat{1}_\kappa \| + \left[G_\kappa^{(0)} \sum_{m \geq 0} A_{m\kappa}^{(2)*} \right. \\
 &\times \|\widehat{1}_m\rangle\rangle^+ \langle\langle \widehat{1}_\kappa \| + \sum_{p,q} \left(G_\kappa^{(0)} \sum_{m \geq 0} A_{m\kappa}^{(1)*} \mathcal{V}_{pq}^{(1)} (1 - \delta_{mp}) \|\widehat{1}_m\rangle\rangle^+ \|\widehat{1}_p\rangle\rangle^+ \|\widehat{1}_q\rangle\rangle^- \langle\langle \widehat{1}_\kappa \| \right. \\
 &- G_\kappa^{(0)} A_{q\kappa}^{(1)*} \mathcal{V}_{pq}^{(1)} \|\widehat{1}_p\rangle\rangle^+ \langle\langle \widehat{1}_\kappa \| + \mathcal{V}_{pq}^{(2)} (1 - \delta_{p\kappa}) \|\widehat{1}_\kappa\rangle\rangle^+ \|\widehat{1}_p\rangle\rangle^+ \|\widehat{1}_q\rangle\rangle^- \langle\langle \widehat{1}_\kappa \| \\
 &- \frac{1}{2} |\mathcal{V}_{pq}^{(1)}|^2 \|\widehat{1}_\kappa\rangle\rangle^+ \langle\langle \widehat{1}_\kappa \| - \frac{1}{2} \sum_{p',q'} \mathcal{V}_{pq}^{(1)} \mathcal{V}_{p'q'}^{(1)} (1 - \delta_{pp'}) (1 - \delta_{qq'}) (1 - \delta_{\kappa p}) (1 - \delta_{\kappa p'}) \\
 &\left. \left. \times \|\widehat{1}_\kappa\rangle\rangle^+ \|\widehat{1}_p\rangle\rangle^+ \|\widehat{1}_{p'}\rangle\rangle^+ \|\widehat{1}_q\rangle\rangle^- \|\widehat{1}_{q'}\rangle\rangle^- \langle\langle \widehat{1}_\kappa \| \right) + \text{H. c.} \right\} + O(h^3). \tag{5.51}
 \end{aligned}$$

Fermionic Single Anti-Particle States

For the single anti-fermion state $\|1_{\kappa'}\rangle\rangle^-$, an excitation in a mode labelled by $\kappa' < 0$, we apply the operator $c_{\kappa'}^\dagger$ of (5.49b), with coefficients expanded as in (4.76c), to the

vacuum state (5.47) to get

$$\begin{aligned}
 \|1_{\kappa'}\rangle\rangle^- &= G_{\kappa'}^{(0)} \|\widehat{1}_{\kappa'}\rangle\rangle^- + h \left[\sum_{m<0} A_{m\kappa'}^{(1)} \|\widehat{1}_m\right\rangle\rangle^- + G_{\kappa'}^{(0)} \sum_{p,q} \mathcal{V}_{pq}^{(1)} (1 - \delta_{q\kappa'}) \|\widehat{1}_p\rangle\rangle^+ \|\widehat{1}_q\rangle\rangle^- \|\widehat{1}_{\kappa'}\rangle\rangle^- \Big] \\
 &+ h^2 \left\{ \sum_{m<0} A_{m\kappa'}^{(2)} \|\widehat{1}_m\right\rangle\rangle^- + \sum_{p,q} \left[\sum_{m<0} A_{m\kappa'}^{(1)} \mathcal{V}_{pq}^{(1)} (1 - \delta_{mq}) \|\widehat{1}_p\rangle\rangle^+ \|\widehat{1}_q\rangle\rangle^- \|\widehat{1}_m\right\rangle\rangle^- \right. \\
 &+ A_{p\kappa'}^{(1)} \mathcal{V}_{pq}^{(1)} \|\widehat{1}_q\rangle\rangle^- + G_{\kappa'}^{(0)} \mathcal{V}_{pq}^{(2)} (1 - \delta_{q\kappa'}) \|\widehat{1}_p\rangle\rangle^+ \|\widehat{1}_q\rangle\rangle^- \|\widehat{1}_{\kappa'}\rangle\rangle^- - \frac{1}{2} G_{\kappa'}^{(0)} |\mathcal{V}_{pq}^{(1)}|^2 \|\widehat{1}_{\kappa'}\rangle\rangle^- \\
 &\left. - \frac{1}{2} G_{\kappa'}^{(0)} \sum_{p',q'} \mathcal{V}_{pq}^{(1)} \mathcal{V}_{p'q'}^{(1)} (1 - \delta_{pp'}) (1 - \delta_{qq'}) (1 - \delta_{\kappa'q}) (1 - \delta_{\kappa'q'}) \right. \\
 &\quad \left. \times \|\widehat{1}_p\rangle\rangle^+ \|\widehat{1}_{p'}\rangle\rangle^+ \|\widehat{1}_q\rangle\rangle^- \|\widehat{1}_{q'}\rangle\rangle^- \|\widehat{1}_{\kappa'}\rangle\rangle^- \right\} + O(h^3). \tag{5.52}
 \end{aligned}$$

In complete analogy to (5.51) we express the density operator for the pure state $\|1_{\kappa'}\rangle\rangle^-$ as

$$\begin{aligned}
 \|1_{\kappa'}\rangle\rangle^- \langle\langle 1_{\kappa'} \| &= \|\widehat{1}_{\kappa'}\rangle\rangle^- \langle\langle \widehat{1}_{\kappa'} \| + h \left[\sum_{p,q} \mathcal{V}_{pq}^{(1)} (1 - \delta_{q\kappa'}) \|\widehat{1}_p\rangle\rangle^+ \|\widehat{1}_q\rangle\rangle^- \|\widehat{1}_{\kappa'}\rangle\rangle^- \langle\langle \widehat{1}_{\kappa'} \| \right. \\
 &+ G_{\kappa'}^{(0)*} \sum_{m<0} A_{m\kappa'}^{(1)} \|\widehat{1}_m\right\rangle\rangle^- \langle\langle \widehat{1}_{\kappa'} \| + \text{H. c.} \Big] + h^2 \left\{ \sum_{m,m'<0} A_{m\kappa'}^{(1)*} A_{m'\kappa'}^{(1)} \|\widehat{1}_m\right\rangle\rangle^- \langle\langle \widehat{1}_{m'} \| \right. \\
 &+ \sum_{\substack{p,q \\ m<0}} \left(G_{\kappa'}^{(0)} A_{m'\kappa'}^{(1)*} \mathcal{V}_{pq}^{(1)} (1 - \delta_{mq}) \|\widehat{1}_p\rangle\rangle^+ \|\widehat{1}_q\rangle\rangle^- \|\widehat{1}_{\kappa'}\rangle\rangle^- \langle\langle \widehat{1}_m \| + \text{H. c.} \right) + \sum_{p,q,p',q'} \mathcal{V}_{pq}^{(1)} \mathcal{V}_{p'q'}^{(1)*} \\
 &\times (1 - \delta_{q\kappa'}) (1 - \delta_{q'\kappa'}) \|\widehat{1}_p\rangle\rangle^+ \|\widehat{1}_q\rangle\rangle^- \|\widehat{1}_{\kappa'}\rangle\rangle^- \langle\langle \widehat{1}_{\kappa'} \| \langle\langle \widehat{1}_{q'} \| \langle\langle \widehat{1}_{p'} \| + \left[G_{\kappa'}^{(0)*} \sum_{m<0} A_{m\kappa'}^{(2)} \right. \\
 &\times \|\widehat{1}_m\right\rangle\rangle^- \langle\langle \widehat{1}_{\kappa'} \| + \sum_{p,q} \left(G_{\kappa'}^{(0)*} \sum_{m<0} A_{m\kappa'}^{(1)} \mathcal{V}_{pq}^{(1)} (1 - \delta_{mq}) \|\widehat{1}_p\rangle\rangle^+ \|\widehat{1}_q\rangle\rangle^- \|\widehat{1}_m\right\rangle\rangle^- \langle\langle \widehat{1}_{\kappa'} \| \\
 &+ G_{\kappa'}^{(0)*} A_{p\kappa'}^{(1)} \mathcal{V}_{pq}^{(1)} \|\widehat{1}_q\rangle\rangle^- \langle\langle \widehat{1}_{\kappa'} \| + \mathcal{V}_{pq}^{(2)} (1 - \delta_{q\kappa'}) \|\widehat{1}_p\rangle\rangle^+ \|\widehat{1}_q\rangle\rangle^- \|\widehat{1}_{\kappa'}\rangle\rangle^- \langle\langle \widehat{1}_{\kappa'} \| \\
 &- \frac{1}{2} |\mathcal{V}_{pq}^{(1)}|^2 \|\widehat{1}_{\kappa'}\rangle\rangle^- \langle\langle \widehat{1}_{\kappa'} \| - \frac{1}{2} \sum_{p',q'} \mathcal{V}_{pq}^{(1)} \mathcal{V}_{p'q'}^{(1)} (1 - \delta_{pp'}) (1 - \delta_{qq'}) (1 - \delta_{\kappa'q}) (1 - \delta_{\kappa'q'}) \\
 &\left. \times \|\widehat{1}_p\rangle\rangle^+ \|\widehat{1}_{p'}\rangle\rangle^+ \|\widehat{1}_q\rangle\rangle^- \|\widehat{1}_{q'}\rangle\rangle^- \|\widehat{1}_{\kappa'}\rangle\rangle^- \langle\langle \widehat{1}_{\kappa'} \| \right\} + \text{H. c.} \Big] + O(h^3). \tag{5.53}
 \end{aligned}$$

Fermionic Particle–Anti-Particle Pair

As a last example we consider the leading order correction in the transformation of a pair of one particle in mode $\kappa \geq 0$ and one antiparticle in mode $\kappa' < 0$. By applying either b_{κ}^{\dagger} to the state of Eq. (5.52), or, equivalently, applying $c_{\kappa'}^{\dagger}$ to (5.50) we obtain

$$\begin{aligned}
 \|1_{\kappa}\rangle\rangle^+ \|1_{\kappa'}\rangle\rangle^- &= G_{\kappa}^{(0)*} G_{\kappa'}^{(0)} \|\widehat{1}_{\kappa}\rangle\rangle^+ \|\widehat{1}_{\kappa'}\rangle\rangle^- + h \left[G_{\kappa'}^{(0)} A_{\kappa'\kappa}^{(1)*} \|\widehat{0}\rangle\rangle \right. \\
 &+ G_{\kappa'}^{(0)} \sum_{m \geq 0} A_{m\kappa}^{(1)*} \|\widehat{1}_m\rangle\rangle^+ \|\widehat{1}_{\kappa'}\rangle\rangle^- + G_{\kappa}^{(0)*} \sum_{n < 0} A_{n\kappa'}^{(1)} \|\widehat{1}_n\rangle\rangle^+ \|\widehat{1}_{\kappa'}\rangle\rangle^- \\
 &\left. + G_{\kappa}^{(0)*} G_{\kappa'}^{(0)} \sum_{p,q} \mathcal{V}_{pq}^{(1)} (1 - \delta_{p\kappa}) (1 - \delta_{q\kappa'}) \|\widehat{1}_p\rangle\rangle^+ \|\widehat{1}_q\rangle\rangle^+ \|\widehat{1}_q\rangle\rangle^- \|\widehat{1}_{\kappa'}\rangle\rangle^- \right] + O(h^2). \tag{5.54}
 \end{aligned}$$

To linear order in \hbar the density operator for the out-region Fock space is

$$\begin{aligned}
 \| |1_\kappa\rangle\rangle^+ \| |1_{\kappa'}\rangle\rangle^- \langle\langle |1_{\kappa'}\rangle\rangle^+ \langle\langle |1_\kappa\rangle\rangle^- &= \| |\hat{1}_\kappa\rangle\rangle^+ \| |\hat{1}_{\kappa'}\rangle\rangle^- \langle\langle |\hat{1}_{\kappa'}\rangle\rangle^+ \langle\langle |\hat{1}_\kappa\rangle\rangle^- + \hbar \left[G_\kappa^{(0)} A_{\kappa'\kappa}^{(1)*} \| |\hat{0}\rangle\rangle^- \langle\langle |\hat{1}_{\kappa'}\rangle\rangle^+ \langle\langle |\hat{1}_\kappa\rangle\rangle^- \right. \\
 &+ G_\kappa^{(0)} \sum_{m \geq 0} A_{m\kappa}^{(1)*} \| |\hat{1}_m\rangle\rangle^+ \| |\hat{1}_{\kappa'}\rangle\rangle^- \langle\langle |\hat{1}_{\kappa'}\rangle\rangle^+ \langle\langle |\hat{1}_\kappa\rangle\rangle^- + G_{\kappa'}^{(0)*} \sum_{n < 0} A_{n\kappa'}^{(1)} \| |\hat{1}_\kappa\rangle\rangle^+ \| |\hat{1}_n\rangle\rangle^- \langle\langle |\hat{1}_{\kappa'}\rangle\rangle^+ \langle\langle |\hat{1}_\kappa\rangle\rangle^- \\
 &\left. + \sum_{p,q} \mathcal{V}_{pq}^{(1)} (1 - \delta_{p\kappa})(1 - \delta_{q\kappa'}) \| |\hat{1}_\kappa\rangle\rangle^+ \| |\hat{1}_p\rangle\rangle^+ \| |\hat{1}_q\rangle\rangle^- \| |\hat{1}_{\kappa'}\rangle\rangle^- \langle\langle |\hat{1}_{\kappa'}\rangle\rangle^+ \langle\langle |\hat{1}_\kappa\rangle\rangle^- + \text{H. c.} \right] + O(\hbar^2).
 \end{aligned} \tag{5.55}$$

We find that the linear Bogoliubov coefficients create coherence between the initial state and those states where either one of the excitations is shifted or an additional particle-antiparticle pair is created.

The states we have considered in this chapter illustrate how the Bogoliubov transformations manifest on the Fock space (or phase space) of all modes of a single cavity. It has been verified that when terms proportional to \hbar^2 are kept the transformed states are normalized, Hermitean and have a non-negative spectrum to second order in the perturbative expansion (see also the discussion in Section 6.1.1). The transformations are hence *implemented unitarily* for smoothly changing accelerations in any dimension, or for sharply varying accelerations in up to $(2 + 1)$ dimensions. In this sense the transformations are *global unitaries* on the Fock space of the cavity modes. We shall see in Chapter 6 how the transformations affect the entanglement between chosen sets of these modes.

Motion Generates Entanglement

In this chapter we discuss the structure of the entanglement that is generated between the modes of quantum fields that are confined to cavities in non-uniform motion. The motivation for this analysis lies in the prospect of employing the specific structure of the created quantum correlations in the verification of the *genuine quantumness* of particle creation phenomena in quantum field theory. In other words, particle creation phenomena and related transformations in the Fock space that occur due to the motion of the cavity boundaries are not arbitrary. They have a rich structure that may allow to unambiguously identify the source of the created particles as a quantum field theory effect, see, e.g., Ref. [201]. Furthermore, in settings similar to those presented in Ref. [7, (xii)] the entanglement between the modes may possibly be used to estimate specific parameters of the transformations with better precision. In addition, via monogamy arguments (see pp. 19) the insights into the entanglement generation within a single cavity will be useful in determining the source of entanglement degradation effects when several entangled cavities are considered in Chapter 7.

This far we have established the Bogoliubov transformations for cavity modes of quantum fields in a cavity that undergoes a change in motion from an inertial in-region to an inertial out-region (see Chapter 4). Consecutively, we have shown in Chapter 5 how initial quantum states in their Fock space or phase space representations are transformed to the out-region. In this chapter we are going to draw from material published in Refs. [82–84, (v-vii)]: Based on the transformed states presented in Chapter 5 we are going to study the reduced states of two modes and the *entanglement* generated therein. As previously the treatment of bosonic Fock states and Gaussian states is separated into Sections 6.1 and 6.2, respectively, before we turn the attention to fermionic states in Section 6.3. The chapter is concluded in Section 6.4 by an analysis of the structure of multipartite entanglement within the non-uniformly moving cavity [84, (vi)].

6.1 Entanglement Generation in Bosonic Fock States

6.1.1 Bosonic Vacuum

A convenient starting point for the analysis of the entanglement in the transformed states is the vacuum state. The out-region decomposition of the in-region vacuum is given by the density matrix (5.17). We are here interested in the bipartite entanglement between a chosen pair of modes labelled by k and k' , respectively. To obtain the reduced out-region state for these two modes we trace out all other modes from (5.17). In contrast to the fermionic case (see Section 3.2.2) this can be done in a straightforward way since mapping bosonic modes to a tensor product space is free of ambiguities. For the purpose of partial traces we can assume a tensor product of mode subspaces and write the resulting reduced state again as a density operator on a Fock space with an appropriately reduced number of modes. Taking into account the structure of the Bogoliubov coefficients (4.76) some lengthy but straightforward algebra reveals

$$\begin{aligned} \text{vac}\rho_{kk'} := \text{Tr}_{-k,k'}(|0\rangle\langle 0|) &= |\widehat{0}\rangle\langle \widehat{0}| - h \left[G_{kk'}^{(0)} \beta_{kk'}^{(1)} |\widehat{0}\rangle\langle \widehat{1}_{k'}| \langle \widehat{1}_k| + \text{H. c.} \right] \\ &+ h^2 \left[(-2f_{k-k'}^\beta - 2f_{k'}^\beta) |\widehat{0}\rangle\langle \widehat{0}| + 2f_{k-k'}^\beta |\widehat{1}_k\rangle\langle \widehat{1}_k| + 2f_{k'-k}^\beta |\widehat{1}_{k'}\rangle\langle \widehat{1}_{k'}| \right. \\ &+ |\beta_{kk'}^{(1)}|^2 |\widehat{1}_k\rangle\langle \widehat{1}_k| \langle \widehat{1}_{k'}| \langle \widehat{1}_k| + \left(V_{kk'}^{(2)*} |\widehat{0}\rangle\langle \widehat{1}_{k'}| \langle \widehat{1}_k| + \frac{1}{\sqrt{2}} V_{kk}^{(2)*} |\widehat{0}\rangle\langle \widehat{2}_k| \right. \\ &\left. \left. + \frac{1}{\sqrt{2}} V_{k'k'}^{(2)*} |\widehat{0}\rangle\langle \widehat{2}_{k'}| + (V_{kk'}^{(1)*})^2 |\widehat{0}\rangle\langle \widehat{2}_{k'}| \langle \widehat{2}_k| + \text{H. c.} \right) \right] + O(h^3), \end{aligned} \quad (6.1)$$

where $\text{Tr}_{-k,k'}$ denotes the trace over all modes except k and k' , $V_{pq}^{(1)}$ and $V_{pq}^{(2)}$ are given by (5.8b) and (5.8c), respectively, and we have introduced the abbreviation

$$f_{m-n}^\beta = \frac{1}{2} \sum_{i \neq n} |\beta_{mi}^{(1)}|^2. \quad (6.2)$$

Cutting off the power expansion at second order effectively truncates each of the two modes in (6.1) to a three dimensional system. Hence, the reduced state can be represented on the tensor product space of two qutrits by the matrix

$$\text{vac}\rho_{kk'} = \begin{pmatrix} 1 - 2h^2(f_{k-k'}^\beta + f_{k'}^\beta) & 0 & \frac{h^2}{\sqrt{2}} V_{k'k'}^{(2)} & 0 & h G_{k'k'}^{(0)*} \beta_{kk'}^{(1)*} + h^2 V_{kk'}^{(2)} & 0 & \frac{h^2}{\sqrt{2}} V_{kk}^{(2)} & 0 & h^2 (V_{kk'}^{(1)})^2 \\ 0 & 2h^2 f_{k'-k}^\beta & 0 & 0 & 0 & 0 & 0 & 0 & 0 \\ \frac{h^2}{\sqrt{2}} V_{k'k'}^{(2)*} & 0 & 0 & 0 & 0 & 0 & 0 & 0 & 0 \\ 0 & 0 & 0 & 2h^2 f_{k-k'}^\beta & 0 & 0 & 0 & 0 & 0 \\ h G_{k'k'}^{(0)} \beta_{kk'}^{(1)} + h^2 V_{kk'}^{(2)*} & 0 & 0 & 0 & h^2 |\beta_{kk'}^{(1)}|^2 & 0 & 0 & 0 & 0 \\ 0 & 0 & 0 & 0 & 0 & 0 & 0 & 0 & 0 \\ \frac{h^2}{\sqrt{2}} V_{kk}^{(2)*} & 0 & 0 & 0 & 0 & 0 & 0 & 0 & 0 \\ 0 & 0 & 0 & 0 & 0 & 0 & 0 & 0 & 0 \\ h^2 (V_{k'k'}^{(1)*})^2 & 0 & 0 & 0 & 0 & 0 & 0 & 0 & 0 \end{pmatrix}, \quad (6.3)$$

where we have neglected terms of order h^3 . The Hilbert-Schmidt condition (5.9) ensures that the quantities $f_{m \rightarrow n}^\beta$ are finite and, consequently, the state in Eq. (6.1) is a well defined density operator. One can easily see that it is normalized and Hermitean. Working out the eigenvalues is somewhat more complicated and needs a more detailed examination.

Perturbative Diagonalization

To determine the eigenvalues of the density operator perturbatively one has to be careful. In typical perturbation theory approaches it is assumed that a given matrix is perturbed by a term that is linear in the expansion parameter. However, in our case the density operator is expanded as

$$\rho = \rho^{(0)} + h \rho^{(1)} + h^2 \rho^{(2)} + O(h^3), \quad (6.4)$$

and we wish to obtain the leading order corrections to the eigenvalues $\lambda_i^{(0)}$ of the unperturbed matrix $\rho^{(0)}$. To begin one may approximate the perturbative corrections to $\rho^{(0)}$ by only the linear term $h\rho^{(1)}$. In that case corrections to the eigenvalues of $\rho^{(0)}$ that are linear in h can be computed using the standard procedure: first the unperturbed matrix is diagonalized, i.e.,

$$\rho^{(0)} | \lambda_i^{(0)} \rangle = \lambda_i^{(0)} | \lambda_i^{(0)} \rangle. \quad (6.5)$$

Subsequently, any degeneracies in the unperturbed eigenvalues need to be taken into account. For any non-degenerate eigenvalues $\lambda_i^{(0)}$ the corrections are computed as the expectation values of the leading order perturbation $\rho^{(1)}$ in the corresponding unperturbed eigenstate $| \lambda_i^{(0)} \rangle$, i.e.,

$$\lambda_i^{(1)} = \langle \lambda_i^{(0)} | \rho^{(1)} | \lambda_i^{(0)} \rangle, \quad (6.6)$$

and one arrives at $\lambda_i = \lambda_i^{(0)} + h\lambda_i^{(1)} + O(h^2)$. For any degenerate eigenvalues $\lambda_{i_1}^{(0)} = \lambda_{i_2}^{(0)} = \dots = \lambda_{i_n}^{(0)}$ the appropriate leading order corrections are given by the eigenvalues of the matrix Λ_i with components

$$(\Lambda_i)_{mn} = \langle \lambda_{i_m}^{(0)} | \rho^{(1)} | \lambda_{i_n}^{(0)} \rangle. \quad (6.7)$$

Similarly, if the linear corrections to the density matrix vanish, i.e., $\rho^{(1)} = 0$, one may perform the same procedure for $\rho^{(2)}$ to obtain leading order corrections that are quadratic in h . We shall use this procedure throughout Chapters 6 and 7 to compute the eigenvalues of partially transposed density operators.

Nonetheless, for finding the corrections to the eigenvalues of the density matrix itself this strategy is not successful. The density matrix of Eq. (6.1) has non-zero linear corrections $\rho^{(1)}$, but no linear corrections to the unperturbed eigenvalues $\{\lambda_1^{(0)} = 1, \lambda_2^{(0)} = 0, \lambda_3^{(0)} = 0, \dots\}$, i.e., $\lambda_i^{(1)} = 0 \forall i \neq 1$. The leading order corrections $\lambda^{(2)}$ must therefore be found by diagonalizing (6.1) by hand. In other words, to determine the diagonal form $\rho_{\text{diag}} = \text{diag}\{\lambda_i | i = 1, 2, \dots\}$ of the density matrix we make the ansatz

$$U = U^{(0)} + hU^{(1)} + h^2U^{(2)} + O(h^3) \quad (6.8)$$

for the *diagonalizing unitary*, such that $\rho_{\text{diag}} = U\rho U^\dagger$. Next, we switch to a more compact notation for the density matrix (6.3) by splitting the matrix into the subspaces corresponding to the unperturbed eigenvalues $\lambda_1^{(0)} = 1$ and $\lambda_{i \neq 1}^{(0)} = 0$, i.e., we write

$$\text{vac}\rho_{kk'} = \begin{pmatrix} 1 & 0 \\ 0 & 0 \end{pmatrix} + h \begin{pmatrix} 0 & \underline{v}^{(1)\dagger} \\ \underline{v}^{(1)} & 0 \end{pmatrix} + h^2 \begin{pmatrix} \rho_{11}^{(2)} & \underline{v}^{(2)\dagger} \\ \underline{v}^{(2)} & \rho^{(2)'} \end{pmatrix} + O(h^3), \quad (6.9)$$

where $\rho_{11}^{(2)} = -2(f_{k \rightarrow k'}^\beta + f_{k'}^\beta)$ and the components of the vectors $\underline{v}^{(1)}$, and $\underline{v}^{(2)}$, and the 6×6 matrix $\rho^{(2)'}$ can be read off directly from $\text{vac}\rho_{kk'}$ in Eq. (6.3). A straightforward computation provides the expansion of the diagonalizing unitary

$$U = \begin{pmatrix} 1 & 0 \\ 0 & \mathbb{1}_6 \end{pmatrix} + h \begin{pmatrix} 0 & \underline{v}^{(1)\dagger} \\ -\underline{v}^{(1)} & 0 \end{pmatrix} + h^2 \begin{pmatrix} -\frac{1}{2}\underline{v}^{(1)\dagger}\underline{v}^{(1)} & \underline{v}^{(2)\dagger} \\ -\underline{v}^{(2)} & -\frac{1}{2}\underline{v}^{(1)}\underline{v}^{(1)\dagger} \end{pmatrix} + O(h^3), \quad (6.10)$$

and the second order corrections to the eigenvalues of (6.1). Including second order terms the non-zero eigenvalues turn out to be

$$\lambda_1 = 1 - h^2 (2f_{k \rightarrow k'}^\beta + 2f_{k' \rightarrow k}^\beta) + O(h^3), \quad (6.11a)$$

$$\lambda_2 = h^2 2f_{k \rightarrow k'}^\beta + O(h^3), \quad (6.11b)$$

$$\lambda_3 = h^2 2f_{k' \rightarrow k}^\beta + O(h^3). \quad (6.11c)$$

Entanglement Generation in the Bosonic Vacuum

From Eqs. (6.11) we clearly see that the eigenvalues of (6.1) are non-negative and well-defined, at least up to and including second order corrections. However, the partial trace leaves the transformed state *mixed*, which can be quickly verified by computing the linear entropy $S_L(\rho)$ (see Definition 1.2),

$$S_L\left(\text{Tr}_{-k, k'}(|0\rangle\langle 0|)\right) = h^2 (2f_{k \rightarrow k'}^\beta + 2f_{k' \rightarrow k}^\beta) + O(h^3). \quad (6.12)$$

To determine the entanglement between the modes k and k' we need to employ a measure that is computable for a mixed state of two qutrits. The *negativity* from Definition 1.10 provides such a tool, although one might miss bound entanglement. To calculate the negativity we determine the eigenvalues of the partially transposed density

matrix. For the state (6.1) it is given by

$$(\text{vac}\rho_{kk'})^{T_{k'}} = \begin{pmatrix} 1 - 2h^2(f_{k-k'}^\beta + f_{k'}^\beta) & 0 & \frac{h^2}{\sqrt{2}}V_{k'k'}^{(2)*} & 0 & 0 & 0 & \frac{h^2}{\sqrt{2}}V_{kk}^{(2)} & 0 & 0 \\ 0 & 2h^2f_{k'-k}^\beta & 0 & hG_{k'}^{(0)*}\beta_{kk'}^{(1)*} + h^2V_{kk'}^{(2)} & 0 & 0 & 0 & 0 & 0 \\ \frac{h^2}{\sqrt{2}}V_{k'k'}^{(2)} & 0 & 0 & 0 & 0 & 0 & h^2(V_{kk'}^{(1)})^2 & 0 & 0 \\ 0 & hG_{k'}^{(0)}\beta_{kk'}^{(1)} + h^2V_{kk'}^{(2)*} & 0 & 2h^2f_{k-k'}^\beta & 0 & 0 & 0 & 0 & 0 \\ 0 & 0 & 0 & 0 & h^2|\beta_{kk'}^{(1)}|^2 & 0 & 0 & 0 & 0 \\ 0 & 0 & 0 & 0 & 0 & 0 & 0 & 0 & 0 \\ \frac{h^2}{\sqrt{2}}V_{kk}^{(2)*} & 0 & h^2(V_{kk'}^{(1)*})^2 & 0 & 0 & 0 & 0 & 0 & 0 \\ 0 & 0 & 0 & 0 & 0 & 0 & 0 & 0 & 0 \\ 0 & 0 & 0 & 0 & 0 & 0 & 0 & 0 & 0 \end{pmatrix}. \quad (6.13)$$

We can proceed as laid out on page 117 to determine the eigenvalues of the partial transpose. If the modes k and k' have opposite parity, that is, if $(k+k')$ is odd, the linear corrections to (6.13) are non-zero, see Eq. (4.22b). Keeping only the linear corrections it becomes evident that the eigenvalues of the matrix

$$h \begin{pmatrix} 0 & G_{k'}^{(0)*}\beta_{kk'}^{(1)*} \\ G_{k'}^{(0)}\beta_{kk'}^{(1)} & 0 \end{pmatrix} \quad (6.14)$$

provide the corrections $\pm h|\beta_{kk'}^{(1)}|$ to the degenerate unperturbed eigenvalue 0. We thus find the linear contribution $\mathcal{N}^{(1)}$ to the negativity

$$\mathcal{N}(\text{vac}\rho_{kk'}) = h\mathcal{N}^{(1)}(\text{vac}\rho_{kk'}) + O(h^2) = h|\beta_{kk'}^{(1)}| + O(h^2). \quad (6.15)$$

We see that, to linear order in h , the entanglement as measured by the negativity (6.15) is generated by the coherent excitation of two particles in the modes k and k' . Now let us turn to the case where $(k+k')$ is even, i.e., the two modes have the same parity. Then $\beta_{kk'}^{(1)} = 0$ and, consequently, also $V_{kk'}^{(1)} = 0$, see Eq. (5.8b). This leaves a non-zero 2×2 block of the second order corrections to the partially transposed state (6.13) in the subspace of the degenerate eigenvalue 0, given by

$$h^2 \begin{pmatrix} 2f_{k'-k}^\beta & V_{kk'}^{(2)} \\ V_{kk'}^{(2)*} & 2f_{k-k'}^\beta \end{pmatrix}. \quad (6.16)$$

There is only one possibly negative correction to the eigenvalue 0 and the leading order correction to the negativity is then simply found to be

$$\begin{aligned} \mathcal{N}(\text{vac}\rho_{kk'}) &= h^2\mathcal{N}^{(2)}(\text{vac}\rho_{kk'}) + O(h^3) \\ &= h^2 \max\left\{0, \sqrt{(f_{k-k'}^\beta - f_{k'-k}^\beta)^2 + |V_{kk'}^{(2)}|^2} - (f_{k-k'}^\beta + f_{k'-k}^\beta)\right\} + O(h^3). \end{aligned} \quad (6.17)$$

The entanglement is now generated by the coefficient $V_{kk'}^{(2)}$ from (5.8c), which has contributions from $\beta_{kk'}^{(2)}$ — pairs of particles that are created directly in the modes k and k' — and products $\beta_{mk}^{(1)*} \alpha_{mk'}^{(1)}$ — a pair of particles is created in modes k and m and the excitation in m is subsequently shifted to k' . These terms compete with the (anti)particle creation where only one constituent of the created pair is generated in k or k' . An illustration of the corrections is shown in Fig. 6.1.

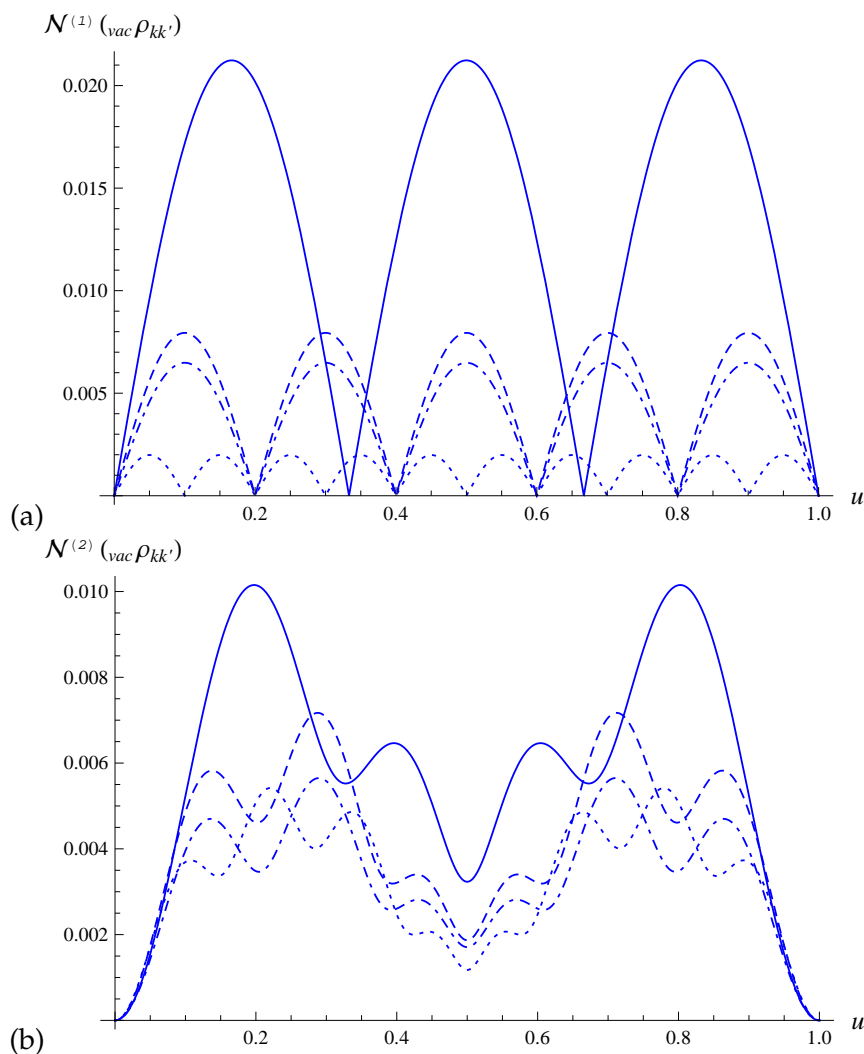


Figure 6.1: Entanglement generation — bosonic vacuum: The coefficients $\mathcal{N}^{(1)}$ [see Eq. (6.15)] and $\mathcal{N}^{(2)}$ [see Eq. (6.17)] of the negativity generated from the vacuum state are plotted in Fig. 6.1 (a) and Fig. 6.1 (b), respectively, for the basic building block travel scenario of Section 4.4.1. For the $(1 + 1)$ dimensional massless scalar field used in this illustration the Bogoliubov coefficients are periodic in the dimensionless parameter $u := h\tau/[4L \operatorname{artanh}(h/2)]$ [see Eq. (4.20)], where τ is the duration, as measured at the centre of the cavity, of the single segment of uniform acceleration. Curves are shown for the mode pairs $(k, k') = (1, 2)$ (solid), $(2, 3)$ (dashed), $(3, 4)$ (dotted), and $(1, 4)$ (dotted-dashed) in Fig. 6.1 (a), and for $(1, 3)$ (solid), $(2, 4)$ (dashed), $(3, 5)$ (dotted), and $(1, 5)$ (dotted-dashed) in Fig. 6.1 (b).

6.1.2 Bosonic Single Particle States

For the bosonic single particle state $|1_k\rangle$ we select the density operator from (5.20) and again trace over all modes except k and k' to obtain the reduced state

$$\begin{aligned}
 {}_{1-k}\rho_{kk'} &:= \text{Tr}_{-k,k'}(|1_k\rangle\langle 1_k|) = |\widehat{1}_k\rangle\langle \widehat{1}_k| - \hbar \left[\sqrt{2} G_k^{(0)} \beta_{k'k}^{(1)} |\widehat{1}_k\rangle\langle \widehat{1}_{k'}| \langle \widehat{2}_k| \right. \\
 &- G_k^{(0)} \alpha_{k'k}^{(1)*} |\widehat{1}_{k'}\rangle\langle \widehat{1}_k| + \text{H. c.} \left. \right] + \hbar^2 \left\{ 2 f_{k-k'}^\alpha |\widehat{0}\rangle\langle \widehat{0}| + |\alpha_{kk'}^{(1)}|^2 |\widehat{1}_{k'}\rangle\langle \widehat{1}_{k'}| \right. \\
 &- 2 (f_k^\alpha + f_{k'-k}^\beta + 2 f_k^\beta) |\widehat{1}_k\rangle\langle \widehat{1}_k| + 2 f_{k'-k}^\beta |\widehat{1}_k\rangle\langle \widehat{1}_{k'}| \langle \widehat{1}_{k'}| \langle \widehat{1}_k| + 4 f_{k-k'}^\beta |\widehat{2}_k\rangle\langle \widehat{2}_k| \\
 &+ 2 |\beta_{kk'}^{(1)}|^2 |\widehat{2}_k\rangle\langle \widehat{1}_{k'}| \langle \widehat{1}_{k'}| \langle \widehat{2}_k| + \left([G_k^{(0)} \alpha_{k'k}^{(2)*} - 2 \text{Re}(G_k^{(0)} G_{k'}^{(0)*} \sum_p \beta_{pk}^{(1)} \beta_{pk'}^{(1)*})] |\widehat{1}_{k'}\rangle\langle \widehat{1}_k| \right. \\
 &- G_k^{(0)} G_{k'}^{(0)} \sum_p \alpha_{pk}^{(1)*} \beta_{pk'}^{(1)} |\widehat{0}\rangle\langle \widehat{1}_{k'}| \langle \widehat{1}_k| - \sqrt{2} (G_k^{(0)})^2 \sum_{p \neq k'} \alpha_{pk}^{(1)*} \beta_{pk}^{(1)} |\widehat{0}\rangle\langle \widehat{2}_k| \\
 &+ \sqrt{2} \alpha_{kk'}^{(1)} \beta_{kk'}^{(1)} |\widehat{1}_{k'}\rangle\langle \widehat{1}_{k'}| \langle \widehat{2}_k| + \sqrt{2} \alpha_{k'k}^{(1)} \beta_{k'k}^{(1)} |\widehat{1}_k\rangle\langle \widehat{2}_{k'}| \langle \widehat{1}_k| + \sqrt{2} V_{kk'}^{(2)*} |\widehat{1}_k\rangle\langle \widehat{1}_{k'}| \langle \widehat{2}_k| \\
 &\left. + \sqrt{\frac{3}{2}} V_{kk}^{(2)*} |\widehat{1}_k\rangle\langle \widehat{3}_k| + \sqrt{3} (G_k^{(0)} \beta_{k'k}^{(1)})^2 |\widehat{1}_k\rangle\langle \widehat{2}_{k'}| \langle \widehat{3}_k| + \text{H. c.} \right\} + O(\hbar^3),
 \end{aligned} \tag{6.18}$$

where, in analogy to (6.2), we define the quantity

$$f_{m-n}^\alpha = \frac{1}{2} \sum_{i \neq n} |\alpha_{mi}^{(1)}|^2. \tag{6.19}$$

As before, a quick computation provides the linear entropy S_L (see Definition 1.2),

$$S_L({}_{1-k}\rho_{kk'}) = \hbar^2 (8 f_{k-k'}^\beta + 4 f_{k'-k}^\beta + 4 f_{k-k'}^\alpha) + O(\hbar^3), \tag{6.20}$$

which immediately reveals that the state (6.18) is mixed, as expected. To evaluate the entanglement that is produced between the modes k and k' we again employ the negativity. If the modes k and k' have opposite parity the partial transpose of (6.18) features corrections linear in \hbar . In the subspace of the degenerate unperturbed eigenvalue 0 we find the linear perturbation

$$\hbar \begin{pmatrix} 0 & G_k^{(0)} \alpha_{k'k}^{(1)*} & 0 \\ G_k^{(0)*} \alpha_{k'k}^{(1)} & 0 & -\sqrt{2} G_k^{(0)} \beta_{k'k}^{(1)} \\ 0 & -\sqrt{2} G_k^{(0)*} \beta_{k'k}^{(1)*} & 0 \end{pmatrix}. \tag{6.21}$$

To leading order this supplies one negative eigenvalue and we get the negativity

$$\mathcal{N}({}_{1-k}\rho_{kk'}) = \hbar \mathcal{N}^{(1)}({}_{1-k}\rho_{kk'}) + O(\hbar^2) = \hbar \sqrt{|\alpha_{kk'}^{(1)}|^2 + 2 |\beta_{kk'}^{(1)}|^2} + O(\hbar^2). \tag{6.22}$$

In contrast to (6.15) the entanglement is now generated by both coherent excitations of particle pairs in the modes k and k' , and the shift of excitations from mode k to mode k' by the coefficient $\alpha_{kk'}^{(1)}$. An illustration of these results is shown in Fig. 6.2 (a).

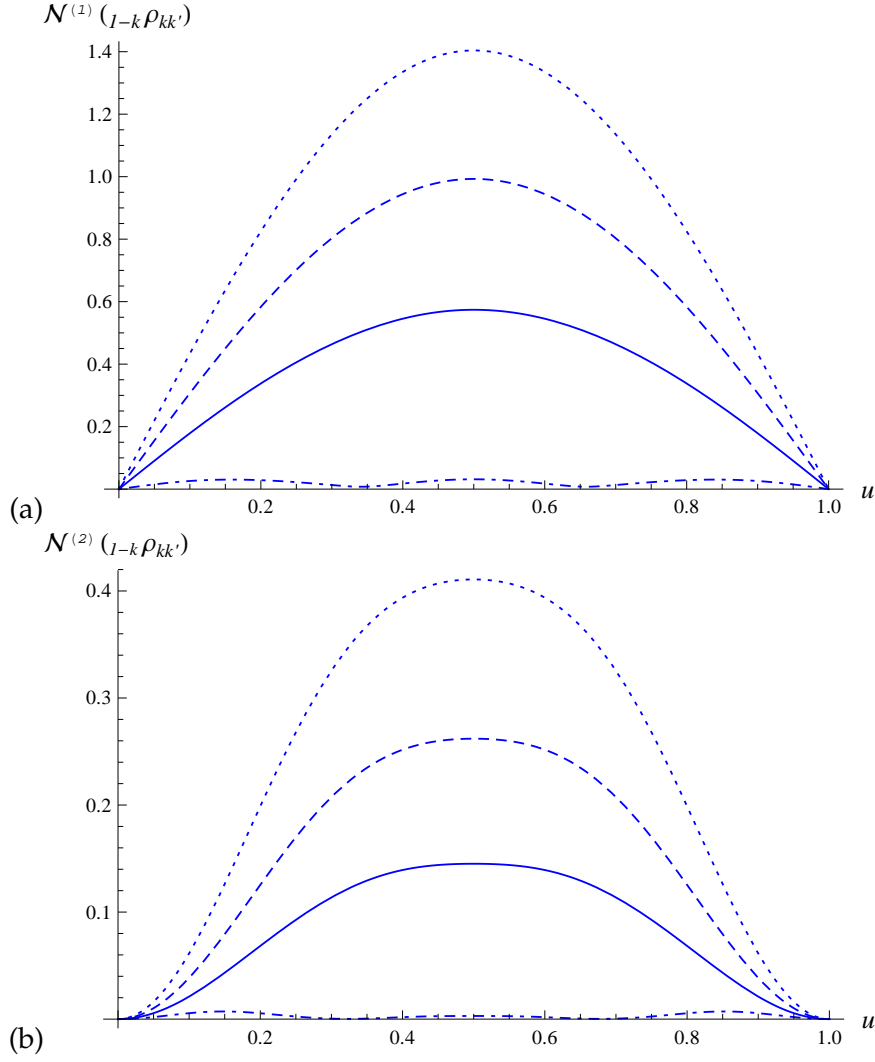


Figure 6.2: Entanglement generation — bosonic single particle state $|1_k\rangle$: The coefficients $\mathcal{N}^{(1)}$ [see Eq. (6.22)] and $\mathcal{N}^{(2)}$ [see Eq. (6.26)] of the negativity generated from the state $|1_k\rangle$ are plotted in Fig. 6.2 (a) and Fig. 6.2 (b), respectively, for the basic building block travel scenario of Section 4.4.1. For the $(1+1)$ dimensional massless scalar field used in this illustration the Bogoliubov coefficients are periodic in the dimensionless parameter $u := h\tau/[4L \operatorname{artanh}(h/2)]$ [see Eq. (4.20)], where τ is the duration, as measured at the centre of the cavity, of the single segment of uniform acceleration. Curves are shown for the mode pairs $(k, k') = (1, 2)$ (solid), $(2, 3)$ (dashed), $(3, 4)$ (dotted), and $(1, 4)$ (dotted-dashed) in Fig. 6.2 (a), and for $(1, 3)$ (solid), $(2, 4)$ (dashed), $(3, 5)$ (dotted), and $(1, 5)$ (dotted-dashed) in Fig. 6.2 (b).

When k and k' have the same parity the situation is slightly more complicated. As previously, all the corrections to the reduced density matrix that are linear in \hbar vanish. We further ignore the row and column of the partial transpose corresponding to the subspace of the unperturbed eigenvalue 1 because a small perturbation cannot possibly change this eigenvalue enough to become negative. The non-zero corrections in the

subspace of the unperturbed eigenvalue 0 decompose into two independent blocks. The first block, given by the matrix

$$h^2 \begin{pmatrix} |\alpha_{kk'}^{(1)}|^2 & \sqrt{2} \alpha_{kk'}^{(1)} \beta_{kk'}^{(1)} \\ \sqrt{2} \alpha_{kk'}^{(1)*} \beta_{kk'}^{(1)*} & 2 |\beta_{kk'}^{(1)}|^2 \end{pmatrix} \quad (6.23)$$

provides one positive eigenvalue, while the other eigenvalue vanishes identically. The second block is represented by

$$h^2 \begin{pmatrix} 2 f_{k-k'}^\alpha & G_k^{(0)} \alpha_{k'k}^{(2)*} - 2 \operatorname{Re}(G_k^{(0)} G_{k'}^{(0)*} g_{kk'}^{\beta\beta*}) & -\sqrt{2} (G_k^{(0)})^2 g_{kk-k'}^{\alpha\beta*} \\ G_k^{(0)*} \alpha_{k'k}^{(2)} - 2 \operatorname{Re}(G_k^{(0)} G_{k'}^{(0)*} g_{kk'}^{\beta\beta*}) & 2 f_{k'-k}^\beta & \sqrt{2} V_{kk'}^{(2)*} \\ -\sqrt{2} (G_k^{(0)*})^2 g_{kk-k'}^{\alpha\beta} & \sqrt{2} V_{kk'}^{(2)} & 4 f_{k-k'}^\beta \end{pmatrix} \quad (6.24)$$

where we have simplified the notation with the abbreviations

$$g_{kk'}^{\beta\beta} = \sum_p \beta_{pk}^{(1)} \beta_{pk'}^{(1)*}, \quad g_{kk-k'}^{\alpha\beta} = \sum_{p \neq k'} \alpha_{pk}^{(1)} \beta_{pk'}^{(1)*}. \quad (6.25)$$

The eigenvalues of (6.24) are given by the solutions to a cubic equation. It is not difficult to see that the off-diagonal elements of this matrix are responsible for possible entanglement generation, competing with the noise that is introduced by the diagonal elements. If the quantities $f_{k-k'}^\alpha$, $f_{k'-k}^\beta$, and $f_{k-k'}^\beta$ were zero, while the off-diagonals are non-vanishing the matrix (6.24) would supply at least one negative eigenvalue. Practically, the negative solutions to the cubic equation mentioned above are best evaluated numerically, and the modulus of the negative eigenvalue of the matrix (6.24) provides the negativity

$$\mathcal{N}_{(1-k\rho_{kk'})} = h^2 \mathcal{N}^{(2)}_{(1-k\rho_{kk'})} + O(h^3) \quad (6.26)$$

illustrated in Fig. 6.2 (b). Finally, it should be noted that the presence of a non-zero negativity allows us to unambiguously conclude that the transformation creates entanglement. Vanishing negativity, on the other hand, does not rule out the presence of entanglement in principle (see pp. 19) because neither are the states under consideration Gaussian, nor can the modes be truncated to qubits. However, in the explicit examples that we have analyzed, e.g., the basic building block (see Section 4.4.1) in Fig. 6.1 and Fig. 6.2, the negativity vanishes only when the corresponding Bogoliubov coefficients also disappear and the state is left unchanged — separable. This indicates that no bound entanglement is produced in the situations considered.

6.2 Entanglement Generation in Bosonic Gaussian States

The analysis of Section 6.1 has demonstrated that entanglement is generated from initially separable Fock states within the cavity. However, as excitations are added the

calculations quickly become computationally demanding. Moreover, there seems to be no natural restriction to the choice of the initial states. Put bluntly, there does not seem to be ample motivation to study, for instance, the state $|5_k\rangle|3_{k'}\rangle$ rather than $|17_k\rangle$. A class of states that distinguishes itself from general bosonic states is the group of *Gaussian states*, see Section 3.1.1, which we are going to restrict ourselves to in this section.

6.2.1 Single-Mode Squeezed States

To study entanglement generation phenomena it is prudent to start with an initial state that is separable. For example, a state where all modes are uncorrelated but individually (single-mode) squeezed, see pp. 106. Since we are particularly interested in the entanglement that is generated between the modes k and k' we allow for non-zero squeezing only for these modes, i.e., $s_n = 0 \forall n \neq k, k'$. The 4×4 covariance matrix for the modes k and k' is decomposed as

$$\widehat{\Gamma} = \begin{pmatrix} \widehat{\Gamma}_k & \widehat{C}_{kk'} \\ \widehat{C}_{kk'}^T & \widehat{\Gamma}_{k'} \end{pmatrix}, \quad (6.27)$$

where the leading order coefficients in the series expansions of the components of the 2×2 matrices $\widehat{\Gamma}_k$, $\widehat{C}_{kk'}$, and $\widehat{\Gamma}_{k'}$ can be read off directly from Eqs. (5.30) and (5.33). Given these perturbative expressions we can proceed to evaluate the entanglement of this state. Taking Theorem 3.2 as a starting point we wish to obtain the smallest symplectic eigenvalue of the partial transpose of the covariance matrix (6.27). Since this essentially entails perturbatively determining the eigenvalues of the matrix

$$i\Omega\widetilde{T}_{k'}\widehat{\Gamma}\widetilde{T}_{k'}, \quad (6.28)$$

where Ω is the symplectic form (3.11) and $\widetilde{T}_{k'} = \mathbb{1} \oplus \text{diag}\{1, -1\}$ represents the partial transposition, we can turn to the procedure described on pp. 117 to do so. The symplectic eigenvalues of the partial transpose of the unperturbed state are given by

$$\text{spectr}(i\Omega\widetilde{T}_{k'}\widehat{\Gamma}^{(0)}\widetilde{T}_{k'}) = \{-1, -1, +1, +1\}, \quad (6.29)$$

as expected for a separable pure state, and we note that the eigenvalues are twice degenerate. Our aim is then to find the leading order negative correction to the eigenvalue $\check{\nu}_-^{(0)} = \check{\nu}_+^{(0)} = 1$. At this stage we specialize to the case where $(k + k')$ is odd, i.e., the modes have opposite parity, such that the leading order correction to $\widehat{\Gamma}^{(0)}$ is linear in \hbar . In the next step we have to diagonalize the subspace of the correction $i\Omega\widetilde{T}_{k'}\widehat{\Gamma}^{(1)}\widetilde{T}_{k'}$ corresponding to the unperturbed eigenvalue $\check{\nu}_\pm^{(0)} = 1$. In other words, the eigenvalues of the matrix

$$\begin{pmatrix} \langle \check{\nu}_+^{(0)} | i\Omega\widetilde{T}_{k'}\widehat{\Gamma}^{(1)}\widetilde{T}_{k'} | \check{\nu}_+^{(0)} \rangle & \langle \check{\nu}_+^{(0)} | i\Omega\widetilde{T}_{k'}\widehat{\Gamma}^{(1)}\widetilde{T}_{k'} | \check{\nu}_-^{(0)} \rangle \\ \langle \check{\nu}_-^{(0)} | i\Omega\widetilde{T}_{k'}\widehat{\Gamma}^{(1)}\widetilde{T}_{k'} | \check{\nu}_+^{(0)} \rangle & \langle \check{\nu}_-^{(0)} | i\Omega\widetilde{T}_{k'}\widehat{\Gamma}^{(1)}\widetilde{T}_{k'} | \check{\nu}_-^{(0)} \rangle \end{pmatrix} \quad (6.30)$$

need to be determined, where the non-zero elements of $\widehat{\Gamma}^{(1)}$ are given by (5.33) and $|\check{\nu}_{\pm}^{(0)}\rangle$ are the eigenstates of $i\Omega\check{T}_{k'}\widehat{\Gamma}^{(0)}\check{T}_{k'}$ with eigenvalue $\check{\nu}_{\pm}^{(0)} = 1$. The eigenstates $|\check{\nu}_{\pm}^{(0)}\rangle$ are given by

$$|\check{\nu}_{+}^{(0)}\rangle = N(s_k, \omega_k \tilde{\tau}) \left(\frac{i \cos(\omega_k \tilde{\tau}) + \exp(s_k) \sin(\omega_k \tilde{\tau})}{\exp(s_k) \cos(\omega_k \tilde{\tau}) - i \sin(\omega_k \tilde{\tau})}, 1, 0, 0 \right)^T, \quad (6.31a)$$

$$|\check{\nu}_{-}^{(0)}\rangle = N(s_{k'}, \omega_{k'} \tilde{\tau}) \left(0, 0, \frac{i \cos(\omega_{k'} \tilde{\tau}) - \exp(s_{k'}) \sin(\omega_{k'} \tilde{\tau})}{\exp(s_{k'}) \cos(\omega_{k'} \tilde{\tau}) + i \sin(\omega_{k'} \tilde{\tau})}, 1 \right)^T, \quad (6.31b)$$

where the normalization constants $N(s_n, \omega_n \tilde{\tau})$ are given by

$$N(s_n, \omega_n \tilde{\tau}) = \left(\frac{1 + \exp(2s_n)}{\exp(2s_n) \cos^2(\omega_n \tilde{\tau}) + \sin^2(\omega_n \tilde{\tau})} \right)^{-\frac{1}{2}}. \quad (6.32)$$

This allows us to obtain the perturbative expansion of the symplectic eigenvalues of the partially transposed covariance matrix to linear order in h , i.e.,

$$\check{\nu}_{\pm} = 1 + h \check{\nu}_{\pm}^{(1)} + O(h^2). \quad (6.33)$$

We find that $\check{\nu}_{+}^{(1)} = -\check{\nu}_{-}^{(1)} \geq 0$, which further allows us to express the leading order correction to the negativity from Eq. (3.22b) in the following form

$$\mathcal{N} = h \mathcal{N}^{(1)} + O(h^2) = h \frac{|\check{\nu}_{-}^{(1)}|}{2} + O(h^2), \quad (6.34)$$

where the leading order coefficient $\mathcal{N}^{(1)}$ is given by

$$\begin{aligned} \mathcal{N}^{(1)} = & \frac{1}{\sqrt{2}} \left(|\alpha_{kk'}^{(1)}|^2 [\cosh(2s_k) \cosh(2s_{k'}) - 1] + |\beta_{kk'}^{(1)}|^2 [\cosh(2s_k) \cosh(2s_{k'}) + 1] \right. \\ & - \text{Re}[(G_k^{(0)*} \alpha_{kk'}^{(1)})^2 + (G_k^{(0)*} \beta_{kk'}^{(1)})^2] \sinh(2s_k) \sinh(2s_{k'}) - 2 \text{Re}[(G_k^{(0)*} \alpha_{kk'}^{(1)})(G_k^{(0)} \beta_{kk'}^{(1)*})] \\ & \left. \times \cosh(2s_k) \sinh(2s_{k'}) + 2 \text{Re}[(G_k^{(0)*} \alpha_{kk'}^{(1)})(G_k^{(0)*} \beta_{kk'}^{(1)})] \sinh(2s_k) \cosh(2s_{k'}) \right)^{\frac{1}{2}}. \quad (6.35) \end{aligned}$$

Alternatively, one may obtain the expression in (6.35) by a different line of argument. To linear order in h the Bogoliubov transformation does not affect the purity of the initial state. In particular, the initially pure states we have chosen remain pure when terms proportional to h^2 are neglected. Recall now that every pure two-mode Gaussian state is equivalent up to local symplectic transformations to a two-mode squeezed state (3.19), see also Ref. [4]. Since we work with small perturbations of the state, the corresponding two-mode squeezing parameter r can be assumed to satisfy $r \ll 1$. We may therefore relate the local symplectic invariant $\det(\widehat{C}_{kk'})$ to r via the relation

$$\det(\widehat{C}_{kk'}) = -\sinh^2(2r) = -4r^2 + O(r^4), \quad (6.36)$$

where we have performed a power expansion assuming $r \ll 1$ in the last step. Since the squeezing parameter is also directly related to $\check{\nu}_{-}$, i.e., $\check{\nu}_{-} = e^{-2|r|}$, the expression

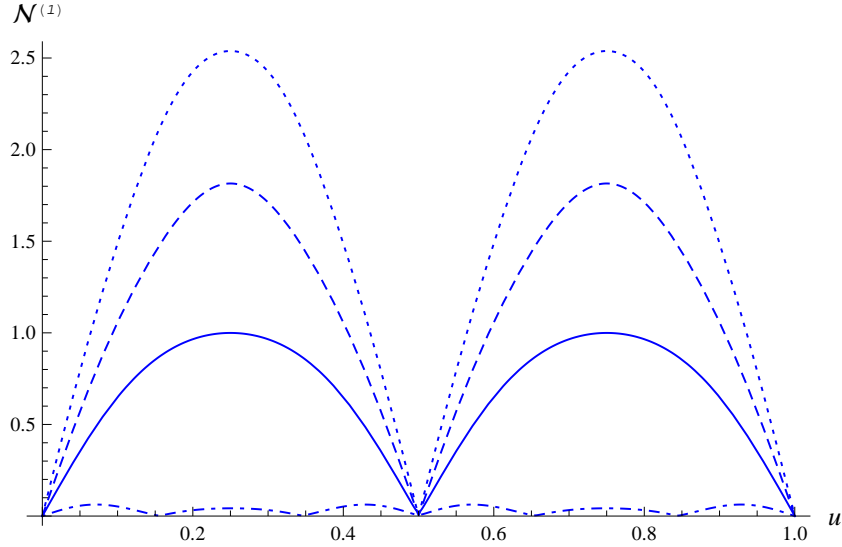


Figure 6.3: Entanglement generation — symmetric single-mode squeezing: The coefficient $\mathcal{N}^{(1)}$ [see Eq. (6.35)] of the negativity generated from a symmetrically single-mode squeezed state is plotted for the basic building block travel scenario of Section 4.4.1 for squeezing parameters $s_k = s_{k'} = 1$. For the $(1+1)$ dimensional massless scalar field in this illustration the Bogoliubov coefficients are periodic in the dimensionless parameter $u := h\tau/[4L \operatorname{artanh}(h/2)]$ [see Eq. (4.20)], where τ is the duration, as measured at the centre of the cavity, of the single segment of uniform acceleration. Curves are shown for the mode pairs $(k, k') = (1, 2)$ (solid), $(2, 3)$ (dashed), $(3, 4)$ (dotted), and $(1, 4)$ (dotted-dashed).

in Eq. (6.35) can be calculated from $\det(\widehat{C}_{kk'})$ in a straightforward manner. Moreover, we can conclude that, to leading order, the transformed state is locally equivalent to a two-mode squeezed state with squeezing parameter $r = h\mathcal{N}^{(1)}$. The correction to the negativity is consistent with the expression obtained for symmetric single-mode squeezing, $s_k = s_{k'}$, in Ref. [83, (vii)], which is illustrated in Fig. 6.3. In the limit of vanishing initial squeezing, i.e., for $s_k = s_{k'} = 0$, we further recover the correct expression for the entanglement generated from the vacuum, see Eq. (6.15).

As expected, and as can be inferred from a quick comparison of Figs. 6.1 and 6.3, the presence of squeezing in the initial state can greatly enhance the entanglement production. However, the perturbative treatment restricts the validity of these considerations. We trust the perturbative corrections as long as the main features of the state, e.g., the *mixedness*, are not significantly altered. More precisely, we quantify the mixedness by the *linear entropy* S_L (see Definition 1.2). For a Gaussian state corresponding to the covariance matrix Γ it is given by (see, e.g., Ref. [1, p. 38])

$$S_L(\Gamma) = 1 - 1/\sqrt{\det(\Gamma)}. \quad (6.37)$$

For the symmetrically single-mode squeezed state ($s_k = s_{k'} = s$) considered in Fig. 6.3 we have

$$\det(\widehat{\Gamma}) = 1 + h^2 \left[4(f_{k \rightarrow k'}^\beta + f_{k' \rightarrow k}^\beta) [\cosh(2s) + 1] + 4(f_{k \rightarrow k'}^\alpha + f_{k' \rightarrow k}^\alpha) [\cosh(2s) - 1] - 4 \sinh(2s) \sum_{n \neq k, k'} \operatorname{Re}(\alpha_{nk'}^{(1)} \beta_{nk}^{(1)*} + \alpha_{nk'}^{(1)} \beta_{nk'}^{(1)*}) \right] + O(h^3), \quad (6.38)$$

with $f_{m \rightarrow n}^\alpha$ and $f_{m \rightarrow n}^\beta$ as in Eqs. (6.19) and (6.2), respectively. The dominant correction in (6.38) is given by the terms proportional to $f_{k \rightarrow k'}^\alpha$ and $f_{k' \rightarrow k}^\alpha$ and it is then easy to see that the validity of the perturbative treatment is expressed in the condition

$$h^2 (f_{k \rightarrow k'}^\alpha + f_{k' \rightarrow k}^\alpha) e^{2|s|} \ll 1. \quad (6.39)$$

Finally, a note on the choice of entanglement measure is in order. To linear order in h we have a symmetric two-mode Gaussian state for which the entanglement of formation (3.23) can be computed. However, this entanglement measure is based on the quantification of the mixedness in the reduced state of one mode arising from tracing out the other mode. But, as we have argued before, the mixedness does not change unless second order terms are included, i.e., if only terms linear in h are kept, the state remains pure. However, when terms proportional to h^2 are kept, we are left with a non-symmetric state, $\det(\widehat{\Gamma}_k) \neq \det(\widehat{\Gamma}_{k'})$, for which the entanglement of formation cannot be computed. Hence, the negativity is the most suitable measure for our purposes.

6.2.2 Resonances of Entanglement Generation

The analysis we have undertaken up to this point has established the entanglement generation from various initial states in terms of the Bogoliubov coefficients for generic travel scenarios, including smoothly varying accelerations, as described in Section 4.4. As we have seen from the examples under scrutiny, for instance in Figs. 6.1, 6.2 and 6.3, the choice of initial state influences the amount of generated entanglement. Now we shall inquire if it is possible to enhance the entanglement production simply by moving the cavity in a particular way — we want to find *entanglement resonances* — possibly with an accompanying restriction of the initial states. The results we present here are based on the results of Section 3.1.4 and the insights gathered from Refs. [42] and [47].

Let us start with the resonance condition of Eq. (3.27). For initial states with a covariance matrix proportional to the identity, i.e., the vacuum or coherent states, a vanishing commutator $[S, S^T]$ indicates that the entanglement produced by the symplectic transformation S can be linearly increased with the number of repetitions of the transformation if the operation represented by S is restricted to contain no overall

single-mode squeezing and if it is possible to perform the transformation successively in principle. Both of these conditions are met by the Bogoliubov transformation for non-uniform cavity motion when we select an arbitrary travel scenario between two inertial regions and terms are kept only up to linear order in h . The latter condition ensures that the coefficients $\beta_{nn}^{(2)}$, which would introduce single-mode squeezing, can be neglected. Under these premises let us proceed by examining the mechanism of the *resonance condition* perturbatively.

First we note that the linear order of corrections introduced by the Bogoliubov transformation for non-uniform cavity motion correlates modes only pairwise. Thus, neglecting second order corrections can be considered as a *two-mode truncation* [42] and we can restrict the analysis to only two modes k and k' . Further assuming that the initial state is represented by $\Gamma_{kk'} = \mathbb{1}$ we write the transformed covariance matrix as

$$\hat{\Gamma}_{kk'} = S S^T = \mathbb{1} + h \hat{\Gamma}_{kk'}^{(1)} + O(h^2). \quad (6.40)$$

The entanglement is determined by the smallest symplectic eigenvalue of the partial transpose, in other words, the smallest positive entry of the diagonal matrix

$$iU \Omega \check{T}_{k'} \hat{\Gamma}_{kk'} \check{T}_{k'} U^\dagger, \quad (6.41)$$

where U is the diagonalizing unitary. In particular, since we start with a separable state it is the correction term

$$iU \Omega \check{T}_{k'} \hat{\Gamma}_{kk'}^{(1)} \check{T}_{k'} U^\dagger = \text{diag}\{\pm \check{\nu}_-^{(1)}, \pm \check{\nu}_+^{(1)}\} \quad (6.42)$$

that generates the entanglement, specifically, the quantity $\check{\nu}_-^{(1)}$, see Eq. (6.34). From Eq. (6.40) it then follows immediately that N -fold repetition of a transformation satisfying the resonance condition of Eq. (3.27) will produce a state represented by the covariance matrix

$$(S)^N (S^T)^N = (S S^T)^N = \mathbb{1} + h N \hat{\Gamma}_{kk'}^{(1)} + O(h^2). \quad (6.43)$$

Consequently, the correction to the smallest symplectic eigenvalue after N repetitions is given by $N \check{\nu}_-^{(1)}$. In other words, the entanglement production grows linearly with the number of repetitions. Let us therefore investigate how the resonance condition can be satisfied by inserting the expansions of (5.23)-(5.25) into (3.14), whilst restricting to the two modes k and k' . To linear order the commutator of the resonance condition (3.27) has two independent non-zero entries

$$\text{Re}(G_k^{(0)} - G_{k'}^{(0)}) \text{Re}(\beta_{kk'}^{(1)}) + \text{Im}(G_k^{(0)} + G_{k'}^{(0)}) \text{Im}(\beta_{kk'}^{(1)}) = 0, \quad (6.44a)$$

$$\text{Re}(G_k^{(0)} - G_{k'}^{(0)}) \text{Im}(\beta_{kk'}^{(1)}) - \text{Im}(G_k^{(0)} + G_{k'}^{(0)}) \text{Re}(\beta_{kk'}^{(1)}) = 0. \quad (6.44b)$$

The two conditions in (6.44) can be conveniently combined into the single requirement

$$(G_k^{(0)*} - G_{k'}^{(0)}) \beta_{kk'}^{(1)} = 0. \quad (6.45)$$

Further noting that $\beta_{kk'}^{(1)}$ needs to be non-zero to create entanglement at all [see Eq. (6.15)] one finds that the resonances are purely governed by the phases that are acquired during the free time evolution. For any mode pair k and k' the *arbitrary* travel scenario that is to be repeated has to be timed appropriately to satisfy $(G_k^{(0)*} - G_{k'}^{(0)}) = 0$, i.e., the duration of a single repetition as measured at the centre of the cavity has to take on one of the discrete values

$$\tau_n = \frac{2\pi n}{\omega_k + \omega_{k'}}, \quad (6.46)$$

with $n = 1, 2, 3, \dots$, for which $\beta_{kk'}^{(1)}$ takes on a non-zero value, see Ref. [42]. An illustration of the resonance peaks of the created entanglement for fixed mode pairs is shown in Fig. 6.4.

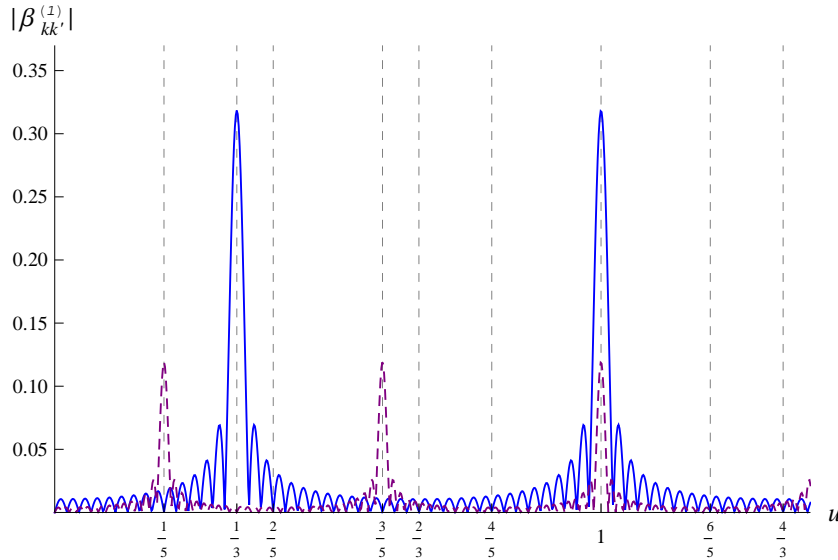


Figure 6.4: Entanglement resonances — β 's: The coefficient $|\beta_{kk'}^{(1)}|$ that generates entanglement from the vacuum [see Eq. (6.15)] is plotted against the dimensionless parameter $u := h\tau/[4L \operatorname{artanh}(h/2)]$ for a massless $(1 + 1)$ dimensional scalar field. The travel scenario, which is illustrated in Fig. 6.5 (b) for $N = 2$, has N segments of uniform proper acceleration h/L and duration $\tau/2$ as measured at the centre of the cavity, separated by $(N - 1)$ segments of inertial coasting of the same duration (to linear order in h). The curves are plotted for $N = 15$, $(k, k') = (1, 2)$ (blue, solid) and $(k, k') = (2, 3)$ (purple, dashed). The vertical dashed lines indicate the potential resonance times as given by Eq. (6.46) for $(k, k') = (1, 2)$ and $(k, k') = (2, 3)$, respectively.

Subsequently, one may ask about possible resonances for states that are not described by a covariance matrix that is proportional to the identity. For instance, inspecting Eqs. (6.22) and (6.35) it seems that a strong increase of $|\beta_{kk'}^{(1)}|$ [see Fig. 6.4 (a)]

may also increase the entanglement that is produced from these states, but the role of the coefficients $\alpha_{kk'}^{(1)}$ requires separate inspection. Indeed, a graphical analysis [see

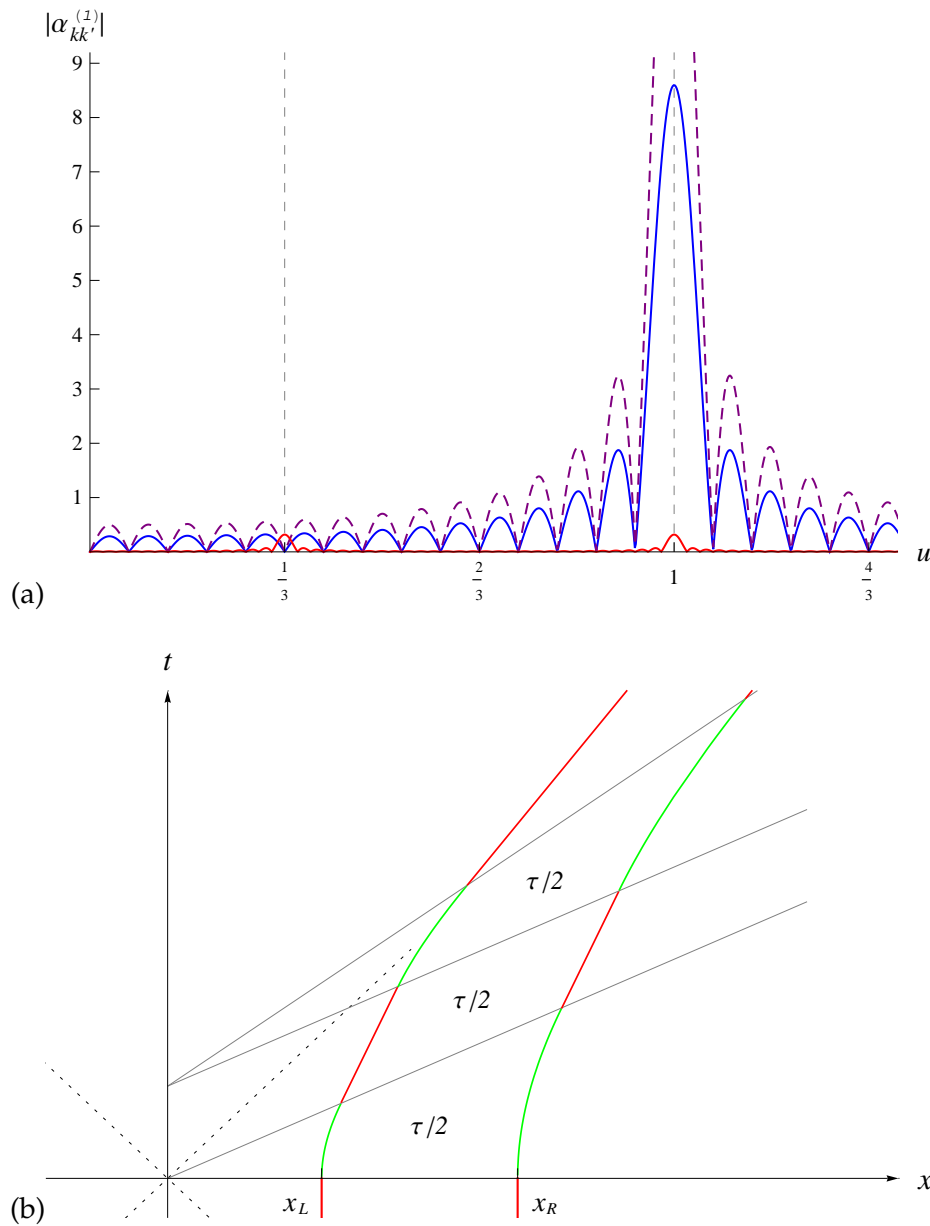


Figure 6.5: Entanglement resonances — α 's: The coefficient $|\alpha_{kk'}^{(1)}|$ that contributes to the entanglement generation, e.g., for squeezed states [see Eqs. (6.22) and (6.35)] is plotted in Fig. 6.5 (a) against the dimensionless parameter $u := h\tau/[4L \operatorname{artanh}(h/2)]$ for a massless $(1+1)$ dimensional scalar field. The travel scenario, which is illustrated in Fig. 6.5 (b) for $N = 2$, has N segments of uniform proper acceleration h/L and duration $\tau/2$ as measured at the centre of the cavity, separated by $(N - 1)$ segments of inertial coasting of the same duration (to linear order in h). The curves in Fig. 6.5 (a) are plotted for $N = 15$, $(k, k') = (1, 2)$ (blue, solid) and $(k, k') = (2, 3)$ (purple, dashed). For comparison the quantity $|\beta_{kk'}^{(1)}|$ (red, dashed) from Fig. 6.4 is shown for $(k, k') = (1, 2)$.

Fig. 6.5 (a)] shows that some resonances occur for both the coefficients $\alpha_{kk'}^{(1)}$ and $\beta_{kk'}^{(1)}$, which suggests that the entanglement production is significantly enhanced, growing (at most) linearly with the number of repetitions, also for squeezed states and single particle states.

Finally, following Ref. [47] we turn to the case of smoothly varying acceleration discussed in Section 4.4.3. Let us assume that the proper acceleration at the centre of the cavity is a sinusoidal function

$$\mathbf{a}_c(\tau) = \mathbf{a}_0 \sin(\omega_c \tau), \quad (6.47)$$

with an amplitude \mathbf{a}_0 that is much smaller than the inverse length of the cavity. The expressions for the leading order Bogoliubov coefficients from Eqs. (4.90b) and (4.90c) are oscillatory for an arbitrary value of the oscillation frequency ω_c . However, for specific choices of ω_c two cases can be distinguished. If $\omega_c = \omega_k + \omega_{k'}$ the integral in (4.90c) for the coefficient ${}_s\beta_{kk'}$ grows linearly with the overall time of acceleration. Such particle creation resonances are at the heart of the *dynamical Casimir effect* (DCE). We refer the interested reader to the recent review Ref. [64] and references therein. In particular, the DCE has been investigated in a variety of media, such as Bose-Einstein condensates (see, e.g., Ref. [115]), or superconducting microwave circuits [116, 123, 201].

On the other hand, for $\omega_c = |\omega_k - \omega_{k'}|$ we obtain a linear growth of the coefficient ${}_s\alpha_{kk'}$ with increasing overall time of the oscillation. Such a *mode-mixing* resonance could in principle be exploited for desktop experiments at mechanical frequencies [47], as well as for entanglement generation, e.g., in simulations of cavity motion in microwave circuitry, see Refs. [89, (ix)] and [186].

Note that in all resonance scenarios that we have discussed here we are still limited by the perturbative regime. The overall perturbation to any quantity of interest still needs to remain small if the approximations we have made are to hold. Nonetheless, the resonance formalism presents an elegant way of enhancing the corrections by orders of magnitude, possibly even to observable levels.

6.3 Entanglement Generation in Fermionic States

In this section we study the entanglement generation between the modes of a Dirac field that is confined to a non-uniformly moving cavity. Mirroring the analysis of the bosonic case in Section 6.1 we start from the vacuum state in Section 6.3.1 before we add particle content in Sections 6.3.2 and 6.3.3. In contrast to the bosonic situation two practical issues already arise at this stage of the analysis. First, in the selection of the

two modes between which entanglement generation is studied we have the choice between distinct particle and antiparticle modes. Second, in the partial tracing to recover the reduced states of the two chosen modes the consistency conditions (3.42) have to be respected, which requires tracing “inside-out.” With these considerations in mind we proceed with the vacuum state.

6.3.1 Entanglement from the Fermionic Vacuum

A quick inspection of the off-diagonal elements of Eq. (5.48) suggests to start by tracing over all modes except a particle mode labelled by κ and an antiparticle mode labelled by κ' . Using (5.43) and (4.77c) one quickly arrives at

$$\begin{aligned} \text{vac} \varrho_{\kappa\kappa'} &= \text{Tr}_{\neg\kappa, \kappa'} (\|0\rangle\rangle\langle\langle 0|) = \|\widehat{0}\rangle\rangle\langle\langle \widehat{0}| + h \left[G_{\kappa'}^{(0)} A_{\kappa\kappa'}^{(1)*} \|\widehat{1}_\kappa\rangle\rangle^+ \|\widehat{1}_{\kappa'}\rangle\rangle^- \langle\langle \widehat{0}| + \text{H. c.} \right] \\ &+ h^2 \left[2\bar{f}_{\kappa\rightarrow\kappa'}^A \|\widehat{1}_\kappa\rangle\rangle^+ \langle\langle \widehat{1}_\kappa| + 2f_{\kappa'\rightarrow\kappa}^A \|\widehat{1}_{\kappa'}\rangle\rangle^- \langle\langle \widehat{1}_{\kappa'}| - 2(\bar{f}_{\kappa\rightarrow\kappa'}^A + f_{\kappa'}^A) \|\widehat{0}\rangle\rangle\langle\langle \widehat{0}| \right. \\ &\left. + |A_{\kappa\kappa'}^{(1)}|^2 \|\widehat{1}_\kappa\rangle\rangle^+ \|\widehat{1}_{\kappa'}\rangle\rangle^- \langle\langle \widehat{1}_{\kappa'}| \langle\langle \widehat{1}_\kappa| + \left(\mathcal{V}_{\kappa\kappa'}^{(2)} \|\widehat{1}_\kappa\rangle\rangle^+ \|\widehat{1}_{\kappa'}\rangle\rangle^- \langle\langle \widehat{0}| + \text{H. c.} \right) \right] + O(h^3), \end{aligned} \quad (6.48)$$

where we have defined the abbreviations

$$f_{m\rightarrow n}^A = \frac{1}{2} \sum_{\substack{i>0 \\ i\neq n}} |A_{mi}^{(1)}|^2, \quad \bar{f}_{m\rightarrow n}^A = \frac{1}{2} \sum_{\substack{i<0 \\ i\neq n}} |A_{mi}^{(1)}|^2. \quad (6.49)$$

For two modes we may unambiguously map the two fermionic modes to two qubits, see Section 3.2.4 and Ref. [86, (viii)], and compute entanglement measures such as the *negativity* (see Definition 1.10) or the *concurrence* (1.17) with respect to the tensor product of the two-qubit space. However, perturbative calculations of the concurrence present practical difficulties, see Ref. [87, (iv)] or Section 7.2.1. It is thus more convenient to compute the negativity instead, which allows for simple comparisons with our previous results for bosons. Hence, we continue by representing the partial transpose of the two-qubit state associated to Eq. (6.48) as

$$\begin{pmatrix} 1 - h^2 2(\bar{f}_{\kappa\rightarrow\kappa'}^A + f_{\kappa'}^A) & 0 & 0 & 0 \\ 0 & h^2 2f_{\kappa'\rightarrow\kappa}^A & h G_{\kappa'}^{(0)} A_{\kappa\kappa'}^{(1)*} + h^2 \mathcal{V}_{\kappa\kappa'}^{(2)*} & 0 \\ 0 & h G_{\kappa'}^{(0)*} A_{\kappa\kappa'}^{(1)} + h^2 \mathcal{V}_{\kappa\kappa'}^{(2)} & h^2 2\bar{f}_{\kappa\rightarrow\kappa'}^A & 0 \\ 0 & 0 & 0 & h^2 |A_{\kappa\kappa'}^{(1)}|^2 \end{pmatrix}. \quad (6.50)$$

Specializing to the case where $(\kappa + \kappa')$ is odd the linear corrections to the off-diagonal elements persist and we find the corrections to the degenerate unperturbed eigenvalues $\lambda_{1,2,3}^{(0)} = 0$ to linear order as $\{\pm h |A_{\kappa\kappa'}^{(1)}|, 0\}$ using the procedure from page 117. We thus find the negativity that is generated from the fermionic vacuum to linear order in h , i.e.,

$$\mathcal{N}(\text{vac} \varrho_{\kappa\kappa'}) = h \mathcal{N}^{(1)}(\text{vac} \varrho_{\kappa\kappa'}) + O(h^2) = h |A_{\kappa\kappa'}^{(1)}| + O(h^2). \quad (6.51)$$

Alternatively, we may select two modes with the same parity, $(\kappa + \kappa')$ even, such that only corrections quadratic in \hbar remain in (6.50). In this case the diagonalization of the 3×3 sub-block corresponding to the unperturbed eigenvalue 0 also has one possibly negative eigenvalue and the negativity

$$\mathcal{N}(\text{vac}\mathcal{Q}_{\kappa\kappa'}) = \hbar^2 \max\left\{0, \sqrt{(\bar{f}_{\kappa-\kappa'}^A - f_{\kappa'-\kappa}^A)^2 + |\mathcal{V}_{\kappa\kappa'}^{(2)}|^2} - (\bar{f}_{\kappa-\kappa'}^A + f_{\kappa'-\kappa}^A)\right\} + O(\hbar^3) \quad (6.52)$$

is obtained, see Fig. 6.6. Note the similarity between the bosonic and fermionic case by comparing Eq. (6.15) with (6.51), and Eq. (6.17) with (6.52), respectively.

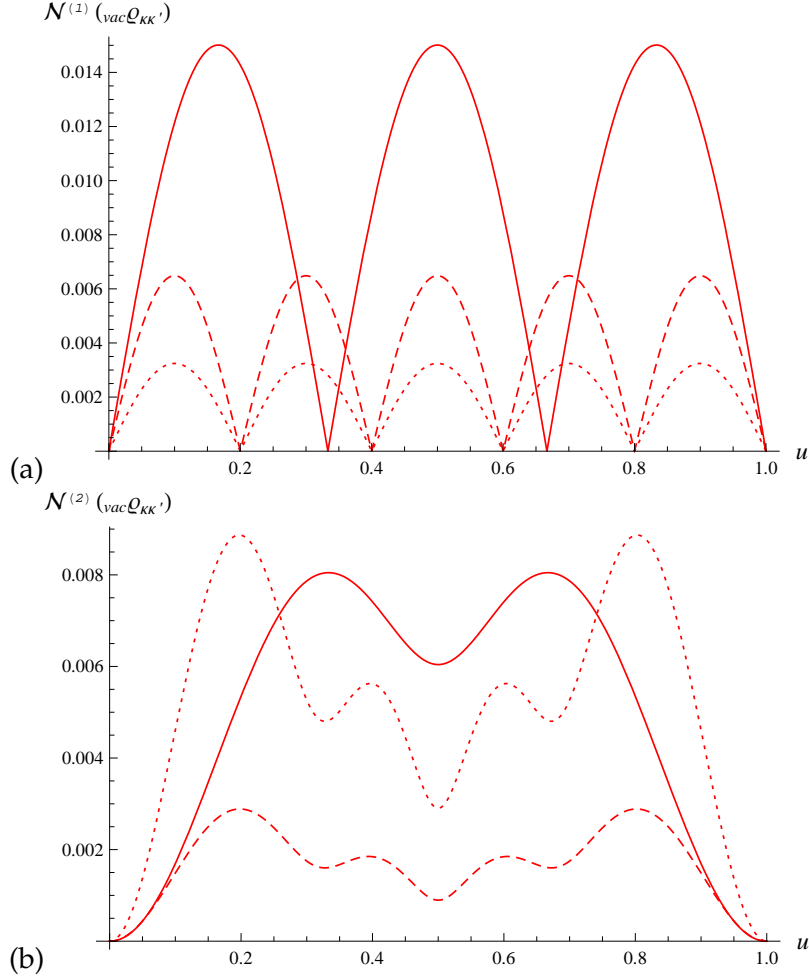


Figure 6.6: Entanglement generation — fermionic vacuum: The coefficients $\mathcal{N}^{(1)}$ and $\mathcal{N}^{(2)}$ [see Eq. (6.51) and (6.52)] of the negativity generated from the fermionic vacuum are plotted in Fig. 6.6 (a) and Fig. 6.6 (b), respectively, for the basic building block travel scenario of Section 4.4.1. The effects for the $(1+1)$ dimensional Dirac field used here are periodic in the dimensionless parameter $u := \hbar\tau/[4L \operatorname{artanh}(\hbar/2)]$ [see Eq. (4.52)], where τ is the duration of the acceleration, as measured at the centre of the cavity. Curves are shown for the modes $(\kappa, \kappa') = (0, -3), (2, -1)$ (solid), $(0, -5), (4, -1)$ (dashed), and $(3, -2), (1, -4)$ (dotted) in Fig. 6.6 (a), and for $(1, -1), (0, -2)$ (solid), $(1, -3), (2, -2)$ (dashed), and $(0, -4), (3, -1)$ (dotted) in Fig. 6.6 (b).

6.3.2 Entanglement from the Fermionic Particle State

Let us pursue the same strategy for the single fermion state as chosen before for the fermionic vacuum in Section 6.3.1, i.e., we consider the density matrix of Eq. (5.51) and trace over (see Section 3.2.3) all modes except for $\kappa \geq 0$ and $\kappa' < 0$ to arrive at

$$\begin{aligned} \text{Tr}_{-\kappa, \kappa'}(\|1_\kappa\rangle\rangle^{++}\langle\langle 1_\kappa\|) &= \|\widehat{1}_\kappa\rangle\rangle^{++}\langle\langle \widehat{1}_\kappa\| + h^2 \left[2 f_{\kappa' \rightarrow \kappa}^A \|\widehat{1}_\kappa\rangle\rangle^+ \|\widehat{1}_{\kappa'}\rangle\rangle^- \langle\langle \widehat{1}_{\kappa'}\| + \langle\langle \widehat{1}_\kappa\| \right. \\ &\quad \left. - 2 (f_{\kappa' \rightarrow \kappa}^A + f_\kappa^A) \|\widehat{1}_\kappa\rangle\rangle^{++}\langle\langle \widehat{1}_\kappa\| + 2 f_\kappa^A \|\widehat{0}\rangle\rangle\langle\langle \widehat{0}\| \right. \\ &\quad \left. - \left(G_\kappa^{(0)*} G_{\kappa'}^{(0)} \sum_{m \geq 0} A_{m\kappa}^{(1)} A_{m\kappa'}^{(1)*} \|\widehat{1}_\kappa\rangle\rangle^+ \|\widehat{1}_{\kappa'}\rangle\rangle^- \langle\langle \widehat{0}\| + \text{H. c.} \right) \right] + O(h^3), \end{aligned} \quad (6.53)$$

(for $\kappa \geq 0, \kappa' < 0$)

where f_κ^A and $f_{\kappa' \rightarrow \kappa}^A$ are as in Eq. (6.49). Mapping this state to two qubits it is quite straightforward to see that the subspace of degenerate eigenvalues of the partial transpose of has no negative corrections to second order in h . Thus, no entanglement is generated from the state $\|1_\kappa\rangle\rangle$ between any chosen pair of modes with opposite sign of frequency. However, we may select two modes of positive frequency instead, such that $\kappa, \kappa' \geq 0$. One then finds the reduced state

$$\begin{aligned} \text{Tr}_{-\kappa, \kappa'}(\|1_\kappa\rangle\rangle^{++}\langle\langle 1_\kappa\|) &= \|\widehat{1}_\kappa\rangle\rangle^{++}\langle\langle \widehat{1}_\kappa\| - h \left[\mathcal{V}_{\kappa\kappa'}^{(1)} \|\widehat{1}_\kappa\rangle\rangle^+ \|\widehat{1}_{\kappa'}\rangle\rangle^+ + \text{H. c.} \right] \\ &\quad + h^2 \left[2 f_{\kappa \rightarrow \kappa'}^A \|\widehat{0}\rangle\rangle\langle\langle \widehat{0}\| + |A_{\kappa\kappa'}^{(1)}|^2 \|\widehat{1}_\kappa\rangle\rangle^{++}\langle\langle \widehat{1}_{\kappa'}\| - (f_\kappa^A + \bar{f}_{\kappa'}^A) \|\widehat{1}_\kappa\rangle\rangle^{++}\langle\langle \widehat{1}_\kappa\| \right. \\ &\quad \left. + 2 \bar{f}_{\kappa'}^A \|\widehat{1}_\kappa\rangle\rangle^+ \|\widehat{1}_{\kappa'}\rangle\rangle^+ \langle\langle \widehat{1}_{\kappa'}\| + \langle\langle \widehat{1}_\kappa\| - \left(\mathcal{V}_{\kappa\kappa'}^{(2)} \|\widehat{1}_\kappa\rangle\rangle^+ \|\widehat{1}_{\kappa'}\rangle\rangle^+ + \text{H. c.} \right) \right] + O(h^3), \end{aligned} \quad (6.54)$$

(for $\kappa, \kappa' \geq 0$)

where we have used the Bogoliubov identities (4.77c) and (4.78c), and the definition of the components \mathcal{V}_{pq} ($p \geq 0, q < 0$) has been extended to indices of all sign combinations via their perturbative expansions in (5.43), such that the indices p and q can take on both negative and non-negative values. For two fermionic modes we can consistently represent (see Section 3.2.4) the reduced state to second order in h as a two-qubit density matrix ${}_{1-\kappa} \rho_{\kappa\kappa'}$ with partial transpose

$$\begin{pmatrix} 2h^2 f_{\kappa \rightarrow \kappa'}^A & 0 & 0 & -h \mathcal{V}_{\kappa\kappa'}^{(1)*} - h^2 \mathcal{V}_{\kappa\kappa'}^{(2)*} \\ 0 & h^2 |A_{\kappa\kappa'}^{(1)}|^2 & 0 & 0 \\ 0 & 0 & 1 - h^2 (f_\kappa^A + \bar{f}_{\kappa'}^A) & 0 \\ -h \mathcal{V}_{\kappa\kappa'}^{(1)} - h^2 \mathcal{V}_{\kappa\kappa'}^{(2)} & 0 & 0 & 2h^2 \bar{f}_{\kappa'}^A \end{pmatrix}. \quad (6.55)$$

If the modes κ and κ' have opposite parity, $(\kappa + \kappa')$ is odd, we find the negativity to be

$$\mathcal{N}({}_{1-\kappa} \rho_{\kappa\kappa'}) = h \mathcal{N}^{(1)}({}_{1-\kappa} \rho_{\kappa\kappa'}) + O(h^2) = h |A_{\kappa\kappa'}^{(1)}| + O(h^2), \quad (6.56)$$

formally the same expression as in Eq. (6.51), but with the appropriate non-negative

value for κ' . Similarly, if the modes have the same parity, i.e., if $(\kappa + \kappa')$ is even, we find

$$\begin{aligned} \mathcal{N}({}_{1-\kappa}\rho_{\kappa\kappa'}) &= h^2 \mathcal{N}^{(2)}({}_{1-\kappa}\rho_{\kappa\kappa'}) + O(h^3) \\ &= h^2 \max\left\{0, \sqrt{(f_{\kappa\rightarrow\kappa'}^A - \bar{f}_{\kappa'}^A)^2 + |\mathcal{V}_{\kappa\kappa'}^{(2)}|^2} - (f_{\kappa\rightarrow\kappa'}^A + \bar{f}_{\kappa'}^A)\right\} + O(h^3). \end{aligned} \quad (6.57)$$

An illustration of the entanglement generated from $\|1_{\kappa}\rangle\rangle^+$ is shown in Fig. 6.7.

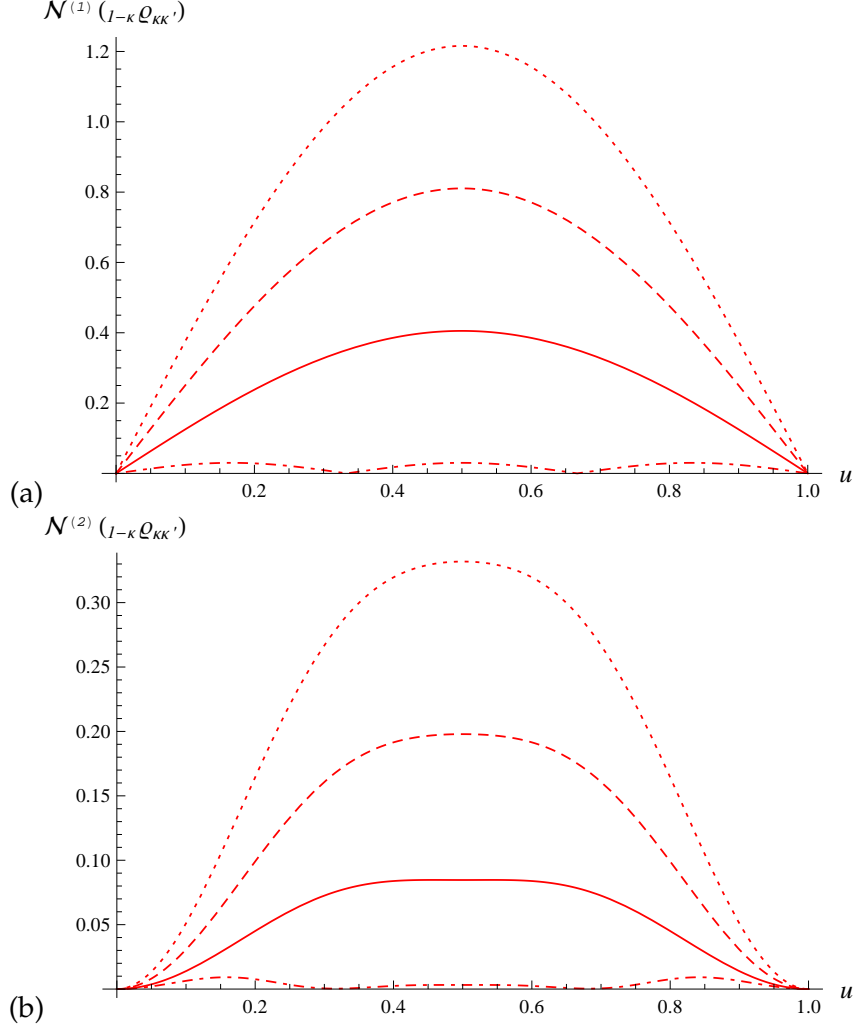


Figure 6.7: Entanglement generation — fermionic particle state: The coefficients $\mathcal{N}^{(1)}$ and $\mathcal{N}^{(2)}$ [see Eq. (6.56) and (6.57)] of the negativity generated from $\|1_{\kappa}\rangle\rangle^+$ are plotted in Fig. 6.7 (a) and Fig. 6.7 (b), respectively, for the basic building block travel scenario of Section 4.4.1. The effects for the $(1+1)$ dimensional Dirac field used here are periodic in the dimensionless parameter $u := h\tau/[4L \operatorname{artanh}(h/2)]$ [see Eq. (4.52)], where τ is the duration of the acceleration, as measured at the centre of the cavity. Curves are shown for the modes $(\kappa, \kappa') = (0, 1)$ (solid), $(1, 2)$ (dashed), $(2, 3)$ (dotted), and $(0, 3)$ (dotted-dashed) in Fig. 6.7 (a), and for $(0, 2)$ (solid), $(1, 3)$ (dashed), $(2, 4)$ (dotted), and $(0, 4)$ (dotted-dashed) in Fig. 6.7 (b).

Entanglement from the Fermionic Antiparticle State

The analysis of Section 6.3.2 can be repeated step by step if we start instead from a single-antiparticle state $\|1_{\hat{\kappa}}\rangle\rangle^-$ and trace over all modes except two modes $\hat{\kappa}, \hat{\kappa}' < 0$. However, since the positive and negative frequency solutions appear symmetrically in the spectrum (see Section 4.3) the corresponding results can be directly obtained by setting κ and κ' in Eq. (6.56) and (6.57) to $|\hat{\kappa} + 1|$ and $|\hat{\kappa}' + 1|$. The same is true for the sample plots in Fig. 6.7.

6.3.3 Entanglement from the Fermionic Particle-Antiparticle Pair

For the initial state $\|1_{\kappa}\rangle\rangle^+ \|1_{\kappa'}\rangle\rangle^-$ of a pair of one particle ($\kappa \geq 0$) and one antiparticle ($\kappa' < 0$) we expand Eq. (5.55) to second order in \hbar . Keeping terms proportional to \hbar^2 and tracing over all modes except κ and κ' one arrives at the expression

$$\begin{aligned} \text{Tr}_{\neg\kappa, \kappa'} (\|1_{\kappa}\rangle\rangle^+ \|1_{\kappa'}\rangle\rangle^- \langle\langle 1_{\kappa'} \| \langle\langle 1_{\kappa} \|) &= \|\hat{1}_{\kappa}\rangle\rangle^+ \|\hat{1}_{\kappa'}\rangle\rangle^- \langle\langle \hat{1}_{\kappa'} \| \langle\langle \hat{1}_{\kappa} \| \quad (6.58) \\ &- \hbar \left[\mathcal{V}_{\kappa\kappa'}^{(1)} \|\hat{1}_{\kappa}\rangle\rangle^+ \|\hat{1}_{\kappa'}\rangle\rangle^- \langle\langle \hat{0} \| + \text{H. c.} \right] + \hbar^2 \left[|A_{\kappa\kappa'}^{(1)}|^2 \|\hat{0}\rangle\rangle \langle\langle \hat{0} \| + 2f_{\kappa}^A \|\hat{1}_{\kappa'}\rangle\rangle^- \langle\langle \hat{1}_{\kappa} \| \right. \\ &+ 2\bar{f}_{\kappa'}^A \|\hat{1}_{\kappa}\rangle\rangle^+ \langle\langle \hat{1}_{\kappa} \| - (2f_{\kappa}^A + 2\bar{f}_{\kappa'}^A + |A_{\kappa\kappa'}^{(1)}|^2) \|\hat{1}_{\kappa}\rangle\rangle^+ \|\hat{1}_{\kappa'}\rangle\rangle^- \langle\langle \hat{1}_{\kappa'} \| \langle\langle \hat{1}_{\kappa} \| \\ &\left. - \left(\mathcal{V}_{\kappa\kappa'}^{(2)} \|\hat{1}_{\kappa}\rangle\rangle^+ \|\hat{1}_{\kappa'}\rangle\rangle^- \langle\langle \hat{0} \| + \text{H. c.} \right) \right] + O(\hbar^3). \end{aligned}$$

Comparing with the case for the fermionic vacuum one immediately finds the negativity

$$\mathcal{N}_{(1-\kappa, 1-\kappa') \varrho_{\kappa\kappa'}} = \hbar \mathcal{N}^{(1)}_{(1-\kappa, 1-\kappa') \varrho_{\kappa\kappa'}} + O(\hbar^2) = \hbar |A_{\kappa\kappa'}^{(1)}| + O(\hbar^2), \quad (6.59)$$

for modes with opposite parity, that is, if $(\kappa + \kappa')$ is odd, while mode pairs with equal parity provide a correction to the negativity that is quadratic in \hbar , i.e.,

$$\begin{aligned} \mathcal{N}_{(1-\kappa, 1-\kappa') \varrho_{\kappa\kappa'}} &= \hbar^2 \mathcal{N}^{(2)}_{(1-\kappa, 1-\kappa') \varrho_{\kappa\kappa'}} + O(\hbar^3) \quad (6.60) \\ &= \hbar^2 \max \left\{ 0, \sqrt{(f_{\kappa}^A - \bar{f}_{\kappa'}^A)^2 + |\mathcal{V}_{\kappa\kappa'}^{(2)}|^2} - (f_{\kappa}^A + \bar{f}_{\kappa'}^A) \right\} + O(\hbar^3). \end{aligned}$$

Formally, these expressions are remarkably similar to the results for the fermionic vacuum in Eq. (6.51) and Eq. (6.52). In fact, the linear corrections are exactly the same and one may consult Fig. 6.6 (a) for an illustration. The quadratic corrections, on the other hand, are slightly different. The sums \bar{f}_{κ}^A and $f_{\kappa'}^A$ in Eq. (6.52) represent particle creation coefficients, while the quantities f_{κ}^A and $\bar{f}_{\kappa'}^A$ in Eq. (6.60) are responsible for shifting excitations from the mode κ (κ') to other positive (negative) frequency modes — mode mixing α -type coefficients. This alteration makes for all the difference: even for a choice of modes with minimal energy for a $(1 + 1)$ dimensional Dirac field the

entanglement generation by the particle creation coefficient $|\mathcal{V}_{\kappa\kappa'}^{(2)}|$ cannot compete with the much larger contributions by f_{κ}^A and $\bar{f}_{\kappa'}^A$ that add noise to the reduced state. The partial transpose of the two-qubit density matrix representing the state (6.58) has one possibly negative eigenvalue, but graphical analysis shows it remains non-negative, see Fig. 6.8. For higher dimensions, higher mode numbers, or increased mass, the noise introduced by f_{κ}^A and $\bar{f}_{\kappa'}^A$ will only increase. Consequently, no entanglement is created from the state $\|1_{\kappa}\rangle\rangle^+ \|1_{\kappa'}\rangle\rangle^-$ for mode pairs (κ, κ') with equal parity.

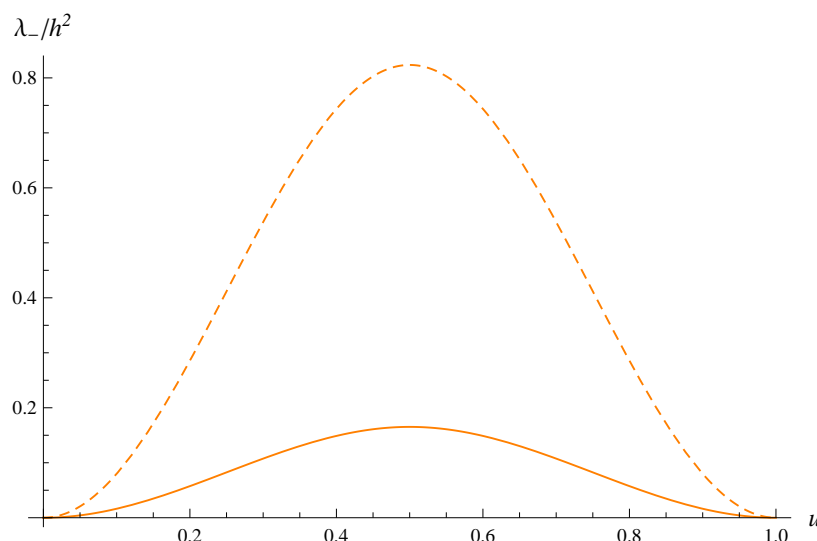


Figure 6.8: Entanglement generation — fermionic particle-antiparticle pair: The second order coefficient of the only possibly negative eigenvalue $\lambda_- = h^2[f_{\kappa}^A + \bar{f}_{\kappa'}^A] - h^2 \sqrt{[f_{\kappa}^A - \bar{f}_{\kappa'}^A]^2 + |\mathcal{V}_{\kappa\kappa'}^{(2)}|^2}$ of the partial transpose of the two qubit representation for the state Eq. (6.58) is shown. Curves are plotted for the basic building block travel scenario of Section 4.4.1 for a $(1 + 1)$ dimensional Dirac field against the dimensionless parameter $u := h\tau/[4L \operatorname{artanh}(h/2)]$ [see Eq. (4.52)], where τ is the duration of the acceleration, as measured at the centre of the cavity. Curves are shown for the modes $(\kappa, \kappa') = (1, -1), (0, -2), (0, -4), (3, -1)$ (solid), and $(1, -3), (2, -2)$ (dashed). Since the correction is positive throughout no entanglement is generated.

6.4 Generation of Genuine Multipartite Entanglement

The investigation carried out up to this point has revealed that entanglement is created by the non-uniform motion between pairs of modes of the quantum fields. The amount of entanglement and, indeed, if any entanglement is created at all, depends on the choice of initial state and chosen modes. In particular, the fermionic systems suffer from limitations in the creation of entanglement due to the Pauli exclusion principle, while bosonic systems are more susceptible to the required particle creation and shifting of excitations. Conceptually, it is of further interest to learn how the quantum

correlations connect more than two modes. We may ask if and how *genuine multipartite entanglement* (GME) emerges from the Bogoliubov transformations. The analysis here is based on material published in Ref. [84, (vi)]. For simplicity we restrict our deliberations to the multipartite entanglement of the transformed vacuum states, the bosonic vacuum in Section 6.4.1, and the fermionic counterpart in Section 6.4.2. It is further useful to recall the discussion of Section 1.4 for the basic concepts and definitions.

6.4.1 Genuine Multipartite Entanglement — Bosonic Vacuum

For the case of bosonic GME we return to the transformed vacuum state of Eq. (5.17) and we reduce the state to three modes, k , k' , and k'' . At this stage we specialize to the case where not all three modes have the same parity. Without loss of generality we pick $(k + k')$ and $(k' + k'')$ to be odd, which implies that $(k + k'')$ is even, such that the first order coefficient $V_{kk''}^{(1)}$ as well as the second order coefficients $V_{kk'}^{(2)}$ and $V_{k'k''}^{(2)}$ vanish. One then obtains the reduced state

$$\begin{aligned}
 \text{vac}\rho_{kk'k''} := & \text{Tr}_{-k,k',k''} (|0\rangle\langle 0|) = |\widehat{0}\rangle\langle\widehat{0}| - h \left[V_{kk'}^{(1)} |\widehat{1}_k\rangle\langle\widehat{1}_k| |\widehat{1}_{k'}\rangle\langle\widehat{1}_{k'}| |\widehat{0}\rangle\langle\widehat{0}| + V_{k'k''}^{(1)} |\widehat{1}_{k'}\rangle\langle\widehat{1}_{k'}| |\widehat{1}_{k''}\rangle\langle\widehat{1}_{k''}| |\widehat{0}\rangle\langle\widehat{0}| \right. \\
 & + \text{H. c.} \left. \right] + h^2 \left[2f_{k-k'}^\beta |\widehat{1}_k\rangle\langle\widehat{1}_k| + 2f_{k'-k,k''}^\beta |\widehat{1}_{k'}\rangle\langle\widehat{1}_{k'}| |\widehat{1}_{k''}\rangle\langle\widehat{1}_{k''}| + 2f_{k''-k'}^\beta |\widehat{1}_{k''}\rangle\langle\widehat{1}_{k''}| |\widehat{1}_k\rangle\langle\widehat{1}_k| - 2(f_{k-k'}^\beta \right. \\
 & + f_{k'-k''}^\beta + f_{k''}^\beta) |\widehat{0}\rangle\langle\widehat{0}| + |\beta_{kk'}^{(1)}|^2 |\widehat{1}_k\rangle\langle\widehat{1}_k| |\widehat{1}_{k'}\rangle\langle\widehat{1}_{k'}| |\widehat{1}_k\rangle\langle\widehat{1}_k| + |\beta_{k'k''}^{(1)}|^2 |\widehat{1}_{k'}\rangle\langle\widehat{1}_{k'}| |\widehat{1}_{k''}\rangle\langle\widehat{1}_{k''}| |\widehat{1}_{k'}\rangle\langle\widehat{1}_{k'}| \\
 & + \left(V_{kk''}^{(2)} |\widehat{1}_k\rangle\langle\widehat{1}_k| |\widehat{1}_{k''}\rangle\langle\widehat{1}_{k''}| |\widehat{0}\rangle\langle\widehat{0}| + \frac{1}{\sqrt{2}} V_{kk}^{(2)} |\widehat{2}_k\rangle\langle\widehat{2}_k| |\widehat{0}\rangle\langle\widehat{0}| + \frac{1}{\sqrt{2}} V_{k'k'}^{(2)} |\widehat{2}_{k'}\rangle\langle\widehat{2}_{k'}| |\widehat{0}\rangle\langle\widehat{0}| + \frac{1}{\sqrt{2}} V_{k''k''}^{(2)} |\widehat{2}_{k''}\rangle\langle\widehat{2}_{k''}| |\widehat{0}\rangle\langle\widehat{0}| \right. \\
 & + (V_{kk'}^{(1)})^2 |\widehat{2}_k\rangle\langle\widehat{2}_k| |\widehat{2}_{k'}\rangle\langle\widehat{2}_{k'}| |\widehat{0}\rangle\langle\widehat{0}| + (V_{k'k''}^{(1)})^2 |\widehat{2}_{k'}\rangle\langle\widehat{2}_{k'}| |\widehat{2}_{k''}\rangle\langle\widehat{2}_{k''}| |\widehat{0}\rangle\langle\widehat{0}| + \sqrt{2} V_{kk'}^{(1)} V_{k''k'}^{(1)} |\widehat{1}_k\rangle\langle\widehat{1}_k| |\widehat{2}_{k'}\rangle\langle\widehat{2}_{k'}| |\widehat{1}_{k''}\rangle\langle\widehat{1}_{k''}| |\widehat{0}\rangle\langle\widehat{0}| \\
 & \left. + \sum_{p \neq k'} V_{pk}^{(1)} V_{pk''}^{(1)} |\widehat{1}_k\rangle\langle\widehat{1}_k| |\widehat{1}_{k''}\rangle\langle\widehat{1}_{k''}| + \text{H. c.} \right] + O(h^3), \tag{6.61}
 \end{aligned}$$

where $V_{mn}^{(1)}$ and $V_{mn}^{(2)}$ are given by (5.8b) and (5.8c), respectively. In the face of the complicated decomposition of the reduced state (6.61) a simple method for the detection of GME is invaluable. It is particularly convenient to invoke the *GME witness inequalities* of Theorem 1.4. Keeping terms proportional to h^2 in the Taylor-Maclaurin expansion effectively truncates the problem at hand to a three qutrit system, i.e., each mode is mapped to a three dimensional Hilbert space. For this situation we use the techniques from [92, 129, 206] to construct the particular witness inequality [84]

$$\begin{aligned}
 2 \left(\left| \langle \widehat{0} | \text{vac}\rho_{kk'k''} | \widehat{1}_k \rangle \langle \widehat{2}_{k'} | \widehat{1}_{k''} \rangle \right| - \sqrt{\langle \widehat{1}_k | \text{vac}\rho_{kk'k''} | \widehat{1}_k \rangle \langle \widehat{1}_{k''} | \widehat{2}_{k'} | \text{vac}\rho_{kk'k''} | \widehat{2}_{k'} \rangle \langle \widehat{1}_{k''} | \widehat{1}_k \rangle} \right. \\
 - \sqrt{\langle \widehat{1}_{k''} | \text{vac}\rho_{kk'k''} | \widehat{1}_{k''} \rangle \langle \widehat{2}_{k'} | \langle \widehat{1}_k | \text{vac}\rho_{kk'k''} | \widehat{1}_k \rangle | \widehat{2}_{k'} \rangle} \\
 \left. - \sqrt{\langle \widehat{2}_{k'} | \text{vac}\rho_{kk'k''} | \widehat{2}_{k'} \rangle \langle \widehat{1}_{k''} | \langle \widehat{1}_k | \text{vac}\rho_{kk'k''} | \widehat{1}_k \rangle | \widehat{1}_{k''} \rangle} \right) \leq 0. \tag{6.62}
 \end{aligned}$$

As we have discussed in Section 1.4 such inequalities are always satisfied by any bi-separable states and their violation therefore unambiguously detects GME. Moreover, the violation of this type of inequality can be regarded as a lower bound to actual measures of GME, see Refs. [206]. Performing the perturbative expansion of Eq. (6.62) we find the simple inequality

$$2|\langle \hat{0} |_{\text{vac}} \rho_{kk'k''} | \hat{1}_k \rangle | \hat{2}_{k'} \rangle | \hat{1}_{k''} \rangle | - O(\hbar^3) = 2\sqrt{2} \hbar^2 |\beta_{kk'}^{(1)}| |\beta_{k'k''}^{(1)}| - O(\hbar^3) \leq 0. \quad (6.63)$$

We find that the inequality indeed is generally violated, showing that GME is created between the three chosen modes by coherently exciting pairs of particles in (k, k') and (k', k'') . Moreover, a quick glance at Fig. 6.4 reveals that joint *entanglement resonances* can occur. For instance, the individual coefficients $|\beta_{kk'}^{(1)}|$ and $|\beta_{k'k''}^{(1)}|$ for a massless scalar field in $(1+1)$ dimensions increase linearly with the number of repetitions of some basic travel scenario when the basic travel time (as measured at the centre of the cavity) is $\tau = 2nL/(k+k')$ or $\tau = 2mL/(k'+k'')$, $n, m \in \mathbb{N}_+$, respectively, see Eq. (6.46). Both of these resonances coincide if $n = p(k+k')$ and $m = p(k'+k'')$, such that $\tau = 2pL$, $p \in \mathbb{N}_+$, see Fig. 6.4.

At this resonance time, which happens to be independent of the chosen modes, the lower bound on the GME increases quadratically with the number N of repetitions of the basic travel scenario. Simultaneously, the terms $f_{k-k'}^\beta$, $f_{k'-k, k''}^\beta$, and $f_{k''-k'}^\beta$, which introduce mixedness into the reduced state, scale quadratically at the mode-independent resonance. Nonetheless, the validity of the perturbative approach is guaranteed because all second order terms are at most proportional to $N^2 \hbar^2 \ll Nh$, which in turn is required to be much smaller than 1 if the perturbative approach is to be justified.

6.4.2 Genuine Multipartite Entanglement — Fermionic Vacuum

For the fermionic counterpart of the situation studied in Section 6.4.1 we may also select three modes κ , κ' , and κ'' , that do not all have the same parity. In addition, we now have the choice between positive and negative frequency modes. The analysis of Section 6.3.1 taught us that entanglement is generated from the vacuum between modes of opposite frequency sign. We thus choose two positive frequency modes, $\kappa \geq 0$ and $\kappa' \geq 0$, of the same parity, $(\kappa + \kappa')$ is even, while the third mode $\kappa'' < 0$ is selected from the negative frequencies such that it has opposite parity to the particle modes, i.e., $(\kappa + \kappa'')$ and $(\kappa' + \kappa'')$ are odd. Tracing out all other modes from the transformed

vacuum of Eq. (5.48) we arrive at

$$\begin{aligned}
 \text{vac}_{\kappa\kappa'\kappa''} &= \text{Tr}_{-\kappa,\kappa'\kappa''} (|0\rangle\rangle\langle\langle 0|) = \|\widehat{0}\rangle\rangle\langle\langle\widehat{0}| + h \left[\mathcal{V}_{\kappa\kappa''}^{(1)} \|\widehat{1}_{\kappa}\rangle\rangle^+ \|\widehat{1}_{\kappa''}\rangle\rangle^- \langle\langle\widehat{0}| \right. \\
 &+ \left. \mathcal{V}_{\kappa'\kappa''}^{(1)} \|\widehat{1}_{\kappa'}\rangle\rangle^+ \|\widehat{1}_{\kappa''}\rangle\rangle^- \langle\langle\widehat{0}| + \text{H. c.} \right] + h^2 \left[-2 (\bar{f}_{\kappa\rightarrow\kappa''}^A + \bar{f}_{\kappa'\rightarrow\kappa''}^A + f_{\kappa''}^A) \|\widehat{0}\rangle\rangle\langle\langle\widehat{0}| \right. \\
 &+ 2 \bar{f}_{\kappa\rightarrow\kappa''}^A \|\widehat{1}_{\kappa}\rangle\rangle^+ \langle\langle\widehat{1}_{\kappa}| + 2 \bar{f}_{\kappa'\rightarrow\kappa''}^A \|\widehat{1}_{\kappa'}\rangle\rangle^+ \langle\langle\widehat{1}_{\kappa'}| + 2 f_{\kappa''\rightarrow\kappa,\kappa'}^A \|\widehat{1}_{\kappa''}\rangle\rangle^- \langle\langle\widehat{1}_{\kappa''}| \\
 &+ |A_{\kappa\kappa''}^{(1)}|^2 \|\widehat{1}_{\kappa}\rangle\rangle^+ \|\widehat{1}_{\kappa''}\rangle\rangle^- \langle\langle\widehat{1}_{\kappa''}| + \langle\langle\widehat{1}_{\kappa}| + |A_{\kappa'\kappa''}^{(1)}|^2 \|\widehat{1}_{\kappa'}\rangle\rangle^+ \|\widehat{1}_{\kappa''}\rangle\rangle^- \langle\langle\widehat{1}_{\kappa''}| + \langle\langle\widehat{1}_{\kappa'}| \\
 &+ \left. \left(\mathcal{V}_{\kappa\kappa''}^{(1)} \mathcal{V}_{\kappa'\kappa''}^{(1)*} \|\widehat{1}_{\kappa}\rangle\rangle^+ \|\widehat{1}_{\kappa''}\rangle\rangle^- \langle\langle\widehat{1}_{\kappa''}| + \langle\langle\widehat{1}_{\kappa'}| + \sum_{\substack{q<0 \\ q\neq\kappa''}} \mathcal{V}_{\kappa q}^{(1)} \mathcal{V}_{\kappa'q}^{(1)*} \|\widehat{1}_{\kappa}\rangle\rangle^+ \|\widehat{1}_{\kappa'}\rangle\rangle^+ \langle\langle\widehat{1}_{\kappa'}| + \text{H. c.} \right) \right] + O(h^3).
 \end{aligned} \tag{6.64}$$

At this stage an impasse is reached. As we have argued in Section 3.2.5, three fermionic modes cannot in general be consistently mapped to three qubits without changing the entanglement properties. However, the specific structure of the Bogoliubov transformations at hand removes some of the otherwise possible elements in the state of Eq. (6.64) as compared to Eq. (3.58). As it happens, this difference is already enough to allow us to write down a consistent three-qubit density matrix representation of (6.64) keeping only terms up to order h^2 , i.e.,

$$\left(\begin{array}{ccccccc}
 1 - 2h^2(\bar{f}_{\kappa\rightarrow\kappa''}^A + \bar{f}_{\kappa'\rightarrow\kappa''}^A + f_{\kappa''}^A) & 0 & 0 & h\mathcal{V}_{\kappa'\kappa''}^{(1)*} & 0 & h\mathcal{V}_{\kappa\kappa''}^{(1)*} & 0 & 0 \\
 0 & 2h^2\bar{f}_{\kappa''\rightarrow\kappa,\kappa'}^A & 0 & 0 & 0 & 0 & 0 & 0 \\
 0 & 0 & 2h^2\bar{f}_{\kappa'\rightarrow\kappa''}^A & 0 & h^2\sum_{\substack{q<0 \\ q\neq\kappa''}} \mathcal{V}_{\kappa q}^{(1)*} \mathcal{V}_{\kappa'q}^{(1)} & 0 & 0 & 0 \\
 h\mathcal{V}_{\kappa'\kappa''}^{(1)} & 0 & 0 & h^2|A_{\kappa'\kappa''}^{(1)}|^2 & 0 & h^2\mathcal{V}_{\kappa\kappa''}^{(1)*} \mathcal{V}_{\kappa'\kappa''}^{(1)} & 0 & 0 \\
 0 & 0 & h^2\sum_{\substack{q<0 \\ q\neq\kappa''}} \mathcal{V}_{\kappa q}^{(1)} \mathcal{V}_{\kappa'q}^{(1)*} & 0 & 2h^2\bar{f}_{\kappa\rightarrow\kappa''}^A & 0 & 0 & 0 \\
 h\mathcal{V}_{\kappa\kappa''}^{(1)} & 0 & 0 & h^2\mathcal{V}_{\kappa\kappa''}^{(1)} \mathcal{V}_{\kappa'\kappa''}^{(1)*} & 0 & h^2|A_{\kappa\kappa''}^{(1)}|^2 & 0 & 0 \\
 0 & 0 & 0 & 0 & 0 & 0 & 0 & 0 \\
 0 & 0 & 0 & 0 & 0 & 0 & 0 & 0
 \end{array} \right). \tag{6.65}$$

In other words, all reductions of the fermionic three-mode state (6.64) are equivalent to the corresponding partial traces of the three-qubit density matrix (6.65). This allows us to employ a witness inequality for GME. However, since we are dealing with fermions restricted by the Pauli exclusion principle the particular witness used in Eq. (6.62) will be of no use. Instead we use the techniques described in Ref. [112] to construct a witness. For convenience let us map the three-qubit witness for *genuine*

tripartite entanglement back to the three fermionic modes and write it as

$$\begin{aligned}
 & \left| \langle \langle \hat{0} \parallel \text{vac}_{\kappa\kappa'\kappa''} \parallel \hat{1}_{\kappa} \rangle \rangle^+ \parallel \hat{1}_{\kappa''} \rangle \rangle^- \right| + \left| \langle \langle \hat{0} \parallel \text{vac}_{\kappa\kappa'\kappa''} \parallel \hat{1}_{\kappa'} \rangle \rangle^+ \parallel \hat{1}_{\kappa''} \rangle \rangle^- \right| - \sqrt{\langle \langle \hat{0} \parallel \text{vac}_{\kappa\kappa'\kappa''} \parallel \hat{0} \rangle \rangle} \\
 & \times \sqrt{-\langle \langle \hat{1}_{\kappa''} \parallel \text{vac}_{\kappa\kappa'\kappa''} \parallel \hat{1}_{\kappa} \rangle \rangle^+ \parallel \hat{1}_{\kappa''} \rangle \rangle^- + \langle \langle \hat{1}_{\kappa''} \parallel \text{vac}_{\kappa\kappa'\kappa''} \parallel \hat{1}_{\kappa'} \rangle \rangle^+ \parallel \hat{1}_{\kappa''} \rangle \rangle^-} \\
 & - \sqrt{\langle \langle \hat{1}_{\kappa''} \parallel \text{vac}_{\kappa\kappa'\kappa''} \parallel \hat{1}_{\kappa''} \rangle \rangle^- + \langle \langle \hat{1}_{\kappa'} \parallel \text{vac}_{\kappa\kappa'\kappa''} \parallel \hat{1}_{\kappa'} \rangle \rangle^+} - \sqrt{-\langle \langle \hat{1}_{\kappa''} \parallel \text{vac}_{\kappa\kappa'\kappa''} \parallel \hat{1}_{\kappa''} \rangle \rangle^-} \\
 & \times \sqrt{\langle \langle \hat{1}_{\kappa} \parallel \text{vac}_{\kappa\kappa'\kappa''} \parallel \hat{1}_{\kappa} \rangle \rangle^+} \leq 0. \tag{6.66}
 \end{aligned}$$

As previously, the inequality is satisfied for all bi-separable pure states and its validity is extended to mixed states by the virtue of the convexity of the absolute value, see Eq. (1.25a), and the concavity of the square roots of the density matrix elements, see Eq. (1.25b). This means that a positive value for the right hand side of (6.66) unambiguously detects GME. We insert the perturbative expansion of the transformed vacuum state of Eq. (6.64) to reduce the witness inequality to

$$|A_{\kappa\kappa''}^{(1)}| + |A_{\kappa'\kappa''}^{(1)}| - \sqrt{|A_{\kappa\kappa''}^{(1)}|^2 + |A_{\kappa'\kappa''}^{(1)}|^2} + O(\hbar) \leq 0. \tag{6.67}$$

One can then use the triangle inequality to see that Eq. (6.67) can be violated whenever $A_{\kappa\kappa''}^{(1)}$ and $A_{\kappa'\kappa''}^{(1)}$ are both nonzero. Hence, we find that even though no mode can be occupied by more than one excitation it is nonetheless the combination of the coefficients that create bipartite entanglement between κ and κ'' , as well as κ' and κ'' , respectively, that are responsible for the generation of genuine tripartite entanglement from the fermionic vacuum.

We can thus conclude this chapter noting that both bipartite and genuine multipartite entanglement are created from a variety of initial states. The Bogoliubov transformations correlate modes depending on their relative parity and energy levels. Most importantly, entanglement can be created between specific modes by selecting appropriate travel scenarios, see Section 6.2.2, which may be used to verify the *quantumness* of the created radiation. In other words, the entanglement that is produced may serve as a clear indicator of the origin of the produced radiation being a quantum field theory effect.

The transformations induced by the motion of the cavity may further be interpreted as *quantum gates* — weak two-mode squeezing [42] or beam-splitting gates [47], or even as gates generating GME states [84, (vi)]. This, in turn, is of conceptual interest and can be considered to be a first step towards the possible future implementation of quantum information processing on the basis of relativistic motion, possibly complemented by alternative approaches [132].

All modes that are being traced over, e.g., which we do not have access to due to limited measurement possibilities, add to the mixedness of the reduced state since information about their correlations with the modes under scrutiny is lost. It is exactly this issue that leads to the entanglement degradation that will be discussed in the final Chapter 7.

Degradation of Entanglement between Moving Cavities

The previous chapters have analyzed the entanglement generation between the modes of quantum fields that are confined to non-uniformly moving cavities. We have argued that, indeed, the radiation produced due to the transitions between orbits of different Killing vector fields (see Section 4.1) is entangled for most initial states and chosen pairs of modes. Such effects may be of interest to identify effects of quantum field theory by distinguishing the produced particles from uncorrelated background noise, see, e.g., Refs. [201] and [43, (xi)]. In principle, the entanglement that is being produced is distillable and could be utilized for quantum information tasks. The transformations effectively act as weak entangling gates on pairs of modes [42, 84], but the perturbative approach limits the practical applications for this scheme of entanglement generation as a resource. However, as we shall see in this chapter, the motion of the cavities may influence quantum information processing tasks in a different way.

Let us now consider *two cavities*, controlled by the observers *Alice* and *Rob*, respectively, see Fig. 7.1. Alice and Rob wish to use entanglement between their cavities as a resource for quantum communication tasks, for instance, for quantum teleportation (see Sections 1.5.3, 7.1.3 and 7.2.2). For practical reasons the entanglement shared between the cavities will be restricted to certain finite sets of modes that are controlled by the observers. For the sake of the argument let us consider entanglement between one mode in each cavity only. The entanglement generation inside individual cavities then entangles the selected modes with all other modes in the respective spectra. Since Alice and Rob do not have access to the entire spectrum of their cavities, information is lost and the resource entanglement between their initial modes is *degraded*. This process may be interpreted as decoherence, and is indeed a consequence of the monogamy of entanglement (see page 19).

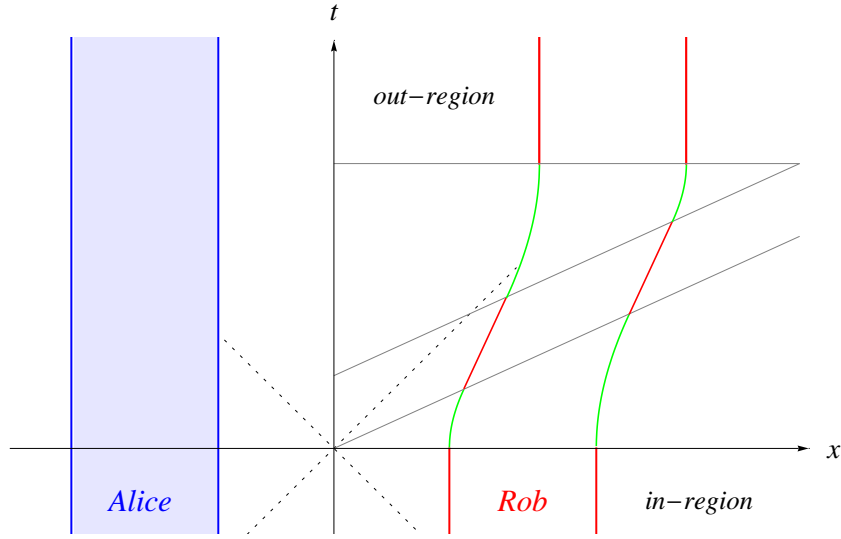


Figure 7.1: Quantum communication between two cavities: Alice and Rob each control a cavity containing a quantum field. They share an initially entangled state between one mode in each cavity to be used in a quantum communication task, e.g., quantum teleportation. Rob’s cavity is undergoing non-uniform motion, which entangles all modes in the spectrum of his cavity. Consequently the entanglement shared between Alice and Rob is degraded by the motion.

In the following we shall make this phenomenological description more precise. In Section 7.1 we analyze the entanglement degradation between two types of entangled initial states for the scalar field — *Bell-states* (based on results presented in Ref. [44]) and *two-mode squeezed states* (based on Ref. [89, (ix)]), accompanied by an application to the continuous variable *teleportation protocol* in Section 7.1.3. We finalize the investigation of the bosonic case with a brief look at a *simulation in superconducting circuits* in Section 7.1.4. At last we perform the corresponding analysis for the Dirac field as investigated in Ref. [87, (iv)], including effects on teleportation and Bell inequality violation, in Section 7.2.

7.1 Entanglement between Two Bosonic Cavities

7.1.1 Bosonic Bell States

For the scalar field we start with the *Bell states* ϕ^+ and ϕ^- from Eq. (1.13a) between two selected modes, k in Alice’s cavity and k' in Rob’s cavity, i.e.,

$$|\phi^\pm\rangle_{AR} = \frac{1}{\sqrt{2}} \left(|0\rangle_A \otimes |0\rangle_R \pm |1_k\rangle_A \otimes |1_{k'}\rangle_R \right), \quad (7.1)$$

where we have written the tensor product explicitly to point out that particles in the two cavities are now distinguishable by their association to either Alice's or Rob's cavity. The corresponding in-region density operator is then given by

$$\rho_{AR}^{\pm} = \frac{1}{2} \left(|0\rangle\langle 0| \otimes |0\rangle\langle 0| \pm |0\rangle\langle 0| \otimes |1_{k'}\rangle\langle 1_{k'}| \pm |1_k\rangle\langle 0| \otimes |1_{k'}\rangle\langle 0| + |1_k\rangle\langle 1_k| \otimes |1_{k'}\rangle\langle 1_{k'}| \right), \quad (7.2)$$

and we have dropped the label for Alice's and Rob's cavity and assume that the position in the tensor product is sufficient for this distinction. Rob now undergoes non-uniform motion as described in Chapter 4, which means that we have to transform the right hand sides of the tensor products in Eq. (7.2) to the out-region. The expressions for the transformed versions of the projectors $|0\rangle\langle 0|$ and $|1_{k'}\rangle\langle 1_{k'}|$ were already obtained in Chapter 5 and are given by Eq. (5.17) and, with appropriate relabelling, by Eq. (5.20). For the off-diagonal matrix element $|0\rangle\langle 1_{k'}|$ we combine Eq. (5.16) with the Hermitean conjugate of Eq. (5.19) with the relabelling $k \rightarrow k'$. Subsequently we trace over all of Rob's modes except k' and we obtain the transformed matrix element

$$\begin{aligned} \text{Tr}_{-k'}(|0\rangle\langle 1_{k'}|) &= G_{k'}^{(0)} |\widehat{0}\rangle\langle \widehat{1}_{k'}| + h^2 G_{k'}^{(0)} \left[(G_{k'}^{(0)*} \alpha_{k'k'}^{(2)} - 4f_{k'}^{\beta}) |\widehat{0}\rangle\langle \widehat{1}_{k'}| - g_{k'k'}^{\alpha\beta} |\widehat{1}_{k'}\rangle\langle \widehat{0}| \right. \\ &\quad \left. + 2\sqrt{2} f_{k'}^{\beta} |\widehat{1}_{k'}\rangle\langle \widehat{2}_{k'}| + \sqrt{2} V_{k'k'}^{(2)} |\widehat{2}_{k'}\rangle\langle \widehat{1}_{k'}| + \sqrt{\frac{3}{2}} V_{k'k'}^{(2)*} |\widehat{0}\rangle\langle \widehat{3}_{k'}| \right] + O(h^3), \end{aligned} \quad (7.3)$$

where we have used the abbreviations $g_{k'k'}^{\alpha\beta}$ and $f_{k'}^{\beta}$ from Eqs. (6.25) and Eq. (6.2), respectively, and $V_{k'k'}^{(2)}$ is given by Eq. (5.8c). The partial traces of the transformed diagonal elements $|0\rangle\langle 0|$ and $|1_{k'}\rangle\langle 1_{k'}|$ are most easily obtained from Eq. (6.1) and, again with appropriate relabelling, from Eq. (6.18), respectively. We obtain

$$\begin{aligned} \text{Tr}_{-k'}(|0\rangle\langle 0|) &= |\widehat{0}\rangle\langle \widehat{0}| + h^2 \left[-2f_{k'}^{\beta} |\widehat{0}\rangle\langle \widehat{0}| + 2f_{k'}^{\beta} |\widehat{1}_{k'}\rangle\langle \widehat{1}_{k'}| \right. \\ &\quad \left. + \frac{1}{\sqrt{2}} \left(V_{k'k'}^{(2)*} |\widehat{0}\rangle\langle \widehat{2}_{k'}| + \text{H. c.} \right) \right] + O(h^3), \end{aligned} \quad (7.4a)$$

$$\begin{aligned} \text{Tr}_{-k'}(|1_{k'}\rangle\langle 1_{k'}|) &= |\widehat{1}_{k'}\rangle\langle \widehat{1}_{k'}| + h^2 \left[2f_{k'}^{\alpha} |\widehat{0}\rangle\langle \widehat{0}| - 2(f_{k'}^{\alpha} + 2f_{k'}^{\beta}) |\widehat{1}_{k'}\rangle\langle \widehat{1}_{k'}| \right. \\ &\quad \left. + 4f_{k'}^{\beta} |\widehat{2}_{k'}\rangle\langle \widehat{2}_{k'}| - \left(\sqrt{2}(G_{k'}^{(0)})^2 g_{k'k'}^{\alpha\beta*} |\widehat{0}\rangle\langle \widehat{2}_{k'}| + \text{H. c.} \right) \right] + O(h^3), \end{aligned} \quad (7.4b)$$

where we have also used the shorthand $f_{k'}^{\alpha}$ from Eq. (6.19). Inserting Eqs. (7.3) and (7.4) into $\text{Tr}_{-k,k'}(\rho_{AR}^{\pm})$ we find that the perturbative expansion truncates the transformed state to a 2×4 dimensional system. Since we are now dealing with a mixed state we can quantify the entanglement of the transformed state via the *negativity* (see Definition 1.10). As can be easily seen from Eq. (7.2) the unperturbed partial transposition has three positive eigenvalues $\lambda_+ = \frac{1}{2}$ and one negative eigenvalue $\lambda_- = -\frac{1}{2}$, while all other eigenvalues vanish, regardless of the sign in $|\phi^{\pm}\rangle$ of Eq. (7.1). The subspace

of the vanishing unperturbed eigenvalues contains only one positive correction $4h^2 f_{k'}^\beta$. The positive unperturbed eigenvalues cannot be turned into negative eigenvalues by the small perturbative corrections. Hence, the only correction to the negativity stems from the leading order perturbation to the unperturbed, non-degenerate eigenvalue $\lambda_- = -\frac{1}{2}$. Following the prescription detailed on page 117 we quickly get the corrected value of the negativity as reported in Ref. [44]

$$\mathcal{N}(\rho_{AR}^\pm) = \mathcal{N}^{(0)} - h^2 \mathcal{N}^{(2)} + O(h^3) = \frac{1}{2} - h^2 (2f_{k'}^\beta + f_{k'}^\alpha) + O(h^3), \quad (7.5)$$

where we have used Eq. (4.78a). The entanglement is thus degraded by information loss due to the generation of particle pairs, where one constituent is created in Rob's mode k' , as well as information loss due to the possibility of shifting excitations from the mode k' to other energy levels in Rob's cavity. The coefficients $f_{k'}^\alpha$ and $f_{k'}^\beta$ that are degrading the entanglement are illustrated in Fig. 7.2 and Fig. 7.3, respectively.

7.1.2 Two-Mode Squeezed States

Although the Bell state that we have analyzed in Section 7.1.1 is a simple example for an entangled two-mode state, more general entangled states — *two-mode squeezed states* (see Section 3.1.3), with superpositions of various particle numbers are allowed. For convenience we shall switch again from the Fock space treatment to the *phase space* and work with the covariance matrix only. As we have explained in Section 3.1 the covariance matrix encodes all relevant information about the entanglement between modes of Gaussian states. Let us assume now that Alice and Rob are sharing a two-mode squeezed state between their modes k (Alice) and k' (Rob), represented by the covariance matrix $\Gamma_{\text{TMS}}(r)$ from Eq. (3.19) that is decomposed into 2×2 blocks, i.e.,

$$\Gamma_{\text{TMS}}(r) = \begin{pmatrix} \Gamma_k & C_{kk'} \\ C_{kk'}^T & \Gamma_{k'} \end{pmatrix}, \quad (7.6)$$

where $\Gamma_k = \Gamma_{k'} = \cosh(2r)\mathbb{1}_2$, $C_{kk'} = \sinh(2r)\sigma_3$, and σ_3 is the third Pauli matrix from Eq. (1.9). Now we employ the formalism of Section 3.1.2 to transform the covariance matrix to the out-region after Rob has undergone non-uniform motion. The 2×2 blocks of the out-region covariance matrix $\hat{\Gamma}_{\text{TMS}}(r)$ are given by $\hat{\Gamma}_k = \Gamma_k$,

$$\hat{\Gamma}_{k'} = \cosh(2r)\mathcal{M}_{k'k'}\mathcal{M}_{k'k'}^T + \sum_{n \neq k'} \mathcal{M}_{m'n}\mathcal{M}_{k'n}^T, \quad (7.7)$$

and $\hat{C}_{kk'} = C_{kk'}\mathcal{M}_{k'k'}^T$, where the matrices \mathcal{M}_{mn} are decomposed into the corresponding Bogoliubov coefficients according to Eq. (3.15). We then proceed with the perturbative expansion of these blocks by inserting the expansions from (4.76a) and (4.76b).

We find

$$\widehat{\Gamma}_{k'} = \widehat{\Gamma}_{k'}^{(0)} + h^2 \widehat{\Gamma}_{k'}^{(2)} + O(h^3), \quad (7.8a)$$

$$\widehat{C}_{kk'} = \widehat{C}_{kk'}^{(0)} + h^2 \widehat{C}_{kk'}^{(2)} + O(h^3), \quad (7.8b)$$

where the leading order is given by $\widehat{\Gamma}_{k'}^{(0)} = \Gamma_k$ and

$$\widehat{C}_{kk'}^{(0)} = \sinh(2r) \begin{pmatrix} \cos(\omega_{k'} \tilde{\tau}) & -\sin(\omega_{k'} \tilde{\tau}) \\ -\sin(\omega_{k'} \tilde{\tau}) & -\cos(\omega_{k'} \tilde{\tau}) \end{pmatrix}, \quad (7.9)$$

with $\omega_{k'}$ from Eq. (4.7) and $\tilde{\tau}$ is the proper time at the centre of the cavity (see Section 4.1). Note that we have not included the time evolution of the mode k in Alice's cavity here explicitly but this may be achieved by replacing $\omega_{k'} \tilde{\tau}$ by $(\omega_{k'} \tilde{\tau} + \omega_k \tilde{\tau}_A)$, where ω_k is the frequency of the mode k and $\tilde{\tau}_A$ is Alice's proper time. The coefficients of the corrections that are quadratic in h are

$$\begin{aligned} \widehat{\Gamma}_{k'}^{(2)} = & 2 \cosh(2r) \begin{pmatrix} f_{k'}^\beta - f_{k'}^\alpha - \operatorname{Re}(G_{k'}^{(0)} \beta_{k'k'}^{(2)}) & \operatorname{Im}(G_{k'}^{(0)} \beta_{k'k'}^{(2)}) \\ \operatorname{Im}(G_{k'}^{(0)} \beta_{k'k'}^{(2)}) & f_{k'}^\beta - f_{k'}^\alpha + \operatorname{Re}(G_{k'}^{(0)} \beta_{k'k'}^{(2)}) \end{pmatrix} \\ & + 2 \begin{pmatrix} f_{k'}^\alpha + f_{k'}^\beta + \operatorname{Re}[(G_{k'}^{(0)})^2 g_{k'k'}^{\alpha\beta*}] & -\operatorname{Im}[(G_{k'}^{(0)})^2 g_{k'k'}^{\alpha\beta*}] \\ -\operatorname{Im}[(G_{k'}^{(0)})^2 g_{k'k'}^{\alpha\beta*}] & f_{k'}^\alpha + f_{k'}^\beta - \operatorname{Re}[(G_{k'}^{(0)})^2 g_{k'k'}^{\alpha\beta*}] \end{pmatrix}, \end{aligned} \quad (7.10a)$$

$$\widehat{C}_{kk'}^{(2)} = \sinh(2r) \begin{pmatrix} \operatorname{Re}(\alpha_{k'k'}^{(2)} - \beta_{k'k'}^{(2)}) & -\operatorname{Im}(\alpha_{k'k'}^{(2)} - \beta_{k'k'}^{(2)}) \\ -\operatorname{Im}(\alpha_{k'k'}^{(2)} + \beta_{k'k'}^{(2)}) & -\operatorname{Re}(\alpha_{k'k'}^{(2)} + \beta_{k'k'}^{(2)}) \end{pmatrix}, \quad (7.10b)$$

where $f_{k'}^\alpha$ and $f_{k'}^\beta$ are given by Eqs. (6.19) and (6.2), respectively, while $g_{k'k'}^{\alpha\beta}$ is as in Eq. (6.25), and we have used the Bogoliubov identity of Eq. (4.78a). As expected from our deliberations in Chapter 6 the reduced state of the two modes k and k' is *mixed*, as can be seen from the determinant of $\widehat{\Gamma}_{\text{TMS}}(r)$ [see Eq. (6.37)], which is found to be

$$\det(\widehat{\Gamma}_{\text{TMS}}) = 1 + 4h^2 \left([\cosh(2r) + 1] f_{k'}^\beta + [\cosh(2r) - 1] f_{k'}^\alpha \right) + O(h^3). \quad (7.11)$$

The perturbative nature of the calculation demands that the corrections do not drastically change the state, in particular, the mixedness. From Eq. (7.11) it can be seen that this imposes the restriction $e^{2|r|} h^2 \ll 1$. Let us now proceed by evaluating the entanglement of the transformed state. Since the transformed state is a mixed Gaussian two-mode state, but it is not symmetric, we again employ the *negativity* (see Definition 1.10). More specifically, we use Eq. (3.22b), which means we have to determine the perturbative corrections to the *smallest symplectic eigenvalue* of the partial transpose. The eigenvalues of the unperturbed matrix $i\Omega \widetilde{T}_{k'} \widehat{\Gamma}_{\text{TMS}}^{(0)} \widetilde{T}_{k'}^*$ are found to be $\{\pm e^{2r}, \pm e^{-2r}\}$. When $\operatorname{sgn}(r) = \pm 1$ the smallest positive eigenvalue is given by $e^{\mp 2r}$. The corresponding eigenvectors are

$$|\widetilde{\nu}_-^{(0)}\rangle = \frac{1}{2} (\mp i G_{k'}^{(0)*}, \mp G_{k'}^{(0)*}, i, 1)^T. \quad (7.12)$$

Since the eigenvalues are non-degenerate and the leading order corrections to the covariance matrix are quadratic in h we expect an expansion of the form

$$\tilde{\nu}_- = \tilde{\nu}_-^{(0)} + h^2 \tilde{\nu}_-^{(2)} + O(h^3), \quad (7.13)$$

and we can compute the correction to the smallest symplectic eigenvalue of the partial transpose as the expectation value [89, (ix)]

$$\tilde{\nu}_-^{(2)} = \langle \tilde{\nu}_-^{(0)} | i\Omega \tilde{T}_{k'} \hat{\Gamma}_{\text{TMS}}^{(2)} \tilde{T}_{k'} | \tilde{\nu}_-^{(0)} \rangle = (1 - e^{-2|r|}) f_{k'}^\alpha + (1 + e^{-2|r|}) f_{k'}^\beta, \quad (7.14)$$

where we have again used the identity (4.78a) in the last step. The result depends on the value of the squeezing parameter r but its validity is limited by the perturbative approach. In particular the small corrections cannot remove the non-degeneracy of the symplectic eigenvalues of the partial transpose, such that $h^2 \ll \sinh(2|r|)$. With this in mind we finally obtain the corrected negativity

$$\begin{aligned} \mathcal{N}(\hat{\Gamma}_{\text{TMS}}) &= \mathcal{N}^{(0)} - h^2 \mathcal{N}^{(2)} + O(h^3) \\ &= \frac{1}{2}(e^{2|r|} - 1) - h^2 e^{2|r|} \left(\frac{1}{2}[e^{2|r|} - 1](f_{k'}^\beta + f_{k'}^\alpha) + f_{k'}^\beta \right) + O(h^3). \end{aligned} \quad (7.15)$$

Illustrations of the functions $f_{k'}^\alpha$ and $f_{k'}^\beta$ that are responsible for the entanglement degradation are shown in Fig. 7.2 and Fig. 7.3, respectively.

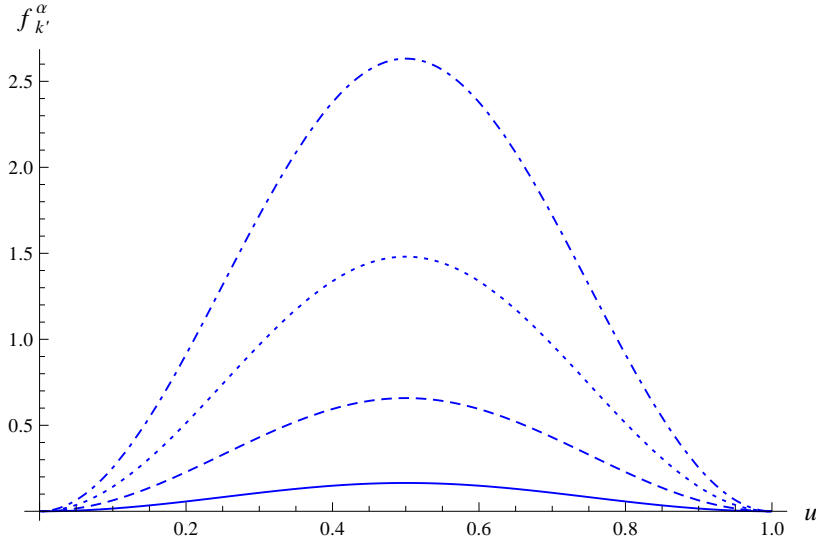


Figure 7.2: Entanglement degradation — $f_{k'}^\alpha$: The coefficient $f_{k'}^\alpha$ that is degrading the entanglement between Alice and Rob as quantified by the negativity [see Eq. (7.5) and Eq. (7.15)] is plotted for the basic building block travel scenario of Section 4.4.1 for a $(1 + 1)$ dimensional massless scalar field. The effects are periodic in the dimensionless parameter $u := h\tau/[4L \operatorname{artanh}(h/2)]$ [see Eq. (4.20)], where τ is the duration of the uniform acceleration, as measured at the centre of the cavity. Curves are shown for the modes $k' = 1$ (solid), $k' = 2$ (dashed), $k' = 3$ (dotted), and $k' = 4$ (dotted-dashed).

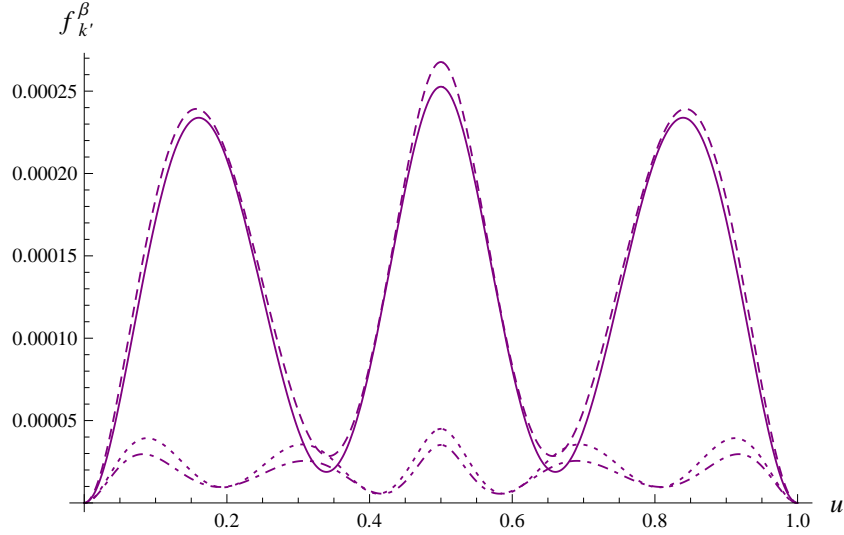


Figure 7.3: Entanglement degradation — $f_{k'}^\beta$: The coefficient $f_{k'}^\beta$ that is degrading the entanglement between Alice and Rob as quantified by the negativity [see Eq. (7.5) and Eq. (7.15)] is plotted for the basic building block travel scenario of Section 4.4.1 for a $(1 + 1)$ dimensional massless scalar field. The effects are periodic in the dimensionless parameter $u := h\tau/[4L \operatorname{artanh}(h/2)]$ [see Eq. (4.20)], where τ is the duration of the uniform acceleration, as measured at the centre of the cavity. Curves are shown for the modes $k' = 1$ (solid), $k' = 2$ (dashed), $k' = 3$ (dotted), and $k' = 4$ (dotted-dashed).

7.1.3 Fidelity of Teleportation

The entanglement between Alice’s mode k and Rob’s mode k' is degraded due to the non-uniform motion. For practical reasons we have used the negativity to quantify the loss of correlations even though this measure does not have a direct operational interpretation. Now we wish to place this result in the context of a practical application — the *teleportation* protocol (see pp. 49). We wish to analyze the influence of the entanglement degradation on the teleportation scheme that is illustrated in Fig. 7.4. The fidelity of the teleportation protocol for Gaussian states is given by Eq. (3.25) (see Ref. [131]). We insert the perturbative expansions of the transformed covariance matrix elements from Eqs. (7.8)-(7.10) into Eq. (3.25) to obtain the expression

$$\mathcal{F}(\widehat{\Gamma}_{\text{TMS}}) = \mathcal{F}^{(0)} - h^2 \mathcal{F}^{(2)} + O(h^3), \quad (7.16)$$

where the coefficients are found to be

$$\mathcal{F}^{(0)} = (1 + \cosh(2r) - \cos(\omega_{k'}\tilde{\tau} + \omega_k\tilde{\tau}_A) \sinh(2r))^{-1}, \quad (7.17a)$$

$$\mathcal{F}^{(2)} = (\mathcal{F}^{(0)})^2 (1 + e^{-2r}) [f_{k'}^\beta + f_{k'}^\alpha \tanh(2r)]. \quad (7.17b)$$

We have specifically included the time evolution of Alice’s mode in Eq. (7.17b) and one should note that the phases accumulated by both modes k and k' affect the un-

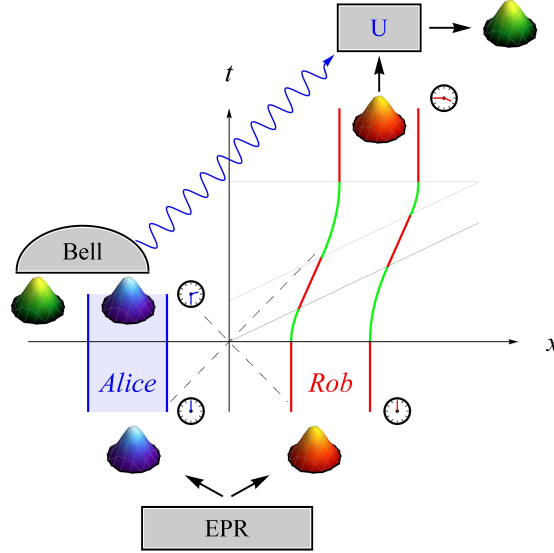


Figure 7.4: Quantum teleportation between two cavities: Alice and Rob wish to use the initially shared entanglement that is supplied by the EPR source to teleport an unknown coherent state. After the initial state has been prepared Alice performs a Bell measurement on the (unknown) state that is to be teleported and her mode k of the entangled resource state. Subsequently, she sends the measurement outcomes to Rob via a classical channel. Meanwhile, Rob undergoes a finite period of non-uniform motion, after which he receives the classical information necessary to retrieve the unknown input state by performing a local unitary U . By measuring their respective proper times and applying corresponding local rotations Alice and Rob can optimize their teleportation scheme.

-perturbed teleportation fidelity $\mathcal{F}^{(0)}$. However, the effect of the time evolution can be easily corrected — Alice and Rob can simply keep track of their respective proper times and apply local rotations to remove the phases. These operations can be performed independently by the two observers and they do not require any knowledge about the other's state of motion. Since these corrections can be implemented by local unitaries the amount of entanglement that is shared is not altered. Incidentally, the local rotations also remove the phase dependence from the correction term in Eq. (7.17b) and we arrive at the *optimal teleportation fidelity*

$$\mathcal{F}_{\text{opt}}(\widehat{\Gamma}_{\text{TMS}}) = \mathcal{F}^{(0)} - h^2 \mathcal{F}^{(2)} + O(h^3), \quad (7.18)$$

where the coefficients are given by [89, (ix)]

$$\mathcal{F}_{\text{opt}}^{(0)} = (1 + e^{-2r})^{-1}, \quad (7.19a)$$

$$\mathcal{F}_{\text{opt}}^{(2)} = \mathcal{F}_{\text{opt}}^{(0)} [f_{k'}^{\beta} + f_{k'}^{\alpha} \tanh(2r)]. \quad (7.19b)$$

Using Eq. (7.13) and (7.14) it can be immediately seen that the upper bound of (3.26) is achieved. The correction $\mathcal{F}_{\text{opt}}^{(2)}$ in Eq. (7.19b) thus isolates the degrading effect of Rob's non-uniform motion.

7.1.4 Simulations in Superconducting Circuits

With the practical application to the teleportation protocol in mind we now want to gain insight about the numerical values of the relative size of the perturbative corrections. So far we have considered the dimensionless expansion parameter h in units where the speed of light is set to unity, $c = 1$. Inserting the speed of light explicitly the perturbative parameter is

$$h := \frac{\mathbf{a}_c L}{c^2}, \quad (7.20)$$

where L is the length of the cavity and \mathbf{a}_c is the proper acceleration at its centre. Assuming that the cavity size is well below the length scale of one meter it becomes clear that the perturbative approach can easily accommodate accelerations of 10^{17}ms^{-2} . In other words, the accelerations must reach extremely large values to produce observable effects for arbitrary setups. However, selecting particular initial states and exploiting the effects of transverse momenta (see Eq. (5.12) and Fig. 4.5) the overall corrections may yet reach observable levels [47]. We shall explore a different route here by studying a setup that simulates the mechanical motion of the cavity walls.

Following Ref. [89, (ix)] we envisage a one-dimensional transmission line for electromagnetic radiation in the microwave domain that is terminated by two *superconducting quantum interference devices* (SQUIDs). Similar setups, e.g., with an open transmission line terminated by a single SQUID, have been extensively used to study the related *dynamical Casimir effect*, see, for instance, Refs. [116, 123, 201]. The role of the SQUID, which consists of a superconducting circuit with two parallel *Josephson junctions*, is to generate the boundary conditions for the electromagnetic field in the transmission line (see Ref. [116] for details). Each SQUID is threaded by a magnetic flux, which can be externally tuned at will, that determines the boundary condition. In particular, the parameters can be tuned to mimic perfectly reflecting mirrors whose distances to the SQUIDs depend on the chosen magnetic fluxes, see Fig. 7.5. Two such SQUIDs thus constitute a cavity for the electromagnetic radiation and the position of the “walls”, i.e., the boundary conditions, can be varied by adjusting the magnetic fluxes. Indeed, the cavity setup we propose has already been implemented in a laboratory, see Ref. [186].

To emulate the motion of a relativistically rigid cavity as described in Section 4.1 the fluxes of the two SQUIDs need to be changed in a particular fashion. Let us imagine an observer undergoing a chosen travel scenario (see Section 4.4 for examples). If the magnetic fluxes are selected such that the positions of the boundary conditions remain at a fixed distance L_{eff} with respect to this observer the effective cavity can be

thought of as rigid and undergoing the same travel scenario. From the point of view of the laboratory no piece of the equipment is in motion, and the magnetic fluxes are not changing symmetrically. The imaginary observer, on the other hand, would see the distance L_0 between the SQUIDs vary in time — the cavity would be contracting and expanding according to the relative velocity of the observer with respect to the laboratory. Finally, let us insert typical values for the parameters to estimate the relative

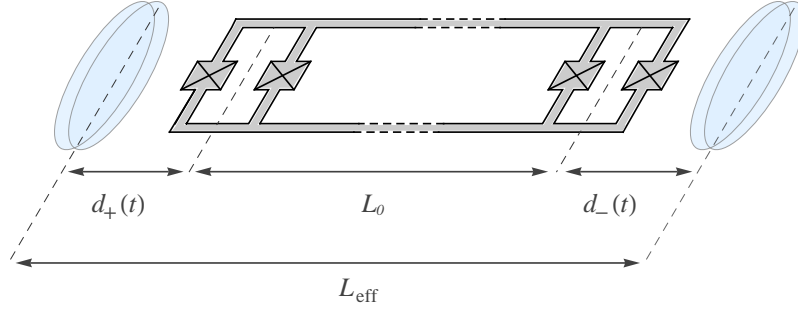


Figure 7.5: Superconducting cavity simulation: A one-dimensional transmission line for microwave radiation is interrupted by two SQUIDs at a distance L_0 with respect to each other. The SQUIDs are threaded by time-dependent magnetic fluxes that create boundary conditions — effective mirrors — at distances $d_{\pm}(t)$ away from the SQUIDs. This creates a cavity of effective length L_{eff} that can simulate non-uniform motion by changing the fluxes in time such that the length $L_{\text{eff}} = d_+ + L_0 + d_- = \text{const.}$, as measured by a potentially co-moving observer, remains constant.

correction. We consider a cavity of length $L = 1.2\text{cm}$ that is undergoing accelerations of up to $\mathbf{a}_c = 3 \times 10^{17}\text{ms}^{-2}$, while the effective speed of light in the transmission line is around $1.2 \times 10^8\text{ms}^{-1}$, similar to the setting in Ref. [201]. This combines to an estimate of $h^2 \approx 0.06$ for the expansion parameter. As a resource we select a two-mode squeezed state with squeezing parameter $r = \frac{1}{2}$, which is well within the limits of current technology [72, 78, 138]. For the mode $k' = 3$, corresponding to an (angular) frequency of $2\pi \times 15\text{GHz}$, the approximate value of the function $f_{k'}^\alpha$ is 1.5, while the contribution from $f_{k'}^\beta$ can be neglected, see Fig. 7.3. Hence, the relative correction to the optimal teleportation fidelity of Eq. (7.18) is given by

$$\frac{h^2 |\mathcal{F}_{\text{opt}}^{(2)}|}{\mathcal{F}_{\text{opt}}^{(0)}} = h^2 [f_{k'}^\beta + f_{k'}^\alpha \tanh(2r)] \approx 0.04, \quad (7.21)$$

that is, a 4% relative correction, which is both reasonably small to fit the perturbative regime, but also large enough to be detected in possible future experiments. We thus conclude that the experimental verification or simulation of the effects of non-uniform motion on entanglement can in principle be achieved in current laboratories.

7.2 Entanglement between Two Fermionic Cavities

To complete our analysis, let us consider the fermionic counterpart of the situation studied in Section 7.1. We copy the previous scenario, i.e., an entangled state shared between Alice's and Rob's cavity and we let Rob undergo non-uniform motion, see Fig. 7.1. However, this time Dirac fields are confined to the cavities in question. In Section 7.2.1 we consider the entanglement degradation of an initially maximally entangled state as reported in Ref. [87, (iv)], before we briefly analyze the consequences for practical applications, *Bell inequalities* and *teleportation*, in Section 7.2.2.

7.2.1 Fermionic Bell States

For the Dirac field we can consider a maximally entangled *Bell state* [see Eqs. (1.13)] between Alice's mode κ and Rob's mode κ' , given by

$$\|\phi^\pm\rangle_{AR} = \frac{1}{\sqrt{2}} \left(\|0\rangle_A \otimes \|0\rangle_R \pm \|1_\kappa\rangle_A \otimes \|1_{\kappa'}\rangle_R^+ \right), \quad (7.22)$$

where we have assumed that $\kappa' \geq 0$ is a positive frequency mode, while the frequency of the mode κ is inconsequential for our present analysis and we therefore have not specifically indicated it in Eq. (7.22). Since the positive and negative frequency modes appear symmetrically in the spectrum we can be content to study the case of $\kappa' \geq 0$, but the interested reader may find the expressions for the case $\kappa' < 0$ in Ref. [87, (iv)]. Assuming that the fermions can be distinguished by their appearance in either Alice's or Rob's cavity we can assume a tensor product between the Fock spaces of different cavities. The density operator that corresponds to the state in Eq. (7.22) is given by

$$\begin{aligned} \varrho_{AR}^\pm = \frac{1}{2} & \left(\|0\rangle\langle 0\| \otimes \|0\rangle\langle 0\| \pm \|0\rangle\langle 1_\kappa\| \otimes \|0\rangle\langle 1_{\kappa'}\|^+ \right. \\ & \left. \pm \|1_\kappa\rangle\langle 0\| \otimes \|1_{\kappa'}\rangle\langle 0\|^+ + \|1_\kappa\rangle\langle 1_\kappa\| \otimes \|1_{\kappa'}\rangle\langle 1_{\kappa'}\|^+ \right), \end{aligned} \quad (7.23)$$

where we have dropped the labels for Alice and Rob. Subsequently, we transform the matrix elements on the right hand side of the tensor product to the out-region to take into account Rob's motion. The corresponding transformed versions of $\|0\rangle$ and $\|1_{\kappa'}\rangle$ are given by (5.45) and, with appropriate relabelling (5.50), respectively. We then trace out all modes except κ and κ' from the relevant matrix elements, i.e.,

$$\text{Tr}_{-\kappa'} \left(\|0\rangle\langle 0\| \right) = (1 - 2h^2 \bar{f}_{\kappa'}^A) \|\hat{0}\rangle\langle \hat{0}\| + 2h^2 \bar{f}_{\kappa'}^A \|\hat{1}_{\kappa'}\rangle\langle \hat{1}_{\kappa'}\|^+ + O(h^3), \quad (7.24a)$$

$$\text{Tr}_{-\kappa'} \left(\|1_{\kappa'}\rangle\langle 1_{\kappa'}\|^+ \right) = (1 - 2h^2 f_{\kappa'}^A) \|\hat{1}_{\kappa'}\rangle\langle \hat{1}_{\kappa'}\|^+ + 2h^2 f_{\kappa'}^A \|\hat{0}\rangle\langle \hat{0}\| + O(h^3), \quad (7.24b)$$

$$\text{Tr}_{-\kappa'} \left(\|0\rangle\langle 1_{\kappa'}\|^+ \right) = G_{\kappa'}^{(0)} \|0\rangle\langle \hat{1}_{\kappa'}\|^+ + h^2 A_{\kappa'}^{(2)} \|0\rangle\langle \hat{1}_{\kappa'}\|^+ + O(h^3), \quad (7.24c)$$

where the functions $f_{\kappa'}^A$ and $\bar{f}_{\kappa'}^A$ are as in Eq. (6.49). For the situation we are dealing with here the two fermionic modes can be mapped to two qubits without problems (see Section 3.2). We represent the transformed state of the modes κ and κ' by the two-qubit density matrix

$$\begin{pmatrix} \frac{1}{2} - h^2 \bar{f}_{\kappa'}^A & 0 & 0 & \pm \frac{1}{2} G_{\kappa'}^{(0)} \pm \frac{1}{2} h^2 A_{\kappa'\kappa'}^{(2)} \\ 0 & h^2 \bar{f}_{\kappa'}^A & 0 & 0 \\ 0 & 0 & h^2 f_{\kappa'}^A & 0 \\ \pm \frac{1}{2} G_{\kappa'}^{(0)*} \pm \frac{1}{2} h^2 A_{\kappa'\kappa'}^{(2)*} & 0 & 0 & \frac{1}{2} - h^2 f_{\kappa'}^A \end{pmatrix}, \quad (7.25)$$

where we have neglected terms of $O(h^3)$. Next, we can compute the *negativity* for this state. The partial transposition shifts the off-diagonals towards the centre along the anti-diagonal and for the unperturbed state one immediately finds three positive eigenvalues $\lambda_+^{(0)} = \frac{1}{2}$ and one negative eigenvalue $\lambda_-^{(0)} = -\frac{1}{2}$. Since there are no corrections linear in h we can find the leading order correction to the negative eigenvalue as the expectation value of the perturbations of ϱ_{AR}^\pm in the eigenvector $|\lambda_-^{(0)}\rangle$ corresponding to the negative unperturbed eigenvalue. That eigenvector is given by

$$|\lambda_-^{(0)}\rangle = \frac{1}{\sqrt{2}}(0, 1, \mp G_{\kappa'}^{(0)}, 0)^T, \quad (7.26)$$

and, using the Bogoliubov identity (4.78c), we find the negativity

$$\mathcal{N}(\varrho_{AR}^\pm) = \mathcal{N}^{(0)} - h^2 \mathcal{N}^{(2)} + O(h^3) = \frac{1}{2} - h^2(f_{\kappa'}^A + \bar{f}_{\kappa'}^A) + O(h^3). \quad (7.27)$$

The quantities $f_{\kappa'}^A$ and $\bar{f}_{\kappa'}^A$ are illustrated in Fig. 7.6.

Perturbative Expressions for the Concurrence

With the results of the previous sections at hand it is not surprising that the entanglement in Eq. (7.27) is degraded due to Rob's motion. Nonetheless, we also wish to supply a quantitative description of the entanglement loss that relates to practical applications. One such measure is the *entanglement of formation*, which, for two qubits, is fully determined by the *concurrence*, see Eq. (1.17). However, as we have hinted at in Section 6.3.1, computing the concurrence in a perturbative approach proves to be somewhat impractical, as we shall demonstrate here. For the calculation we need to determine the eigenvalues of the matrix $\varrho_{AR}^\pm(\sigma_2 \otimes \sigma_2)\varrho_{AR}^{\pm*}(\sigma_2 \otimes \sigma_2)$, where σ_2 is the second Pauli matrix from Eq. (1.9) and ϱ_{AR}^\pm is taken from (7.25), which, to second order in h , can be written as

$$\begin{pmatrix} \frac{1}{2} - h^2(f_{\kappa'}^A + \bar{f}_{\kappa'}^A) & 0 & 0 & \pm \frac{1}{2} G_{\kappa'}^{(0)} \pm h^2(\frac{1}{2} A_{\kappa'\kappa'}^{(2)} - G_{\kappa'}^{(0)} \bar{f}_{\kappa'}^A) \\ 0 & 0 & 0 & 0 \\ 0 & 0 & 0 & 0 \\ \pm \frac{1}{2} G_{\kappa'}^{(0)*} \pm h^2(\frac{1}{2} A_{\kappa'\kappa'}^{(2)*} - G_{\kappa'}^{(0)*} f_{\kappa'}^A) & 0 & 0 & \frac{1}{2} - h^2(f_{\kappa'}^A + \bar{f}_{\kappa'}^A) \end{pmatrix}. \quad (7.28)$$

The unperturbed matrix has the eigenvalues $\lambda_1^{(0)} = 1$ and $\lambda_{2,3,4}^{(0)} = 0$. Applying the techniques described on pp. 117 to determine the corrections to these eigenvalues, and with the help of Eq. (4.78c) we find that none of the degenerate eigenvalues are perturbed when terms proportional to h^2 are included. The non-degenerate eigenvalue, on the other hand, is corrected such that

$$\lambda_1 = \lambda_1^{(0)} + h^2 \lambda_1^{(2)} + O(h^3) = 1 - 2h^2 (f_{\kappa'}^A + \bar{f}_{\kappa'}^A) + O(h^3). \quad (7.29)$$

When we now wish to evaluate the concurrence from Eq. (1.17) we have to take the square roots of the perturbed eigenvalues and we encounter an issue. The expansion $\sqrt{\lambda_1} = 1 - h^2 (f_{\kappa'}^A + \bar{f}_{\kappa'}^A) + O(h^3)$ is easily determined, but all other square roots vanish to leading order. However, without further computations we cannot exclude the possibility that the eigenvalues $\lambda_{2,3,4}$ receive fourth order corrections when terms proportional to h^4 are kept throughout the calculation. These corrections could contribute to the second order corrections of the concurrence. The present calculation thus only allows us to specify an *upper bound* on the degraded concurrence. But, with the aid of the inequality (1.23) and the negativity from Eq. (7.27) we can supply also a *lower bound*, such that the perturbed concurrence is bounded by

$$1 - 2h^2 (f_{\kappa'}^A + \bar{f}_{\kappa'}^A) \leq C(\varrho_{AR}^\pm) + O(h^3) \leq 1 - h^2 (f_{\kappa'}^A + \bar{f}_{\kappa'}^A). \quad (7.30)$$

7.2.2 Non-Locality & Fidelity of Teleportation

Since the perturbative evaluation of the concurrence proved to be rather intricate, let us turn to more accessible means of supplying an operational picture for the entanglement degradation in fermionic systems. In Sections 1.5.2 and 1.5.3 we have seen that the *correlation matrix* $t[\rho]$ (see Theorem 1.8 or Ref. [102]) of a two-qubit state can be used to determine the maximally possible violation of the *CHSH inequality* as well as the optimal *teleportation fidelity*. We thus determine the matrix $M_{\varrho_{AR}^\pm} = t[\varrho_{AR}^\pm]^T t[\varrho_{AR}^\pm]$ for the two-qubit density matrix in Eq. (7.25) and we obtain

$$\begin{pmatrix} 1 - 2h^2 (f_{\kappa'}^A + \bar{f}_{\kappa'}^A) & 0 & 0 \\ 0 & 1 - 2h^2 (f_{\kappa'}^A + \bar{f}_{\kappa'}^A) & 0 \\ 0 & 0 & 1 - 4h^2 (f_{\kappa'}^A + \bar{f}_{\kappa'}^A) \end{pmatrix} + O(h^3), \quad (7.31)$$

where we have again used Eq. (4.78c). Since the matrix is already diagonal we can straightforwardly find the maximally possible violation of the CHSH inequality from Theorem 1.8 as

$$\langle \mathcal{O}_{\text{CHSH}}^{\max} \rangle_{\varrho_{AR}^\pm} = 2\sqrt{2} (1 - h^2 [f_{\kappa'}^A + \bar{f}_{\kappa'}^A]) + O(h^3), \quad (7.32)$$

while the maximal teleportation fidelity, optimized over Rob's local rotations, is found to be

$$\mathcal{F}_{\max}(\varrho_{AR}^{\pm}) = 1 - \frac{2}{3} h^2 (f_{\kappa'}^A + \bar{f}_{\kappa'}^A) + O(h^3). \quad (7.33)$$

An illustration of the functions $f_{\kappa'}^A$ and $\bar{f}_{\kappa'}^A$ is shown in Fig. 7.6. The quantities of Eqs. (7.32) and (7.33) provide clear operational meaning for the entanglement degradation effects of the fermionic modes, and may hopefully allow for simulations of these effects in analogue materials, see, e.g., Refs. [31, 114, 208].

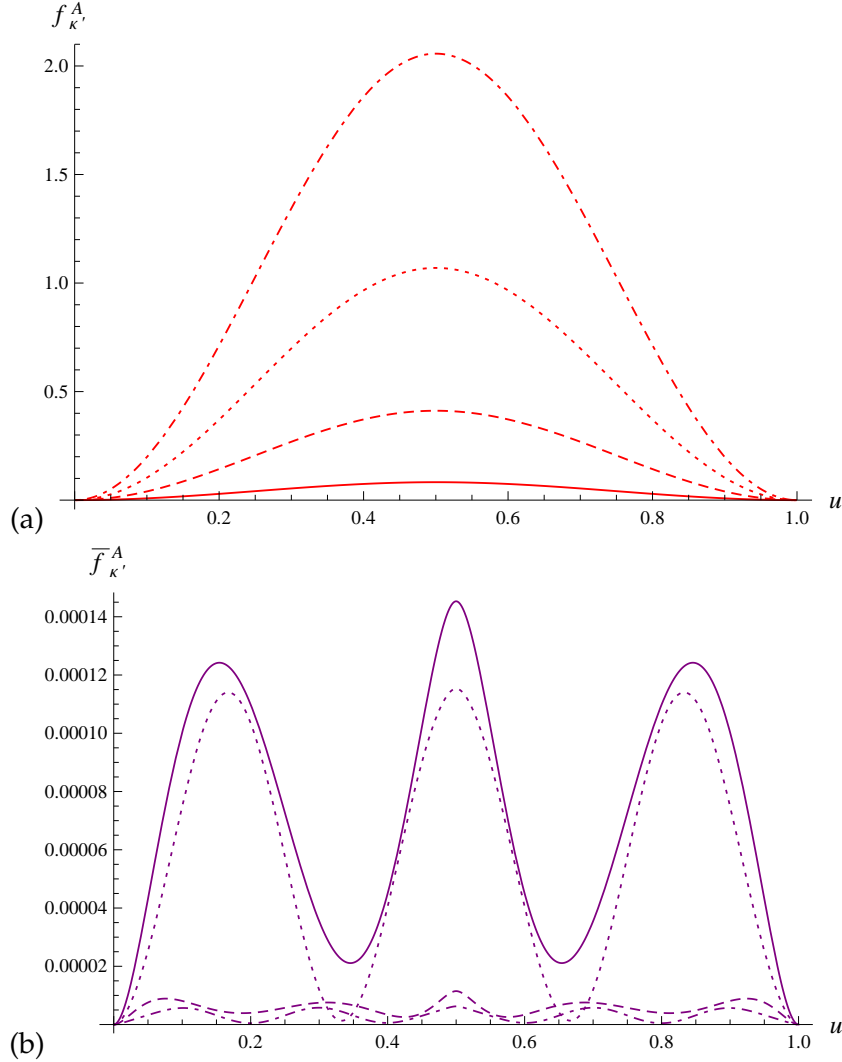


Figure 7.6: Entanglement degradation — $f_{\kappa'}^A$ and $\bar{f}_{\kappa'}^A$: The quantities $f_{\kappa'}^A$ and $\bar{f}_{\kappa'}^A$ that are degrading the entanglement between Alice and Rob [see Eqs. (7.27), (7.32) and (7.33)] are shown in Fig. 7.6 (a) and Fig. 7.6 (b), respectively, for the basic building block travel scenario of Section 4.4.1 for a $(1 + 1)$ dimensional massless Dirac field. The horizontal axis shows the dimensionless parameter $u := h\tau/[4L \operatorname{artanh}(h/2)]$ [see Eq. (4.20)], where τ is the duration of the uniform acceleration at the centre of the cavity. Curves are shown for the modes $\kappa' = 0$ (solid), $\kappa' = 1$ (dashed), $\kappa' = 2$ (dotted), and $\kappa' = 3$ (dotted-dashed).

Conclusions

In this thesis we have presented the model of *relativistically rigid cavities* in the context of relativistic quantum information (RQI), which was first introduced in Ref. [44]. We have discussed the geometric aspects of the rigid cavity in Minkowski spacetime and we have analyzed the confinement of bosonic scalar fields as well as fermionic Dirac fields to the cavity when it is undergoing non-uniform motion. The quantum fields can be massless or have non-zero mass and are confined to the cavity by boundary conditions that enforce that either the mode functions or the spatial probability current vanish at the cavity walls. The motion can consist of individual segments of inertial motion and uniform acceleration that are related by sharp transitions, or the proper acceleration can vary smoothly. For $(1 + 1)$ and $(2 + 1)$ dimensions both options can be implemented unitarily on the Fock spaces of the bosonic and fermionic field operators, respectively. However, in $(3 + 1)$ dimensions unitarity fails for non-smooth transitions [88, (x)].

The main focus of the analysis was aimed at the investigation of the role of the cavity as a system for the storage and manipulation of quantum information. We have shown how the Bogoliubov transformations that are induced by the non-uniform motion create entanglement between previously unentangled modes of the quantum fields inside the cavities. Quantum correlations are created for various initial states, including bosonic Fock states [82, (v)] and squeezed states [83, (vii)], as well as for different fermionic Fock states. Moreover, we have reviewed how the production of entanglement can be resonantly enhanced, see Refs. [42] and [43, (xi)] and even generate genuine multipartite entanglement [84, (vi)]. These entanglement generation effects may be of interest for the identification of the quantumness of particle creation phenomena similar to the *dynamical Casimir effect* via the specific signature of the created quantum correlations. This may allow to assign observed radiation unambiguously to the effects of non-uniform motion. Moreover, the entanglement generation is conceptually interesting since it suggests that the motion of the cavity may be interpreted as (weak)

quantum gates [42, 47]. Certainly, this opens avenues for further investigation around the central motive: “*Can quantum information processing tasks or quantum computation be performed by simply moving quantum systems in spacetime?*”

Finally, we have turned our attention to *entanglement degradation* effects when quantum communication tasks, for instance, *teleportation* between two different cavities, are considered. If the observers do not have access to all of the modes in the spectrum — typically only a finite number of modes can be addressed — the motion of the individual cavities degrades the initially shared entanglement. This is the case because the particle creation and shifting of excitations within one cavity entangles the modes in the spectrum with each other. Subsequently, some of the entangled modes are traced over, which leads to a loss of information that can be viewed as *decoherence*. We have studied such situations for cavities containing scalar fields [44] as well as Dirac fields [87, (iv)]. For the special case of Gaussian two-mode squeezed states of the bosonic fields we have investigated the effects on the *quantum teleportation* protocol [89, (ix)], and we have presented a setup where the mechanical motion of the cavity mirrors may be simulated in superconducting circuits.

The significance of this direction of our research lies in the basic need to establish assessments of the *robustness* of quantum communication procedures against the effects of relativistic motion. Our treatment has significantly advanced the previous toy models in RQI addressing such questions, taking them from the realm of thought experiments with global modes, and eternal uniform accelerations towards practical settings that may be emulated with current technology, see Refs. [116, 123, 186, 201] and [89, (ix)]. However, the analysis presented here covers only one specific type of quantum system used for the manipulation of quantum information, and it will hence be of interest for future investigations to study relativistic effects on other tools for quantum communication. In addition, a whole zoo of other relativistic effects, besides those described here, may emerge from further research in this direction.

We have also come across issues relating to the practical treatment of fermionic modes for the purpose of quantum information processing [86, (viii)]. Although computations can be carried out in a meaningful way for the situations we have considered here, we showed that this is not the case in general. Briefly summarized, *fermionic modes are not qubits*, which calls for a reevaluation of standard techniques in quantum information for fermionic modes. In particular, the quantification of fermionic mode entanglement remains an open question for theoretical research that might possibly also inspire experimental tests.

We conclude that the effects of the non-uniform motion, although small compared to common day-to-day experience, may be large enough for experimental observation in modern cutting-edge laboratories, for instance using superconducting technology that was recently employed for the confirmation of the dynamical Casimir effect [201]. The rapidly progressing technological advancement, e.g., in the control and manipulation of individual quantum systems [164], suggests that even previously negligible effects may become relevant in the near future. Quantum communication is already operating at length scales where relativity plays a role [49, 130, 168], and so it seems prudent to study relativistic effects on such tasks. Moreover, relativistic effects may provide novel ways to estimate kinematical parameters and spacetime properties [7, 67].

In combination, recently established, as well as well-known theoretical and experimental techniques, and yet-to-be-made discoveries in the overlap of relativity and quantum information science will form the core for the next generation of quantum technologies.

References

- [1] G. Adesso, *Entanglement of Gaussian states*, Ph.D. thesis, University of Salerno, 2007 [[arXiv:quant-ph/0702069](#)].
- [2] G. Adesso, I. Fuentes-Schuller, and M. Ericsson, *Continuous-variable entanglement sharing in noninertial frames*, *Phys. Rev. A* **76**, 062112 (2007) [[arXiv:quant-ph/0701074](#)].
- [3] G. Adesso and F. Illuminati, *Equivalence between Entanglement and the Optimal Fidelity of Continuous Variable Teleportation*, *Phys. Rev. Lett.* **95**, 150503 (2005) [[arXiv:quant-ph/0412125](#)].
- [4] G. Adesso and F. Illuminati, *Gaussian measures of entanglement versus negativities: Ordering of two-mode Gaussian states*, *Phys. Rev. A* **72**, 032334 (2005) [[arXiv:quant-ph/0506124](#)].
- [5] G. Adesso, A. Serafini, and F. Illuminati, *Extremal entanglement and mixedness in continuous variable systems*, *Phys. Rev. A* **70**, 022318 (2004) [[arXiv:quant-ph/0402124](#)].
- [6] G. Adesso, A. Serafini, and F. Illuminati, *Multipartite entanglement in three-mode Gaussian states of continuous-variable systems: Quantification, sharing structure, and decoherence*, *Phys. Rev. A* **73**, 032345 (2006) [[arXiv:quant-ph/0512124](#)].
- [7] M. Ahmadi, D. E. Bruschi, N. Friis, C. Sabín, G. Adesso, and I. Fuentes, *Relativistic Quantum Metrology: Exploiting relativity to improve quantum measurement technologies*, e-print [arXiv:1307.7082](#) [quant-ph] (2013).
- [8] D. Ahn, H. Lee, and S. W. Hwang, *Lorentz-covariant reduced-density-operator theory for relativistic-quantum-information processing*, *Phys. Rev. A* **67**, 032309 (2003) [[arXiv:quant-ph/0207053](#)].
- [9] D. Ahn, H. Lee, Y. H. Moon, and S. W. Hwang, *Relativistic entanglement and Bell's inequality*, *Phys. Rev. A* **67**, 012103 (2003) [[arXiv:quant-ph/0209164](#)].

-
- [10] P. M. Alsing and I. Fuentes, *Observer dependent entanglement*, *Class. Quantum Grav.* **29**, 224001 (2012), Focus Issue on ‘Relativistic Quantum Information’ [arXiv:1210.2223 [quant-ph]].
- [11] P. M. Alsing, I. Fuentes-Schuller, R. B. Mann, and T. E. Tessier, *Entanglement of Dirac fields in noninertial frames*, *Phys. Rev. A* **74**, 032326 (2006) [arXiv:quant-ph/0603269].
- [12] P. M. Alsing and G. J. Milburn, *On Entanglement and Lorentz Transformations*, *Quant. Inf. Comp.* **2**, 487 (2002) [arXiv:quant-ph/0203051].
- [13] P. M. Alsing, G. J. Stephenson Jr., and P. Kilian, *Spin-induced non-geodesic motion, gyroscopic precession, Wigner rotation and EPR correlations of massive spin 1/2 particles in a gravitational field*, e-print arXiv:0902.1396 [quant-ph] (2009).
- [14] D. T. Alves, E. R. Granhen, and W. P. Pires, *Quantum radiation reaction force on a one-dimensional cavity with two relativistic moving mirrors*, *Phys. Rev. D* **82**, 045028 (2010) [arXiv:0912.1802 [hep-th]].
- [15] M. A. Andreatta and V. V. Dodonov, *Dynamics of entanglement between field modes in a one-dimensional cavity with a vibrating boundary*, *J. Opt. B: Quant. Semiclass. Opt.* **7**, 11 (2005).
- [16] Arvind, B. Dutta, N. Mukunda, and R. Simon, *The real symplectic groups in quantum mechanics and optics*, *Pramana* **45**, 471 (1995) [arXiv:quant-ph/9509002].
- [17] M. Aspachs, G. Adesso, and I. Fuentes, *Optimal quantum estimation of the Unruh-Hawking effect*, *Phys. Rev. Lett.* **105**, 151301 (2010) [arXiv:1007.0389].
- [18] J. L. Ball, I. Fuentes-Schuller, and F. P. Schuller, *Entanglement in an expanding space-time*, *Phys. Lett. A* **359**, 550 (2006) [arXiv:quant-ph/0506113].
- [19] J. S. Bell, *On the Einstein Podolsky Rosen Paradox*, *Physics* **1**, 195 (1964).
- [20] M.-C. Bañuls, J. I. Cirac, and M. M. Wolf, *Entanglement in fermionic systems*, *Phys. Rev. A* **76**, 022311 (2007) [arXiv:0705.1103].
- [21] C. Barceló, S. Liberati, and M. Visser, *Analogue Gravity*, *Living Rev. Relativity* **8**, 12 (2005) [arXiv:gr-qc/0505065].
- [22] H. Bauke, S. Ahrens, C. H. Keitel, and R. Grobe, *What is the relativistic spin operator?* e-print arXiv:1303.3862 [quant-ph] (2013).

-
- [23] B. Belchev and M. A. Walton, *Robin boundary conditions and the Morse potential in quantum mechanics*, *J. Phys. A* **43**, 085301 (2010) [[arXiv:1002.2139](#) [quant-ph]].
- [24] F. Belgiorno, S. L. Cacciatori, M. Clerici, V. Gorini, G. Ortenzi, L. Rizzi, E. Rubino, V. G. Sala, and D. Faccio, *Hawking Radiation from Ultrashort Laser Pulse Filaments*, *Phys. Rev. Lett.* **105**, 203901 (2010) [[arXiv:1009.4634](#) [gr-qc]].
- [25] C. H. Bennett, G. Brassard, C. Crépeau, R. Jozsa, A. Peres, and W. K. Wootters, *Teleporting an unknown quantum state via dual classical and Einstein-Podolsky-Rosen channels*, *Phys. Rev. Lett.* **70**, 1895 (1993).
- [26] C. H. Bennett, D. P. Di Vincenzo, J. A. Smolin, and W. K. Wootters, *Mixed-state entanglement and quantum error correction*, *Phys. Rev. A* **54**, 3824 (1996) [[arXiv:quant-ph/9604024](#)].
- [27] R. A. Bertlmann and P. Krammer, *Geometric entanglement witnesses and bound entanglement*, *Phys. Rev. A* **77**, 024303 (2008) [[arXiv:0710.1184](#) [quant-ph]].
- [28] R. A. Bertlmann and P. Krammer, *Bloch vectors for qudits*, *J. Phys. A: Math. Theor.* **41**, 235303 (2008) [[arXiv:0806.1174](#) [quant-ph]].
- [29] R. A. Bertlmann, H. Narnhofer, and W. Thirring, *A Geometric Picture of Entanglement and Bell Inequalities*, *Phys. Rev. A* **66**, 032319 (2002) [[arXiv:quant-ph/0111116](#)].
- [30] N. D. Birrell and P. C. W. Davies, *Quantum Fields in Curved Space* (Cambridge University Press, Cambridge, England, 1982).
- [31] O. Boada, A. Celi, J. I. Latorre, and M. Lewenstein, *Dirac equation for cold atoms in artificial curved spacetimes*, *New J. Phys.* **13**, 035002 (2011) [[arXiv:1010.1716](#) [cond-mat.quant-gas]].
- [32] D. Bohm and Y. Aharonov, *Discussion of Experimental Proof for the Paradox of Einstein, Rosen, and Podolsky*, *Phys. Rev.* **108**, 1070 (1957).
- [33] N. Bohr, *Can quantum-mechanical description of physical reality be considered complete?* *Phys. Rev.* **48**, 696 (1935).
- [34] G. Bonneau, J. Faraut, and G. Valent, *Self-adjoint extensions of operators and the teaching of quantum mechanics*, *Am. J. Phys.* **69**, 322 (2001) [[arXiv:quant-ph/0103153](#)].
- [35] A. Botero and B. Reznik, *BCS-like Modewise Entanglement of Fermion Gaussian States*, *Phys. Lett. A* **331**, 39 (2004) [[arXiv:quant-ph/0404176](#)].

-
- [36] K. Brádler, *On two misconceptions in current relativistic quantum information*, e-print [arXiv:1108.5553](https://arxiv.org/abs/1108.5553) [quant-ph] (2011).
- [37] K. Brádler and R. Jáuregui, *Comment on "Fermionic entanglement ambiguity in non-inertial frames"*, *Phys. Rev. A* **85**, 016301 (2012) [[arXiv:1201.1045](https://arxiv.org/abs/1201.1045) [quant-ph]].
- [38] S. L. Braunstein, *Squeezing as an irreducible resource*, *Phys. Rev. A* **71**, 055801 (2005) [[arXiv:quant-ph/9904002](https://arxiv.org/abs/quant-ph/9904002)].
- [39] S. L. Braunstein and H. J. Kimble, *Teleportation of Continuous Quantum Variables*, *Phys. Rev. Lett.* **80**, 869 (1998).
- [40] E. G. Brown, E. Martín-Martínez, N. C. Menicucci, and R. B. Mann, *Detectors for probing relativistic quantum physics beyond perturbation theory*, *Phys. Rev. D* **87**, 084062 (2013) [[arXiv:1212.1973](https://arxiv.org/abs/1212.1973) [quant-ph]].
- [41] D. E. Bruschi, A. Dragan, I. Fuentes, and J. Louko, *Particle and anti-particle bosonic entanglement in non inertial frames*, *Phys. Rev. D* **86**, 025026 (2012) [[arXiv:1205.5296](https://arxiv.org/abs/1205.5296) [quant-ph]].
- [42] D. E. Bruschi, A. Dragan, A. R. Lee, I. Fuentes, and J. Louko, *Relativistic Motion Generates Quantum Gates and Entanglement Resonances*, *Phys. Rev. Lett.* **111**, 090504 (2013) [[arXiv:1201.0663](https://arxiv.org/abs/1201.0663) [quant-ph]].
- [43] D. E. Bruschi, N. Friis, I. Fuentes, and S. Weinfurter, *On the robustness of entanglement in analogue gravity systems*, *New J. Phys.* **15**, 113016 (2013) [[arXiv:1305.3867](https://arxiv.org/abs/1305.3867) [quant-ph]].
- [44] D. E. Bruschi, I. Fuentes, and J. Louko, *Voyage to Alpha Centauri: Entanglement degradation of cavity modes due to motion*, *Phys. Rev. D* **85**, 061701(R) (2012) [[arXiv:1105.1875](https://arxiv.org/abs/1105.1875) [quant-ph]].
- [45] D. E. Bruschi, A. R. Lee, and I. Fuentes, *Time evolution techniques for detectors in relativistic quantum information*, *J. Phys. A: Math. Theor.* **46**, 165303 (2013) [[arXiv:1212.2110](https://arxiv.org/abs/1212.2110) [quant-ph]].
- [46] D. E. Bruschi, J. Louko, and D. Faccio, *Entanglement generation in relativistic cavity motion*, *J. Phys.: Conf. Ser.* **442**, 012024 (2013) [[arXiv:1301.2988](https://arxiv.org/abs/1301.2988) [quant-ph]].
- [47] D. E. Bruschi, J. Louko, D. Faccio, and I. Fuentes, *Mode-mixing quantum gates and entanglement without particle creation in periodically accelerated cavities*, *New J. Phys.* **15**, 073052 (2013) [[arXiv:1210.6772](https://arxiv.org/abs/1210.6772) [quant-ph]].
-

-
- [48] D. E. Bruschi, J. Louko, E. Martín-Martínez, A. Dragan, and I. Fuentes, *Unruh effect in quantum information beyond the single-mode approximation*, *Phys. Rev. A* **82**, 042332 (2010) [[arXiv:1007.4670](#) [quant-ph]].
- [49] D. E. Bruschi, C. Sabín, A. White, V. Baccetti, D. K. L. Oi, and I. Fuentes, *Testing the effects of gravity and motion on quantum entanglement in space-based experiments*, e-print [arXiv:1306.1933](#) [quant-ph] (2013).
- [50] D. Bruß, *Characterizing Entanglement*, *J. Math. Phys.* **43**, 4237 (2002) [[arxiv:quant-ph/0110078](#)].
- [51] P. Caban, K. Podlaski, J. Rembieliński, K. A. Smoliński, and Z. Walczak, *Entanglement and tensor product decomposition for two fermions*, *J. Phys. A: Math. Gen.* **38**, L79 (2005).
- [52] P. Caban, J. Rembieliński, and M. Włodarczyk, *Spin observable for a Dirac particle*, *Annals of Physics* **330**, 263 (2013).
- [53] P. Caban, J. Rembieliński, and M. Włodarczyk, *Covariant Abstract Description for a Dirac Particle*, *Open Syst. Inf. Dyn.* **19**, 1250027 (2012) [[arXiv:1206.3074](#) [quant-ph]].
- [54] P. Caban, J. Rembieliński, and M. Włodarczyk, *Spin operator in the Dirac theory*, *Phys. Rev. A* **88**, 022119 (2013) [[arXiv:1308.4313](#) [quant-ph]].
- [55] E. Castro-Ruiz and E. Nahmad-Achar, *On the Relativistic Invariance of Entanglement*, *Rev. Mex. Fis. S* **57**, No. 3, 65 (2011).
- [56] E. Castro-Ruiz and E. Nahmad-Achar, *Entanglement properties of a system of two spin-1 particles under a Lorentz transformation*, *Phys. Rev. A* **86**, 052331 (2012) [[arXiv:1210.1889](#) [quant-ph]].
- [57] A. Chodos, R. L. Jaffe, K. Johnson, C. B. Thorn, and V. F. Weisskopf, *A new extended model of hadrons*, *Phys. Rev. D* **9**, 3471 (1974).
- [58] J. F. Clauser, M. A. Horne, A. Shimony, and R. A. Holt, *Proposed Experiment to Test Local Hidden-Variable Theories*, *Phys. Rev. Lett.* **23**, 880 (1969).
- [59] V. Coffman, J. Kundu, and W. K. Wootters, *Distributed entanglement*, *Phys. Rev. A* **61**, 052306 (2000).
- [60] M. Czachor, *Einstein-Podolsky-Rosen-Bohm experiment with relativistic massive particles*, *Phys. Rev. A* **55**, 72 (1997) [[arXiv:quant-ph/9609022](#)].
-

-
- [61] D. A. R. Dalvit and F. D. Mazzitelli, *Creation of photons in an oscillating cavity with two moving mirrors*, *Phys. Rev. A* **59**, 3049 (1999).
- [62] T. Debarba and R. O. Vianna, *Quantum state of a free spin- $\frac{1}{2}$ particle and the inextricable dependence of spin and momentum under Lorentz transformations*, *Int. J. Quant. Inf.* **10**, 1230003 (2012) [arXiv:1203.3147 [quant-ph]].
- [63] V. V. Dodonov, *Nonstationary Casimir Effect and analytical solutions for quantum fields in cavities with moving boundaries*, *Adv. Chem. Phys.* **119**, 309 (2001) [arXiv:quant-ph/0106081].
- [64] V. V. Dodonov, *Current status of the dynamical Casimir effect*, *Phys. Scr.* **82**, 038105 (2010) [arXiv:1004.3301 [quant-ph]].
- [65] V. V. Dodonov, A. B. Klimov, and V. I. Man'ko, *Generation of squeezed states in a resonator with a moving wall*, *Phys. Lett. A* **149**, 225 (1990).
- [66] T. G. Downes, I. Fuentes, and T. C. Ralph, *Entangling Moving Cavities in Noninertial Frames*, *Phys. Rev. Lett.* **106**, 210502 (2011) [arXiv:1007.4035 [quant-ph]].
- [67] T. G. Downes, G. J. Milburn, and C. M. Caves, *Optimal Quantum Estimation for Gravitation*, e-print arXiv:1108.5220 [gr-qc] (2012).
- [68] T. G. Downes, T. C. Ralph, and N. Walk, *Quantum communication with an accelerated partner*, *Phys. Rev. A* **87**, 012327 (2013) [arXiv:1203.2716 [quant-ph]].
- [69] A. Dragan, J. Doukas, and E. Martín-Martínez, *Localized detection of quantum entanglement through the event horizon*, *Phys. Rev. A* **87**, 052326 (2013) [arXiv:1207.4275 [quant-ph]].
- [70] T. M. Dunster, *Bessel functions of purely imaginary order, with an application to second-order linear differential equations having a large parameter*, *SIAM J. Math. Anal.* **21**, 995 (1990).
- [71] K. Eckert, J. Schliemann, D. Bruß, and M. Lewenstein, *Quantum Correlations in Systems of Indistinguishable Particles*, *Annals Phys.* **299**, 88 (2002) [arXiv:quant-ph/0203060].
- [72] C. Eichler, D. Bozyigit, C. Lang, M. Baur, L. Steffen, J. M. Fink, S. Filipp, and A. Wallraff, *Observation of Two-Mode Squeezing in the Microwave Frequency Domain*, *Phys. Rev. Lett.* **107**, 113601 (2011) [arXiv:1101.2136 [quant-ph]].
- [73] A. Einstein, B. Podolsky, and N. Rosen, *Can quantum-mechanical description of physical reality be considered complete?* *Phys. Rev.* **47**, 777 (1935).
-

-
- [74] E. Elizalde, M. Bordag, and K. Kirsten, *Casimir energy for a massive fermionic quantum field with a spherical boundary*, *J. Phys. A: Math. Gen.* **31**, 1743 (1998) [[arXiv:hep-th/9707083](#)].
- [75] A. Fabbri and J. Navarro-Salas, *Modeling Black Hole Evaporation* (Imperial College Press, London, 2005).
- [76] U. Fano, *Pairs of two-level systems*, *Rev. Mod. Phys.* **55**, 855 (1983).
- [77] A. Ferraro, S. Olivares, and M. G. A. Paris, *Gaussian states in continuous variable quantum information*, (Bibliopolis, Napoli, 2005) [[arXiv:quant-ph/0503237](#)].
- [78] E. Flurin, N. Roch, F. Mallet, M. H. Devoret, and B. Huard, *Generating Entangled Microwave Radiation Over Two Transmission Lines*, *Phys. Rev. Lett.* **109**, 183901 (2012) [[arXiv:1204.0732](#) [cond-mat.mes-hall]].
- [79] S. J. Freedman and J. F. Clauser, *Experimental Test of Local Hidden-Variable Theories*, *Phys. Rev. Lett.* **28**, 938 (1972).
- [80] N. Friis, *Relativistic Effects in Quantum Entanglement*, *Diploma thesis, University of Vienna, 2010* ([arXiv:1003.1874](#) [quant-ph]).
- [81] N. Friis, R. A. Bertlmann, M. Huber, and B. C. Hiesmayr, *Relativistic entanglement of two massive particles*, *Phys. Rev. A* **81**, 042114 (2010) [[arXiv:0912.4863](#) [quant-ph]].
- [82] N. Friis, D. E. Bruschi, J. Louko, and I. Fuentes, *Motion generates entanglement*, *Phys. Rev. D* **85**, 081701(R) (2012) [[arXiv:1201.0549](#) [quant-ph]].
- [83] N. Friis and I. Fuentes, *Entanglement generation in relativistic quantum fields*, *J. Mod. Opt.* **60**, 22 (2013) [[arXiv:1204.0617](#) [quant-ph]].
- [84] N. Friis, M. Huber, I. Fuentes, and D. E. Bruschi, *Quantum gates and multipartite entanglement resonances realized by non-uniform cavity motion*, *Phys. Rev. D* **86**, 105003 (2012) [[arXiv:1207.1827](#) [quant-ph]].
- [85] N. Friis, P. Köhler, E. Martín-Martínez, and R. A. Bertlmann, *Residual entanglement of accelerated fermions is not nonlocal*, *Phys. Rev. A* **84**, 062111 (2011) [[arXiv:1107.3235](#) [quant-ph]].
- [86] N. Friis, A. R. Lee, and D. E. Bruschi, *Fermionic mode entanglement in quantum information*, *Phys. Rev. A* **87**, 022338 (2013) [[arXiv:1211.7217](#) [quant-ph]].
- [87] N. Friis, A. R. Lee, D. E. Bruschi, and J. Louko, *Kinematic entanglement degradation of fermionic cavity modes*, *Phys. Rev. D* **85**, 025012 (2012) [[arXiv:1110.6756](#) [quant-ph]].
-

-
- [88] N. Friis, A. R. Lee, and J. Louko, *Scalar, spinor, and photon fields under relativistic cavity motion*, *Phys. Rev. D* **88**, 064028 (2013) [arXiv:1307.1631 [quant-ph]].
- [89] N. Friis, A. R. Lee, K. Truong, C. Sabín, E. Solano, G. Johansson, and I. Fuentes, *Relativistic Quantum Teleportation with Superconducting Circuits*, *Phys. Rev. Lett.* **110**, 113602 (2013) [arXiv:1211.5563 [quant-ph]].
- [90] I. Fuentes, R. B. Mann, E. Martín-Martínez, and S. Moradi, *Entanglement of Dirac fields in an expanding spacetime*, *Phys. Rev. D* **82**, 045030 (2010) [arXiv:1007.1569 [quant-ph]].
- [91] I. Fuentes-Schuller and R. B. Mann, *Alice Falls into a Black Hole: Entanglement in Noninertial Frames*, *Phys. Rev. Lett.* **95**, 120404 (2005) [arXiv:quant-ph/0410172].
- [92] A. Gabriel, B. C. Hiesmayr, and M. Huber, *Criterion for k -separability in mixed multipartite systems*, *Quant. Inf. Comp.* **10**, 0829 (2010) [arXiv:1002.2953 [quant-ph]].
- [93] J. C. Garrison and R. Y. Chiao, *Quantum Optics* (Oxford University Press, Oxford, England, 2008).
- [94] G. C. Ghirardi and L. Marinatto, *General criterion for the entanglement of two indistinguishable particles*, *Phys. Rev. A* **70**, 012109 (2004) [arXiv:quant-ph/0401065].
- [95] G. Giedke, M. M. Wolf, O. Krüger, R. F. Werner, and J. I. Cirac, *Entanglement of Formation for Symmetric Gaussian States*, *Phys. Rev. Lett.* **91**, 107901 (2003) [arXiv:quant-ph/0304042].
- [96] R. M. Gingrich and C. Adami, *Quantum Entanglement of Moving Bodies*, *Phys. Rev. Lett.* **89**, 270402 (2002) [arXiv:quant-ph/0205179].
- [97] N. Gisin, *Bell's inequality holds for all non-product states*, *Phys. Lett. A* **154**, 201 (1991).
- [98] O. Gühne and G. Tóth, *Entanglement detection*, *Phys. Rep.* **474**, 1 (2009) [arXiv:0811.2803 [quant-ph]].
- [99] L. Heaney and V. Vedral, *Natural Mode Entanglement as a Resource for Quantum Communication*, *Phys. Rev. Lett.* **103**, 200502 (2009) [arXiv:0907.5404 [quant-ph]].
- [100] T. Hiroshima, G. Adesso, and F. Illuminati, *Monogamy Inequality for Distributed Gaussian Entanglement*, *Phys. Rev. Lett.* **98**, 050503 (2007) [arXiv:quant-ph/0605021].
- [101] R. Honegger and A. Rieckers, *Squeezing Bogoliubov transformations on the infinite mode CCR-algebra*, *J. Math. Phys.* **37**, 4292 (1996).
-

-
- [102] M. Horodecki, P. Horodecki, and R. Horodecki, *Violating Bell inequality by mixed spin- $\frac{1}{2}$ states: necessary and sufficient condition*, *Phys. Lett. A* **200**, 340 (1995).
- [103] M. Horodecki, P. Horodecki, and R. Horodecki, *Separability of mixed states: necessary and sufficient conditions*, *Phys. Lett. A* **223**, 1 (1996) [arXiv:quant-ph/9605038].
- [104] M. Horodecki, P. Horodecki, and R. Horodecki, *Mixed-State Entanglement and Distillation: Is there a “Bound” Entanglement in Nature?* *Phys. Rev. Lett.* **80**, 5239 (1998) [arXiv:quant-ph/9801069].
- [105] M. Horodecki, P. Horodecki, and R. Horodecki, *General teleportation channel, singlet fraction, and quasidistillation*, *Phys. Rev. A* **60**, 1888 (1999) [arXiv:quant-ph/9807091].
- [106] R. Horodecki, M. Horodecki, and P. Horodecki, *Teleportation, Bell’s inequalities and inseparability*, *Phys. Lett. A* **222**, 21 (1996) [arXiv:quant-ph/9606027].
- [107] R. Horodecki, P. Horodecki, M. Horodecki, and K. Horodecki, *Quantum Entanglement*, *Rev. Mod. Phys.* **81**, 865 (2009) [arXiv:quant-ph/0702225].
- [108] D. J. Hosler, *Relativistic Quantum Communication*, Ph.D. thesis, University of Sheffield, 2013 [arXiv:1306.4853 [quant-ph]].
- [109] D. J. Hosler and P. Kok, e-print arXiv:1306.3144 [quant-ph] (2013).
- [110] B. L. Hu, S.-Y. Lin, and J. Louko, *Relativistic Quantum Information in Detectors-Field Interactions*, *Class. Quantum Grav.* **29**, 224005 (2012), Focus Issue on ‘Relativistic Quantum Information’ [arXiv:1205.1328 [quant-ph]].
- [111] M. Huber, N. Friis, A. Gabriel, C. Spengler, and B. C. Hiesmayr, *Lorentz invariance of entanglement classes in multipartite systems*, *Europhys. Lett.* **95**, 20002 (2011) [arXiv:1011.3374 [quant-ph]].
- [112] M. Huber, F. Mintert, A. Gabriel, and B. C. Hiesmayr, *Detection of high-dimensional genuine multi-partite entanglement of mixed states*, *Phys. Rev. Lett.* **104**, 210501 (2010) [arXiv:0912.1870 [quant-ph]].
- [113] F. Iemini, R. O. Vianna, *Computable Measures for the Entanglement of Indistinguishable Particles*, *Phys. Rev. A* **87**, 022327 (2013) [arXiv:1211.1886 [quant-ph]].
- [114] A. Iorio, *Using Weyl symmetry to make graphene a real lab for fundamental physics*, *Eur. Phys. J. Plus* **127**, 156 (2012) [arXiv:1207.6929 [hep-th]].
-

-
- [115] J.-C. Jaskula, G. B. Partridge, M. Bonneau, R. Lopes, J. Ruaudel, D. Boiron, and C. I. Westbrook, *An acoustic analog to the dynamical Casimir effect in a Bose-Einstein condensate*, *Phys. Rev. Lett.* **109**, 220401 (2012) [arXiv:1207.1338 [cond-mat]].
- [116] J. R. Johansson, G. Johansson, C. M. Wilson, and F. Nori, *Dynamical Casimir effect in superconducting microwave circuits*, *Phys. Rev. A* **82**, 052509 (2010) [arXiv:1007.1058 [quant-ph]].
- [117] T. F. Jordan, A. Shaji, and E. C. G. Sudarshan, *Lorentz transformations that entangle spins and entangle momenta*, *Phys. Rev. A* **75**, 022101 (2007) [arXiv:quant-ph/0608061].
- [118] R. Josza, *Fidelity for Mixed Quantum States*, *J. Mod. Opt.* **41**, 2315 (1994).
- [119] J. S. Kim, A. Das, and B. C. Sanders, *Entanglement monogamy of multipartite higher-dimensional quantum systems using convex-roof extended negativity*, *Phys. Rev. A* **79**, 012329 (2009) [arXiv:0811.2047 [quant-ph]].
- [120] M. Koashi and A. Winter, *Monogamy of entanglement and other correlations*, *Phys. Rev. A* **69**, 022309 (2004) [arXiv:quant-ph/0310037].
- [121] S. Kochen and E. P. Specker, *The Problem of Hidden Variables in Quantum Mechanics*, *Indiana Univ. Math. J. (formerly: J. Math. Mech.)* **17**, 59 (1967).
- [122] G. Labonté, *On the nature of 'strong' Bogoliubov transformations for fermions*, *Commun. Math. Phys.* **36**, 59 (1974).
- [123] P. Lähteenmäki, G. S. Paraoanu, J. Hassel, and P. J. Hakonen, *Dynamical Casimir effect in a Josephson metamaterial*, *Proc. Natl. Acad. Sci. U.S.A.* **110**, 4234 (2013) [arXiv:1111.5608 [cond-mat.mes-hall]].
- [124] A. Lambrecht, M.-T. Jaekel, and S. Reynaud, *Motion Induced Radiation from a Vibrating Cavity*, *Phys. Rev. Lett.* **77**, 615 (1996) [arXiv:quant-ph/9606029].
- [125] P. Langlois, *Hawking radiation for Dirac spinors on the \mathbb{RP}^3 geon*, *Phys. Rev. D* **70**, 104008 (2004) [Erratum-ibid. **72**, 129902(E) (2005); arXiv:gr-qc/0403011].
- [126] P. Langlois, *Imprints of spacetime topology in the Hawking-Unruh effect*, Ph.D. Thesis, University of Nottingham, 2005 [arXiv:gr-qc/0510127].
- [127] A. R. Lee and I. Fuentes, *Spatially extended Unruh-DeWitt detectors for relativistic quantum information*, e-print arXiv:1211.5261 [quant-ph] (2012).

-
- [128] Y. S. Li, B. Zeng, X. S. Liu, and G. L. Long, *Entanglement in a two-identical-particle system*, *Phys. Rev. A* **64**, 054302 (2001).
- [129] Z.-H. Ma, Z.-H. Chen, J.-L. Chen, C. Spengler, A. Gabriel, and M. Huber, *Measure of genuine multipartite entanglement with computable lower bounds*, *Phys. Rev. A* **83**, 062325 (2011) [arXiv:1101.2001 [quant-ph]].
- [130] X.-S. Ma, T. Herbst, T. Scheidl, D. Wang, S. Kropatschek, W. Naylor, A. Mech, B. Wittmann, J. Kofler, E. Anisimova, V. Makarov, T. Jennewein, R. Ursin, and A. Zeilinger, *Quantum Teleportation over 143 Kilometers Using Active Feed-Forward*, *Nature (London)* **489**, 269 (2012) [arXiv:1205.3909 [quant-ph]].
- [131] A. Mari and D. Vitali, *Optimal fidelity of teleportation of coherent states and entanglement*, *Phys. Rev. A* **78**, 062340 (2008) [arXiv:0808.2829 [quant-ph]].
- [132] E. Martín-Martínez, D. Aasen, and A. Kempf, *Processing Quantum Information with Relativistic Motion of Atoms*, *Phys. Rev. Lett.* **110**, 160501 (2013) [arXiv:1209.4948 [quant-ph]].
- [133] E. Martín-Martínez and I. Fuentes, *Redistribution of particle and antiparticle entanglement in noninertial frames*, *Phys. Rev. A* **83**, 052306 (2011) [arXiv:1102.4759 [quant-ph]].
- [134] E. Martín-Martínez, L. J. Garay, and J. León, *Unveiling quantum entanglement degradation near a Schwarzschild black hole*, *Phys. Rev. D* **82**, 064006 (2010) [arXiv:1006.1394 [quant-ph]].
- [135] E. Martín-Martínez, L. J. Garay, and J. León, *Quantum entanglement produced in the formation of a black hole*, *Phys. Rev. D* **82**, 064028 (2010) [arXiv:1007.2858 [quant-ph]].
- [136] E. Martín-Martínez, L. J. Garay, and J. León, *The fate of non-trivial entanglement under gravitational collapse*, *Class. Quantum Grav.* **29**, 224006 (2012), Focus Issue on ‘Relativistic Quantum Information’ [arXiv:1205.1263 [quant-ph]].
- [137] D. McMahon, P. M. Alsing, and P. Embid, *The Dirac equation in Rindler space: A pedagogical introduction*, e-print arXiv:gr-qc/0601010 (2006).
- [138] E. P. Menzel, R. Di Candia, F. Deppe, P. Eder, L. Zhong, M. Ihmig, M. Haeberlein, A. Baust, E. Hoffmann, D. Ballester, K. Inomata, T. Yamamoto, Y. Nakamura, E. Solano, A. Marx, and R. Grossard, *Path Entanglement of Continuous-Variable Quantum Microwaves*, *Phys. Rev. Lett.* **109**, 250502 (2012) [arXiv:1210.4413 [cond-mat.mes-hall]].

-
- [139] N. D. Mermin, *Simple Unified Form for the Major No-Hidden-Variables Theorems*, *Phys. Rev. Lett.* **65**, 3373 (1990).
- [140] M. Montero and E. Martín-Martínez, *Fermionic entanglement ambiguity in noninertial frames*, *Phys. Rev. A* **83**, 062323 (2011) [arXiv:1104.2307 [quant-ph]].
- [141] M. Montero and E. Martín-Martínez, *Reply to “Comment on ‘Fermionic entanglement ambiguity in noninertial frames’ ”*, *Phys. Rev. A* **85**, 016302 (2012) [arXiv:1108.6074 [quant-ph]].
- [142] M. Montero and E. Martín-Martínez, *Convergence of fermionic field entanglement at infinite acceleration in relativistic quantum information*, *Phys. Rev. A* **85**, 024301 (2012) [arXiv:1111.6070 [quant-ph]].
- [143] G. T. Moore, *Quantum theory of the electromagnetic field in a variable-length one-dimensional cavity*, *J. Math. Phys.* **11**, 2679 (1970).
- [144] M. A. Nielsen and I. L. Chuang, *Quantum Computation and Quantum Information* (Cambridge University Press, Cambridge, England, 2000).
- [145] *NIST Digital Library of Mathematical Functions*, <http://dlmf.nist.gov/>, Release 1.0.6 of 2013-05-06.
- [146] F. W. J. Olver, *The asymptotic expansion of Bessel functions of large order*, *Philos. Trans. Roy. Soc. London. Ser. A.* **247**, 328 (1954).
- [147] T. J. Osborne, *Entanglement measure for rank-2 mixed states*, *Phys. Rev. A* **72**, 022309 (2005) [arXiv:quant-ph/0203087].
- [148] T. J. Osborne and F. Verstraete, *General Monogamy Inequality for Bipartite Qubit Entanglement*, *Phys. Rev. Lett.* **96**, 220503 (2006) [arXiv:quant-ph/0502176].
- [149] Y. C. Ou, *Violation of monogamy inequality for higher-dimensional objects*, *Phys. Rev. A* **75**, 034305 (2007) [arXiv:quant-ph/0612127].
- [150] V. Palge, *Relativistic entanglement of single and two particle systems*, *Ph.D. thesis*, University of Leeds, 2013.
- [151] V. Palge and J. Dunningham, *Generation of maximally entangled states with subluminal Lorentz boosts*, *Phys. Rev. A* **85**, 042322 (2012) [arXiv:1207.5351 [quant-ph]].
- [152] M. C. Palmer, M. Takahashi, and H. F. Westman, *Localized qubits in curved spacetimes*, *Annals Phys.* **327**, 1078 (2012) [arXiv:1108.3896 [quant-ph]].

-
- [153] M. C. Palmer, M. Takahashi, and H. F. Westman, *WKB analysis of relativistic Stern-Gerlach measurements*, *Annals Phys.* **336** 505 (2013) [arXiv:1208.6434 [quant-ph]].
- [154] R. Paškauskas and L. You, *Quantum correlations in two-boson wave functions*, *Phys. Rev. A* **64**, 042310 (2001) [arXiv:quant-ph/0106117].
- [155] A. Peres, *Two simple proofs of the Kochen-Specker theorem*, *J. Phys. A: Math. Gen.* **24**, L175 (1991).
- [156] A. Peres, *Higher order Schmidt decompositions*, *Phys. Lett. A* **202**, 16 (1995) [arXiv:quant-ph/9504006].
- [157] A. Peres, *Separability Criterion for Density Matrices*, *Phys. Rev. Lett.* **77**, 1413 (1996) [arXiv:quant-ph/9604005].
- [158] A. Peres, P. F. Scudo, and D. R. Terno, *Quantum Entropy and Special Relativity*, *Phys. Rev. Lett.* **88**, 230402 (2002) [arXiv:quant-ph/0203033].
- [159] A. Peres and D. R. Terno, *Quantum information and relativity theory*, *Rev. Mod. Phys.* **76**, 93 (2004) [arXiv:quant-ph/0212023].
- [160] M. E. Peskin and D. V. Schroeder, *An Introduction to Quantum Field Theory* (Westview Press, 1995).
- [161] M. B. Plenio, *The logarithmic negativity: A full entanglement monotone that is not convex*, *Phys. Rev. Lett.* **95**, 090503 (2005) [arXiv:quant-ph/0505071].
- [162] M. B. Plenio and S. Virmani, *An introduction to entanglement measures*, *Quant. Inf. Comput.* **7**, 1 (2007) [arXiv:quant-ph/0504163].
- [163] S. Popescu, *Bell's inequalities versus teleportation: What is nonlocality?* *Phys. Rev. Lett.* **72**, 797 (1994).
- [164] J. M. Raimond, S. Brune, and S. Haroche, *Manipulating quantum entanglement with atoms and photons in a cavity*, *Rev. Mod. Phys.* **73**, 565 (2001).
- [165] S. Rana, *Negative eigenvalues of partial transposition of arbitrary bipartite states*, *Phys. Rev. A* **87**, 054301 (2013) [arXiv:1304.6775 [quant-ph]].
- [166] A. Recati, N. Pavloff, and I. Carusotto, *Bogoliubov theory of acoustic Hawking radiation in Bose-Einstein condensates*, *Phys. Rev. A* **80**, 043603 (2009) [arXiv:0907.4305 [quant-ph]].
- [167] M. Reed and B. Simon, *Methods of modern mathematical physics I: functional analysis*, (Academic Press, New York and London, 1972).

-
- [168] D. Rideout, T. Jennewein, G. Amelino-Camelia, T. F. Demarie, B. L. Higgins, A. Kempf, A. Kent, R. Laflamme, X. Ma, R. B. Mann, E. Martín-Martínez, N. C. Menicucci, J. Moffat, C. Simon, R. Sorkin, L. Smolin, and D. R. Terno, *Fundamental quantum optics experiments conceivable with satellites – reaching relativistic distances and velocities*, *Class. Quantum Grav.* **29**, 224011 (2012), Focus Issue on ‘Relativistic Quantum Information’ [[arXiv:1206.4949](#) [quant-ph]].
- [169] E. Rubino, J. McLenaghan, S. C. Kehr, F. Belgiorno, D. Townsend, S. Rohr, C. E. Kuklewicz, U. Leonhardt, F. König, and D. Faccio, *Negative-Frequency Resonant Radiation*, *Phys. Rev. Lett.* **108**, 253901 (2012) [[arXiv:1201.2689](#) [physics.optics]].
- [170] C. Sabín, A. White, L. Hackermüller, and I. Fuentes, *Dynamical phase quantum thermometer for an ultracold Bose-Einstein Condensate*, e-print [arXiv:1303.6208](#) [quant-ph] (2013).
- [171] P. L. Saldanha and V. Vedral, *Physical interpretation of the Wigner rotations and its implications for relativistic quantum information*, *New J. Phys.* **14**, 023041 (2012) [[arXiv:1111.7145](#) [quant-ph]].
- [172] P. L. Saldanha and V. Vedral, *Spin quantum correlations of relativistic particles*, *Phys. Rev. A* **85**, 062101 (2012) [[arXiv:1112.1272](#) [quant-ph]].
- [173] P. L. Saldanha and V. Vedral, *Wigner rotations and an apparent paradox in relativistic quantum information*, *Phys. Rev. A* **87**, 042102 (2013) [[arXiv:1303.4367](#) [quant-ph]].
- [174] A. Sanpera, R. Tarrach, and G. Vidal, *Quantum inseparability as local pseudomixture*, *Phys. Rev. A* **58**, 826 (1998) [[arXiv:quant-ph/9801024](#)].
- [175] J. Schliemann, J. I. Cirac, M. Kuś, M. Lewenstein, and D. Loss, *Quantum Correlations in Two-Fermion Systems*, *Phys. Rev. A* **64**, 022303 (2001) [[arXiv:quant-ph/0012094](#)].
- [176] J. Schliemann, D. Loss, and A. H. MacDonald, *Double-Occupancy Errors, Adiabaticity, and Entanglement of Spin-Qubits in Quantum Dots*, *Phys. Rev. B* **63**, 085311 (2001) [[arXiv:cond-mat/0009083](#)].
- [177] E. Schmidt, *Zur Theorie der linearen und nichtlinearen Integralgleichungen*, *Math. Ann.* **63** (4), 433 (1907).
- [178] D. Shale, *Linear symmetries of free boson fields*, *Trans. Am. Math. Soc.* **103**, 149 (1962).
-

-
- [179] D. Shale and W. F. Stinespring, *Spinor representations of infinite orthogonal groups*, *Indiana Univ. Math. J. (formerly: J. Math. Mech.)* **14**, 315 (1965).
- [180] Y. Shi, *Quantum entanglement of identical particles*, *Phys. Rev. A* **67**, 024301 (2003) [[arXiv:quant-ph/0205069](#)].
- [181] Y. Shi, *Entanglement in relativistic quantum field theory*, *Phys. Rev. D* **70**, 105001 (2004) [[arXiv:hep-th/0408062](#)].
- [182] R. Simon, *Peres-Horodecki Separability Criterion for Continuous Variable Systems*, *Phys. Rev. Lett.* **84**, 2726 (2000) [[arXiv:quant-ph/9909044](#)].
- [183] A. Smith and R. B. Mann, *Persistence of Tripartite Nonlocality for Non-inertial Observers*, *Phys. Rev. A* **86**, 012306 (2012) [[arXiv:1107.4633 \[quant-ph\]](#)].
- [184] R. D. Sorkin, *Impossible Measurements on Quantum Fields*, in: *Directions in General Relativity: Proceedings of the 1993 International Symposium, Maryland*, Vol. 2, pp. 293, edited by B.-L. Hu and T. A. Jacobson (Cambridge University Press, Cambridge, England, 1993) [[arXiv:gr-qc/9302018](#)].
- [185] F. Strocchi and A. S. Wightman, *Proof of the charge superselection rule in local relativistic quantum field theory*, *J. Math. Phys.* **15**, 2198 (1974).
- [186] I.-M. Svensson, *Photon generation in a doubly tunable resonator*, *M.Sc. thesis, Chalmers University of Technology*, 2012.
- [187] S. Takagi, *Vacuum noise and stress induced by uniform acceleration: Hawking-Unruh effect in Rindler manifold of arbitrary dimension*, *Prog. Theor. Phys. Suppl.* **88**, 1 (1986).
- [188] H. Terashima and M. Ueda, *Einstein-Podolsky-Rosen correlation seen from moving observers*, *Quantum Inf. Comput.* **3**, 224 (2003) [[arXiv:quant-ph/0204138](#)].
- [189] H. Terashima and M. Ueda, *Relativistic Einstein-Podolsky-Rosen correlation and Bell's inequality*, *Int. J. Quantum Inform.* **1**, 93 (2003) [[arXiv:quant-ph/0211177](#)].
- [190] B. M. Terhal, *Detecting quantum entanglement*, *Theor. Comput. Sci.* **287**, 313 (2002) [[arXiv:quant-ph/0101032](#)].
- [191] L. Vaidman, *Teleportation of quantum states*, *Phys. Rev. A* **49**, 1473 (1994).
- [192] F. Verstraete, K. Audenaert, J. Dehaene, and B. De Moor, *A comparison of the entanglement measures negativity and concurrence*, *J. Phys. A: Math. Gen.* **34**, 10327 (2001) [[arXiv:quant-ph/0108021](#)].

-
- [193] F. Verstraete and H. Verschelde, *Optimal teleportation with a mixed state of two qubits*, *Phys. Rev. Lett.* **90**, 097901 (2003) [[arXiv:quant-ph/0303007](#)].
- [194] G. Vidal and R. F. Werner, *Computable measure of entanglement*, *Phys. Rev. A* **65**, 032314 (2002) [[arXiv:quant-ph/0102117](#)].
- [195] R. M. Wald, *On particle creation by black holes*, *Comm. Math. Phys.* **45**, 9 (1975) [project Euclid [1103899393](#)].
- [196] R. M. Wald, *General Relativity*, (University of Chicago Press, Chicago, Illinois, USA, 1984).
- [197] S. Weinfurtner, E. W. Tedford, M. C. J. Penrice, W. G. Unruh, and G. A. Lawrence, *Measurement of stimulated Hawking emission in an analogue system*, *Phys. Rev. Lett.* **106**, 021302 (2011) [[arXiv:1008.1911](#) [gr-qc]].
- [198] S. Weinfurtner, E. W. Tedford, M. C. J. Penrice, W. G. Unruh, and G. A. Lawrence, *Classical aspects of Hawking radiation verified in analogue gravity experiment*, *Lect. Notes Phys.* **870**, 167 (2013) [[arXiv:1302.0375](#) [gr-qc]].
- [199] H. A. Weldon, *Fermions without vierbeins in curved space-time*, *Phys. Rev. D* **63**, 104010 (2001) [[arXiv:gr-qc/0009086](#)].
- [200] J. Williamson, *On the Algebraic Problem Concerning the Normal Forms of Linear Dynamical Systems*, *Am. J. Math.* **58**, 141 (1936).
- [201] C. M. Wilson, G. Johansson, A. Pourkabirian, M. Simoen, J. R. Johansson, T. Duty, F. Nori, and P. Delsing, *Observation of the dynamical Casimir effect in a superconducting circuit*, *Nature (London)* **479**, 376 (2011) [[arXiv:1105.4714](#) [quant-ph]].
- [202] H. M. Wiseman, S. D. Bartlett, and J. A. Vaccaro, *Ferretting out the Fluffy Bunnies: Entanglement constrained by Generalized superselection rules*, *Laser Spectroscopy, Proceedings of the XVI International Conference*, pp.307 (World Scientific, 2004) [[arXiv:quant-ph/0309046](#)].
- [203] H. M. Wiseman and J. A. Vaccaro, *Entanglement of Indistinguishable Particles Shared between Two Parties*, *Phys. Rev. Lett.* **91**, 097902 (2003) [[arXiv:quant-ph/0210002](#)].
- [204] M. M. Wolf, J. Eisert, and M. B. Plenio, *The entangling power of passive optical elements*, *Phys. Rev. Lett.* **90**, 047904 (2003) [[arXiv:quant-ph/0206171](#)].
- [205] W. K. Wootters, *Entanglement of Formation of an Arbitrary State of Two Qubits*, *Phys. Rev. Lett.* **80**, 2245 (1998) [[arXiv:quant-ph/9709029](#)].
-

- [206] J.-Y. Wu, H. Kampermann, D. Bruß, C. Klöckl, and M. Huber , *Determining lower bounds on a measure of multipartite entanglement from few local observables*, *Phys. Rev. A* **86**, 022319 (2012) [[arXiv:1205.3119](#) [quant-ph]].
- [207] P. Zanardi, *Quantum entanglement in fermionic lattices*, *Phys. Rev. A* **65**, 042101 (2002) [[arXiv:quant-ph/0104114](#) [quant-ph]].
- [208] D.-W. Zhang, Z.-D. Wang, and S.-L. Zhu, *Relativistic quantum effects of Dirac particles simulated by ultracold atoms*, *Front. Phys.* **7**, 31 (2012) [[arXiv:1203.5949](#) [cond-mat.quant-gas]].

List of Figures

- 4.1 **Inertial rigid cavity:** From the point of view of a co-moving observer with coordinates (t, x) , the inertial, rigid cavity has boundaries at $x = x_L$ and $x = x_R$, such that the cavity has the proper length $L = x_R - x_L$ 69
- 4.2 **Rindler coordinates:** Lines of constant χ (dashed green confocal hyperbolae) and constant η (solid blue radial lines) are shown for selected values of the coordinates in the right Rindler wedge $|t| < x$. The Rindler horizon is indicated by the solid black lines $t = x$ and $t = -x$. The hyperbolae $\chi = \text{const.}$ describe a family of (point-like) observers that are eternally uniformly accelerated. 70
- 4.3 **Relativistically rigid cavity:** The rigid inertial (region I) and uniformly accelerated (region II) cavities can be combined by pasting together the boundaries $x = x_L$ and $x = x_R$, with $\chi = \chi_L$ and $\chi = \chi_R$, respectively, at $\eta = t = 0$. The proper length with respect to a co-moving observer is $L = x_R - x_L$. The dashed lines indicate the light cone at the origin. 71
- 4.4 **Minkowski to Rindler Bogoliubov transformation — scalar field:** The cavity modes ϕ_n in the inertial region and the modes $\tilde{\phi}_m$ in the uniformly accelerated region are related by a Bogoliubov transformation with coefficients ${}_o\alpha_{mn}$ and ${}_o\beta_{mn}$, see Eq. (4.16). 75
- 4.5 **Minkowski to Rindler Bogoliubov coefficients — scalar field α 's:** The behaviour of the leading order “mode mixing” Bogoliubov coefficients ${}_o\alpha_{mn}^{(1)}$ from (4.22a) is shown for increasing mass of the (1+1)-dimensional real scalar field with Dirichlet boundary conditions. A selection of the coefficients ${}_o\alpha_{mn}^{(1)}$ is plotted against the dimensionless combination $M := mL$. The coefficients are proportional to M^2 as $M \rightarrow \infty$, while the intersections with the vertical axis give the massless limit, $m \rightarrow 0$, of Eq. (4.22a). 76

4.6 **Minkowski to Rindler Bogoliubov coefficients — scalar field β 's:** The behaviour of the leading order “particle creation” Bogoliubov coefficients ${}_o\beta_{mn}^{(1)}$ from (4.22b) is shown for increasing mass of the (1+1)-dimensional real scalar field with Dirichlet boundary conditions. A selection of the coefficients ${}_o\beta_{mn}^{(1)}$ is plotted against the dimensionless combination $M := mL$. The coefficients are proportional to M^{-4} as $M \rightarrow \infty$, while the intersections with the vertical axis give the massless limit, $m \rightarrow 0$, of Eq. (4.22b). 77

4.7 **Acceleration to the left:** The cavity is mirrored to the left Rindler wedge $|t| < -x$. The spatial reflection leaves the Bogoliubov coefficients unchanged but the inverted signs of the odd modes have to be taken into account when matching the phases of the modes. 78

4.8 **Transcendental equation:** For fixed parameters m and L the allowed frequencies ω_{k_n} from Eq.(4.30) for the Dirac field modes in the cavity are determined by the positive and negative numbers k_n that satisfy the transcendental equation (4.35). The roots of the function $\tan(kL)/(kL) + 1/M$ determine the possible values of (k_nL) . Curves are shown here for discrete steps, $M \in \{\frac{2l}{100} | l = 1, 2, \dots, 50\}$ (l increasing from top to bottom), of the dimensionless combination $M = mL$ 81

4.9 **Minkowski to Rindler Bogoliubov transformation — Dirac field:** The cavity modes ψ_{k_n} in the inertial region and the modes $\tilde{\psi}_{\Omega_m}$ in the uniformly accelerated region are related by a Bogoliubov transformation with coefficients ${}_oA_{mn}$, see Eq. (4.53). 85

4.10 **Minkowski to Rindler Bogoliubov coefficients — Dirac field:** The behaviour of the leading order Bogoliubov coefficients ${}_oA_{mn}^{(1)}$ from (4.59) for the (1 + 1)-dimensional Dirac field with MIT bag boundary conditions is shown for increasing mass. The coefficient ${}_oA_{mn}^{(1)}$ is plotted against the dimensionless combination $M := mL$. Figure 4.10 (a) shows a selection of Bogoliubov coefficients that relate modes with the same sign of the frequency (α -type coefficients): These mode-mixing coefficients are proportional to M^2 as $M \rightarrow \infty$. Figure 4.10 (b) shows a selection of Bogoliubov coefficients that relate positive frequency modes with negative frequency modes (β -type coefficients). These particle creation coefficients are proportional to M^{-6} as $M \rightarrow \infty$. For all curves the intersections with the vertical axis are given by the massless coefficients of Eq. (4.60). 87

- 4.11 **Basic building block:** The rigid cavity is at rest initially (region I), then undergoes a period of uniform acceleration from $t = 0$ to Rindler coordinate time $\eta = \eta_1$ (region II) and is thereafter again inertial (region III). The transitions between periods of inertial motion and uniform acceleration induce Bogoliubov transformations ${}_oB$ (I \rightarrow II) and ${}_oB^{-1}$ (II \rightarrow III). 89
- 4.12 **Trip to Alpha Centauri:** The travel scenario contains two periods of uniform acceleration of the same duration $\tilde{\tau}$ and proper acceleration as measured at the centre of the cavity. One of these segments is towards increasing, the other towards decreasing values of x . The periods of uniform acceleration are separated by a segment of inertial coasting at fixed velocity for the (proper) time τ , allowing the cavity to reach a (possibly) remote location such as *Alpha Centauri* [44]. 94
- 6.1 **Entanglement generation — bosonic vacuum:** The coefficients $\mathcal{N}^{(1)}$ [see Eq. (6.15)] and $\mathcal{N}^{(2)}$ [see Eq. (6.17)] of the negativity generated from the vacuum state are plotted in Fig. 6.1 (a) and Fig. 6.1 (b), respectively, for the basic building block travel scenario of Section 4.4.1. For the (1 + 1) dimensional massless scalar field used in this illustration the Bogoliubov coefficients are periodic in the dimensionless parameter $u := h\tau/[4L \operatorname{artanh}(h/2)]$ [see Eq. (4.20)], where τ is the duration, as measured at the centre of the cavity, of the single segment of uniform acceleration. Curves are shown for the mode pairs $(k, k') = (1, 2)$ (solid), $(2, 3)$ (dashed), $(3, 4)$ (dotted), and $(1, 4)$ (dotted-dashed) in Fig. 6.1 (a), and for $(1, 3)$ (solid), $(2, 4)$ (dashed), $(3, 5)$ (dotted), and $(1, 5)$ (dotted-dashed) in Fig. 6.1 (b). . 120
- 6.2 **Entanglement generation — bosonic single particle state $|1_k\rangle$:** The coefficients $\mathcal{N}^{(1)}$ [see Eq. (6.22)] and $\mathcal{N}^{(2)}$ [see Eq. (6.26)] of the negativity generated from the state $|1_k\rangle$ are plotted in Fig. 6.2 (a) and Fig. 6.2 (b), respectively, for the basic building block travel scenario of Section 4.4.1. For the (1 + 1) dimensional massless scalar field used in this illustration the Bogoliubov coefficients are periodic in the dimensionless parameter $u := h\tau/[4L \operatorname{artanh}(h/2)]$ [see Eq. (4.20)], where τ is the duration, as measured at the centre of the cavity, of the single segment of uniform acceleration. Curves are shown for the mode pairs $(k, k') = (1, 2)$ (solid), $(2, 3)$ (dashed), $(3, 4)$ (dotted), and $(1, 4)$ (dotted-dashed) in Fig. 6.2 (a), and for $(1, 3)$ (solid), $(2, 4)$ (dashed), $(3, 5)$ (dotted), and $(1, 5)$ (dotted-dashed) in Fig. 6.2 (b). 122

- 6.3 **Entanglement generation — symmetric single-mode squeezing:** The coefficient $\mathcal{N}^{(1)}$ [see Eq. (6.35)] of the negativity generated from a symmetrically single-mode squeezed state is plotted for the basic building block travel scenario of Section 4.4.1 for squeezing parameters $s_k = s_{k'} = 1$. For the $(1 + 1)$ dimensional massless scalar field in this illustration the Bogoliubov coefficients are periodic in the dimensionless parameter $u := h\tau/[4L \operatorname{artanh}(h/2)]$ [see Eq. (4.20)], where τ is the duration, as measured at the centre of the cavity, of the single segment of uniform acceleration. Curves are shown for the mode pairs $(k, k') = (1, 2)$ (solid), $(2, 3)$ (dashed), $(3, 4)$ (dotted), and $(1, 4)$ (dotted-dashed). 126
- 6.4 **Entanglement resonances — β 's:** The coefficient $|\beta_{kk'}^{(1)}|$ that generates entanglement from the vacuum [see Eq. (6.15)] is plotted against the dimensionless parameter $u := h\tau/[4L \operatorname{artanh}(h/2)]$ for a massless $(1 + 1)$ dimensional scalar field. The travel scenario, which is illustrated in Fig. 6.5 (b) for $N = 2$, has N segments of uniform proper acceleration h/L and duration $\tau/2$ as measured at the centre of the cavity, separated by $(N - 1)$ segments of inertial coasting of the same duration (to linear order in h). The curves are plotted for $N = 15$, $(k, k') = (1, 2)$ (blue, solid) and $(k, k') = (2, 3)$ (purple, dashed). The vertical dashed lines indicate the potential resonance times as given by Eq. (6.46) for $(k, k') = (1, 2)$ and $(k, k') = (2, 3)$, respectively. 129
- 6.5 **Entanglement resonances — α 's:** The coefficient $|\alpha_{kk'}^{(1)}|$ that contributes to the entanglement generation, e.g., for squeezed states [see Eqs. (6.22) and (6.35)] is plotted in Fig. 6.5 (a) against the dimensionless parameter $u := h\tau/[4L \operatorname{artanh}(h/2)]$ for a massless $(1 + 1)$ dimensional scalar field. The travel scenario, which is illustrated in Fig. 6.5 (b) for $N = 2$, has N segments of uniform proper acceleration h/L and duration $\tau/2$ as measured at the centre of the cavity, separated by $(N - 1)$ segments of inertial coasting of the same duration (to linear order in h). The curves in Fig. 6.5 (a) are plotted for $N = 15$, $(k, k') = (1, 2)$ (blue, solid) and $(k, k') = (2, 3)$ (purple, dashed). For comparison the quantity $|\beta_{kk'}^{(1)}|$ (red, dashed) from Fig. 6.4 is shown for $(k, k') = (1, 2)$ 130

- 6.6 **Entanglement generation — fermionic vacuum:** The coefficients $\mathcal{N}^{(1)}$ and $\mathcal{N}^{(2)}$ [see Eq. (6.51) and (6.52)] of the negativity generated from the fermionic vacuum are plotted in Fig. 6.6 (a) and Fig. 6.6 (b), respectively, for the basic building block travel scenario of Section 4.4.1. The effects for the $(1 + 1)$ dimensional Dirac field used here are periodic in the dimensionless parameter $u := h\tau/[4L \operatorname{artanh}(h/2)]$ [see Eq. (4.52)], where τ is the duration of the acceleration, as measured at the centre of the cavity. Curves are shown for the modes $(\kappa, \kappa') = (0, -3), (2, -1)$ (solid), $(0, -5), (4, -1)$ (dashed), and $(3, -2), (1, -4)$ (dotted) in Fig. 6.6 (a), and for $(1, -1), (0, -2)$ (solid), $(1, -3), (2, -2)$ (dashed), and $(0, -4), (3, -1)$ (dotted) in Fig. 6.6 (b). 133
- 6.7 **Entanglement generation — fermionic particle state:** The coefficients $\mathcal{N}^{(1)}$ and $\mathcal{N}^{(2)}$ [see Eq. (6.56) and (6.57)] of the negativity generated from $\|1_{\kappa}\rangle\rangle^{\dagger}$ are plotted in Fig. 6.7 (a) and Fig. 6.7 (b), respectively, for the basic building block travel scenario of Section 4.4.1. The effects for the $(1 + 1)$ dimensional Dirac field used here are periodic in the dimensionless parameter $u := h\tau/[4L \operatorname{artanh}(h/2)]$ [see Eq. (4.52)], where τ is the duration of the acceleration, as measured at the centre of the cavity. Curves are shown for the modes $(\kappa, \kappa') = (0, 1)$ (solid), $(1, 2)$ (dashed), $(2, 3)$ (dotted), and $(0, 3)$ (dotted-dashed) in Fig. 6.7 (a), and for $(0, 2)$ (solid), $(1, 3)$ (dashed), $(2, 4)$ (dotted), and $(0, 4)$ (dotted-dashed) in Fig. 6.7 (b). . 135
- 6.8 **Entanglement generation — fermionic particle-antiparticle pair:** The second order coefficient of the only possibly negative eigenvalue $\lambda_{-} = h^2[f_{\kappa}^A + \bar{f}_{\kappa}^A] - h^2\sqrt{[f_{\kappa}^A - \bar{f}_{\kappa'}^A]^2 + |\mathcal{V}_{\kappa\kappa'}^{(2)}|^2}$ of the partial transpose of the two qubit representation for the state Eq. (6.58) is shown. Curves are plotted for the basic building block travel scenario of Section 4.4.1 for a $(1 + 1)$ dimensional Dirac field against the dimensionless parameter $u := h\tau/[4L \operatorname{artanh}(h/2)]$ [see Eq. (4.52)], where τ is the duration of the acceleration, as measured at the centre of the cavity. Curves are shown for the modes $(\kappa, \kappa') = (1, -1), (0, -2), (0, -4), (3, -1)$ (solid), and $(1, -3), (2, -2)$ (dashed). Since the correction is positive throughout no entanglement is generated. 137

-
- 7.1 **Quantum communication between two cavities:** Alice and Rob each control a cavity containing a quantum field. They share an initially entangled state between one mode in each cavity to be used in a quantum communication task, e.g., quantum teleportation. Rob's cavity is undergoing non-uniform motion, which entangles all modes in the spectrum of his cavity. Consequently the entanglement shared between Alice and Rob is degraded by the motion. 144
- 7.2 **Entanglement degradation — f_k^α :** The coefficient $f_{k'}^\alpha$ that is degrading the entanglement between Alice and Rob as quantified by the negativity [see Eq. (7.5) and Eq. (7.15)] is plotted for the basic building block travel scenario of Section 4.4.1 for a $(1 + 1)$ dimensional massless scalar field. The effects are periodic in the dimensionless parameter $u := h\tau/[4L \operatorname{artanh}(h/2)]$ [see Eq. (4.20)], where τ is the duration of the uniform acceleration, as measured at the centre of the cavity. Curves are shown for the modes $k' = 1$ (solid), $k' = 2$ (dashed), $k' = 3$ (dotted), and $k' = 4$ (dotted-dashed). 148
- 7.3 **Entanglement degradation — f_k^β :** The coefficient $f_{k'}^\beta$ that is degrading the entanglement between Alice and Rob as quantified by the negativity [see Eq. (7.5) and Eq. (7.15)] is plotted for the basic building block travel scenario of Section 4.4.1 for a $(1 + 1)$ dimensional massless scalar field. The effects are periodic in the dimensionless parameter $u := h\tau/[4L \operatorname{artanh}(h/2)]$ [see Eq. (4.20)], where τ is the duration of the uniform acceleration, as measured at the centre of the cavity. Curves are shown for the modes $k' = 1$ (solid), $k' = 2$ (dashed), $k' = 3$ (dotted), and $k' = 4$ (dotted-dashed). 149
- 7.4 **Quantum teleportation between two cavities:** Alice and Rob wish to use the initially shared entanglement that is supplied by the EPR source to teleport an unknown coherent state. After the initial state has been prepared Alice performs a Bell measurement on the (unknown) state that is to be teleported and her mode k of the entangled resource state. Subsequently, she sends the measurement outcomes to Rob via a classical channel. Meanwhile, Rob undergoes a finite period of non-uniform motion, after which he receives the classical information necessary to retrieve the unknown input state by performing a local unitary U . By measuring their respective proper times and applying corresponding local rotations Alice and Rob can optimize their teleportation scheme. . . 150
-

-
- 7.5 **Superconducting cavity simulation:** A one-dimensional transmission line for microwave radiation is interrupted by two SQUIDs at a distance L_0 with respect to each other. The SQUIDs are threaded by time-dependent magnetic fluxes that create boundary conditions — effective mirrors — at distances $d_{\pm}(t)$ away from the SQUIDs. This creates a cavity of effective length L_{eff} that can simulate non-uniform motion by changing the fluxes in time such that the length $L_{\text{eff}} = d_+ + L_0 + d_- = \text{const.}$, as measured by a potentially co-moving observer, remains constant. 152
- 7.6 **Entanglement degradation — $f_{\kappa'}^A$ and $\bar{f}_{\kappa'}^A$:** The quantities $f_{\kappa'}^A$ and $\bar{f}_{\kappa'}^A$ that are degrading the entanglement between Alice and Rob [see Eqs. (7.27), (7.32) and (7.33)] are shown in Fig. 7.6 (a) and Fig. 7.6 (b), respectively, for the basic building block travel scenario of Section 4.4.1 for a $(1 + 1)$ dimensional massless Dirac field. The horizontal axis shows the dimensionless parameter $u := h\tau/[4L \operatorname{artanh}(h/2)]$ [see Eq. (4.20)], where τ is the duration of the uniform acceleration at the centre of the cavity. Curves are shown for the modes $\kappa' = 0$ (solid), $\kappa' = 1$ (dashed), $\kappa' = 2$ (dotted), and $\kappa' = 3$ (dotted-dashed). 156

Index

- action principle, 32
- active (optical) transformation, 45
- algebra
 - anticommutation relation, 39
 - commutation relation, 35
- beam splitter, 46
- Bell
 - inequality, 24
 - measurement, 26
 - states, 15, 144, 153
 - theorem, 24, 25
- Bessel
 - equation, modified, 73, 83
 - functions, modified, 1st kind, 74, 83
- Bloch
 - decomposition, 12
 - decomposition; generalized, 13
 - vector, 12
- Boch-Messiah reduction, 45, 46
- Bogoliubov coefficients bosons
 - Alpha Centauri, 94
 - basic building block, 90–91
 - general, 35
 - general expansion, 92
 - Minkowski to Rindler, 74
 - smooth acceleration, 96
- Bogoliubov coefficients fermions
 - Alpha Centauri, 94
- basic building block, 91
 - general, 39
 - general expansion, 92
 - Minkowski to Rindler, 86
 - smooth acceleration, 96
- Bogoliubov identities bosons
 - expansion order h , 93
 - expansion order h^2 , 93
 - general, 35
- Bogoliubov identities fermions
 - expansion order h , 93
 - expansion order h^2 , 93
 - general, 39
- Bogoliubov transformation
 - Alpha Centauri, 93
 - basic building block, 90
 - bosons, 35, 44, 74
 - fermions, 39, 85
 - smooth acceleration, 96
- boundary conditions
 - MIT bag, 80, 83
 - Dirichlet, 72, 73
- canonical
 - commutation relation, 42
- characteristic function, 42
- CHSH
 - criterion, 16, 25
 - inequality, 25, 155

-
- operator, 25
 - CKW monogamy inequality, 19
 - Clauser-Horne-Shimony-Holt, 16
 - Coffman-Kundu-Wootters, *see* CKW
 - coherent state, 43
 - concurrence, 17, 18, 59, 61, 154
 - convex roof construction, 18
 - correlation matrix, 26, 155
 - covariance
 - matrix, 42, 105
 - criterion
 - CHSH, 16
 - PPT, 16
 - density operator, 11
 - Dirac
 - equation, curved space, 36
 - equation, Minkowski coord., 79
 - equation, Rindler coordinates, 82
 - fermions, 37
 - field, 79
 - gamma matrices, 36
 - inner product, 84
 - Dirichlet boundary conditions, 72
 - displacement operator, 43
 - dynamical Casimir effect, 4, 29, 68, 97, 131, 151, 159
 - Einstein summation convention, 12
 - Einstein-Podolsky-Rosen, *see* EPR
 - entanglement, 14–63
 - detection, 15–17
 - entropy of, 14
 - genuine multipartite, 21, 138
 - genuine tripartite, 141
 - maximal, 14
 - measures, 17–20
 - monogamy, *see* CKW
 - multipartite, 20–23
 - of formation, 18
 - resonances, 127, 139
 - witness, 16
 - witness theorem, 16
 - entropy
 - inequalities, 15
 - linear, 11, 118, 121, 126
 - of entanglement, 14
 - Shannon, 12
 - von Neumann, 11
 - EPR paradox, 23–24
 - Euler-Lagrange equation, 32, 36
 - expectation value
 - mixed states, 11
 - pure states, 10
 - fermionic concurrence, 61
 - Fock
 - space, bosonic, 34, 100
 - space, fermionic, 37–39, 107
 - states, 34, 103, 110
 - Gaussian
 - state, 42–51, 105
 - group
 - Poincaré, 30
 - symplectic, 44
 - Hadamard Lemma, 100, 108
 - Hermitean operator, 10
 - Hilbert space, 9
 - Hilbert-Schmidt
 - condition, 101, 108
 - inner product, 11
 - space, 11
 - homodyne detection, 49
 - isometry, 31
-

-
- Josephson junction, 151
- Killing vector, 31, 69, 71, 73, 74
- Klein-Gordon
 equation, curved spacetime, 32
 equation, Minkowski coord., 72
 equation, Rindler coordinates, 73
 field, 33, 72
 inner product, 32, 72
- Lagrangian
 Dirac field, 36
 real, scalar field, 31
- Laplacian, 72
- Lie
 derivative, 31
- linear operator, 10
- local operations & classical communication, *see* LOCC, 17
- local unitary operations, 17
- LOCC, 15, *see* local operations & classical communication
- Lorentz
 invariance, 30
 metric, 30
- metric tensor, 30
- Minkowski metric, 30
- mixedness, 11, 126
- negativity, 20, 59, 118, 132, 145, 154
 logarithmic, 20
- Noether current, 32
- non-locality, 24–26
- observable, 10
- partial transposition, 16, 19, 47, 59, 119,
 121, 124, 132, 134, 137, 145, 147,
 154
- passive (optical) transformation, 45
- Pauli exclusion principle, 52, 110, 137,
 140
- Pauli matrices, 12, 25, 146, 154
- Peres-Horodecki criterion, *see* PPT
- phase space, 42
- Poincaré group, 30
- Positive
 semi-definite operator, 11
- PPT criterion, 16, 47
- proper
 acceleration, 70, 75, 99, 131, 151
 length, 31, 71
 time, 31, 70, 147, 150
- quadratures, 42
- quantum gates, 141, 158
- resonance condition, 50, 127
- Riemann
 sum, 101, 108
 zeta function, 101, 108
- Rindler coordinates, 69, 73, 82
- Schmidt decomposition, 13
- separability
 bi-separable, 21
 mixed states, 15
 n-separable, 21
 pure states, 14
- Shannon entropy, 12
- space-like, 30
- spin connection, 82
- squeezed state
 single-mode, 43, 106, 124
 two-mode, 46, 146
- squeezing parameter
 single-mode, 43
 two-mode, 46, 47
-

-
- SQUID, 151
- state
- Bell, 15, 144, 153
 - bipartite, pure, 13
 - coherent, 43
 - Fock, 34, 103, 110
 - Gaussian, 42–51, 105
 - mixed, 10–13
 - pure, 9
 - single-mode squeezed, 43, 106
 - symmetric two-mode Gaussian, 47
 - thermal, 43
 - two-mode squeezed, 46, 146
- stress-energy-momentum tensor, 32
- superconducting quantum interference device, *see* SQUID
- superposition principle, 10
- symplectic
- eigenvalues, 45
 - form, 44
 - group, 44
 - local invariants, 47
 - local operations, 47
 - spectrum, 45
 - transformation, 44, 105
 - transformation, active, 45
 - transformation, passive, 45
- tangle, 19
- Taylor-Maclaurin expansion, 75, 85, 99
- teleportation, 26, 49
- fidelity, 27, 155
 - fidelity, Gaussian states, 49
- thermal state, 43
- time-like, 30
- transcendental equation, 81
- transformation
- Bogoliubov, 35, 39
 - global unitary, 55
 - local symplectic, 47
 - local unitary, 17
 - symplectic, 44, 105
 - unitary, 85
- unitarity, 93
- bosons, 101–102
 - fermions, 108–109
- unitary
- operator, 10
 - transformation, 85
- vacuum
- bosons, 33, 43, 50, 100, 103, 116–120
 - fermions, 37, 107, 110, 132–133
- volume form, 32
- Von Neumann
- entropy, 11
- Wigner function, 42
- Williamson normal form, 45
- worldline, 31
-